July 2018

Novel Mass Spectrometry Methods for the Analysis of Covalent and Non-Covalent Protein Structures and Their Influence on the Functions of Therapeutic Proteins

Jake Pawlowski

NOVEL MASS SPECTROMETRY METHODS FOR THE ANALYSIS OF COVALENT AND NON-COVALENT PROTEIN STRUCTURES AND THEIR INFLUENCE ON THE FUNCTIONS OF THERAPEUTIC PROTEINS

A Dissertation Presented

by

JAKE WALTER PAWLOWSKI

Submitted to the Graduate School of the
University of Massachusetts Amherst in partial fulfillment
of the requirements for the degree of

DOCTOR OF PHILOSOPHY

MAY 2018

Chemistry Department

NOVEL MASS SPECTROMETRY METHODS FOR THE ANALYSIS OF COVALENT AND NON-COVALENT PROTEIN STRUCTURES AND THEIR INFLUENCE ON THE FUNCTIONS OF THERAPEUTIC PROTEINS

A Dissertation Presented

By

JAKE WALTER PAWLOWSKI

Approved as to style and content by:

_____

Igor A. Kaltashov, Chair

_____

Richard W. Vachet, Member

_____

Anne B. Mason, Member

_____

Daniel N. Hebert, Outside Member, BMB Department

_____

Richard W. Vachet, Department Head Chemistry

DEDICATION

My friends and family

ACKNOWLEDGMENTS

First I would like to thank Igor Kaltashov who has been my mentor and advisor since he first accepted me into his lab as an undergraduate back in 2009. I would not be the scientist or mass spectrometrist I am today without his feedback and thoughtful discussions. I would also like to thank my committee members Prof. Braun, Prof. Vachet, Prof. Hebert, and Prof. Mason for all their guidance and feedback during my graduate career.

A special thanks is necessary for my aunt Helena Madden for bringing me into her lab at Biogen as a teenager that helped inspired my pursuit of science. I would like to give my sincerest thanks to my family Paul, Janet, and Walter as well as my girlfriend Barbara for their full love and support during my graduate school work. To all my friends in the graduate school I would like to thank you all for making my time here very fulfilling with all the memories we created and shared.

A big thanks is needed for Cedric Bobst for all his help and advice during my time as an undergraduate and graduate student. To all current and past lab members of the Kaltashov lab I would like to extend my thanks for all the help and thoughtful discussions throughout the years as well as for making coming to lab an enjoyable experience. To Ian, Noel, Peter, and Jake who worked with me as undergraduate researchers thank you for all the help that made my research that much easier and eventually lead to two publications. I had the opportunity to work with some great collaborates from Biogen: Damian, Tyler, Marian, and Adriana. I am extremely grateful for the help and feedback during our collaboration together. Finally I would like to give a big thanks to Bill Schmitt for all his help in the analytical teaching labs.

ABSTRACT

NOVEL MASS SPECTROMETRY METHODS FOR THE ANALYSIS OF COVALENT AND NON-COVALENT PROTEIN STRUCTURES AND THEIR INFLUENCE ON THE FUNCTIONS OF THERAPEUTIC PROTEINS

MAY 2018

JAKE WALTER APWLOWSKI, B.S., UNIVERSITY OF MASSACHUSETTS AMHERST

Ph.D., UNIVERSITY OF MASSACHUSETTS AMHERST

Directed by: Professor Igor A. Kaltashov

Biotherapeutics consist of biopolymers (proteins, polysaccharides, DNA, and RNA) that are used to treat a wide range of conditions from cancer to autoimmune disease to enzyme replacement. In recent years biotherapeutics have experience tremendous growth due to advances in technology and our understanding of human biology. They are very important to modern medicine due to their ability to treat diseases which are unable to be treated with small molecule-based drugs. Unlike small molecule drugs which are synthetically produced, biotherapeutics are expressed inside cells. Produced biotherapeutics are not made up of a single homogenous population but instead a population of highly similar variants. The source of these variations are enzymatic and non-enzymatic post-translational modifications. By characterizing these modification, a

profile is built that links the *in vivo* response of a drug to its modifications. The complexity and size of these biopolymers makes their characterization very challenging and demands the development of robust analytical techniques.

Mass spectrometry- and liquid chromatography-base methods are an integral part of protein characterization. Mass spectrometry provides accurate mass measurements that are invaluable for confirming the identity of a protein and any modifications. Additionally, mass spectrometry is used to assess a protein's higher order structure. Liquid chromatography is a very powerful tool that allows for different post-translational modified populations of a biotherapeutic sample to separate by their chemical or physical properties. Separated populations can further be characterized to identify and analyze their chemical or structural composition. The presented work utilized a blend of mass spectrometry and liquid chromatography methods to characterize proteins with biotherapeutic potential.

TABLE OF CONTENTS

Page

LIST OF TABLES

LIST OF FIGURES

CHAPTER 1

INTRODUCTION

1.1 Biopharmaceuticals and Their Importance to Modern Medicine

In 1982 from Eli Lily recombinant human insulin was the first marketed biopharmaceutical leading to a transformation in the pharmaceutical industry.[1] Previously, most commercial drugs consisted of small molecules or biological products purified from biological sources (*i.e.* blood). A biopharmaceutical is a protein- or nucleic acid-based product that is manufactured by any means other than direct extraction from a natural biological source.[2] In recent years, biopharmaceuticals have experienced a rise in market approvals due to the increased understanding of human and cellular biology and the underlying mechanisms which lead to diseases.

Perhaps the two most important advances accounting for the rise of biopharmaceuticals were the developments of recombinant DNA technology and monoclonal antibody (mAb) production through hybridoma technology.[2] The majority of proteins with therapeutic promise are produced in limiting amounts by the body and are challenging or impossible to purify economically from biological sources. Fortunately, recombinant DNA technology, first utilized in 1972[3,4], permits genes encoding therapeutically relevant proteins to be expressed in large quantities in cell culture. Secondly but no less important is the ability to produce monoclonal antibodies (mAb) by hybridomas technology, developed in 1975.[5] A hybridoma is an immortal cell line, created by the fusion of a B cell and myeloma cell, that produces antibodies with identical structure and sequence, known as a mAb.[6] The ability to produce an almost unlimited amount of an

identical antibody has made it feasible to treat diseases with mAbs. Examples include cancer and autoimmune disorders.

Biopharmaceuticals are not limited in their scope to diseases in the body. As the understanding of human biology moves forward, new treatment opportunities for disease are possible. In 2016, newly approved biopharmaceuticals covered a diverse range of ailments that include cancer, autoimmune disorders, psoriasis, and bacterial infections. This highlights the versatility of biopharmaceuticals as they can be utilized to target and treat a wide spectrum of diseases.

1.2 Complexity of Biopharmaceuticals

Biopharmaceuticals are produced in cells and are orders of magnitude more complex than traditional small molecule production.[7] Cell lines used for protein expression include mammalian (Chinese hamster ovary, human embryonic kidney 293, baby hamster kidney cells, etc.) and non-mammalian (yeast, insect, bacteria, and plant) cell lines.[8] A cell line is chosen depending on the requirements for the biopharmaceutical to be expressed.[9] For example, bacterial expression systems benefit from being simple to grow and produce protein in high yields. However, these expression systems lack the proper glycosylation enzymes to decorate expressed proteins with human-like glycans.[10,11] If human-like glycans or disulfides are necessary for the biopharmaceutical then mammalian cell lines are used. Care must still be taken as non-human mammalian cell lines can add glycans not found in humans such as N-glycolylneuraminic acid and galactose-α1.3-galactose.[8] Due to humans possessing antibodies against these glycans, any biopharmaceutical

containing these glycans could generate an immune response and thus possibly neutralize the drug.[12]

Unlike a small molecule drug whose production is highly controlled, it is impossible to maintain this same level of control over protein production due to the complexity inside a cell.[7] As a result, a produced therapeutically relevant protein will not be composed of a single homogeneous protein population but rather a heterogeneous one. Heterogeneity is due in part to cellular expression, cell culture media, manufacturing processes, transport, and protein storage.[13-18] Additionally, changes in any of these factors are known to potentially affect the composition of the final product. It is essential to identify these composition differences and assess they cause a change in efficacy. Even changes in the headspace of a vial[19] or its oxygen level[20] are known to alter the composition of a stored protein drug. These are excellent examples of how even trivial changes in storage can lead to a different final product. Therefore great effort is exerted to minimize heterogeneity during production to ensure the safety and efficacy of a biotherapeutic.

As mentioned *vide supra* a produced biopharmaceutical is not made up of a single homogenous population but rather a population of highly similar variant forms due to post-translational modifications (PTMs). The number, range, and variety of these forms are all dependent on the cell line used, cell culture conditions, and purification processes.[7] Variation in the population of highly similar variants is commonly referred to as microheterogeneity. As described by the well know biological phrase "structure determines function", changes in biopharmaceutical's structure may adversely affect its function. Therefore, it is of great importance to characterize and understand at what thresholds PTMs will change the function of a protein drug.

1.3 Post-Translational Modifications of Proteins

The majority of heterogeneity in a biopharmaceutical is due to PTMs that occur inside a cell or during the manufacturing process and storage. PTMs control a protein's activity state, cell locations, degradation, and other protein interactions.[21] Moreover, PTMs are not encoded in a protein's genetic sequence but rather are a product of both enzymatic and non-enzymatic processes. The lack of ability to directly encode PTMs through a protein's DNA sequence makes it difficult to precisely control these modifications and gives rise to the possibility of a heterogeneous expressed protein. While **Table 1.1** describes a small sampling of all the possible PTMs and their effects, there are many PTMs which makes protein characterization a challenging goal. Therefore, it is important to detect and quantitate PTMs to ensure that a biopharmaceutical population contains the correct modifications (*i.e.* glycosylation) as well as minimal amounts of damaging PTMs (*i.e.* oxidation, glycation and deamidation).

Once a biopharmaceutical is characterized, a PTM profile is created to describe all possible modifications and their effect on a biopharmaceutical. The profile is used as a standard to compare all future manufactured lots of the biotherapeutic to a quality control measurement. Additionaly, the PTM profile is linked to the function and efficacy of the protein drug. Changes to this profile may have significant changes for a biotherapeutic's *in vivo* function.[22] Therefore, to ensure different batches of a protein drug will elicit the same therapeutic response *in vivo* it is crucial to establish the acceptable presence and range of PTMs. Also, improvements to a biopharmaceutical's production and storage can be

assessed and compared to previously produced protein lots as a way to ensure the drug will provide the same efficacy.

Table 1.1 List of common PTMs

Type	Description
Enzymatic Post-Translational Modifications	
Glycosylation	Addition of a glycan chain to an asparagine (N-linked) or a serine/threonine (O-linked). Glycans are important for proper protein folding,[23] protein stability,[24] modulating a protein's function,[25-30] and cell-cell / protein-protein interaction.[31]
Phosphorylation	Phosphate group is added by a kinase to (most commonly) a serine, threonine, or tyrosine as a way to control the function of protein in response to a stimuli.[32]
Non-Enzymatic Post-Translational Modifications	
Oxidation	Covalent modification of a protein by a reactive oxygen species. Addition of an oxygen is known to affect the structure and function of a protein.[33] Oxidation is a sign of protein stress and may lead to immunogenicity, aggregation, or degradation.[34-37]
Deamidation	Asparagine (or glutamine) is converted, through a succinimide intermediate, to aspartic (or glutamic acid) which may affect a proteins structure and function due to the introduction of a negative charge (and possible isomerization).[38] Can enhance[39] or reduce[40] the potency of a biopharmaceutical.
Disulfide Bridge	Covalent bond between two cysteines and is important for maintaining a protein's structure.[41] Disulfide scrambling affects the proteins structure and may lead to aggregation.[42] Trisulfide formation is also possible and is found in mAbs.[43]
Glycation	Hexose is covalently attached to a protein. May affect the efficacy and stability of a biopharmaceutical.[44]
Designer Post-Translational Modifications	
Pegylation	Addition of a PEG polymer chain to a protein. Increases a protein's half-life and solubility.[45]
Drug Conjugates	Covalent labeling of a protein with a linker and drug. A drug attached to a mAb can be effectively delivered to its target with an increased half-life.[46]

1.4 Characterization of Biopharmaceuticals

Protein PTMs are complex to understand with regard to the function and stability of the protein. Additionally there are hundreds of know PTMs[15] which makes understanding their effects even more challenging requiring a multivariable equation. It is important to keep in mind that a completely homogenous (structure, sequence, and PTMs) biopharmaceutical is impossible to produce on a large scale. Fortunately, there are acceptable ranges in the amount of PTMs in a biopharmaceutical in which they will deliver a reproducible clinical performance.[47] Great effort goes into defining the acceptable range of PTMs in a biopharmaceutical's population. Robust analytical methods must be implemented to *i.* identify at what percent of a biopharmaceutical's population will a PTM alter its clinical efficacy and *ii.* accurately quantitate these PTMs to ensure confidence of the measurements. This will contribute to ensuring that different production lots of a biopharmaceutical, even with alteration to its PTM profile, will deliver reproducible results.

Unfortunately, there is not a single analytical tool that can provide all the necessary information to fully characterize a therapeutic protein. Instead a punctilious suite of analytical tools is necessary to fully characterize a protein. These tools range in complexity from simple (UV absorbance) to complicated (hydrogen-deuterium exchange). All these analytical measurements of a biopharmaceutical are needed to build a profile of a protein. Once a protein's profile is established it is used as a standard for the acceptable variations in the protein's population. It is with this standard of acceptable ranges for PTMs that the quality of the protein can be judged

1.5 Toolbox for Biopharmaceuticals Characterization

There is a wide range of tools varying from spectroscopic- to imaging- to thermodynamic-based methods that are used for characterizing a biopharmaceutical. Generally, each tool provides a single straightforward piece of information such as concentration, percent aggregation, melting point, or hydrodynamic radius. By using all these measurements, a profile of a biopharmaceutical's chemical and physical attributes is generated. Two tools vital for characterizing a protein involve liquid chromatography (LC)-based, mass spectrometry (MS)-based, or combined LC-MS methods. MS and LC measurements provide an abundance of information about a protein such as its mass, heterogeneity, and present PTMs.

1.6 Liquid Chromatography Characterization

It is very rare for a biopharmaceutical to be produced as a single component but more often as a complex mixture with a variety of components. These complex mixtures are problematic for protein characterization due to analytical measurements generating convoluted responses from multicomponent samples. Fortuitously, there are methods which allow for not only purification but characterization of the therapeutic protein shrouded in these complex mixtures.

Liquid chromatography is a blanket term used to encompass a diverse group ofmethods that allow for the separation, identification, and quantitation of similar components in complex samples. Different types of chromatography separate proteins based on their size, polarity, and charge among other intrinsic properties. Chromatographic methods are extremely versatile and an important part of a protein characterization.

1.6.1 Size Exclusion Chromatography

Size exclusion chromatography (SEC) is unique because that molecules inside the column do not physically interact with the stationary phase unlike nearly all other types of chromatography. SEC separates molecules based on their hydrodynamic volume not their molecular weight as commonly confused (though it is generally a correct assumption that a larger molecular weight protein will have a larger hydrodynamic volume). Molecules are able be separated by their hydrodynamic volume by a porous silica bead stationary phase. If the molecule is small enough to enter these pores the time spent is dependent on the molecule's hydrodynamic volume. It is through this process of entering and exiting pores that molecules are separated from largest to smallest hydrodynamic volumes. An isocratic elution is used for SEC and the mobile phase can be an aqueous, salt-containing solution that mimics the ionic strength in the blood (~150mM). The purpose of the mobile phase is to preserve the structure of the protein in solution and to mask the stationary phase from non-specific interaction with molecules in solution. Eluting molecules are detected by UV/VIS absorbance (typically 280nm for aromatic amino acids) but fluorescent or light scattering detectors may also be used. If MS compatible solutions are used, a mass spectrometer can be used to further characterize eluting species.

SEC is useful in a variety of ways. One use is to assist with sample purification by separating the protein(s) of interest from a complex biological mixture of different sized proteins and molecules. Most commonly SEC is used to detect and estimate aggregation to ensure the quality of the protein sample. Aggregation of a biopharmaceutical is known to induce an immune response so it is vital to keep aggregation to a minimum.[48]

1.6.2 Reverse Phase Chromatography

Reverse phase chromatography utilizes a non-polar stationary phase to separate molecules based on their polarity. The stationary phase consists of a silica bead functionalized with C_4, C_8, or C_{18} alkyl chains. More polar molecules will elute first followed by less polar. Molecules are eluted with a mobile phase gradient that changes the mobile phase from a weak polar mobile phase (H_2O) to less polar (acetonitrile or methanol) mobile phase. An optimized gradient is extremely useful because it allows a large number of different analytes (i.*e.* proteolytic digest of a protein) to be separated in a single run. Due to the use of MS friendly solvents, a mass spectrometer can be used as a detector to help further measure eluting analytes.

Reverse phase chromatography is most commonly used to separate peptides from a proteolytic digest of a protein.[49] Most PTMs will affect the retention of the modified peptide, as compared to the unmodified peptide, allowing for separation. A mass spectrometer measures the mass of eluting peptides to identify its sequence and modifications that are presentZ. This is extremely useful when characterizing a protein as it allows a PTM to be identified and localized on a protein.

1.6.3 Ion Exchange Chromatography

Ion exchange chromatography utilizes a charged stationary phase (negative or positive) to separate analytes based on their charge. A cation exchange column has a negatively charged stationary phase with the column packing being functionalized with a carboxylic acid or sulfonic acid. An anion exchange column has a positively charged

stationary phase with the column packing functionalized with a primary or quaternary amine. The pI of the analyte and the pH of the mobile phase dictates which type of ion exchange column is used. Molecules are eluted with a mobile phase gradient where the pH is adjusted or the salt concentration is increased. If MS friendly solvents are used a mass spectrometer can be used to measure eluting analytes. Ion exchange chromatography is very powerful because of its ability to take advantage of the charge heterogeneity in protein samples.

1.6.4 Other Types of Chromatography

Polar compounds (*i.e.* glycans and some peptides) are weakly retained in reverse phase columns, eluting at or close to the void volume and are thus unable to be effectively separated. Hydrophilic interaction liquid chromatography (HILIC) offers an alternative to reverse phase chromatography for separation of polar samples.[50] Glycan characterization is an important part of drug discovery and HILIC is a great tool for separating glycan chains.[51] Additionaly, due to HILIC's use of MS-friendly solutions, eluting samples can be analyzed online via MS.

Affinity chromatography is generally used as a purification method to remove a biopolymer of interest from a complex solution but has some application as a characterization tool. A protein G, protein A and FcRn affinity column all can be used to detect and measure oxidation of a mAb in its Fc domain.[52-54] Oxidation of two conserved methionines (252,428) at the CH2-CH3 interface negatively affects the half-life of a mAb.[55] Therefore, it is vital to ensure there is not significant amount of a mAb oxidized at these methionines as it will affect the therapeutic efficacy of a mAb. Affinity

chromatography offers the unique ability to specifically target and separate a specific protein from a complex mixture.

1.7 Mass Spectrometry Characterization

Mass spectrometry (MS) is a powerful characterization tool that has experienced rapid growth in recent years due to both improved hardware and software. No other technique offers the ability to accurately and precisely measure the mass of a biopolymer. Electrospray ionization (ESI) MS and matrix assisted laser desorption ionization (MALDI) are soft ionization techniques that were a fundamental part to the rise of MS. Both ionization techniques can preserve covalent and non-covalent bonds during ionization with little to no induced fragmentation making them ideal for measuring biopolymers.

MS is an excellent tool for measuring the primary structure of a biopolymer. If the sequence of a biopolymer is known then a theoretical mass can be calculated and compared against the experimentally measured mass. This is an important part of protein identification and characterization since it confirms that the correct protein has been produced as well as providing an assessment of its quality and purity. Additionaly, PTMs can be identified by measuring mass shifts in comparison to an unmodified protein. While the presence or absence of a PTM is important information, the location of the PTM is just as significant. Tandem MS measurements localize PTMs on a protein by inducing fragmentation of a polypeptide backbone in the gas phase. Produced fragments are measured and provide more localized data of to identify the location of the PTM. Ideally this is performed at the whole protein level, known as top-down MS, but for proteins over 30 kDa[56] it becomes nearly impossible to achieve the necessary resolution for PTM

localization. For large proteins, a bottom-up or middle-down approach must be implemented that typically involve enzymatic digestion of a protein. Using a reverse phase column, digested protein fragments or peptides are separated and eluting molecules are measured by tandem MS. These measurements are indispensable for characterizing the primary structure and PTMs of a biopharmaceutical.

In addition to measuring the mass of a biopolymer to confirm its identity and associated PTMs, mass spectrometry is also used to for higher order structure measurements. Two methods, fast photochemical oxidation of proteins (FPOP) and hydrogen deuterium exchange (HDX), utilize covalent labeling to measure the higher order structure and dynamics of a protein in solution. FPOP covalently labels solvent exposed amino acid residues by oxidation with hydroxyl radicals produced by photolysis of H_2O_2.[57] Oxidation is detected by MS in a bottom-up or top-down approach depending on the complexity and size of the protein. HDX exchanges the backbone amide hydrogen of a protein with deuterium using a D_2O solution. Unprotected (*i.e.* not participating in a hydrogen bond) or solvent exposed amide hydrogens will quickly exchange with deuterium while protected regions will undergo a slower exchange. Mass shift from deuterium labeling are measured by MS, usually in a bottom-up approach. Both FPOP and HDX provide data about the structure and dynamics of a protein in solution by the distribution of their covalent labels. Changes to a protein's structure due to a PTM or solvent conditions can be measured to elucidate their effect to a protein's higher order structure. These measurements when combined with NMR or x-ray crystallography provide in depth information about a protein's conformation and dynamics in solution.

1.7.1 Native MS

Native MS is an excellent tool for studying a protein's higher order structure. Unlike traditional MS measurements, native MS utilizes near native solutions (150mM ammonium acetate) that preserve the native structure of a protein in solution. ESI MS, first used in the 1980s,[58] is a soft ionization technique that allows a protein remain folded during the ionization process.[59] The combination of a gentle ionization technique and a native solution allows for non-covalent interactions and protein complexes to be preserved for MS measurement. From these measurements, some structural information can be extracted based on the charge state distribution. Unlike traditional MS which uses solvents that denature a protein, native MS preserves the structure thus making it more compact in the gas phase. This more compact molecule carries less charge due to a decrease in available surface area for protonation and a narrower charge state distribution.[60] If a portion of the protein is unfolded in solution a bimodal charge state distribution will be observed indicating as both unfolded and folded species are present in solution. In the case of quaternary structures the measured mass can help identify components which make up the multimeric protein structure. Native MS is a valuable tool which allows the native fold of a protein to be preserved during measurement to provide structural and composition information.

1.8 Monoclonal Antibodies

Immuglobulins possess properties that make them excellent candidates as biopharmaceuticals. These properties include robustness to harsh conditions, a long half-life, a versatile mechanism of action, and possible immune system activation. An

immuglobulin is a heterodimeric protein composed of two light (L) and heavy (H) chains as shown in **Figure 1.1**. An immuglobulin is divided into two domains that are a fragment antigen binding (Fab) and fragment crystallizable (Fc) domain. As the name suggests, the Fab domain is responsible for binding its cognate target. The Fc domain is responsible for a mAb's effector functions that includes complement activation, antibody-dependent cellular cytotoxicity, antibody-dependent phagocytosis, degranulation, cytokine release, and inhibition of cell activities among other functions.[61,62] The majority of these effector functions are mediated through binding of Fc gamma receptors (FcγRs) present on immune system related cells. How the adaptive immune system responds to an antigen depends on the bound antibody and its associated effector functions.

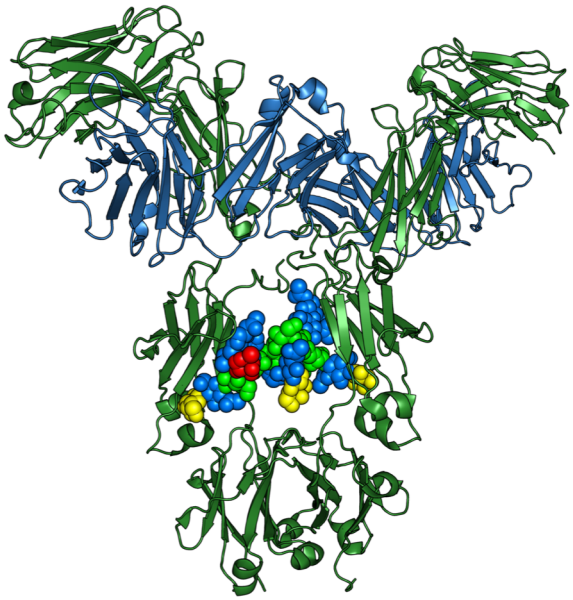

Figure 1.1 Two H (green) and L (blue) chains make up an immuglobulin. Colored spheres represent glycan chains.

There are five classes of immuglobulins IgA, IgD, IgE, IgG, and IgM that each serve unique functions inside the body. All currently approved clinical mAbs are based on the IgG template due it its favorable biological qualities.[63,64] IgG is glycosylated in its Fc domain on each of its H chains at Asn^{297}. Both glycan chains help provide structure to the Fc domain and the glycan composition is known to affect the effector functions of the IgG.[61,65-70]

While all therapeutic mAbs bind their target through the Fab domain, a mAb's specific mechanism of action is quite diverse and includes: drug delivery, target

neutralization, cell destruction, and imaging. Depending on the mechanism of action of a mAb the effector function needs to be tailored to ensure the correct *in vivo* response. One option to tailor the effector function of aa mAb is through its glycan chain.[62] For example, if the mechanism of action is cell destruction then an elevated antibody dependent cellular cytotoxicity would be beneficial. An afucosylated mAb is known to exhibit a much greater antibody dependent cellular cytotoxicity thus making it more effective at destroying its cellular target.[25] If the mAb is to be strictly a drug delivery vehicle or is being used for imaging, an immune response may be unnecessary or even detrimental to its target. Removal of the glycan chain offers an attractive option to abrogate a mAb's effector function[65,66] and thus preventing an immune response to its target. It is clear that all these factors need to be considered when producing the final product and necessitates proper characterization of these mAbs to elucidate their *in vivo* properties.

1.9 Transferrin

There are several plasma proteins, other than antibodies, that have biopharmaceutical potential. Transferrin (Tf) is an excellent candidate due to favorable *in vivo* qualities. The most important quality (in terms of its usefulness as a protein drug) of Tf is its ability to cross the blood brain barrier. Tf offers the ability to transport attached drugs to targets in the brain or central nervous system[71-73] Unlike a mAb which directly affects its target, Tf may act as a passive carrier for an attached drug. Additionally, quantitative information about the drug distribution can be measured by taking advantage of Tf's ability to bind metals other than iron (*i.e.* indium).[71] The ability for Tf to cross the

blood brain barrier and bind metals other than iron gives it great potential as a biopharmaceutical.

1.9.1 The Role of Transferrin in Iron Homeostasis

Tf is not only has potential as a biopharmaceutical but has an important biological role in the body as the iron transporter in the serum. Iron is the 4th most abundant element in the earth's crust[74] and is essential to almost every living organism due to its intrinsic redox properties. During the appearance of the first single cell organisms the Earth's atmosphere was composed of very little O_2.[75] The lack of atmospheric oxygen provided cells with an abundance of readily available Fe^{2+} thus establishing a foothold in biological processes.[75] As the Earth's atmosphere changed to high oxygen conditions iron became more scarce due to Fe^{3+} forming insoluble iron oxides. This necessitated that organisms to develop strategies to capture Fe^{3+} which is extremely insoluble (K_{sp} $1.6x10^{-39}$) in aqueous solutions. Furthermore, the same attractive redox properties of iron for biological processes makes them potentially dangerous. Fe^{2+} reduces O_2 and can lead to a hydroxyl radical which is extremely damaging to cells.[75] Additionaly, due to iron being a scarce essential resource for invading pathogens it is imperative to sequester iron as an immune system strategy. Iron must be tightly controlled to help prevent damage by free radicals or invading pathogens.

Tf is a key player in iron homeostasis inside the body. It is an 80kDa bilobal glycoprotein and the major iron transport protein inside the blood. Each lobe of Tf (**Figure 1.2**) is capable of binding Fe^{3+} tightly (Kd ~10^{22}) but reversibly.[76] Iron is coordinated by two tyrosines, one histidine, and one aspartic acid (Tyr95, Tyr188, Asp63, and His249 in

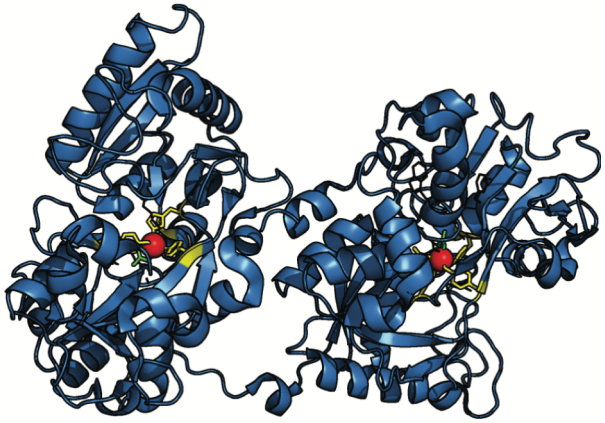

Figure 1.2 Diferric Tf with two irons (red) bound. PDB: 1HZH

the N-lobe and Tyr426, Tyr517, Asp392, and His585 in the C-lobe, respectively) in each lobe. A synergistic anion, usually carbonate, is required to complete iron binding in transferrin. However, oxalate can also coordinate with Fe in Tf and is known to prevent the release of Fe inside of cells. Iron is delivered to cells through Tf interacting with a Tf receptor to enter the cell. Once inside an endosome, the pH is lowered to assist with iron release after which the Tf-Tf receptor complex is returned to the cell surface.[76] Disruptions to the ability of Tf to bind and release iron is troublesome to iron homeostasis in the body.

1.10 Objectives

The complexity of biopharmaceuticals necessitates the need for robust analytical methods to characterize biopolymers and their PTMs. It is through PTMs that a protein's function is defined and allows for proteins to be adaptable with their function in the body. Careful measurements are needed to link the presence and amount of PTMs with a protein's *in vivo* function. LC- and MS-based methods are a valuable tool for characterizing biopharmaceuticals by providing a wealth of information about a protein's sequence, structure, and modifications. The work presented in the following chapters discuss the development of LC and MS methods to characterize proteins with biopharmaceutical value

(mAb and Tf). Specifically, the chapters discuss: *i.* development of a method to extract Tf from a clinical sample (serum) and utilizing native MS to determine its metal and synergistic anion composition, *ii.* Modification of a mAb's glycan chain and the effect on its biophysical properties and effector function and, *iii* development of a novel cross path reactive chromatography method for in column reduction or oxidation of disulfide-containing proteins.

1.11 References

1 Nielsen, J. Production of biopharmaceutical proteins by yeast: Advances through metabolic engineering. *Bioengineered* **4**, 207-211, doi:10.4161/bioe.22856 (2013).

2 Cornely, K. Biopharmaceuticals: Biochemistry and biotechnology, 2nd edition: Walsh, Gary, John Wiley & Sons. *Biochem. Mol. Biol. Educ.* **32**, 137-138, doi:10.1002/bmb.2004.494032029997 (2004).

3 Jackson, D. A., Symons, R. H. & Berg, P. Biochemical Method for Inserting New Genetic Information into DNA of Simian Virus 40: Circular SV40 DNA Molecules Containing Lambda Phage Genes and the Galactose Operon of Escherichia coli. *Proc. Natl. Acad. Sci. U. S. A.* **69**, 2904-2909 (1972).

4 Mertz, J. E. & Davis, R. W. Cleavage of DNA by R(1) Restriction Endonuclease Generates Cohesive Ends. *Proc. Natl. Acad. Sci. U. S. A.* **69**, 3370-3374 (1972).

5 Milstein, C. The hybridoma revolution: an offshoot of basic research. *Bioessays* **21**, 966-973 (1999).

6 Murphy, K., Travers, P., Walport, M. & Janeway, C. *Janeway's immunobiology*. (Garland Science, 2012).

7 Berkowitz, S. A. & J. Houde, D. in *Biophysical Characterization of Proteins in Developing Biopharmaceuticals* 1-21 (Elsevier, 2015).

8 Dumont, J., Euwart, D., Mei, B., Estes, S. & Kshirsagar, R. Human cell lines for biopharmaceutical manufacturing: history, status, and future perspectives. *Crit. Rev. Biotechnol.* **36**, 1110-1122, doi:10.3109/07388551.2015.1084266 (2016).

9 Estes, S. & Melville, M. Mammalian cell line developments in speed and efficiency. *Adv. Biochem. Eng. Biotechnol.* **139**, 11-33, doi:10.1007/10_2013_260 (2014).

10 Graumann, K. & Premstaller, A. Manufacturing of recombinant therapeutic proteins in microbial systems. *Biotechnol J* **1**, 164-186, doi:10.1002/biot.200500051 (2006).

11 Huang, C.-J., Lin, H. & Yang, X. Industrial production of recombinant therapeutics in Escherichia coli and its recent advancements. *J. Ind. Microbiol. Biotechnol.* **39**, 383-399, doi:10.1007/s10295-011-1082-9 (2012).

12 Ghaderi, D., Taylor, R. E., Padler-Karavani, V., Diaz, S. & Varki, A. Implications of the presence of N-glycolylneuraminic acid in recombinant therapeutic glycoproteins. *Nat. Biotechnol.* **28**, 863-867, doi:10.1038/nbt.1651 (2010).

13 Berkowitz, S. A., Engen, J. R., Mazzeo, J. R. & Jones, G. B. Analytical tools for characterizing biopharmaceuticals and the implications for biosimilars. *Nat Rev Drug Discov* **11**, 527-540 (2012).

14 Rathore, A. S. & Bhambure, R. Establishing analytical comparability for "biosimilars": filgrastim as a case study. *Anal. Bioanal. Chem.* **406**, 6569-6576, doi:10.1007/s00216-014-7887-4 (2014).

15 Walsh, G. Post-translational modifications of protein biopharmaceuticals. *Drug Discovery Today* **15**, 773-780, doi:http://dx.doi.org/10.1016/j.drudis.2010.06.009 (2010).

16 Wang, W., Singh, S., Zeng, D. L., King, K. & Nema, S. Antibody Structure, Instability, and Formulation. *J. Pharm. Sci.* **96**, 1-26, doi:http://dx.doi.org/10.1002/jps.20727 (2007).

17 Daugherty, A. L. & Mrsny, R. J. Formulation and delivery issues for monoclonal antibody therapeutics. *Advanced Drug Delivery Reviews* **58**, 686-706, doi:http://dx.doi.org/10.1016/j.addr.2006.03.011 (2006).

18 Maa, Y. F. & Hsu, C. C. Protein denaturation by combined effect of shear and air-liquid interface. *Biotechnol. Bioeng.* **54**, 503-512, doi:10.1002/(sici)1097-0290(19970620)54:6<503::aid-bit1>3.0.co;2-n (1997).

19 Kiese, S., Papppenberger, A., Friess, W. & Mahler, H. C. Shaken, not stirred: mechanical stress testing of an IgG1 antibody. *J. Pharm. Sci.* **97**, 4347-4366, doi:10.1002/jps.21328 (2008).

20 Mahajan, R., Templeton, A., Harman, A., Reed, R. A. & Chern, R. T. The Effect of Inert Atmospheric Packaging on Oxidative Degradation in Formulated Granules. *Pharm. Res.* **22**, 128-140, doi:10.1007/s11095-004-9018-y (2005).

21 Mann, M. & Jensen, O. N. Proteomic analysis of post-translational modifications. *Nat. Biotechnol.* **21**, 255-261, doi:10.1038/nbt0303-255 (2003).

22 Houde, D. J. & Berkowitz, S. A. in *Biophysical Characterization of Proteins in Developing Biopharmaceuticals* 23-47 (Elsevier, 2015).

23 Xu, C. & Ng, D. T. W. Glycosylation-directed quality control of protein folding. *Nat. Rev. Mol. Cell Biol.* **16**, 742-752, doi:10.1038/nrm4073 (2015).

24 SolÁ, R. J. & Griebenow, K. A. I. Effects of Glycosylation on the Stability of Protein Pharmaceuticals. *J. Pharm. Sci.* **98**, 1223-1245, doi:10.1002/jps.21504 (2009).

25 Shields, R. L. *et al.* Lack of fucose on human IgG1 N-linked oligosaccharide improves binding to human Fcgamma RIII and antibody-dependent cellular toxicity. *J. Biol. Chem.* **277**, 26733-26740, doi:10.1074/jbc.M202069200 (2002).

26 Raju, T. S. Terminal sugars of Fc glycans influence antibody effector functions of IgGs. *Curr. Opin. Immunol.* **20**, 471-478, doi:http://doi.org/10.1016/j.coi.2008.06.007 (2008).

27 Scallon, B. J., Tam, S. H., McCarthy, S. G., Cai, A. N. & Raju, T. S. Higher levels of sialylated Fc glycans in immunoglobulin G molecules can adversely impact functionality. *Mol. Immunol.* **44**, 1524-1534, doi:10.1016/j.molimm.2006.09.005 (2007).

28 Liu, L. Antibody glycosylation and its impact on the pharmacokinetics and pharmacodynamics of monoclonal antibodies and Fc-fusion proteins. *J. Pharm. Sci.* **104**, 1866-1884, doi:10.1002/jps.24444 (2015).

29 Anthony, R. M. & Ravetch, J. V. A Novel Role for the IgG Fc Glycan: The Anti-inflammatory Activity of Sialylated IgG Fcs. *J. Clin. Immunol.* **30**, 9-14, doi:10.1007/s10875-010-9405-6 (2010).

30 Reslan, L., Dalle, S. & Dumontet, C. Understanding and circumventing resistance to anticancer monoclonal antibodies. *mAbs* **1**, 222-229 (2009).

31 Varki, A. *Essentials of glycobiology*. (Cold Spring Harbor Laboratory Press, 2009).

32 Siegel, G. J. & Agranoff, B. W. *Basic Neurochemistry: Molecular, Cellular, and Medical Aspects*. (Lippincott Williams & Wilkins, 1999).

33 Dunlop, R. A., Brunk, U. T. & Rodgers, K. J. Oxidized proteins: mechanisms of removal and consequences of accumulation. *IUBMB Life* **61**, 522-527, doi:10.1002/iub.189 (2009).

34 Yan, B., Yates, Z., Balland, A. & Kleemann, G. R. Human IgG1 hinge fragmentation as the result of H2O2-mediated radical cleavage. *J. Biol. Chem.* **284**, 35390-35402, doi:10.1074/jbc.M109.064147 (2009).

35 Ratanji, K. D., Derrick, J. P., Dearman, R. J. & Kimber, I. Immunogenicity of therapeutic proteins: Influence of aggregation. *J. Immunotoxicol.* **11**, 99-109, doi:10.3109/1547691X.2013.821564 (2014).

36 Mulinacci, F., Poirier, E., Capelle, M. A. H., Gurny, R. & Arvinte, T. Influence of methionine oxidation on the aggregation of recombinant human growth hormone. *Eur. J. Pharm. Biopharm.* **85**, 42-52, doi:http://doi.org/10.1016/j.ejpb.2013.03.015 (2013).

37 Kim, Y. H., Berry, A. H., Spencer, D. S. & Stites, W. E. Comparing the effect on protein stability of methionine oxidation versus mutagenesis: steps toward engineering oxidative resistance in proteins. *Protein Eng.* **14**, 343-347 (2001).

38 Robinson, N. E. & Robinson, A. B. Molecular clocks. *Proc. Natl. Acad. Sci. U. S. A.* **98**, 944-949, doi:10.1073/pnas.98.3.944 (2001).

39 Mastrangeli, R. *et al.* Biological Functions of Interferon beta-1a Are Enhanced By Deamidation. *J. Interferon Cytokine Res.* **36**, 534-541, doi:10.1089/jir.2016.0025 (2016).

40 Phillips, J. J. *et al.* Rate of Asparagine Deamidation in a Monoclonal Antibody Correlating with Hydrogen Exchange Rate at Adjacent Downstream Residues. *Anal. Chem.* **89**, 2361-2368, doi:10.1021/acs.analchem.6b04158 (2017).

41 Zavodszky, M. *et al.* Disulfide bond effects on protein stability: Designed variants of Cucurbita maxima trypsin inhibitor-V. *Protein Science : A Publication of the Protein Society* **10**, 149-160 (2001).

42 Yang, M., Dutta, C. & Tiwari, A. Disulfide-Bond Scrambling Promotes Amorphous Aggregates in Lysozyme and Bovine Serum Albumin. *The Journal of Physical Chemistry B* **119**, 3969-3981, doi:10.1021/acs.jpcb.5b00144 (2015).

43 Gu, S. *et al.* Characterization of trisulfide modification in antibodies. *Anal. Biochem.* **400**, 89-98, doi:10.1016/j.ab.2010.01.019 (2010).

44 Wei, B., Berning, K., Quan, C. & Zhang, Y. T. Glycation of antibodies: Modification, methods and potential effects on biological functions. *MAbs* **9**, 586-594, doi:10.1080/19420862.2017.1300214 (2017).

45 Dozier, J. K. & Distefano, M. D. Site-Specific PEGylation of Therapeutic Proteins. *Int. J. Mol. Sci.* **16**, 25831-25864, doi:10.3390/ijms161025831 (2015).

46 Dyachenko, A. *et al.* Tandem Native Mass-Spectrometry on Antibody–Drug Conjugates and Submillion Da Antibody–Antigen Protein Assemblies on an Orbitrap EMR Equipped with a High-Mass Quadrupole Mass Selector. *Anal. Chem.* **87**, 6095-6102, doi:10.1021/acs.analchem.5b00788 (2015).

47 Schiestl, M. *et al.* Acceptable changes in quality attributes of glycosylated biopharmaceuticals. *Nat Biotech* **29**, 310-312, doi:http://www.nature.com/nbt/journal/v29/n4/abs/nbt.1839.html - supplementary-information (2011).

48 Ratanji, K. D., Derrick, J. P., Dearman, R. J. & Kimber, I. Immunogenicity of therapeutic proteins: influence of aggregation. *J. Immunotoxicol.* **11**, 99-109, doi:10.3109/1547691x.2013.821564 (2014).

49 Krokhin, O. Peptide retention prediction in reversed-phase chromatography: proteomic applications. *Expert Review of Proteomics* **9**, 1-4, doi:10.1586/epr.11.79 (2012).

50 Jandera, P. Stationary and mobile phases in hydrophilic interaction chromatography: a review. *Anal. Chim. Acta* **692**, 1-25, doi:10.1016/j.aca.2011.02.047 (2011).

51 Strege, M. A. Hydrophilic Interaction Chromatography−Electrospray Mass Spectrometry Analysis of Polar Compounds for Natural Product Drug Discovery. *Anal. Chem.* **70**, 2439-2445, doi:10.1021/ac9802271 (1998).

52 Gaza-Bulseco, G., Faldu, S., Hurkmans, K., Chumsae, C. & Liu, H. Effect of methionine oxidation of a recombinant monoclonal antibody on the binding affinity to protein A and protein G. *Journal of Chromatography B* **870**, 55-62, doi:http://dx.doi.org/10.1016/j.jchromb.2008.05.045 (2008).

53 Wang, W. *et al.* Impact of methionine oxidation in human IgG1 Fc on serum half-life of monoclonal antibodies. *Mol. Immunol.* **48**, 860-866, doi:10.1016/j.molimm.2010.12.009 (2011).

54 Schlothauer, T. *et al.* Analytical FcRn affinity chromatography for functional characterization of monoclonal antibodies. *MAbs* **5**, 576-586, doi:10.4161/mabs.24981 (2013).

55 Gao, X. *et al.* Effect of individual Fc methionine oxidation on FcRn binding: Met252 oxidation impairs FcRn binding more profoundly than Met428 oxidation. *J. Pharm. Sci.* **104**, 368-377, doi:10.1002/jps.24136 (2015).

56 Pan, J., Zhang, S., Chou, A. & Borchers, C. H. Higher-order structural interrogation of antibodies using middle-down hydrogen/deuterium exchange mass spectrometry. *Chemical Science* **7**, 1480-1486, doi:10.1039/C5SC03420E (2016).

57 Gau, B. C., Sharp, J. S., Rempel, D. L. & Gross, M. L. Fast Photochemical Oxidation of Proteins Footprints Faster than Protein Unfolding. *Anal. Chem.* **81**, 6563-6571, doi:10.1021/ac901054w (2009).

58 Kaltashov, I. A. & Eyles, S. J. *Mass spectrometry in biophysics : conformation and dynamics of biomolecules*. (Hoboken, N.J. : John Wiley, 2005., 2005).

59 Heck, A. J. Native mass spectrometry: a bridge between interactomics and structural biology. *Nat Methods* **5**, 927-933, doi:10.1038/nmeth.1265 (2008).

60 Konermann, L. & Douglas, D. J. Acid-Induced Unfolding of Cytochrome c at Different Methanol Concentrations: Electrospray Ionization Mass Spectrometry Specifically Monitors Changes in the Tertiary Structure. *Biochemistry* **36**, 12296-12302, doi:10.1021/bi971266u (1997).

61 Vidarsson, G., Dekkers, G. & Rispens, T. IgG subclasses and allotypes: from structure to effector functions. *Front. Immunol.* **5**, 520, doi:10.3389/fimmu.2014.00520 (2014).

62 Kapur, R., Einarsdottir, H. K. & Vidarsson, G. IgG-effector functions: "The Good, The Bad and The Ugly". *Immunol. Lett.* **160**, 139-144, doi:http://dx.doi.org/10.1016/j.imlet.2014.01.015 (2014).

63 Jefferis, R. Isotype and glycoform selection for antibody therapeutics. *Arch. Biochem. Biophys.* **526**, 159-166, doi:http://dx.doi.org/10.1016/j.abb.2012.03.021 (2012).

64 Irani, V. *et al.* Molecular properties of human IgG subclasses and their implications for designing therapeutic monoclonal antibodies against infectious diseases. *Mol. Immunol.* **67**, 171-182, doi:http://dx.doi.org/10.1016/j.molimm.2015.03.255 (2015).

65 Yamaguchi, Y. *et al.* Glycoform-dependent conformational alteration of the Fc region of human immunoglobulin G1 as revealed by NMR spectroscopy. *Biochimica et Biophysica Acta (BBA) - General Subjects* **1760**, 693-700, doi:http://doi.org/10.1016/j.bbagen.2005.10.002 (2006).

66 Krapp, S., Mimura, Y., Jefferis, R., Huber, R. & Sondermann, P. Structural analysis of human IgG-Fc glycoforms reveals a correlation between glycosylation and structural integrity. *J. Mol. Biol.* **325**, 979-989 (2003).

67 Scallon, B. J., Tam, S. H., McCarthy, S. G., Cai, A. N. & Raju, T. S. Higher levels of sialylated Fc glycans in immunoglobulin G molecules can adversely impact functionality. *Molecular Immunology* **44**, 1524-1534, doi:http://dx.doi.org/10.1016/j.molimm.2006.09.005 (2007).

68 Anthony, R. M. & Ravetch, J. V. A novel role for the IgG Fc glycan: the anti-inflammatory activity of sialylated IgG Fcs. *Journal of clinical immunology* **30 Suppl 1**, S9-14, doi:10.1007/s10875-010-9405-6 (2010).

69 Crispin, M., Yu, X. & Bowden, T. A. Crystal structure of sialylated IgG Fc: Implications for the mechanism of intravenous immunoglobulin therapy. *Proc. Natl. Acad. Sci. U. S. A.* **110**, E3544-E3546, doi:10.1073/pnas.1310657110 (2013).

70 Anthony, R. M. *et al.* Recapitulation of IVIG anti-inflammatory activity with a recombinant IgG Fc. *Science* **320**, 373-376, doi:10.1126/science.1154315 (2008).

71 Zhao, H., Wang, S., Nguyen, S. N., Elci, S. G. & Kaltashov, I. A. Evaluation of Nonferrous Metals as Potential In Vivo Tracers of Transferrin-Based Therapeutics. *J. Am. Soc. Mass Spectrom.* **27**, 211-219, doi:10.1007/s13361-015-1267-y (2016).

72 Kaltashov, I. A., Bobst, C. E., Nguyen, S. N. & Wang, S. Emerging mass spectrometry-based approaches to probe protein-receptor interactions: focus on overcoming physiological barriers. *Adv Drug Deliv Rev* **65**, 1020-1030, doi:10.1016/j.addr.2013.04.014 (2013).

73 Nguyen, S. N., Bobst, C. E. & Kaltashov, I. A. Mass Spectrometry-Guided Optimization and Characterization of a Biologically Active Transferrin–Lysozyme Model Drug Conjugate. *Mol. Pharm.*, doi:10.1021/mp400026y (2013).

74 Lutgens, F. K. & Tarbuck, E. J. *Essentials of geology*. (Boston : Pearson, [2015] Twelfth edition., 2015).

75 Lutsenko, S. & Argüello, J. M. *Metal transporters. [electronic resource]*. (San Diego : Elsevier Science, 2012., 2012).

76 Luck, A. N., Bobst, C. E., Kaltashov, I. A. & Mason, A. B. Human serum transferrin: is there a link among autism, high oxalate levels, and iron deficiency anemia? *Biochemistry* **52**, 8333-8341, doi:10.1021/bi401190m (2013).

CHAPTER 2

ASSESSING THE IRON DELIVERY EFFICACY OF TRANSFERRIN IN CLINICAL SAMPLES BY NATIVE ELECTROSPRAY IONIZATION MASS SPECTROMETRY

This chapter has been adapted from a paper published as: Pawlowski, J. W., Kellicker, N., Bobst, C. E. & Kaltashov, I. A. Assessing the iron delivery efficacy of transferrin in clinical samples by native electrospray ionization mass spectrometry. *Analyst* **141**, 853-861, doi:10.1039/C5AN02159F (2016).

2.1 Abstract

Serum transferrin is a key player in iron homeostasis, and its ability to deliver iron to cells via the endosomal pathway critically depends on the presence of carbonate that binds this protein synergistically with ferric ion. Oxalate is another ubiquitous anionic species that can act as a synergistic anion, and in fact its interaction with transferrin is notably stronger compared to carbonate, preventing the protein from releasing the metal in the endosomal environment. While this raises concerns that high oxalate levels in plasma may interfere with iron delivery to tissues, concentration of free oxalate in blood appears to be a poor predictor of impeded availability of iron, as previous studies showed that it cannot displace carbonate from ferro-transferrin on a physiologically relevant time scale under the conditions mimicking plasma. In this work we present a new method that allows different forms of ferro-transferrin (carbonate- vs oxalate-bound) to be distinguished from each other by removing this protein from plasma without altering the composition of the protein/metal/synergistic anion complexes, and determining their accurate masses using native electrospray ionization mass spectrometry (ESI MS). The new method has been

validated using a mixture of recombinant proteins, followed by its application to the analysis of clinical samples of human plasma, demonstrating that native ESI MS can be used in clinical analysis.

2.2 Introduction

Iron is an essential element that is required for nearly all living organisms. There are 3-5 grams of iron present in a healthy adult body with over 2 grams found in hemoglobin of erythrocytes.[152] Despite the attention paid in the field of nutraceuticals to iron dietary supplements, the majority of iron circulating in plasma is actually recycled from reticuloendothelial macrophages through the degradation of erythrocytes as well as other cells.[212] Although it is one of the most abundant elements in the Earth's crust, iron bioavailability is limited due to the extremely low solubility of the ferric ion (Fe^{3+}, the predominant form under aerobic conditions), forcing all living organisms to devise various strategies to solubilize this element. In vertebrates, this problem is solved using proteins that bind iron tightly while in circulation and release it in cells via receptor-mediated endocytosis.[85,123] Human serum transferrin (Tf), a protein intimately involved in iron homeostasis, transports iron to cells that need this metal and express the Tf receptor on their surface; meanwhile, Tf sequesters iron from pathogens that also require this element for growth and proliferation.

Tf is an 80 kDa bilobal glycoprotein, with each lobe capable of binding Fe^{3+} strongly ($K_d \sim 10^{22}$) but reversibly at physiological pH (7.4).[120] Following its association with the Tf receptor at the cell surface, Tf is internalized and releases iron under the mildly acidic conditions of the endosome, before being recycled back to the cell surface and released to

circulation for another cycle of iron acquisition and delivery.[2] An intriguing feature of Tf (shared across the entire family of Tf-related proteins, including lactoferrin and ovotransferrin) is the presence of a synergistic anion (typically carbonate, CO_3^{2-}) in the Fe^{3+}/Tf complex, which is required to complete the metal's coordination sphere[124] (see Supplementary Material for more detail). Oxalate ($C_2O_4^{2-}$) is another ubiquitous anionic species capable of acting as a synergistic anion.[65] While its concentration in serum (10-30 μM[26]) is significantly lower compared to the total pool of carbonate (20-30 mM[26]), it has significantly higher Tf affinity.[175]

The documented ability of oxalate to prevent iron release from Tf under endosomal conditions[67] has led to concerns that it may interfere with iron trafficking by inhibiting its release from Tf inside the endosome and, therefore, deprive cells of this essential nutrient even though there is no iron deficiency in the diet or circulation. Under these circumstances the clinical symptoms of anaemia would not correlate with the results of laboratory testing, which commonly relies on total iron and protein-bound iron as the biomarkers. While anaemia is involved in the etiology of a range of pathologies,[117] iron deficiency is particularly devastating for the function of the central nervous system, adversely affecting *inter alia* sleep, attention, and cognitive development.[103,149,183] In the past decade several studies have reported an increased prevalence of iron deficiency in autistic children,[20,40,41] suggesting the involvement of anaemia in the etiology of autism spectrum disorders, although more recent studies failed to confirm this correlation.[164]

One possible explanation for the lack of an obvious correlation between iron status and the occurrence/severity of autism is based on a recent observation by Konstantynowicz *et al*. of a three-fold greater plasma oxalate levels in autistic children compared to their

symptom-free peers.[104] Oxalate replacing Tf-bound carbonate is likely to disturb iron homeostasis by inhibiting metal release in the endosome (**Figure 2.1**). However, Mason *et al*. have pointed out that the serum level of oxalate could be a poor predictor of the disturbed iron homeostasis, as this anion fails to displace carbonate from transferrin on a physiologically relevant time scale in solution that has the same pH and ionic strength as blood serum.[120] While it is possible that oxalate may easily out-compete carbonate during the iron loading of transferrin, especially under mildly acidic conditions, the molecular mechanisms of iron loading remain a subject of debate, and it remains unclear if there is correlation between serum oxalate levels and the presence of oxalate as a synergistic anion in circulating Fe_2Tf.

Clearly, a meaningful diagnostic test in this case should specifically focus on the relative amounts of oxalate and carbonate bound to Tf (rather than on the total oxalate concentration in the plasma). Together with the total amount of Tf-bound iron, this number should provide a true measure of Tf potency *vis-a-vis* iron delivery to cells. While the existing analytical protocols cannot accomplish this task, native electrospray ionization mass spectrometry (ESI MS) has been shown in the past to be a powerful tool capable of determining the composition of the protein/metal complexes.[65,145,221,225] However, such measurements are always carried out *in vitro* using solvent systems compatible with the ESI process; to the best of our knowledge, no reports have been published on applying native ESI MS to characterize metalloproteins in clinical samples. Another complication arises from the very small difference between the two synergistic anions (28 Da, which is less than 0.04% of the mass of Tf). Although modern mass spectrometry allows even smaller mass differences to be measured for polypeptide ions, these measurements are

typically carried out under denaturing conditions; the gentle nature of native ESI MS typically results in formation of multiple adducts, leading to ion peak broadening and making high-resolution and high-accuracy mass measurements extremely challenging.[118] In this work we present a new method for the analysis of clinical blood samples that allows the composition of the endogenous ternary complexes $(Fe{\cdot}CO_3^{2-}/C_2O_4^{2-})_2$Tf to be probed using a combination of size exclusion and albumin-depletion chromatographic separations and native ESI MS detection. The new method is tested with a mixture of recombinant proteins of known $CO_3^{2-}/C_2O_4^{2-}$ composition and then applied to clinical samples. The technique is ready to be used in clinical studies, to search for a correlation between autism and iron deprivation caused by Tf-bound oxalate.

2.3 Experimental

Materials. Recombinant human Tf used in this work was a generous gift from Prof. Anne B. Mason (University of Vermont College of Medicine, Burlington, VT, USA), and the glycosylated form of human Tf was purchased from Sigma-Aldrich Chemical Company (St. Louis, MO, USA). Clinical samples of human serum from anonymous volunteers were provided by Prof. Barry Braun (University of Massachusetts-Amherst, Department of Kinesiology). Amicon Ultracel membrane microconcentrator devices (10 kDa molecular weight cut-off) were purchased from EMD Millipore (Billerica, MA, USA). Cibacron F3GA resin was purchased from Pall Corporation (Westborough, MA, USA). Oxalate, EDTA, ammonium acetate, and formic acid were purchased from Sigma-Aldrich Chemical Company (St. Louis, MO, USA); all other solvents and buffers were of analytical grade or higher.

Preparation of Tf Standards. The apo- (iron-free) form of Tf was prepared by lowering the pH of Tf solution in 150 mM ammonium acetate to 4.5, followed by addition of EDTA (to a final concentration of 10 mM). This solution was incubated at room temperature for an hour, and then buffer exchanged repeatedly to a 150 mM ammonium acetate solution containing 10 mM EDTA with pH adjusted to 5.5 using a microconcentrator. During the final step the Tf solution was buffer exchanged to 150 mM ammonium acetate with pH adjusted to 6.8. The complete removal of both metal and synergistic anion from the protein was verified by native ESI MS (*vide infra*). The oxalate-bound form of holo-Tf, $(Fe^{3+}\cdot C_2O_4^{2-})_2$Tf, was prepared by adding oxalic acid to the holo-Tf solution (dissolved in 150 mM ammonium acetate) to a final concentration of 10 mM followed by adjusting the pH down to 5.0 with acetic acid and one-hour incubation at room temperature prior to raising the pH back up to 6.8 with ammonium hydroxide. Excess of carbonate, bicarbonate and oxalate was removed from the protein solution by repeated buffer-exchange to 150mM ammonium acetate (pH 6.8). The composition of the protein/metal/synergistic anion complex in the final solution was confirmed as $(Fe^{3+}\cdot C_2O_4^{2-})_2$Tf by native ESI MS (*vide infra*).

Tf Purification from Clinical Samples. Tf was extracted from the clinical serum samples using a two-dimensional chromatography comprising size exclusion chromatography (SEC) and affinity chromatography (albumin depletion). Briefly, a 125 μL aliquot of unprocessed serum was injected onto a Superose 12 SEC column using a 150 mM solution of ammonium acetate (pH 6.8) as a mobile phase and a 0.45 mL/min flow rate. Absorption at 470 nm was used to identify eluting Tf. Multiple injections were used to collect Tf-containing fractions, which were subsequently pooled. Removal of serum

albumin from these pooled fractions was carried out using a home-made gravity-driven affinity column packed with Cibacron F3GA resin (BDR). A step gradient was used to allow hTf to be eluted from the column while retaining HSA. Three buffers were used for the step gradient: a no-salt buffer (pH 6.8, 150 mM ammonium acetate), a low salt buffer (pH 6.8, 0.25 M NaCl, 150 mM ammonium acetate), and a high salt buffer (pH 6.8, 2 M NaCl, 150 mM ammonium acetate). All holo-Tf eluted during the no-salt step, which was collected and buffer-exchanged to 150 mM ammonium acetate (pH 6.8) using a microconcentrator (*vide supra*).

Native ESI MS Analyses. All mass spectral data were acquired with a SolariX 7T Fourier transform ion cyclotron resonance (FT ICR) mass spectrometer (Bruker Daltonics, Billerica, MA, USA). All samples were directly infused at a flow rate of 3 μL/min. A 4500 V capillary voltage was used for all measurements. The dry gas was set to a flow of 4.6 L/min and a temperature of 200^{o}C. Each measurement had a 0.52 second transient time and a 32,000-point time-domain. All spectra were acquired in a 3,500-5,000 m/z range with 400 scans were averaged for each measurement to achieve adequate signal-to-noise ratio. The ESI source parameters were adjusted to minimize collisional activation in the ESI interface region in order to preserve the integrity of the protein/metal/synergistic anion complexes. Reference mass spectra of metal- and synergistic anion-free protein for each sample were acquired by lowering the pH of the protein solution to 3.7. Data analysis was performed using Compass Data Analysis software (Bruker Daltonics). Generally, the m/z value was assigned for each Tf charge state peak observed. Mass shifts were calculated by subtracting m/z values, of the same charge state, and multiplying the difference by the charge state. Experimentally determined mass shifts were compared to expected calculated

values in order to assign the synergistic anion and metal composition (an example of using this procedure is shown in Supplementary Material).

2.4 Results and Discussion

The unequivocal proof that oxalate does disturb iron homeostasis in a specific patient can only be provided by measuring the fraction of Tf molecules in circulation in which carbonate is replaced with oxalate. Existing methods that measure plasma oxalate do not provide such information; however, the ligand composition of Tf/metal complexes can be probed by native ESI MS *in vitro*.[221] In the past, we used this technique to determine the presence of oxalate as a synergistic ion in a fragment of Tf molecule (its N-lobe),[65] but the subsequent attempts to extend this method to the full-length protein produced mixed results, as the broad shape of the mass spectral peaks typical of native ESI MS prevented us from being able to make unequivocal assignments, while collisional desolvation led to facile dissociation of the synergistic anion form the protein prior to the mass measurement.[66,225] Another problem related to the use of native ESI MS for the analysis of a clinical sample is the presence of significant amounts of strong electrolytes (*e.g.*, NaCl), which are incompatible with the ESI process and must be removed/replaced with volatile electrolytes (*e.g.*, $CH_3CO_2NH_4$) during the sample preparation step. The problem here lies with the possibility of altering the composition of the Tf/metal/synergistic anion complexes prior to MS analysis, which would obviously render the results of the testing meaningless.

In order to circumvent these problems, we initially worked with recombinant and commercially available protein molecules to explore the utility of thermal desolvation as a tool capable of removing non-specific adducts from the Tf/metal/synergistic anion

complexes in the ESI interface without altering their composition. This was followed by designing a protocol of Tf extraction from clinical samples and placing them in "ESI-friendly" solutions without altering the composition of the Tf/metal/synergistic anion complexes. The absence of any alteration of these complexes' make-up (either due to loss/exchange of synergistic anions or due to a bias introduced by the procedure that would preferentially extract one particular form of the protein at the expense of others) was verified using a mixture of $(Fe^{3+}\cdot CO_3^{2-})_2\cdot Tf$, $(Fe^{3+}\cdot CO_3^{2-})\cdot(Fe^{3+}\cdot C_2O_4^{2-})\cdot Tf$ and $(Fe^{3+}\cdot C_2O_4^{2-})_2Tf$ complexes that were prepared using recombinant human Tf. Finally, the procedure was applied to test several anonymized blood samples for the presence of oxalate bound to serum Tf. Intriguingly, while most of the analyzed samples contained only carbonate-bound Tf, one contained $(Fe^{3+}\cdot C_2O_4^{2-})_2Tf$ as a major component with a mixed complex $(Fe^{3+}\cdot CO_3^{2-})\cdot(Fe^{3+}\cdot C_2O_4^{2-})\cdot Tf$ also present (no $(Fe^{3+}\cdot CO_3^{2-})_2\cdot Tf$ signal was detected in this anomalous sample).

Native ESI MS can make a distinction between the carbonate- and oxalate-bound forms of Fe_2Tf. The mass difference between carbonate and oxalate dianions is 28 Da; this number dictates the minimal level of precision that must be attained in the protein mass measurements in order for the meaningful analysis of the composition of serum transferrin to be carried out. The ability to resolve a mass difference of 28 Da would allow a distinction to be made *e.g*. between a mixed complex $(Fe^{3+}\cdot CO_3^{2-})\cdot(Fe^{3+}\cdot C_2O_4^{2-})Tf$ and the carbonate-bound form $(Fe^{3+}\cdot CO_3^{2-})_2\cdot Tf$). Although this mass difference corresponds to < 0.04% of the total protein mass, the resolving power of many modern MS instruments allows such measurements to be readily made. One complication that arises in our particular case is that such measurements must be carried out under the so-called native conditions, which

presents two challenges. First, protein ions accumulate relatively low number of charges in native ESI MS, giving rise to the ionic signal in the high m/z range (> 3,500 for Tf[94]), where most instruments typically have sub-optimal resolution. Second, the gentle nature of native ESI MS results in production of multiple adducts, leading to broadening of ion peaks in mass spectra, which affects both the accuracy of the mass measurements and the ability to resolve closely spaced ion peaks. While mild collisional activation of ions representing protein complexes frequently enhances the ionic peak shapes (via adduct dissociation), it also leads to partial dissociation of non-covalent assemblies in the gas phase.[63,111] In the case of Tf, it results in facile removal of the synergistic anion from the protein,[65,66] which obviously invalidates the measurements aimed at determining the composition of Tf/ferric ion/synergistic anion complexes.

Recently we reported that such complexes exhibit surprising stability when subjected to thermal desolvation, even though the adduct ions dissociate readily, allowing high mass accuracy measurements to be made.[120] **Figure 2.2** shows native ESI mass spectra of recombinant human Tf reconstituted with carbonate and oxalate, where both carbonate- and oxalate-bound forms of Tf can be readily identified based on their masses. The identification becomes particularly straightforward when the ligand composition of the complex is determined based on the mass difference between the complex ion and the apo-Tf ion (228.8 Da and 287.2 Da for the peaks shown in **Figure 2.2**); the theoretical mass differences are 229.7 Da for the carbonate-bound form (calculated as a mass of $2Fe^{3+} + 2CO_3^{2-} - 2H^+$) and 285.8 Da ($2Fe^{3+} + 2\ C_2O_4^{2-} - 2H^+$) for the oxalate-bound Tf.

Extraction of Tf from serum for the synergistic anion analysis. Although native MS with thermal ion desolvation in the ESI interface does allow the distinction to be made

between the carbonate- and oxalate-bound Tf, it is important to remember that the mass spectra shown in **Figure 2.2** were acquired using a sample prepared with volatile electrolytes (ammonium acetate). Direct analysis of a serum sample by ESI MS generates abundant, but unresolved (and, therefore, analytically meaningless) ion signal due to the presence of (*i*) multiple protein species and (*ii*) non-volatile electrolytes leading to facile cluster ion and adduct ion formation. To circumvent this problem, we ran the serum sample through a size exclusion column using an "electrospray-friendly" solvent system (150 mM ammonium acetate) whose ionic strength and pH are close to those of serum. While the protein signal spans over a significant time range (**Figure 2.3**), only three chromatographic bands showed strong absorbance at 470 nm (characteristic of the holo-form of Tf). The elution time of the second band (9 min) was consistent with the molecular weight of Tf; indeed, when this fraction was collected and analyzed by MS, Tf could be readily detected (see inset in **Figure 2.3**). Unfortunately, this fraction also contained a significant amount of albumin, whose molecular weight is close to that of Tf, but abundance in serum is an order of magnitude higher. Ionic peaks representing these two proteins had significant overlap, which made accurate mass measurement of Tf ions (and identification of the synergistic anion) very challenging. Albumin depletion is a common task in blood proteomic analyses, and is usually accomplished by running the sample through an affinity column containing antibodies to the fourteen most abundant plasma proteins.[79] Unfortunately, Tf is one of the proteins depleted using these commercial kits, making it necessary to seek alternative ways of albumin depletion. We accomplished this using blue dye resin (BDR), which has a high affinity to albumin.[187] Injecting the Tf/albumin containing SEC fraction through the BDR column allowed holo-Tf to elute at low ionic

strength while albumin was retained and could only be eluted under high salt conditions. Ammonium acetate was used as a salt in the affinity separation (or, more correctly, depletion) step, allowing all eluting fractions to be analyzed by native ESI MS without additional sample work-up.

The combination of SEC fractionation with albumin depletion produces a serum Tf sample suitable for the analysis of its composition *vis-a-vis* the synergistic anion by native ESI MS; however, it also introduces the possibility that the ratio of carbonate- vs. oxalate-bound forms of Tf is altered prior to MS analyses. This can occur through two possible mechanisms. First, it is not inconceivable that the recoveries of the two forms of Tf could be different from each other; in this case, the extraction procedure would introduce a bias. Second, both apo-Tf and mono-ferric Tf may acquire iron during the extraction and albumin depletion steps if the metal is present in the soluble form *e.g.* in BDR. Should this occur, a bias would be introduced favouring the carbonated form of holo-Tf (although neither oxalate nor carbonate salts were used in preparation of solvents used for protein extraction and albumin depletion, ambient CO_2 is likely to contribute to formation of carbonate in solution which can be utilized as a synergistic anion by Tf upon metal binding). In order to prove that no bias is introduced prior to the MS measurements by either the SEC fractionation or the albumin depletion step, a mixture of the three forms of diferric Tf (carbonate-bound form, $(Fe^{3+}\cdot CO_3^{2-})_2\cdot Tf$; the oxalate-bound form, $(Fe^{3+}\cdot C_2O_4^{2-})_2\cdot Tf$; and the mixed form $(Fe^{3+}\cdot CO_3^{2-})\cdot(Fe^{3+}\cdot C_2O_4^{2-})\cdot Tf$) was prepared and subjected to the established Tf extraction workflow prior to native ESI MS (**Figure 2.4**). Comparison of the protein peak profiles in each case before and after the procedure provided unequivocal evidence that no detectable bias is introduced by either the SEC fractionation

or the albumin depletion step. Additionally, the apo-form of Tf was tested for its ability to scavenge for iron (which could conceivably be present in either SEC or BDR columns due to contamination or carry-over) during either of the two sample preparation steps. Once again, the result of this study was negative, as neither step lead to detectable acquisition of iron by the metal-free form of the protein (**Figure 2.5**).

Synergistic anions bound to endogenous Tf in human blood: analysis of clinical samples. Once the procedure for Tf extraction from serum followed by identification and quantitation of synergistic anions had been validated, it was applied to the analysis of clinical samples. One significant difference between the recombinant proteins discussed above and endogenous Tf encountered in plasma is that the protein mass of the latter may differ from the mass based on the published wild-type sequence and glycosylation pattern. Tf glycosylation is known to be affected by several disorders (with alcoholism being perhaps the best known,[11] but certainly not the only example).[231] Glycosylation is an enzymatic post-translational modification (PTM) that generally leads to heterogeneous protein populations. Tf is rather unusual in that regard, as it exhibits surprising level of homogeneity with over 80% of all protein molecules being modified with two fully sialylated biantennary glycan chains,[213] while other glycosylation patterns make minor contributions[213,231] Mass profiling of both commercial Tf and Tf extracted from patients' blood confirms the paucity of minor Tf glycoforms (see Supplementary Material for more detail). However, the protein mass can also be affected by various non-enzymatic post-translational modifications as a result of stress or protein aging; the presence of Tf mutants in some patients cannot be excluded either. Therefore, confident identification of the synergistic anions bound to Tf *in vivo* would not be possible without the knowledge of the

apo-Tf mass in each patient. To obtain this information, we carried out the analysis of each serum sample in two steps. First, following the SEC fraction collection and albumin depletion on the BDR column, the sample was analyzed by native ESI MS, yielding the total mass of the protein/metal/synergistic anion complex. After that, the sample was quickly acidified, causing the complex to dissociate, and the mass spectrum was recorded, yielding the mass of the endogenous protein in its apo-form. This allowed the total mass of the ligands (metal and synergistic anion) to be calculated as a mass difference between the two forms of the protein (**Figure 2.6**).

Five out of six anonymized blood samples revealed nearly identical MS patterns; one example is presented in **Figure 2.6A**. The extracted metal-bound Tf population consists of both mono-ferric and di-ferric species, each utilizing carbonate as a synergistic anion. The presence of the mono-ferric form of Tf is consistent with the known pattern of Tf metal loading in healthy subjects, which typically contains a distribution of apo-, mono-ferric and di-ferric protein species. Interestingly, one of the patients exhibited a very different metal loading pattern, with only di-ferric protein species present in the sample. The two distinct peaks present in the mass spectrum (**Figure 2.6B**) correspond to the oxalate-bound form $(Fe^{3+}\cdot C_2O_4^{2-})_2\cdot$Tf and to the mixed form $(Fe^{3+}\cdot CO_3^{2-})\cdot(Fe^{3+}\cdot C_2O_4^{2-})\cdot$Tf.

The fact that the oxalate-bound Tf species were detected in one of the clinical samples is exciting, as it clearly signals the ability of oxalate to act as a synergistic anion *in vivo*, and not just *in vitro*, as had been previously demonstrated.[121] We note that this anomalous clinical sample did not reveal the presence of mono-ferric forms of Tf, which may be indirect evidence of the inhibition of iron release *in vivo* by oxalate acting as a

synergistic anion. Indeed, the inability of Tf to unload iron in the endosome coupled with continuous iron uptake would result in complete saturation of the protein with the metal. Since the focus of this work was on method development, and we did not have access to the patients' medical records, it is impossible to draw any definitive conclusions regarding the interference of Tf-bound oxalate and iron homeostasis. It is clear, however, that oxalate can act as a synergistic anion, likely interfering with the iron delivery to cells. The ability to differentiate between carbonate- and oxalate-bound Tf in clinical samples will provide clinicians with a powerful tool that can be used to establish an actual role of oxalate in symptomatic iron deprivation, as well as in the etiology of neuropathologies caused by insufficient supply of iron to the brain during its development.

So far, in the majority of cases autism has eluded attempts to discover its genetic origins,[194] hinting at the importance of complex gene-environment interactions in the etiology of this disease.[25] Extensive efforts to identify metabolic biomarkers of autism have also met only with limited success.[140,191,206] Nevertheless, a relentless pursuit of autism biomarkers continues with the ultimate goal of improving both diagnosis of the disease and evaluation of the effectiveness of therapeutic interventions, and currently the most promising strategies appear to be those integrating Omics-based approaches and clinical data.[73] Surprisingly, oxalate does not appear on the list of candidate biomarkers despite wide-spread anecdotal evidence for its involvement in autism progression,[3] and a clinical study suggesting a correlation between the elevated levels of oxalate in plasma and the occurrence of autism.[104] Oxalate is an endogenous anion, which is both produced internally (as a final product of metabolism of glyoxalate and glycerate), and acquired with food (especially through diets reach in leafy greens, but also from a variety of other sources

ranging from chocolate to tofu). As there are no enzymes in humans that can degrade oxalate, the only channel of its elimination from circulation is through the kidney, with a typical plasma concentration in healthy adults being 10-30 μM.[26] While kidney stone formation is probably the best known pathology linked to increased levels of oxalate, hyperoxaluria may also affect other organs and tissues, including the myocardium and bone marrow, through systemic oxalosis.[19]

Anemia is also one of the well-documented clinical presentations of systemic oxalosis, which is linked to oxalate deposition in the bones.[34] Conceivably, limited availability of iron may also be caused by oxalate interfering with iron delivery to cells (*e.g.*, increased levels of oxalate may lead to this anion replacing carbonate from the $(Fe^{3+}\cdot CO_3^{2-})_2\cdot$Tf complexes in circulation; with the resulting $(Fe^{3+}\cdot C_2O_4^{2-})_2$Tf complexes unable to release iron in the mildly acidic endosomal environment, see **Figure 2.1)**. Since the insufficient supply of iron to the developing brain is known to have devastating consequences,[15,60,86,119,134,155,216] arguments have been repeatedly made that iron deprivation may also play a role in the etiology of autism. However, multiple studies of the iron status in autistic children failed to reach a consensus whether oxalate is a contributing factor to iron deprivation.

However, it is important to note that even abundant plasma oxalate may not necessarily interfere with iron delivery to the central nervous system via receptor-mediated transcytosis, as this anion fails to displace carbonate from Tf *in vitro* at neutral pH *on a* physiologically relevant time scale.[120] The ability to determine the level of Tf complexed with oxalate in clinical samples opens a host of exciting opportunities in this field by providing a powerful analytical tool to establish the role of this ubiquitous metabolite in

modulating iron supply within the developing organism. Definitive proof of oxalate interference with iron delivery in autistic patients would provide an explanation for the frequent ineffectiveness of iron supplementation. Otherwise, it would bring into question the effectiveness of the aggressively marketed low-oxalate diets, at least with respect to ensuring sufficient iron supply, which appear to be common dietary interventions in autistic children.[3]

2.5 Conclusions

Tf-bound oxalate is expected to disturb iron homeostasis by inhibiting its release during Tf receptor-mediated endocytosis, potentially leading to a range of pathological conditions triggered by iron deprivation. Although the plasma levels of oxalate can be readily determined using a variety of techniques, currently there are no methods to determine the extent of oxalate bound to Tf in circulation. We have developed an analytical procedure that uses native ESI MS to identify synergistic anions bound to Tf in clinical blood samples without introducing artefacts that alter the carbonate/oxalate ratio. Therefore, this procedure may allow direct quantitation of different forms of Tf to be carried out. Application of this new technique to the analysis of blood samples of patients with various forms of anaemia and/or hyperoxaluria will allow the role of oxalate in limiting iron bioavailability to be established. This information will be invaluable for the design of a targeted and effective treatment of various pathologies triggered by iron deprivation without relying on iron supplementation, which frequently fails. The work presented in this report had focused specifically on the composition of Tf/metal/synergistic anion complexes *in vivo*. However, a similar strategy may also be used for the analysis of

other clinically relevant non-covalent complexes whose composition may provide important information regarding disease diagnosis, its progression or the treatment progress.

2.6 Acknowledgements

The authors are grateful to Prof. Anne B. Mason (University of Vermont College of Medicine, Department of Biochemistry) for providing the recombinant form of human Tf and to Prof. Barry Braun (University of Massachusetts-Amherst, Department of Kinesiology) for providing anonymized blood samples of human volunteers. This work was supported in part by a grant R01 GM061666 from the National Institutes of Health, and the FT ICR mass spectrometer was acquired through the grant CHE-0923329 from the National Science Foundation (Major Research Instrumentation program).

2.7 Figures

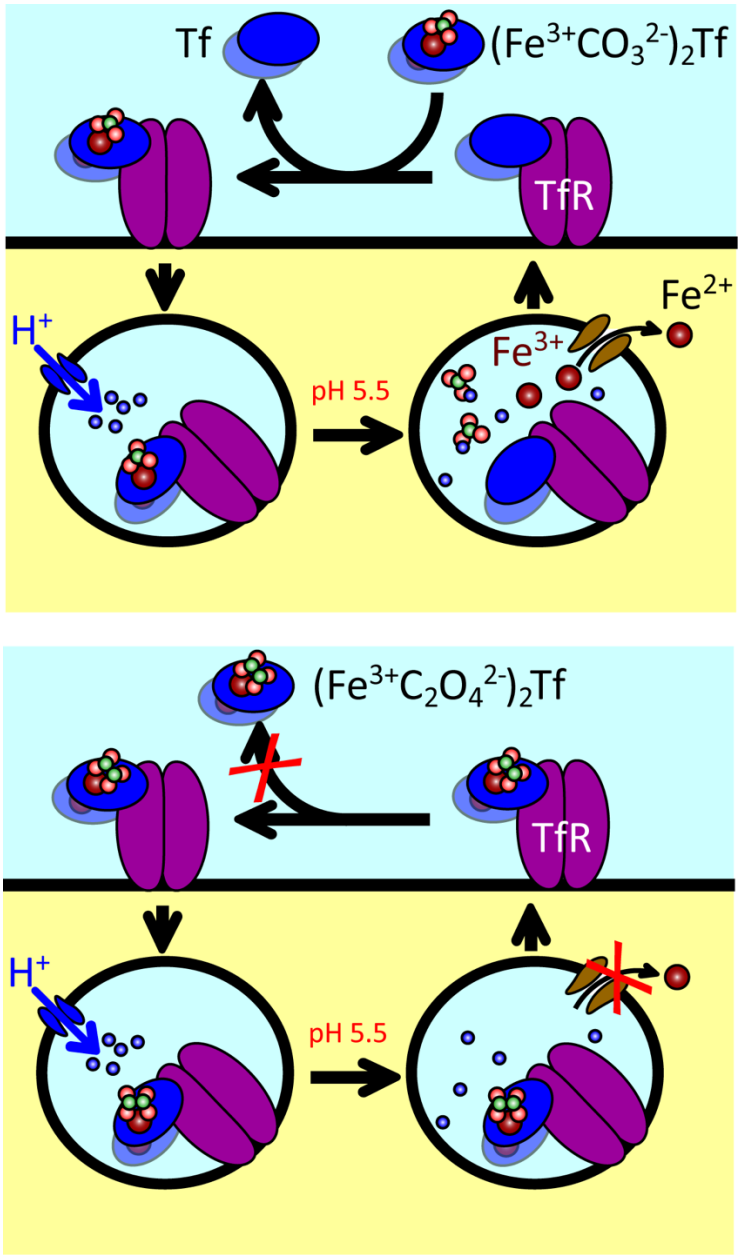

Figure 2.1. Iron delivery to cells by Tf via receptor-mediated endocytosis (top) and inhibition of this process by oxalate acting as a synergistic anion instead of carbonate (bottom). Top (counter-clockwise, from upper left corner): binding of $(Fe{\cdot}CO_3^{2-}/C_2O_4^{2-})_2Tf$ to TfR at the cell surface is followed by internalization of this complex in an endosome. Activation of proton pumps (blue) leads to the endosome acidification, a process that eventually triggers iron release from Tf and its subsequent transport from the endosomal compartment to the cytosol, while the iron-free Tf is recycled back to the cell surface, where it is made available for another cycle of iron delivery. Bottom: presence of oxalate prevent iron dissociation from Tf at mildly acidic endosomal pH.

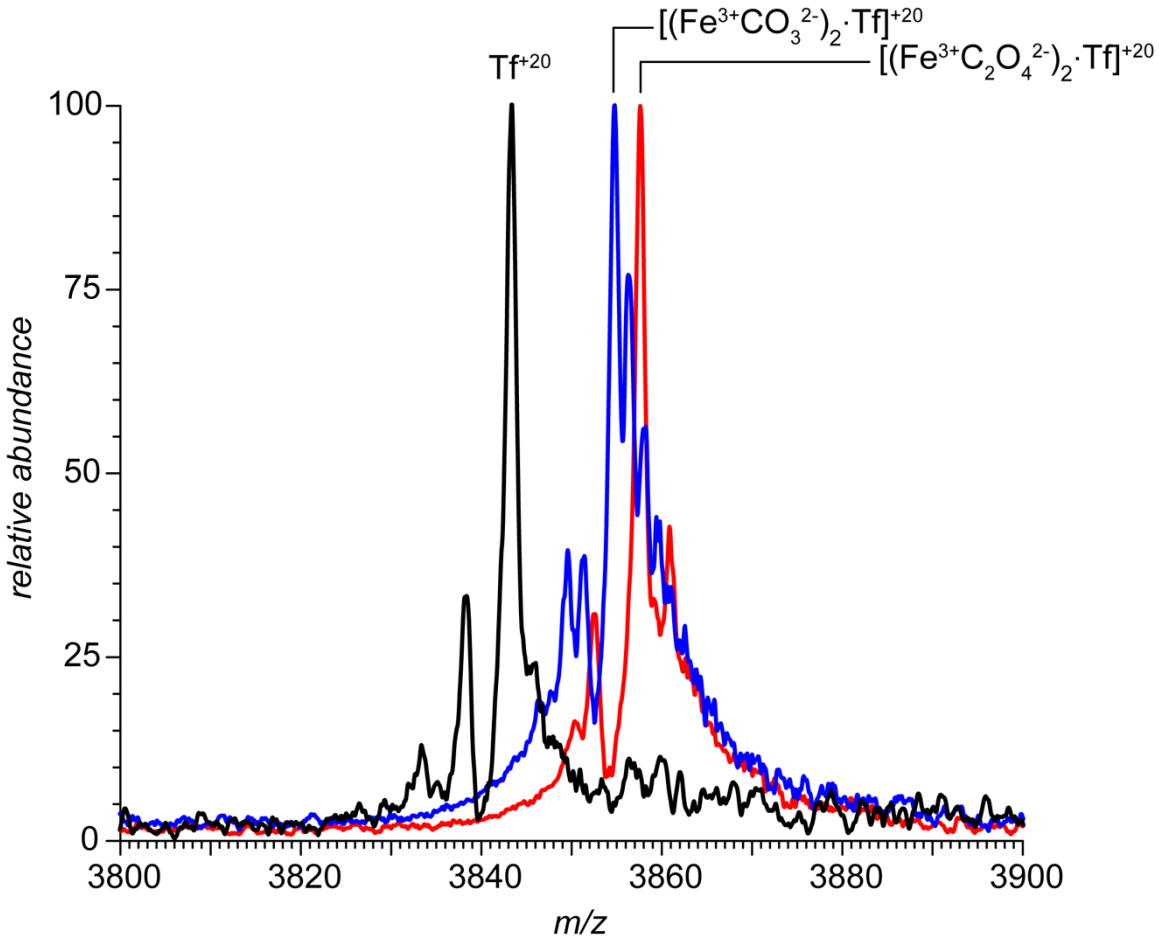

Figure 2.2. Zoomed views of the native ESI mass spectra of recombinant Tf reconstituted with iron using carbonate (blue trace) and oxalate (red) as synergistic anions. The black trace represents the ionic signal of the apo-form of recombinant Tf. Only peaks corresponding to ionic species at charge state +20 are shown for clarity.

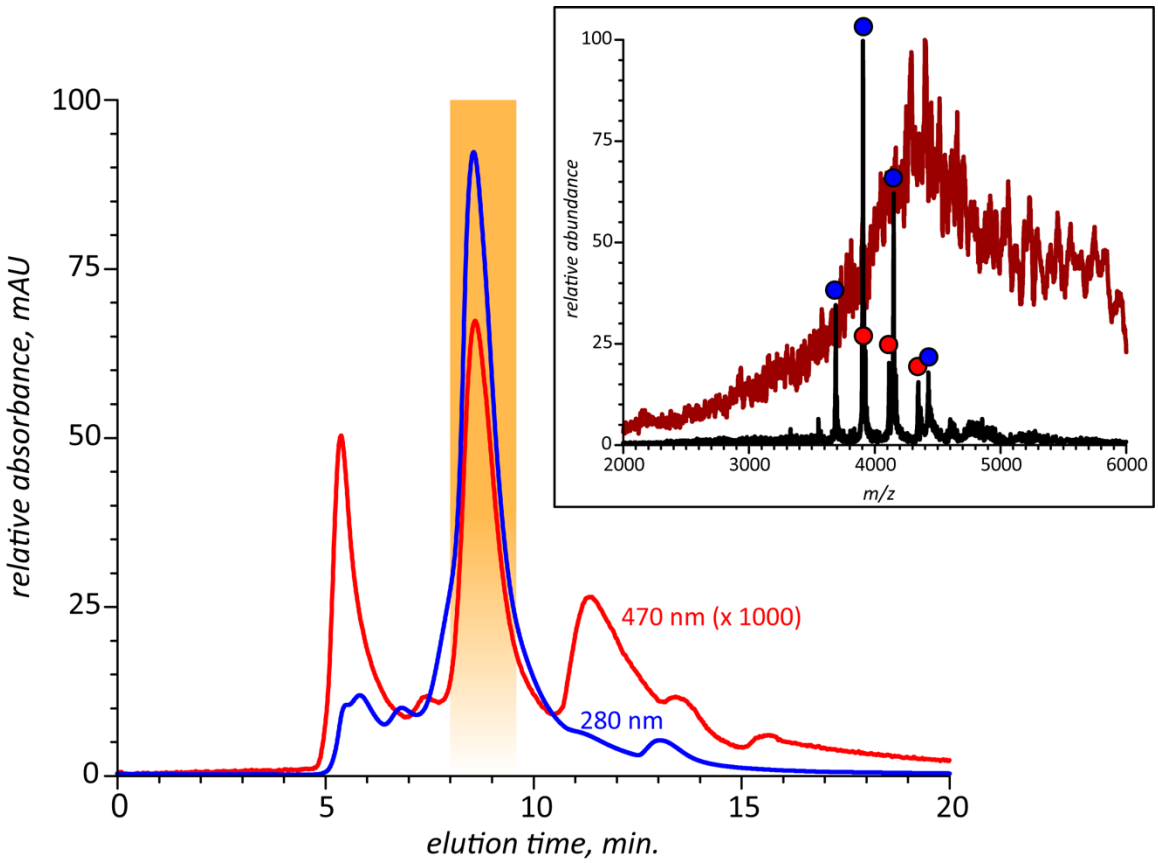

Figure 2.3. SEC chromatograms of bovine serum showing the Tf-containing fraction (highlighted in orange); native ESI mass spectrum of this fraction is shown in the inset (black trace). Serum albumin and Tf peaks are labeled with blue and red circles, respectively. The brown trace shows a mass spectrum of unfractionated serum.

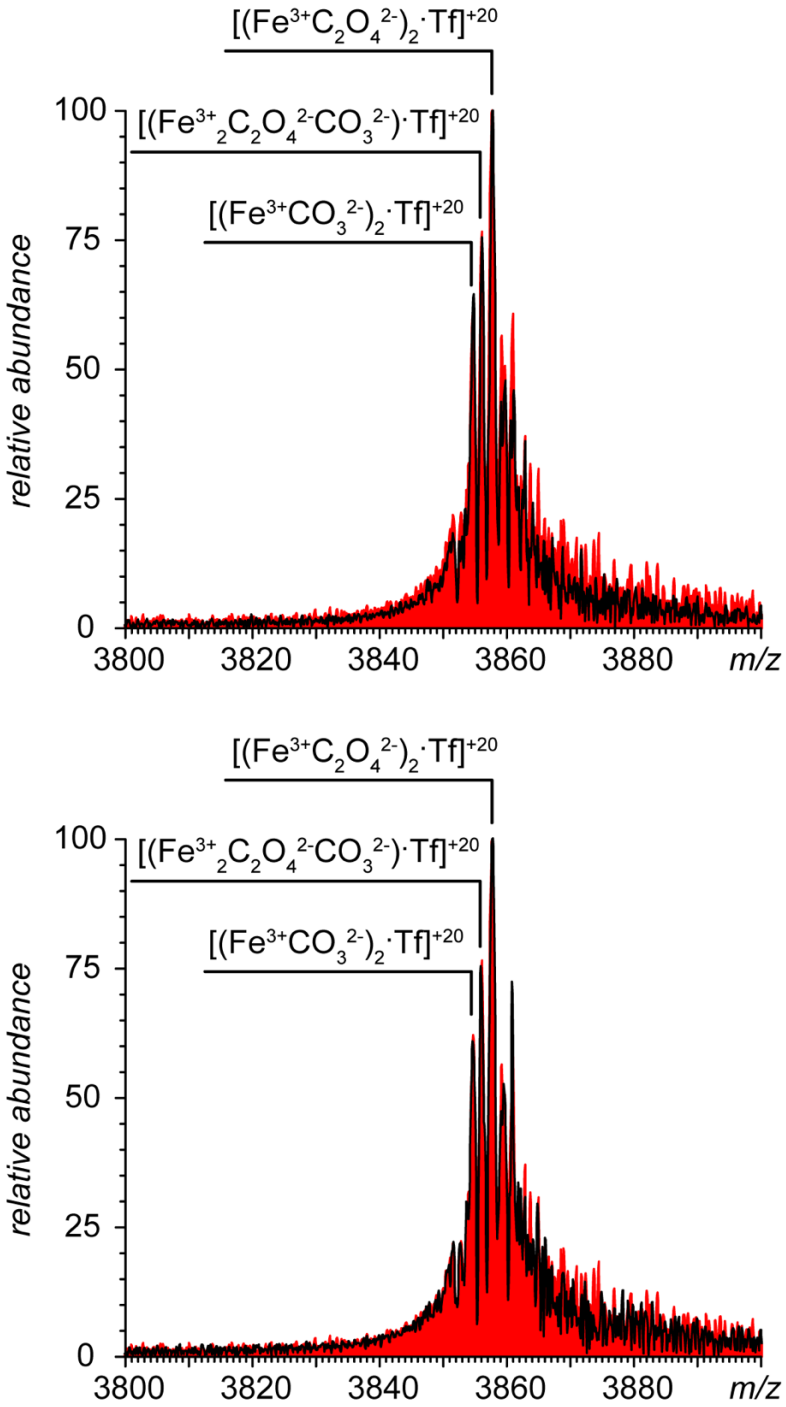

Figure 2.4. Zoomed views of the native ESI mass spectra of mixtures of recombinant Tf reconstituted with iron using carbonate and oxalate as synergistic anions subjected to SEC fractionation (top) and albumin depletion on a BDR column (bottom). The black traces represent the spectra acquired after the treatments, and the red-filled curves represent the mass spectra of the initial mixtures. Only peaks corresponding to ionic species at charge state +20 are shown for clarity.

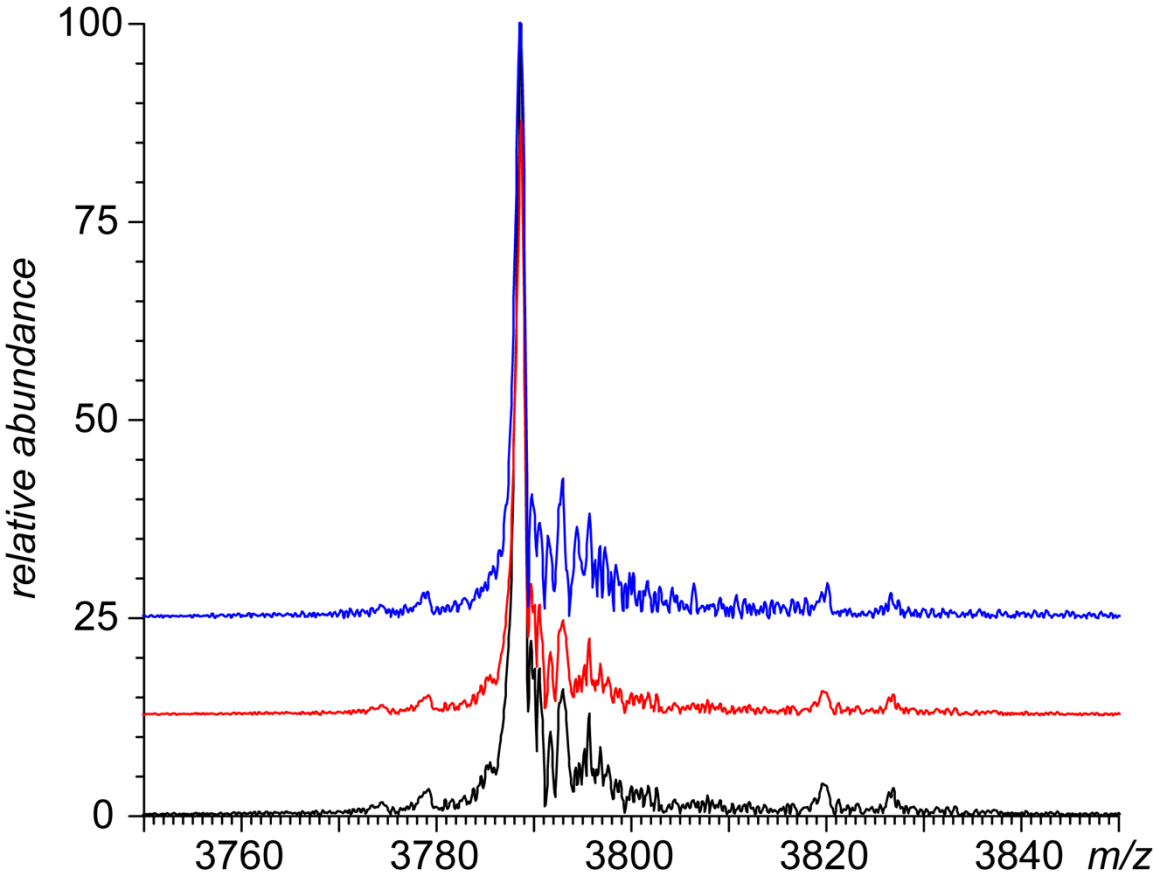

Figure 2.5. Zoomed views of the native ESI mass spectra of the apo-form of human Tf subjected to SEC fractionation (red trace) and albumin depletion on the BDR column (blue). The black trace represents the reference mass spectrum of the apo-Tf.

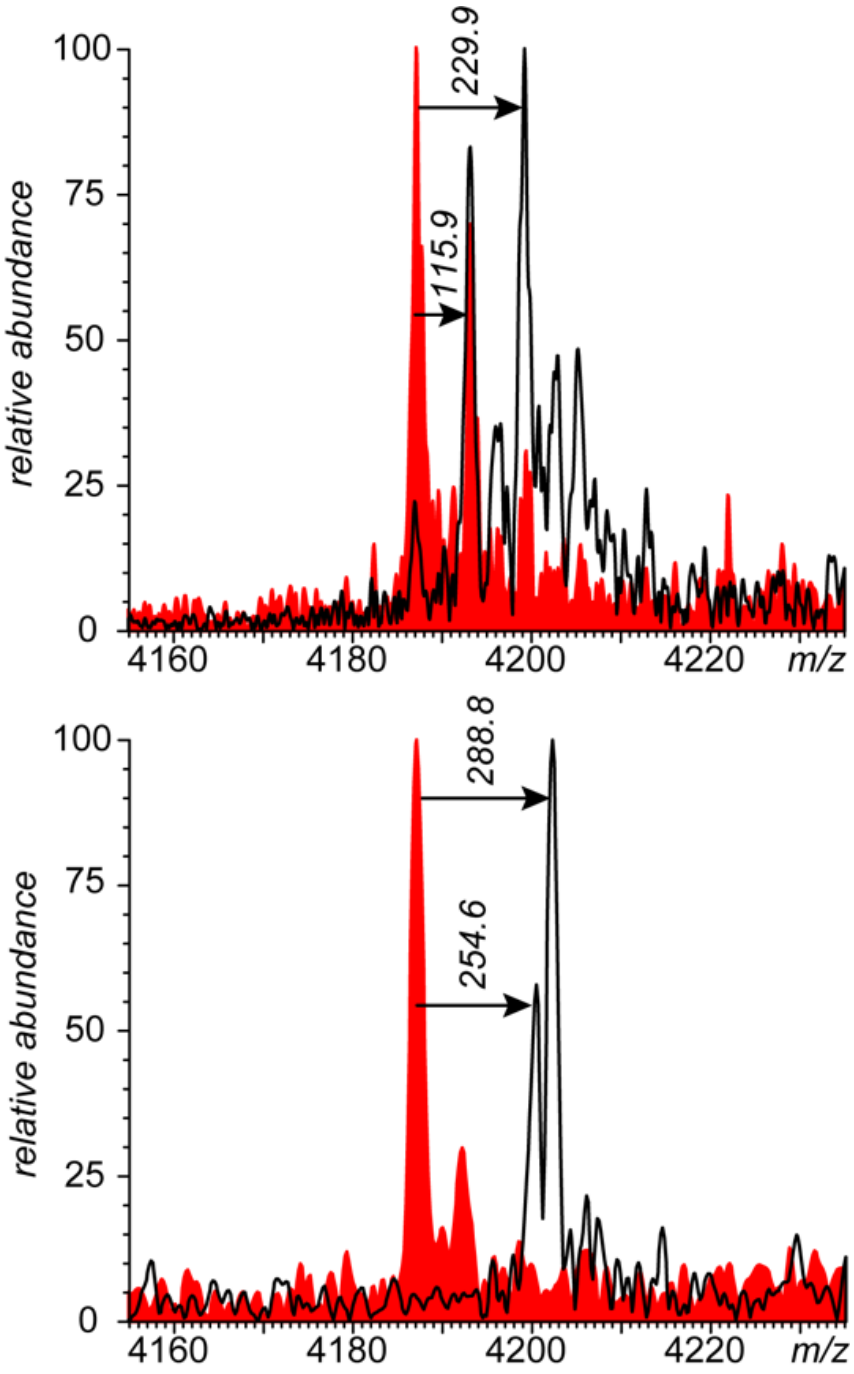

Figure 2.6. Representative native ESI mass spectra of endogenous Tf extracted from serum of two patients (black traces). The red-filled curves represent reference mass spectra of the apo-forms of endogenous Tf acquired following acidification of the extracts to induce dissociation of both iron and synergistic anions from the protein. Only peaks corresponding to ionic species at charge state +19 are shown for clarity.

2.9 Supplemental Figures

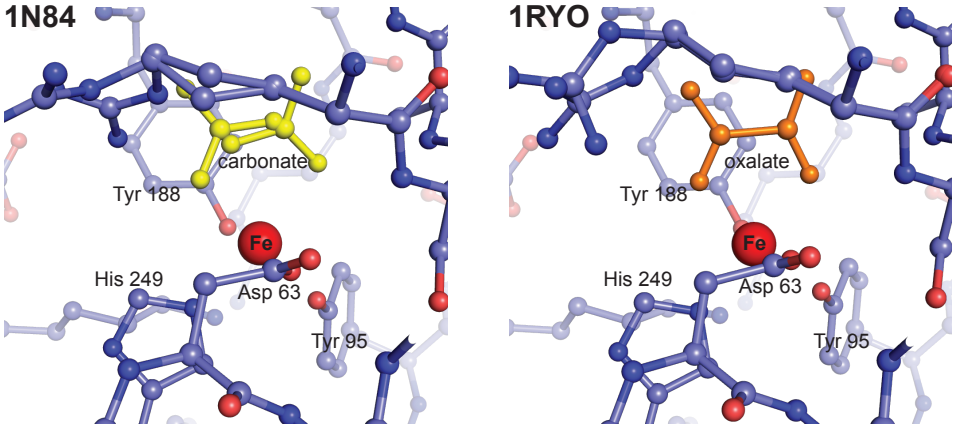

Figure S2.1. Carbonate (left) and Oxalate (right) coordinated Fe in the N-lobe of Tf

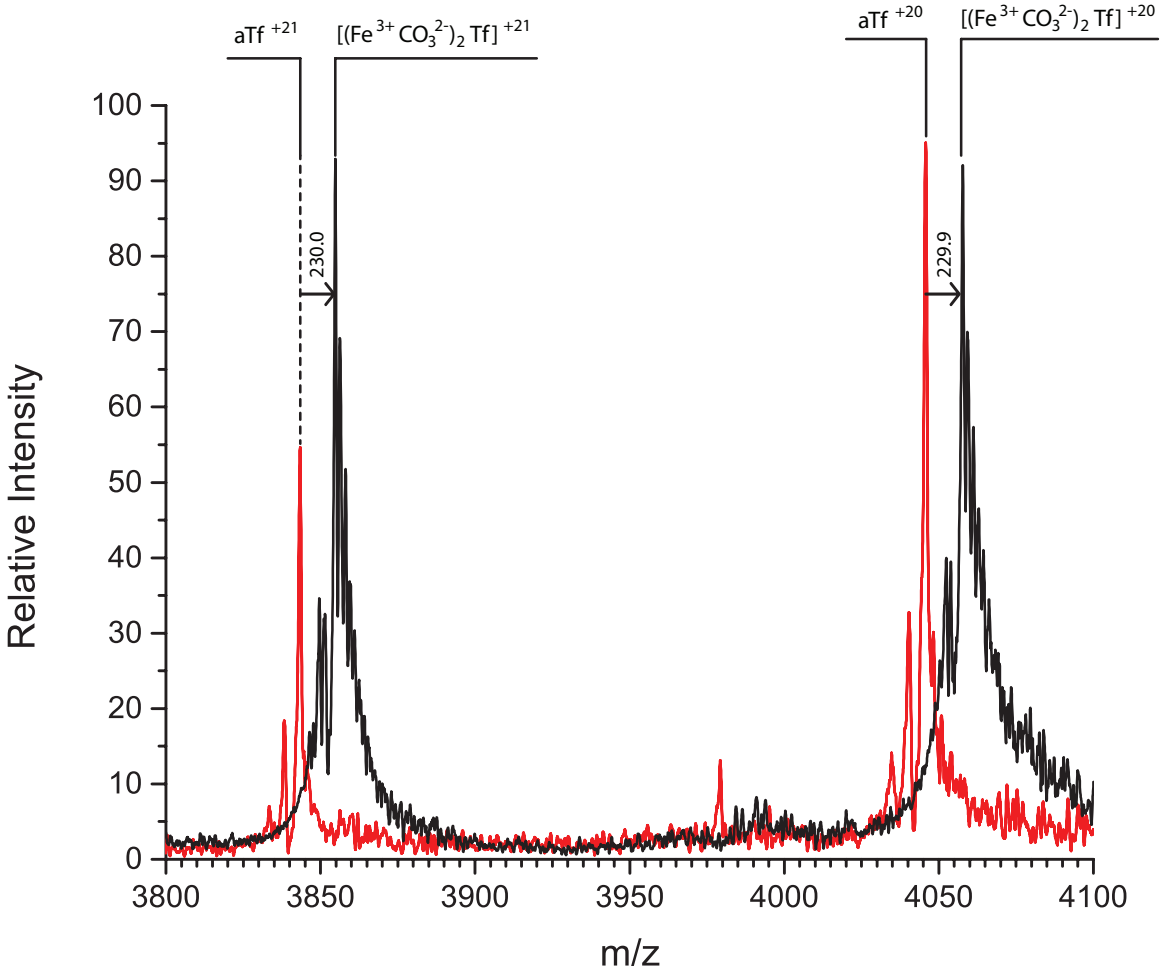

Figure S2.2. Calculated mass shifts between holo- and apo-Tf for the +21 and +20 charge states. Theoretical mass shift is for two Fe^{3+} and CO_3^{2-} is 229.7Da.

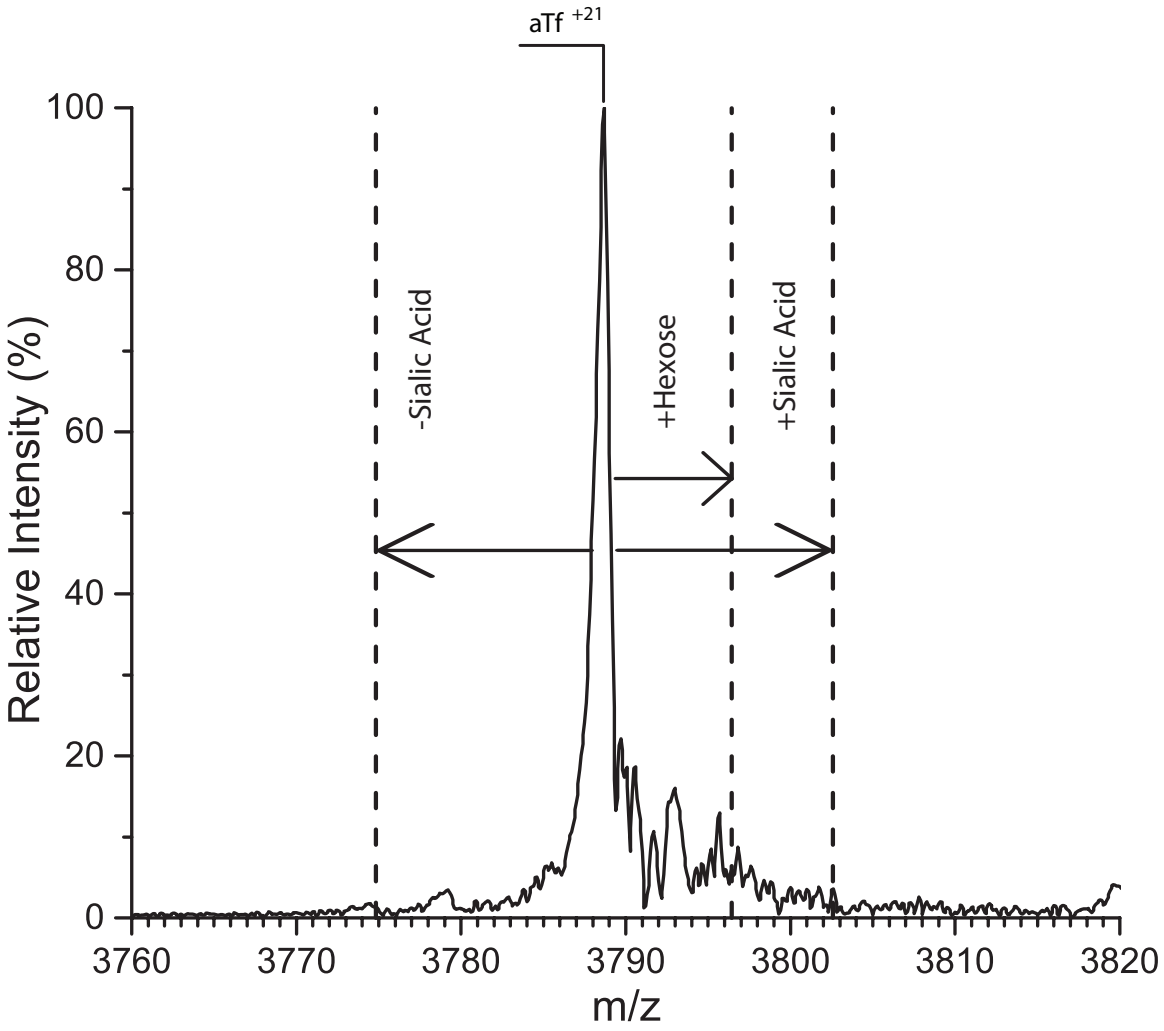

Figure S2.3. Shown is the +21 charge state of aTf. Dashed lines represent the calculated mass shift for either the addition of a hexose due to glycation (162.1 Da) as well as the addition or absence of a sialic acid (291.2 Da).

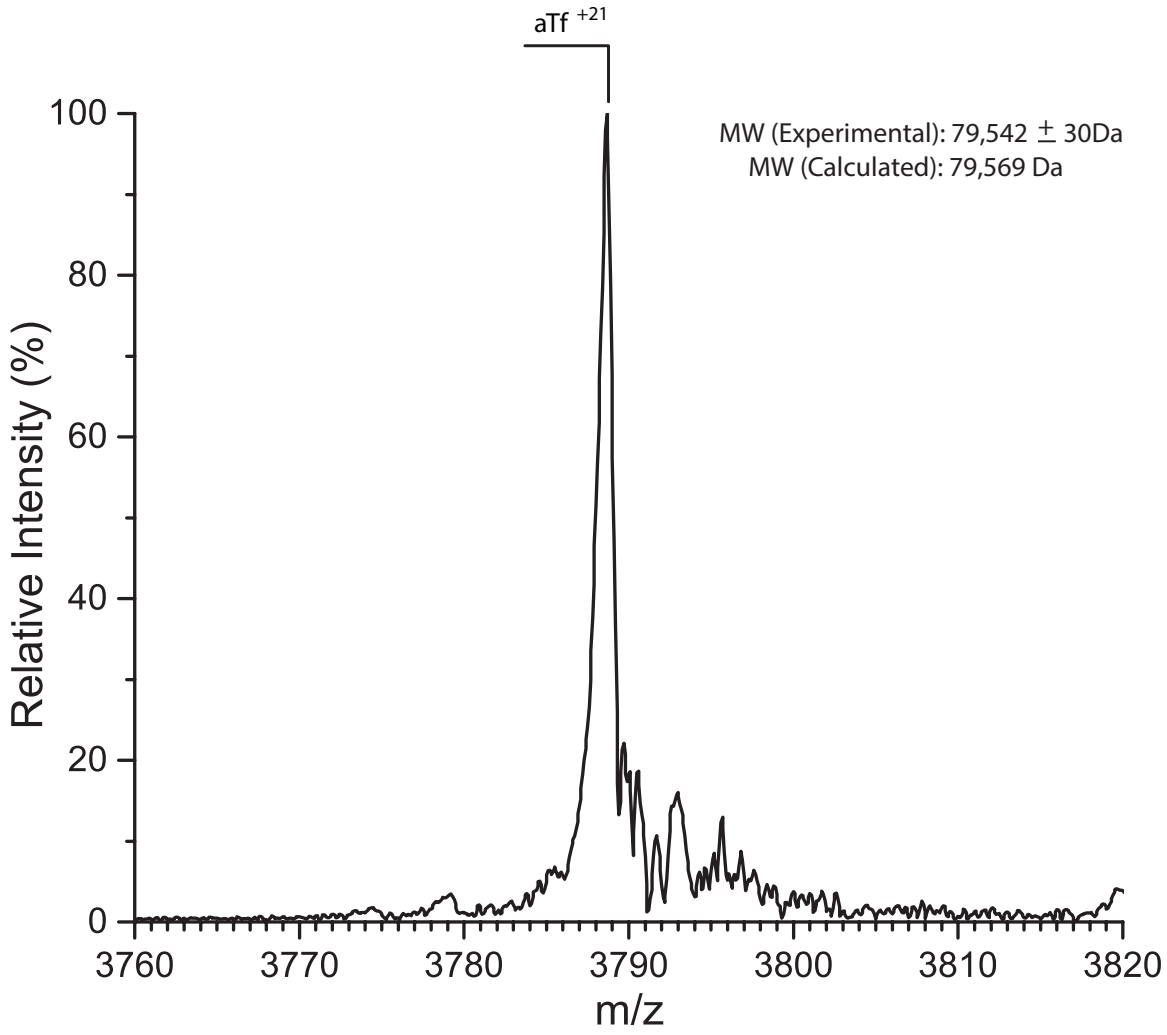

Figure S2.4. Calculated mass is based on the amino acid sequence of Tf and the mass of two fully sialylated biantennary glycan chains. This figure highlights the importance of experimentally determining the mass of aTf in order for the correct synergistic anion and metal composition to be assigned.

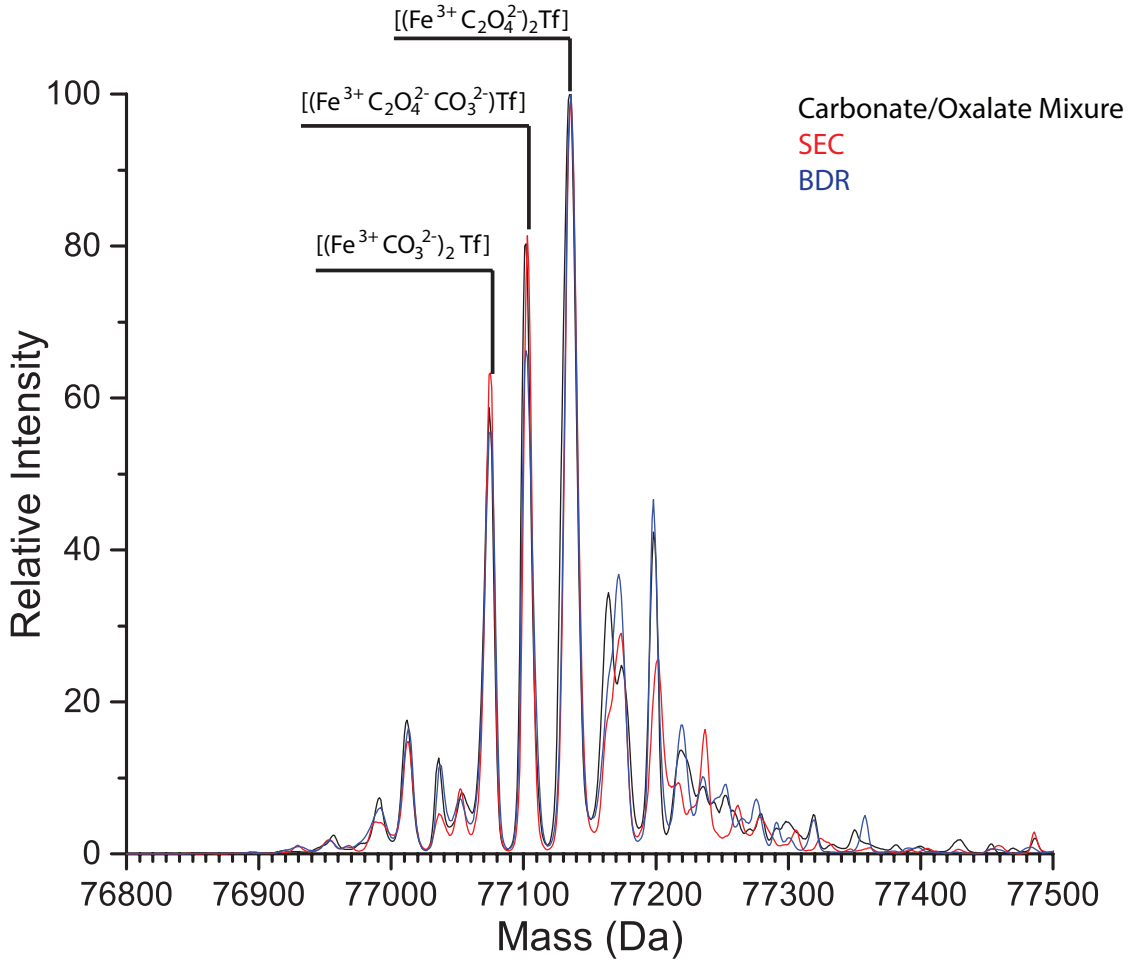

	% Area		
Synergistic Anion Composition	**Orig. Mix**	**SEC**	**BDR**
2 CO_3^{2-}	21.5%	23.8%	24.0%
CO_3^{2}/ $C_2O_4^{2}$	28.5%	27.1%	27.9%
2 $C_2O_4^{2}$	50.0%	49.1%	48.0%

Figure S2.5. Deconvoluted spectra of recombinant Tf reconstituted with iron using carbonate and oxalate as synergistic anions subjected to SEC fractionation (red) and albumin depletion on a BDR column (blue). Peak area's were integrated and there was no significant change in the percent area for any of the three synergistic anion peaks.

2.9 References

1 Pantopoulos, K., Porwal, S. K., Tartakoff, A. & Devireddy, L. Mechanisms of mammalian iron homeostasis. *Biochemistry* **51**, 5705-5724, doi:10.1021/bi300752r (2012).

2 Weiss, G. & Goodnough, L. T. Anemia of chronic disease. *N. Engl. J. Med.* **352**, 1011-1023, doi:10.1056/NEJMra041809 (2005).

3 Luck, A. N. & Mason, A. B. in *Metal Transporters* Vol. 69 *Current Topics in Membranes* (eds S. Lutsenko & J. M. Arguello) 3-35 (Elsevier Academic Press Inc, 2012).

4 Jandl, J. H. & Katz, J. H. The plasma-to-cell cycle of transferrin. *J. Clin. Invest.* **42**, 314-326, doi:10.1172/JCI104718 (1963).

5 Luck, A. N., Bobst, C. E., Kaltashov, I. A. & Mason, A. B. Human serum transferrin: is there a link among autism, high oxalate levels, and iron deficiency anemia? *Biochemistry* **52**, 8333-8341, doi:10.1021/bi401190m (2013).

6 Aisen, P. Transferrin, the transferrin receptor, and the uptake of iron by cells. *Met. Ions Biol. Syst.* **35**, 585-631 (1998).

7 Luck, A. N. & Mason, A. B. Transferrin-mediated cellular iron delivery. *Curr. Top. Membr.* **69**, 3-35, doi:10.1016/b978-0-12-394390-3.00001-x (2012).

8 Gumerov, D. R. & Kaltashov, I. A. Dynamics of iron release from transferrin N-lobe studied by electrospray ionization mass spectrometry. *Anal. Chem.* **73**, 2565-2570 (2001).

9 Burtis, C. A., Ashwood, E. R. & Tietz, N. W. *Tietz Textbook of Clinical Chemistry*. 3 edn, (W.B. Saunders, 1999).

10 Schlabach, M. R. & Bates, G. W. The synergistic binding of anions and Fe3+ by transferrin. Implications for the interlocking sites hypothesis. *J. Biol. Chem.* **250**, 2182-2188 (1975).

11 Halbrooks, P. J., Mason, A. B., Adams, T. E., Briggs, S. K. & Everse, S. J. The oxalate effect on release of iron from human serum transferrin explained. *J. Mol. Biol.* **339**, 217-226 (2004).

12 Lopez, A., Cacoub, P., Macdougall, I. C. & Peyrin-Biroulet, L. Iron deficiency anaemia. *Lancet*, in press, doi:10.1016/s0140-6736(15)60865-0 (2015).

13 Konofal, E. *et al.* Impact of restless legs syndrome and iron deficiency on attention-deficit/hyperactivity disorder in children. *Sleep Med.* **8**, 711-715, doi:http://dx.doi.org/10.1016/j.sleep.2007.04.022 (2007).

14 Simakajornboon, N., Kheirandish-Gozal, L. & Gozal, D. Diagnosis and management of restless legs syndrome in children. *Sleep Med. Rev.* **13**, 149-156, doi:http://dx.doi.org/10.1016/j.smrv.2008.12.002 (2009).

15 Otero, G. A., Pliego-Rivero, F. B., Porcayo-Mercado, R. & Mendieta-Alcántara, G. Working memory impairment and recovery in iron deficient children. *Clin. Neurophysiol.* **119**, 1739-1746, doi:http://dx.doi.org/10.1016/j.clinph.2008.04.015 (2008).

16 Dosman, C. F. *et al.* Ferritin as an indicator of suspected iron deficiency in children with autism spectrum disorder: prevalence of low serum ferritin concentration. *Dev. Med. Child Neurol.* **48**, 1008-1009, doi:10.1017/s0012162206232225 (2006).

17 Dosman, C. F. *et al.* Children with autism: Effect of iron supplementation on sleep and ferritin. *Pediatr. Neurol.* **36**, 152-158, doi:10.1016/j.pediatrneurol.2006.11.004 (2007).

18 Bilgic, A. *et al.* Iron deficiency in preschool children with autistic spectrum disorders. *Res. Autism Spectr. Disord.* **4**, 639-644, doi:10.1016/j.rasd.2009.12.008 (2010).

19 Reynolds, A. *et al.* Iron Status in Children With Autism Spectrum Disorder. *Pediatrics* **130**, S154-S159, doi:10.1542/peds.2012-0900M (2012).

20 Konstantynowicz, J. *et al.* A potential pathogenic role of oxalate in autism. *Eur. J. Paediatr. Neurol.* **16**, 485-491, doi:http://dx.doi.org/10.1016/j.ejpn.2011.08.004 (2012).

21 Zhang, M., Gumerov, D. R., Kaltashov, I. A. & Mason, A. B. Indirect detection of protein-metal binding: Interaction of serum transferrin with In^{3+} and Bi^{3+}. *J. Am. Soc. Mass Spectrom.* **15**, 1658-1664 (2004).

22 Yu, X., Wojciechowski, M. & Fenselau, C. Assessment of metals in reconstituted metallothioneins by electrospray mass spectrometry. *Anal. Chem.* **65**, 1355-1359 (1993).

23 Nemirovskiy, O. V. & Gross, M. L. Determination of calcium binding sites in gas-phase small peptides by tandem mass spectrometry. *J. Am. Soc. Mass Spectrom.* **9**, 1020-1028 (1998).

24 Lossl, P., Snijder, J. & Heck, A. J. Boundaries of mass resolution in native mass spectrometry. *J. Am. Soc. Mass Spectrom.* **25**, 906-917, doi:10.1007/s13361-014-0874-3 (2014).

25 Gumerov, D. R., Mason, A. B. & Kaltashov, I. A. Interlobe communication in human serum transferrin: metal binding and conformational dynamics investigated by electrospray ionization mass spectrometry. *Biochemistry* **42**, 5421-5428 (2003).

26 Kaltashov, I. A., Bobst, C. E., Zhang, M., Leverence, R. & Gumerov, D. R. Transferrin as a model system for method development to study structure, dynamics and interactions of metalloproteins using mass spectrometry. *Biochim. Biophys. Acta* **1820**, 417-426 (2012).

27 Lei, Q. P. *et al.* Electrospray mass spectrometry studies of non-heme iron-containing proteins. *Anal. Chem.* **70**, 1838-1846 (1998).

28 Griffith, W. P. & Kaltashov, I. A. Highly asymmetric interactions between globin chains during hemoglobin assembly revealed by electrospray ionization mass spectrometry. *Biochemistry* **42**, 10024-10033 (2003).

29 Hyung, S. W. *et al.* Microscale depletion of high abundance proteins in human biofluids using IgY14 immunoaffinity resin: analysis of human plasma and cerebrospinal fluid. *Anal Bioanal Chem* **406**, 7117-7125, doi:10.1007/s00216-014-8058-3 (2014).

30 Steel, L. F. *et al.* Efficient and specific removal of albumin from human serum samples. *Mol. Cell. Proteomics* **2**, 262-270, doi:10.1074/mcp.M300026-MCP200 (2003).

31 Arndt, T. Carbohydrate-deficient transferrin as a marker of chronic alcohol abuse: a critical review of preanalysis, analysis, and interpretation. *Clinical chemistry* **47**, 13-27 (2001).

32 Zühlsdorf, A. *et al.* It Is Not Always Alcohol Abuse—A Transferrin Variant Impairing the CDT Test. *Alcohol Alcohol.*, doi:10.1093/alcalc/agv099 (2015).

33 Weykamp, C. *et al.* Toward standardization of carbohydrate-deficient transferrin (CDT) measurements: III. Performance of native serum and serum spiked with disialotransferrin proves that harmonization of CDT assays is possible. *Clin. Chem. Lab. Med.* **51**, 991-996, doi:10.1515/cclm-2012-0767 (2013).

34 Luck, A. N., Bobst, C. E., Kaltashov, I. A. & Mason, A. B. Human serum transferrin: Is there a link between autism, high oxalate and iron deficiency anemia? *Biochemistry* **52**, 8333-8341, doi:10.1021/bi401190m (2013).

35 Sykes, N. H. & Lamb, J. A. Autism: the quest for the genes. *Expert Reviews in Molecular Medicine* **9**, 1-15, doi:doi:10.1017/S1462399407000452 (2007).

36 Broek, J. A. C. *et al.* The need for a comprehensive molecular characterization of autism spectrum disorders. *International Journal of Neuropsychopharmacology* **17**, 651-673, doi:10.1017/s146114571300117x (2014).

37 Wang, H. *et al.* Potential serum biomarkers from a metabolomics study of autism. *J. Psychiatry Neurosci.* **40**, in press, doi:10.1503/jpn.140009 (2015).

38 Suganya, V., Geetha, A. & Sujatha, S. Urine proteome analysis to evaluate protein biomarkers in children with autism. *Clinica Chimica Acta* **450**, 210-219, doi:http://dx.doi.org/10.1016/j.cca.2015.08.015 (2015).

39 Mizejewski, G. J., Lindau-Shepard, B. & Pass, K. A. Newborn screening for autism: in search of candidate biomarkers. *Biomark. Med.* **7**, 247-260, doi:10.2217/bmm.12.108 (2013).

40 Higdon, R. *et al.* The Promise of Multi-Omics and Clinical Data Integration to Identify and Target Personalized Healthcare Approaches in Autism Spectrum Disorders. *Omics* **19**, 197-208, doi:10.1089/omi.2015.0020 (2015).

41 Aitken, K. J. Dietary interventions in autism spectrum disorders why they work when they do, why they don't when they don't. (2009).

42 Bhasin, B., Urekli, H. M. & Atta, M. G. Primary and secondary hyperoxaluria: Understanding the enigma. *World J. Nephrol.* **4**, 235-244, doi:10.5527/wjn.v4.i2.235 (2015).

43 Coulter-Mackie, M. B., White, C. T., Lange, D. & Chew, B. H. Primary Hyperoxaluria Type 1. *GeneReviews* (2014).

44 Beard, J. One person's view of iron deficiency, development, and cognitive function. *Am. J. Clin. Nutr.* **62**, 709-710 (1995).

45 Pollitt, E. IRON-DEFICIENCY AND COGNITIVE FUNCTION. *Annu. Rev. Nutr.* **13**, 521-537, doi:10.1146/annurev.nutr.13.1.521 (1993).

46 Yager, J. Y. & Hartfield, D. S. Neurologic manifestations of iron deficiency in childhood. *Pediatr. Neurol.* **27**, 85-92, doi:http://dx.doi.org/10.1016/S0887-8994(02)00417-4 (2002).

47 Gordon, N. Iron deficiency and the intellect. *Brain Dev.* **25**, 3-8, doi:http://dx.doi.org/10.1016/s0387-7604(02)00148-1 (2003).

48 Lozoff, B. & Georgieff, M. K. Iron Deficiency and Brain Development. *Sem. Pediatr. Neurol.* **13**, 158-165, doi:http://dx.doi.org/10.1016/j.spen.2006.08.004 (2006).

49 McCann, J. C. & Ames, B. N. An overview of evidence for a causal relation between iron deficiency during development and deficits in cognitive or behavioral function. *Am. J. Clin. Nutr.* **85**, 931-945 (2007).

50 Jáuregui-Lobera, I. Iron deficiency and cognitive functions. *Neuropsychiatr. Dis. Treat.* **10**, 2087-2095, doi:10.2147/NDT.S72491 (2014).

CHAPTER 3

INFLUENCE OF GLYCAN MODIFICATGION ON IGG1 BIOCHEMICAL AND BIOPHYSICAL PROPERTIES

This chapter has been adapted from a paper submitted as: Pawlowski, J. W., Bajardi-Taccioli, A., Houde, D., Feschenko, M., Carlage, T. & Kaltashov, I. A. Influence of glycan modification on IgG1 biochemical and biophysical properties. *J. Pharm. Biomed. Anal.* **151**, 133-144, doi:https://doi.org/10.1016/j.jpba.2017.12.061 (2018).

3.1 Abstract

Monoclonal antibodies (mAbs) are the fastest growing class of biopharmaceuticals. The specific therapeutic tasks vary among different mAbs, which may include neutralization of soluble targets, activation of cytotoxic pathways, targeted drug delivery, and diagnostic imaging. The specific therapeutic goal defines which interactions of the antibody with its multiple physiological partners are most critical for function, and which ones are irrelevant or indeed detrimental. In this work, we explored the ability of the glycan chains to affect IgG1 interaction with two key receptor families, FcRn and γ-type Fc receptors, as well as the influence of glycan composition on the conformation and stability of the antibody molecule. Three different glycan-modified forms of IgG1 (fully deglycosylated, hypergalactosylated and hypersialylated) were produced and characterized alongside the unmodified mAb molecule. Biophysical measurements did not reveal any changes that would be indicative of alterations in the higher order structure or increased aggregation propensity for any of the three glycoforms compared to the unmodified mAb, although the CH2 domain was shown to have reduced thermal stability in the fully deglycosylated form. No significant changes were observed for the hypergalactosylated and hypersialylated forms of IgG1 with regards to binding to FcRn, FcγRIIA and FcγRIIIA, suggesting that neither half-life in circulation nor their ability to induce an immune response are likely to be affected by these modifications of the glycan chains. In contrast, no measurable binding was observed for the deglycosylated form of IgG1 with either FcγRIIA or FcγRIIIA, although this form of the antibody retained the ability to associate

with FcRn. These highly specific patterns of attenuation of Fc receptor recognition can be exploited in the future for therapeutic purposes.

3.2 Introduction

Monoclonal antibodies (mAbs) are a large and fast growing class of biopharmaceuticals used to treat a wide range of diseases. Of the five classes of antibodies, the majority of all currently licensed therapeutic mAbs use immuglobulin gamma (IgG) as their framework [1,2]. IgG consists of a fragment antigen binding (Fab) domain and a fragment crystalline (Fc) domain. The latter is responsible for Fc gamma receptor (FcγR) and neonatal Fc receptor (FcRn) binding. There are four major subtypes of IgG (IgG1, IgG2, IgG3, and IgG4), each having different properties with respect to antigen target, complement activation, and affinity for FcγRs [3].

The most important IgG effector functions are achieved through binding to FcγRs on the surface of leukocytes leading to the activation of the immune system.[4] There is one inhibiting (FcγRIIb) and four activating (FcγRI, FcγRIIa, FcγRIIIa, FcγRIIIb) receptors present in humans [5,6]. IgG effector functions that are mediated through the binding of FcγRs-presenting cells include antibody-dependent cellular cytotoxicity, antibody-dependent phagocytosis, degranulation, cytokine release, and inhibition of cell activities among other functions.[3,4] Neonatal Fc receptor (FcRn) is a unique type of Fc receptor responsible for IgG longevity in circulation (half-life of up to three weeks) [7]. Circulating IgG molecules are taken up by cells through pinocytosis and directed to endosomal compartments. Upon endosome acidification (pH < 6.5) FcRn binds to the CH2/C_H3 region of IgG and rescues it from being routed to and degraded in the lysosome. FcRn-bound IgG is then returned to the cell surface and released at physiological pH (7.4) back into circulation. This pH dependent binding is thought to be due to several pH-titratable residues at the FcRn-Fc binding interface [8]. FcRn is also able to transport IgG molecules across epithelial barriers [9] including the placenta (and thus playing a critical role in establishing and maintaining immunity by transferring antibodies from mother to child) [10].

Interactions of the antibody with its targets and receptors must be considered when developing a new therapeutic mAb, as they ultimately determine all aspects of its activity and pharmacokinetic (PK) properties, *e.g.*, target recognition (Fab/antigen binding),

activation of the immune response (Fc/FcγR binding) and half-life (Fc/FcRn association and interaction with neutralizing antibodies [11]). However, the relative importance of each individual type of interaction depends upon the specific task the new biotherapeutic is designed to accomplish (e.g., soluble target neutralization, cell destruction, drug delivery, imaging, etc.). For example, in drug delivery or imaging applications the emphasis is placed on the Fab/antigen interaction (in fact, an immune response to the target of interest is likely to be an unwanted side effect in this case, and the mAb effector function should be diminished or eliminated). In contrast, effective targeting of cancer cells would depend upon a strong immune response, placing emphasis on optimizing Fc/FcγR interactions.

Glycosylation is a structural feature common to many therapeutic proteins, including most mAbs used in clinical applications. In mAbs, glycan chains can have a significant impact on both PK properties and the effector function. The single (and highly conserved) glycosylation site is located at position N297 in the CH2 domains of each heavy chain (**Figure 3.1**), and each glycan chain interacts with the CH2 domain and the opposite glycan chain [3,12]. While the localization of the glycan chains within the Fc region makes their influence on antigen binding highly unlikely, their unique "introverted" arrangement plays an important role in forming and maintaining the conformation of Fc; it is therefore not surprising that changes in the glycan composition alter many aspects of functionality, stability and PK profile of mAbs [13]. It has been reported that sialylation of IgG molecules enhances their anti-inflammatory properties through a decreased affinity to FcγRIIIa [12] and a proposed interactions with dendritic cell-specific intercellular adhesion molecule-3-grabbing non-integrin [3,14-16]. Furthermore, afucosylated, terminal galactose, and high mannose glycan species have all been reported to affect the PK profile and effector function of IgG [17,18]. It is very important to understand how glycosylation may affect the effector function and PK profile of mAb for efficacy and safety reasons. It may also enable rational design of engineered glycoforms with receptor-binding properties optimized for a specific therapeutic function.

In this work, two glycotransferases were used to add a terminal galactose or sialic acid to the glycan chain of an antibody (IgG1 subclass), while the glycosidase PNGase F was used to completely remove the glycan chain. The glycan-modified mAbs were then extensively characterized with regards to changes in stability and function (with an

emphasis on binding to FcγRs and FcRn). Since certain steps during enzymatic modification of mAbs may introduce non-enzymatic post-translational modifications (PTMs) in addition to the desired enzymatic PTMs, the levels of oxidation and deamidation were carefully controlled in the final products and compared to those in the starting material. Furthermore, changes in the glycan composition can influence both structure and functional properties of mAbs via two distinct routes, (*i*) packing and steric effects and (*ii*) electrostatic effects, which were evaluated separately in this work. The glycan modifications were optimized to minimize other structural changes to the mAb, and these modifications did not appear to have a significant effect on the mAbs biophysical and/or biochemical properties. Addition of galactose and/or sialic acid did not significantly interfere with the mAb's binding to FcRn or FcγRIIA/IIIA. Deglycosylation of the mAb produced a modest decrease of its affinity for FcRn, and completely abrogated binding to FcγRIIA/IIIA, as previously reported [19,20]. Modification of a mAb's glycan composition opens exciting new possibilities to fine-tune its properties with the purpose of achieving a desired therapeutic outcome [21-23]. The results of this study help to further understand the impact of Fc glycosylation on the function and structure of an IgG1 molecule.

3.3 Results

Three glycoprotein variants (deglycosylated IgG1, hypergalactosylated IgG1 and hypersialylated IgG1) were produced from the same mAb sample as described in the ***Experimental*** section. All three glycan-modified mAb samples, as well as the reaction control (IgG1 incubated in the same buffer and temperature as the glycan-modified samples) and unmodified IgG1 were characterized as described below.

Intact Mass Spectrometry Analysis. Successful enzymatic modification of the IgG1 glycans was verified by comparing the mass spectra of the modified (enzymatically treated) IgG1 to control (unmodified) IgG1 species (**Figure 3.2**). The unmodified mAb has four major glycan chain variants, which range from having no terminal galactoses (G0/G0 in **Figure 3.2**) to 3 terminal galactose residues (G1/G2). A list of all possible glycan species is shown in the Supplementary Material (**Figure S3.1**). Based on the mass shift from the G0/G0 peak of the unmodified IgG1, hypergalactosylation was shown to convert the

heterogeneous ensemble of unmodified IgG1 molecules to a fully galactosylated species (G2/G2 in **Figure 3.2**). Hypersialylated IgG1 exhibited a combination of 2, 3, and 4 terminal sialic acid residues, with the glycoforms bearing 2 and 3 sialic acid residues being the major species (G2S1/G2S1+G2S0/G2S2 and G2S1/G2S2 in **Figure 3.2**). The mass of the deglycosylated IgG1 species is consistent with a complete removal of both glycan chains from the protein. No significant increase in either oxidation or glycation was observed in the enzymatically modified IgG1 samples (**Table 3.1**, **Figure S3.2** in Supplementary Material).

Size Exclusion Chromatography. Size exclusion chromatography (SEC) was used to evaluate the extent of aggregation of enzymatically treated IgG1 samples by monitoring formation of both soluble aggregates. None of the enzymatic modifications used in this work resulted in a detectable shift of the retention time for the main (monomer) peak. The level of the soluble aggregate formation was found to be less than 2% (by absorbance) for all IgG1 samples, including fully deglycosylated one (Table S1), suggesting that no the experimental conditions to modify the glycan did not significantly alter molecular stability or lead to increased levels of protein aggregates.

Lys-C peptide mapping. Lys-C peptide mapping of all IgG1 samples was carried out using reversed phase liquid chromatography with detection by mass spectrometry (LC/MS). The generated peptide maps were used to detect and quantitate several possible PTMs that could be present in the intact IgG1 sample and generated as side products of the glyco-modification treatment (e.g., oxidation, deamidation, and glycosylation). Possible oxidation of the protein was a particular concern, as the FcRn binding interface incorporates two conserved [24] methionine residues present on each HC (Met^{252} and Met^{428}, located in peptides L17 and L32, respectively). Oxidation of either methionine has been shown to negatively affect the binding of IgG1 to FcRn, provided its twin methionine residue (located on another HC chain) is also oxidized [24-26]. Deamidation introduces a negative charge into a protein and in some cases, is accompanied by isomerization which elongates the polypeptide backbone. Somewhat elevated levels of deamidation were observed in peptide L19-20 containing Asn^{304} and Asn^{322}, and of which are located close to the FcRn binding interface (see **Figure 3.1**) and are known to be prone to deamidation [27,28]. Glycosylated peptides were monitored to confirm the glycan composition of the

hypergalactosylated and hypersialylated IgG1 samples; in the case of the deglycosylated IgG1, successful removal of the glycan chain was verified by the absence of any glycopeptides in the Lys-C digest (Table 3.2).

An example of non-enzymatic PTM quantitation (oxidation of Met^{252}) using LC/MS is illustrated in **Figure 3.3**, and **Table 3.1** compares the relative levels of oxidation and deamidation in both modified and unmodified IgG1 molecules. Peptide maps for the hypergalactosylated and hypersialyated IgG1 species show a modest increase of oxidation of Met^{252} and Met^{428}. Importantly, the estimated percentage of modified IgG1 molecules with oxidation at both methionine residues is less than 2% for all samples; therefore, oxidation is not expected to impact FcRn binding. There is a slight increase of deamidation for both hypergalactosylated and hypersialyated IgG1 (**Table 3.1**), although this has not been reported to affect FcRn binding (*vide supra*). Deglycosylated IgG1 showed a decrease in oxidation of the two methionine residues, and a modest increase of deamidation. The decrease in oxidation is due variability in sample handling of the deglycosylated IgG1 from the other samples were prepared from aliquots held at 2-8 C^o for > 2 weeks. The reaction control IgG1 sample showed a minor increase in oxidation and deamidation levels following exposure to the reaction conditions for hypersialylated IgG1 *sans* sialyltransferase as, but the absence of major changes indicates reaction conditions do not adversely affect IgG1.

Relative abundance of observed glycopeptides for each IgG1 sample was calculated (**Table 3.2**). For hypergalactosylated IgG1, the only identified glycopeptide was found to have a G2 glycan chain (core complex glycan moiety with two terminal galactoses). This is consistent with the intact mass measurement which showed IgG1 being fully galactosylated (see **Figure 3.2**). Hypersialylated IgG1 contained a mixture of glycopeptides with one or two terminal sialic acid glycans (G2S1 and G2S2, one and two terminal sialic acids respectively), consistent with the intact mass measurement which showed only IgG1 glycans with 2, 3, and 4 terminal sialic acids (see **Figure 3.2**). No glycopeptides were detected in the deglycosylated IgG1 sample, as was expected since the intact mass measurement shows no glycans attached to IgG1 (see **Figure 3.2**).

Second Order Derivative UV-VIS Spectroscopy. Second order derivative UV-VIS spectroscopy was performed to monitor changes in absorbance of aromatic residues in the modified IgG1 samples. Plots of second order derivatives of the absorption spectra for all IgG1 samples are shown in **Figure 3.4**. No significant change is observed, consistent with the absence of global structural change for any of the IgG1 samples.

Differential Scanning Calorimetry. Differential scanning calorimetry was used to assess the thermal stability of the IgG1 samples. Thermograms of the IgG1 samples examined in this work (**Figure 3.5**) show multiple transitions, the lower of which is assigned as thermal unfolding of the CH2 domain (T_m1), while the higher-temperature transitions ($T_m2/3$) are assigned as thermal unfolding of the Fab and CH3 domains.[29,30] No temperature change of either thermal transition was observed for the hypergalactosylated IgG1 as compared to unmodified IgG1, while deglycosylated IgG1 had noticeably lower T_m1, consistent with a previous study.[31] Interestingly, hypersialylated IgG1 had slightly lower temperatures for both transitions, with the downward shift of the higher-temperature transition being more pronounced. Regardless of the reason for the modest decrease of Tm2 in the hypersialylated IgG1, it is not expected to have significant impact on its long-term stability.[30]

Biolayer Interferometry Binding Kinetics. A biolayer interferometry assay was used to measure the kinetics of IgG1 association to and dissociation from the FcRn fusion protein. The experimental curves (**Figure 3.6**) were fitted using a 1:1 binding model to generate association and dissociation rate constants (k_{on} and k_{off}), as well as the dissociation constant (K_D, calculated as k_{off}/k_{on}) [32]. The calculated K_D values are presented in **Table 3.3**. The reaction control IgG1 sample did not show a change in its K_D value as compared to the unmodified IgG1. Deglycosylated IgG1 was found to have a modest increase in K_D, while both hypergalactosylated and hypersialylated IgG1 samples showed a modest decrease in K_D values.

Fcγ Receptor Binding. AlphaScreen-based competitive FcRn, FcγRIIa, and FcγRIIIa assays were used to measure the relative potency for each modified form of the IgG1 (compared to the unmodified IgG1). The results are shown in **Figure 3.7** and **Figure 3.8**. Deglycosylated and hypergalactosylated IgG1s were observed to have a decrease of their relative potency for FcRn. Conversely, the reaction control and hypersialylated IgG1s were

observed to have an increase of their relative potency for FcRn. Deglycosylated IgG1 was not observed to bind either FcγRIIa or FcγRIIIa. Hypergalactosylated and hypersialylated IgG1 showed a minor decrease and increase of its relative potency for FcγRIIa and FcγRIIIa, respectively.

3.4 Discussion

The goal of this study was to understand how specific changes to this IgG1 glycan chain affect both biophysical properties of the protein and its ability to bind to Fc receptors. To that end, fully deglycosylated, hypergalactosylated, and hypersialylated IgG1 molecules were prepared enzymatically, and their structural and receptor-binding characteristics were assessed using a variety of biophysical tools and compared to those of intact (unmodified) IgG1. Successful modification of the glycan chains was verified by measuring the mass of intact IgG1 molecules with ESI MS [33,34] (**Figure 3.1**), as well as profiling glycopeptides in the Lys-C map of each glycoform of IgG1, including the unmodified molecule. In addition to modifying the glycan chains, the enzymatic treatment of the IgG1 sample may inadvertently introduce unintended non-enzymatic PTMs (such as oxidation, deamidation and glycation). Among the several non-enzymatic PTMs that frequently affect monoclonal antibodies during both production and storage, oxidation is particularly critical in the context of this study. First, extensive oxidation is known to have a negative impact on the conformational integrity of proteins [35-37]. Second, oxidation of both methionine residues at the FcRn binding interface (Met^{252} and Met^{428}) is known to be detrimental to FcRn binding [24-26]. Should the extensive oxidation occur during the enzymatic treatment of IgG1, the resulting instability of the protein and/or its inability to interact with FcRn might be incorrectly correlated with a particular structural feature of the glycan chain. Both the occurrence and the extent of non-enzymatic PTMs were determined by careful examination of the Lys-C peptide maps for each of the glycoforms. No significant increase in non-enzymatic PTMs (deamidation or oxidation) were observed that would be detrimental to the stability of IgG1 or its ability to bind FcRn. Indeed, it would require the oxidation level for Met^{252} and Met^{428} to exceed 50% (a recent study failed to observe a significant difference in serum clearance profiles between the intact IgG1 and its modified version in which the oxidation level of one of the key Met residues was 50% [25]).

The absence of extensive non-enzymatic PTMs triggered by glycan chain modification procedures in IgG1 samples is important, as it allows all observed changes in the stability of the higher order structure, as well as receptor-binding characteristics of the modified protein samples to be attributed directly to the change in the glycan structure. The only exception is the deamidation observed in the fully deglycosylated IgG1, where elevated deamidation levels were observed (**Table 3.1**). The affected residue (Asn^{322}) are located near the FcRn binding interface of the antibody (see **Figure 3.1**) and are highly unlikely to have any influence on its association with either of the Fcγ receptors examined in this work; there are no reports of deamidation in this region of the IgG1 Fc having any impact on FcRn binding.

Second-order derivative UV-VIS does not provide any indication of a tertiary structure change for any of the modified IgG1s (**Figure 3.4**). Second order derivative UV-VIS spectroscopy is a sensitive probe of the environment of aromatic side chains in protein molecules.[38,39] These residues are present in all domains of the molecule (see the inset in **Figure 3.4**, where positions of Tyr, Phe and Trp residues are shown within the IgG1 structure), lending them a useful probe of the changes in conformational integrity.[40] Therefore, absence of any changes in the second order derivative UV-VIS absorption spectra provides a strong indication that there are no significant (large-scale) conformational changes. Consistent with this conclusion, changes in the glycan composition (including complete deglycosylation) did not result in a detectable change in the elution time of the IgG1 monomer peak in SEC chromatograms (Table S1 in Supplementary Material), suggesting the consistency of the hydrodynamic radius across the different variants studied. Furthermore, the extent of dimerization (based on the relative abundance of the dimer peak in the SEC chromatograms) is also unaffected by the composition of the glycan chain. This provides a strong indication that the aggregation propensity of the IgG1 molecules (which is commonly thought of as being linked to the changes in the higher order structure) [41-43] is not altered by either modification or removal of the glycans. Deglycosylation can have a profound negative effect on the solubility of many proteins [44,45] (a loss of even a single glycan chain may lead to significant aggregation [46]); furthermore, removal of the glycan chains has been shown to have a detrimental effect on the stability of the CH2 domain of an antibody under acidic conditions [47]. However, we

have not observed any loss of solubility for the antibody molecule after deglycosylation at physiologically relevant pH; this should not be surprising, given the unusual "inward" orientation of the glycan chains within the native conformation of the homo-dimeric IgG1 molecule, where it can hardly act as a solubility enhancer.

While the higher order structure of the IgG1 molecules does not appear to be compromised as a result of its complete deglycosylation, the conformational stability does change upon removal of the glycan chains. DSC measurements clearly demonstrate a significant (> 5^{O}C) decrease of Tm1 in the deglycosylated IgG1 sample compared to the unmodified molecule (**Figure 3.5**). This transition is usually interpreted as thermal unfolding of the CH2 domain,[30] and the dramatic decrease in the melting temperature of this domain upon the complete removal of glycans suggests that the inward orientation of the glycans within the homo-dimer enhances its stability by providing additional interactions between the two units forming the homo-dimeric structure. While it might be tempting to speculate that the increased level of deamidation in the CH2 domain observed in the deglycosylated IgG1 sample may also contribute to decreased thermal stability, a significant fraction of the IgG1 molecules in this sample are not affected by deamidation. Should this PTM result in loss of thermal stability, a split peak would be observed in the thermogram representing both deamidated (Asp^{322}) and intact (Asn^{322}) populations; in contrast to this, a single well-defined peak is observed in the Tm1 region of the thermogram, indicating that the entire ensemble of the deglycosylated IgG1 molecules suffers from the decrease of thermal stability. Above and beyond the CH2 domain, deglycosylation does not appear to affect the thermal stability of the IgG1 molecule (no shift in Tm2/3 is evident in **Figure 3.5**), consistent with the notion that the stabilizing effects of the glycan chains are localized within the CH2 domain and to not affect thermal stability of either CH3 or Fab regions of the molecule.

Hypergalactosylation does not result in any detectable changes in either T_m1 or $T_m2/3$, which is hardly surprising given the relatively modest increase of the length of the glycan chain (compared to the unmodified IgG1). On the other hand, hypersialylation of IgG1 does give rise to modest, but detectable shifts of both T_m1 and $T_m2/3$ (**Figure 3.5**). The slight (*ca*. 1.5 ^{O}C) decrease in Tm1 is not surprising, as the introduction of two to four negative charges within the relatively small interstitial space between the two CH2

domains is likely to exert at least some destabilizing effect due to Coulombic repulsion. Intriguingly, the effect of the electrostatic repulsion is also felt outside of the CH2 domains, as indicated by a modest decrease of $T_m2/3$ (ca. 2 ^{O}C) compared to all other IgG1 samples. This modest decrease of $T_m2/3$ is suspected to be destabilization of the CH3 domain due to the proximity of the glycan chain.

Even though the DSC measurements clearly demonstrate a modest decrease of thermal stability of IgG1 following hypersialylation, these changes are too small to have a measurable negative impact on the protein stability at either room or body temperature. Furthermore, even though the CH2 domain appears to be sensitive to the effects of hypersialylation, neither FcRn nor FcγRIIA/FcγRIIIA binding is affected by hypersialylation (for which the binding interfaces are located in the CH2/CH3 and the CH2/lower hinge regions, respectively [23]), as demonstrated by the results of the biolayer interferometry and the AlphaScreen measurements. FcRn is responsible for the long half-life of IgG1 molecules in circulation (by rescuing them from lysosomal degradation in macrophages [8], which is the major clearance route for large proteins in circulation), while the FcRγ receptors are responsible for activation of the immune system. Highly sialylated IgG1 molecules have been shown to possess anti-inflammatory properties [48-50]. The absence of any measurable influence of sialylation on IgG1, interaction with either FcRn or γ-type Fc receptors demonstrated in this work, suggests that hypersialylation can be exploited for therapeutic purposes without a significant impact on PK characteristics of antibodies, at least with respect to the receptors explored in this work.

All biophysical characteristics of hypergalactosylated IgG1 assessed in this work remain unchanged compared to the intact (unmodified) antibody, and its ability to interact with FcγRIIA and FcγRIIIA is also preserved. This also has important practical implications, as the increase in the content of terminal galactose residues of antibodies' glycan chains is known to be correlated with greater complement dependent cytotoxicity as a result of greater affinity for C1q [51]. The results of our work suggest that this trait may be exploited for therapeutic purposes without compromising PK and PD profiles of the antibody.

Biolayer interferometry and AlphaScreen assays for FcRn displayed similar trends with relative potency and affinity (**Figure 3.7** and **Table 3.3)** for all modified samples excluding

hypergalactosylated IgG1mAb. Hypergalactosylated showed contradictory results with a lower relative potency (AlphaScreen) and higher affinity (biolayer interferometry) as compared to the unmodified IgG1 but the minor changes observed are likely within the range of assay variability and are not significant. Deglycosylated IgG1 was observed to have the largest change in both assays but it has been previously reported that deglycosylated IgG1s do not have a different *in vivo* half-life [52-54]. None of the observed changes in relative potency and K_D values are expected to manifest in a detectable change in the half-lives for any of the modified mAbs.

The AlphaScreen assays for FcγRIIA and FcγRIIIA showed changes in the relative potency for hypergalatocylated and hypersialylated IgG1 (see **Figure 3.8**). These changes, however, are relatively minor compared to those that are known to elicit observable changes in the *in vivo* behavior of IgG1. For example, afucosylated IgG1 is reported to have a fifty-fold affinity increase towards FcγRIIIA, and exhibited a higher antibody dependent cellular cytotoxicity [21]. The magnitude of the changes observed for both hypergalactosylated and hypersialylated forms of the IgG1 is not significant enough to result in measureable changes *in vivo*. Additionaly, deglycosylated IgG1 was not observed to bind either FcγRIIA or FcγRIIIA. Consistent with earlier reports [19,20], this inability for deglycosylated IgG1 to interact with either FcγRIIA or FcγRIIIA is expected to eliminate its ability to activate immune cells expressing these receptors.

Perhaps the most important observation related to IgG1 glycoforms' interactions with Fc receptors is a complete loss of the ability of the deglycosylated IgG1 to interact with FcγRIIA and FcγRIIIA receptors, while maintaining FcRn affinity A modest decrease in FcRn affinity for deglycosylated mAbs had been reported previously [55] and the complete obliteration of their ability to associate with FcγRIIA or FcγRIIIA is also consistent with the previously published work [12]. However, it seems puzzling that the complete removal of the glycan chains from the IgG1 molecule (a process which is shown in our work to have a negative influence on conformational stability of the CH2 domain) exerts such vastly different effects on its interactions with two Fc receptors (modest decrease of FcRn binding and completely obliterating γ-receptor binding), even though each relies on CH2's structure to provide a part of a binding interface (see **Figure 3.1**). A more detailed study would be needed to understand the differential effect of the glycan chains on the

stability/integrity of different parts of the CH2 domain that are involved in the interactions with these two different types of Fc receptors. Regardless of the specific mechanisms involved in attenuating the receptor-binding properties, this behavior of glycan-free antibodies makes them highly attractive as vehicles in targeted drug delivery applications, where both the long half-life and the absence of immune response are needed. The former would be guaranteed by conformational integrity of the molecule at both room and body temperature, as well as enhanced interactions with a "rescue" receptor (FcRn), while the latter (an abrogated effector function) is ensured by the lost ability to interact with the γ-type Fc receptors, thereby avoiding an undesirable immune response. While disrupting a mAb's interaction with FcγR's can be readily achieved by mutating key residues in the binding interface located in the CH2/lower hinge region, an unintended consequence of this could be an immune response to the neo-epitope not present in the wild-type molecule; elimination of the glycan chain might provide an alternative approach to this problem that would not trigger productions of the neutralizing antibodies by the host.

The study of the impact of glycosylation attributes on specific IgG functions can be leveraged for risk assessments of therapeutic mAbs. The risk assessment performed on product quality attributes of biopharmaceuticals (see ICH Q8(R2) and Q11) requires assessment of the potential impact of different attributes on a drug's efficacy, pharmacokinetic properties, and safety [56,57]. These risk assessments can help inform process development, and enable an analytical control strategy that can be used to ensure proper control of critical quality attributes (CQAs) within the process. Often, structure-activity relationship studies are performed to provide relevant data to help inform these risk assessments to understand which product attributes are most critical. Previous studies have shown the criticality of specific glycan species such as afucosylated glycans and high mannose glycans on effector function via the FcγRIIIa pathway [17,18]. This study queried the potential impact of elevated levels of terminal galactose or terminal sialic acid on Fc receptor interactions. In both cases, no significant impact was observed. The data shown here provides important context when assessing the criticality of IgG1 glycosylation, in terms of any potential impact on PK and effector function.

3.5 Conclusions

Three different glycan-modified forms of mAb (deglycosylated, hypergalactosylated and hypersialylated) were produced and characterized alongside the intact mAb molecule. Biophysical measurements have not revealed any changes that would be indicative of alterations in the higher order structure of the mAb or increased aggregation propensity for any of the three forms compared to the intact mAb, although reduced thermal stability in the CH2 domain was observed for the fully deglycosylated form by DSC. The deglycosylated mAb showed a modest decrease in FcRn affinity (though not expected to affect its half-life) while having no binding to FcγRIIa and FcγRIIIa. Depending on the mechanism of action required for a mAb, an aglycosylated or deglycosylated mAb may be attractive for use if effector functions are undesirable while retaining a long half-life. No significant changes were noted for binding of the hypergalactosylated and hypersialylated forms of IgG1 to both FcRn, FcγRIIA, and FcγRIIIA suggesting that neither the half-life in circulation nor the ability to induce an immune response are affected by these modifications of the glycan chains. The results described provide valuable information regarding the criticality of IgG1 galactosylation and sialylation that can be leveraged during risk assessments and process characterization studies. These attributes may also be of interest to researchers using a therapeutic mAb with a high percentage of terminal galactose and or sialylated glycan chains.

3.6 Experimental

IgG1 Deglycosylation. IgG1 was buffer exchanged into a 100 mM tris-acetate buffer (pH 7.5). 20 mg of IgG1 was added to a 1.5 mL vial with 10 µL of PNGase F (500,000 U/mL, New England Biolabs, Ipswich, MA) and diluted up to 600 µL with 100 mM tris-acetate buffer (pH 7.5). The sample was incubated in a water bath at 37 ^{o}C for 24 hours. After incubation, deglycosylated IgG1 was buffer exchanged into a 50 mM MOPS buffer (pH 7.2) and stored at -80 ^{o}C.

IgG1 Hypergalactosylation. IgG1 was buffer exchanged into a 100 mM tris-acetate buffer (pH 7.5). 20 mg of IgG1 was added to a 2 mL vial with 10 µL of $MnCl_2$ (10 mM), 200 µL UDP-Galactose (EMD Millipore Corp., Billerica, MA) (25mg/mL), and 250 µL galactosyltransferase (Sigma-Aldrich Co., St. Louis, MO) (2 U/mL). The volume of the solution was adjusted to 1000 µL with 100 mM tris-acetate buffer (pH 7.5) and incubated

in a water bath at 37 ^{o}C for 24 hours. After 24 hours, 10 µL of a 10 mM solution of $MnCl_2$ (Fisher Scientific, Hampton, NH), 5 mg UDP-Galactose (25 mg/mL), and 0.5 units of galactosyltransferase (2 U/mL) were added to vial and incubated in a water bath at 37 ^{o}C for an additional 24 hours. After incubation, hypergalactosylated IgG1 was purified by size exclusion chromatography to remove excess reagents. Hypergalactosylated IgG1 was buffer exchanged into a 50 mM MOPS buffer (pH 7.2) and stored at -80 ^{o}C.

IgG1 Hypersialylation. IgG1 was first hypergalactosylated as described above, since the sialyltransferase used will only add sialic acid to glycan chain with a terminal galactose. Two hypersialylation reactions were run in parallel as follows: 12.5 mg of hypergalactosylated IgG1, 30 mg of CMP-Sialic Acid, and 0.5 mg sialyltransferase (Roche Life Science, Penzberg,Germany)(5.7 mg/mL) were added to a 2 mL vial. The volume of the solution was adjusted to 1500 µL with 100 mM tris-acetate buffer (pH 7.5) giving the final concentration of the enzyme 0.33 mg/mL. and incubated in a water bath at 37 ^{o}C for 8 hours. After incubation, hypersialylated IgG1 was purified by size exclusion chromatography to remove excess reagents. Hypersialylated IgG1 was buffer exchanged into a 50 mM MOPS buffer (pH 7.2) and stored at -80 ^{o}C.

Size Exclusion Chromatography. Size exclusion chromatography (SEC) measurements were carried out using an Agilent 1100 HPLC system (Agilent Technologies, Santa Clara, CA). IgG1 samples (100 µg total protein mass) were individually injected onto an SEC column (Tosoh TSKgel G3000SWxl, Tosoh, Tokyo, Japan) using a 150 mM ammonium acetate buffer (pH 6.8) with at a 1 mL/min flow rate. Absorbance was monitored at 280 nm and peaks were integrated manually using ChemStation software (Agilent Technologies).

Mass Spectrometry. Electrospray ionization mass spectrometry (ESI MS) was used to monitor modification or complete removal of the IgG1 glycan chain by measuring intact protein mass. IgG1 samples (50 µg) were injected onto a MassPREP online desalting (Waters, Milford, MA) column and using a two mobile phase gradient (A: H_2O, 0.1% (v/v) formic acid B: 10:90 (v/v) H_2O/ acetonitrile, 0.1% (v/v) formic acid). The eluting protein fraction was collected for ESI MS analysis. A SolariX 7 (Bruker Daltonics, Billerica, MA) Fourier transform ion cyclotron resonance mass spectrometer (FT ICR MS) with a 7.0 T superconducting magnet was used to acquire MS data of desalted IgG1 samples.

Lys-C Peptide Mapping. IgG1 samples were digested with a Lys-C protease (Wako Pure Chemical Industries, Richmond, VA) and reversed phase (Agilent Zorbax 300-SD-C18) liquid chromatography (HP 1100, Agilent Technologies, Santa Clara, CA) coupled with a SolariX 7 FT ICR MS was used to generate peptide maps. Solution aliquots containing 5 μg of peptides (total peptide mass) were injected onto the C18 column and eluted using a two mobile phase gradient (A: H_2O, 0.1% (v/v) formic acid B: 10:90 (v/v) H_2O/acetonitrile, 0.1% (v/v) formic acid). Each peptide map was used to detect occurrence and evaluate the extent of two specific non-enzymatic PTMs (oxidation and deamidation). The presence of glycopeptides was also monitored to confirm the addition of sugars to the glycan chain. Peak areas for various PTMs were integrated manually using built-in data analysis software to calculate their relative abundance.

Second Order Derivative UV-VIS Spectroscopy. Normalized second order derivative UV-VIS absorbance spectra of the protein samples were calculated based on the absorbance measurements carried out over a wavelength range of 200 nm to 600 nm using Agilent Technologies (Santa Clara, CA) 8453 spectrophotometer.

Differential Scanning Calorimetry (DSC). DSC thermograms were obtained with a MicroCal VP DSC (Malvern, Westborough, MA) in the temperature range from 25 ^{o}C to 100 ^{o}C at a 200 ^{o}C/hour scan rate and analyzed using Origin 9.0 (Origin Lab, Northampton, MA).

FcRn binding assessment by Biolayer Interferometry. FcRn-Fc fusion protein: FcRn-huM4Fc, a soluble dimeric Fc binding protein was constructed by genetically fusing the extracellular domain of a neonatal receptor with the Fc region of an IgG1 antibody, as described in US 8,618,252 B2[58] (Farrington et al., Biogen Idec, Cambridge, MA) to use as reagent in the binding assays. FcRn-huM4Fc is a FcRn-Fc fusion protein, consisting of two beta-2-microglobulin and two FcRn alpha-Fc fusion chains, where the Fc region was mutated by site-directed mutagenesis from the wild type sequence at residues 388, 389, 511, and 512 to eliminate the likelihood of the FcRn-huM4Fc binding to itself.

Biotin-FcRn-Fc: FcRn-huM4Fc was biotinylated using ChromaLink Biotin (catalog # B-1001-1005, Solulink, San Diego, CA) at a biotin/protein molar ratio of 3/1 following manufacturer's procedure.

Biolayer Interferometry: A fortéBio Octet® QKe system and streptavidin (SA) biosensors (cat# 18-0009) were purchased from Pall ForteBio Corp. (Menlo Park, CA). This instrument was used to study kinetics of IgG1 protein samples binding to FcRn. The assays were performed in solid black 96-well plates (Greiner Greiner Bio-One, cat #65520), using streptavidin biosensors (SA), with agitation set at1000 rpm, and temperature set at 30°C. All reagents were diluted in assay diluent containing MES Buffer, pH 5.8, supplemented with 150mM NaCl, 1.0% BSA Bovine Serum Albumin (BSA), and 0.02% Polysorbate-20. Biotin- FcRn at 5µg/ml was used in a loading step for 300 seconds to bind FcRn to the SA-biosensor surface. A 60 seconds biosensor washing step was applied prior to the association of the IgG1 protein samples to FcRn on the biosensor. All samples were tested at the same concentrations, 33.3 nM, 16.7 nM, and 8.33 nM, 4.17nM, with an association step of 150 seconds, and a dissociation step of 100 seconds. Experimental data was fit with the 1:1 binding model and was analyzed with global fitting using Octet software (v. 7.1) to calculate k_{on} and k_{off} rates.

FcRn binding assessment by by AlphaScreen®screen. A competition assay was used to measure the relative potency for each modified mAb for FcRn binding. Biotin-FcRn-Fc: FcRn-huM4Fc was biotinylated using ChromaLink Biotin (catalog # B-1001-1005, Solulink, San Diego, CA) at a biotin/protein molar ratio of 20/1 following manufacturer's procedure. AlphaScreen® beads (streptavidin-coated donor beads and Human IgG1-conjugated acceptor beads) were purchased from Perkin Elmer, Waltham, MA. MES (N-morpholine ethanesulfonic acid) buffer, pH 5.8, supplemented with 150mM NaCl, and 0.1% Bovine Serum Albumin (BSA) was used as a binding assay diluent.

AlphaScreen®-based FcRn competitive binding assay was performed as described in elsewhere [32], using the following reagents: biotin–FcRn (0.6 µg/mL), hIgG1-conjugated acceptor beads (10µg/mL), and streptavidin-coated donor beads (20µg/mL), final concentrations. This assay is based on the competition between the Fc-fusion protein and hIgG1-conjugated to acceptor beads for binding to biotin-FcRn. Biotin–FcRn and the Fc-fusion protein samples were incubated for 30 minutes, followed by the addition of hIgG1-acceptor beads and 30 minutes incubation, and a final step with addition of streptavidin-donor beads and incubation for 60 minutes. All incubations were done in the dark with

shaking at 22° C. All reagents were diluted in assay diluent containing. Plates were read on EnVision Multilabel 2101, (Perkin Elmer, Waltham, MA). Each sample was tested in triplicates. Parallel Line Analysis software (Stegmann Systems, Germany) was used to assess the linearity, parallelism, and potency of the sample in relation to the standard.

FcγRIIa and FcγRIIIa binding assessment by AlphaScreen®screen. A competition assay was used to measure the relative potency for each modified mAb for FcγRIIa and FcγRIIIa binding.

FcγRIIa and FcγRIIIa reagents: Glutathione-S-Transferase (GST)-FcγRIIa and GST-FcγRIIIa were constructed at Biogen (Cambridge, MA).

AlphaScreen® beads: Reduced Glutathione (GSH)-coated donor beads (Catalog # 6765302), and human IgG1-conjugated acceptor beads (custom made) were purchased from Perkin Elmer, Waltham, MA.

FcγRIIa Binding assay diluent: 50 mM Tris Buffer, pH 7.2, supplemented with 25 mM NaCl, 0.1% Bovine Serum Albumin (BSA), and 0.01% Tween-20.

FcγRIIIa Assay Diluent: PBS, pH 7.2, supplemented with 0.1% Bovine Serum Albumin (BSA), 0.01% Tween-20

AlphaScreen®-based FcγRIIa and FcγRIIIa binding assays: The assays are based on the competition between the IgG1 protein and hIgG1- conjugated to acceptor beads for binding to GST-FcγRIIa or GST-FcγRIIIa. The FcγRIIa and FcγRIIIa binding assays, were carried out in white ½ area 96-well plates (catalog #3693, Corning, Tewksbury, MA), using the following reagents: GST-FcγRIIa (6µg/mL) and GST-FcγRIIIa (10µg/mL), hIgG1-conjugated acceptor beads (2µg/mL), and GSH-coated donor beads (2µg/mL), final concentrations. The assays were performed as follows, IgG1 protein samples, hIgG1-acceptor beads, and GST-FcγRIIa, or GST-FcγRIIIa, were incubated for 2 hours in the dark with shaking at 22° C. All reagents were diluted in binding assay diluent. Plates were read on EnVision Multilabel 2101, (Perkin Elmer, Waltham, MA). Each sample was tested in triplicates. Parallel Line Analysis software (Stegmann Systems, Germany) was used to assess the linearity, parallelism, and potency of the sample in relation to a reference standard.

3.7 Acknowledgements

This work was supported in part by the President's Enhancement Funding from the Graduate School of the University of Massachusetts-Amherst. FT ICR mass spectrometer was acquired through the Major Research Instrumentation program (grant CHE-0923329 from the National Science Foundation), and is now a part of the Mass Spectrometry Core facility at UMass-Amherst.

3.8 Tables

Table 3.1. Relative levels of oxidation and deamidation of Lys-C peptide fragments.

Peptide #	Met^{34}	Met^{83}/ Met^{111}	Met^{259}	Asn^{322}	Met^{365}	Met^{435}
Unmodified IgG1	0.0%	2.5%	10.1%	2.4%	1.7%	6.6%
Reaction Control IgG1	0.0%	3.6%	10.3%	2.7%	2.4%	7.2%
Hypersialylated IgG1	0.0%	3.8%	12.6%	3.9%	3.0%	5.1%
Hypergalactosylated IgG1	0.0%	4.5%	14.3%	3.9%	3.0%	10.7%
Deglycosylated IgG1	0.0%	1.4%	6.8%	9.6%	1.0%	3.6%

Table 3.2. Relative abundance of various glycoforms present within the only glycopeptide ion (L19/20) detected in the entire complement of Lys-C peptide fragments.

Peptide #	G0	G1	G2	G2+SA	G2+2SA
Unmodified IgG1	59.5%	36.4%	4.1%	0.0%	0.0%
Reaction Control IgG1	64.6%	32.0%	3.4%	0.0%	0.0%
Hypersialylated IgG1	0.0%	0.0%	0.0%	62.6%	37.4%
Hypergalactosylated IgG1	0.0%	0.0%	100.0%	0.0%	0.0%
Deglycosylated IgG1	0.0%	0.0%	0.0%	0.0%	0.0%

Table 3.3. Values of k_{on}, k_{off}, and K_D for IgG1/FcRn interactions calculated from the biolayer interferometry assay.

Sample	K_D (M)	k_{on}(1/M*s)	k_{off}(1/s)	% Change
Unmodified IgG1	4.8E-09	9.2E+05	4.5E-03	100%
Reaction Control IgG1	4.7E-09	8.9E+05	4.2E-03	103%
Hypersialylated IgG1	4.0E-09	8.5E+05	3.4E-03	122%
Hypergalactosylated IgG1	4.4E-09	8.5E+05	3.7E-03	110%
Deglycosylated IgG1	5.9E-09	9.0E+05	5.3E-03	83%

Table 3.4. Retention time, %HMW, and %HMW change (as compared to unmodified IgG1) for each IgG1 sample.

Sample	Ret. Time (min)	%HMW	%HMW Increase
Unmodified IgG1	9.74	0.6%	--
Reaction Control IgG1	9.78	0.6%	0.0%
Hypersialylated IgG1	9.77	0.2%	-0.4%
Hypergalactosylated IgG1	9.79	0.3%	-0.3%
Deglycosylated IgG1	9.76	1.1%	0.5%

3.9 Figures

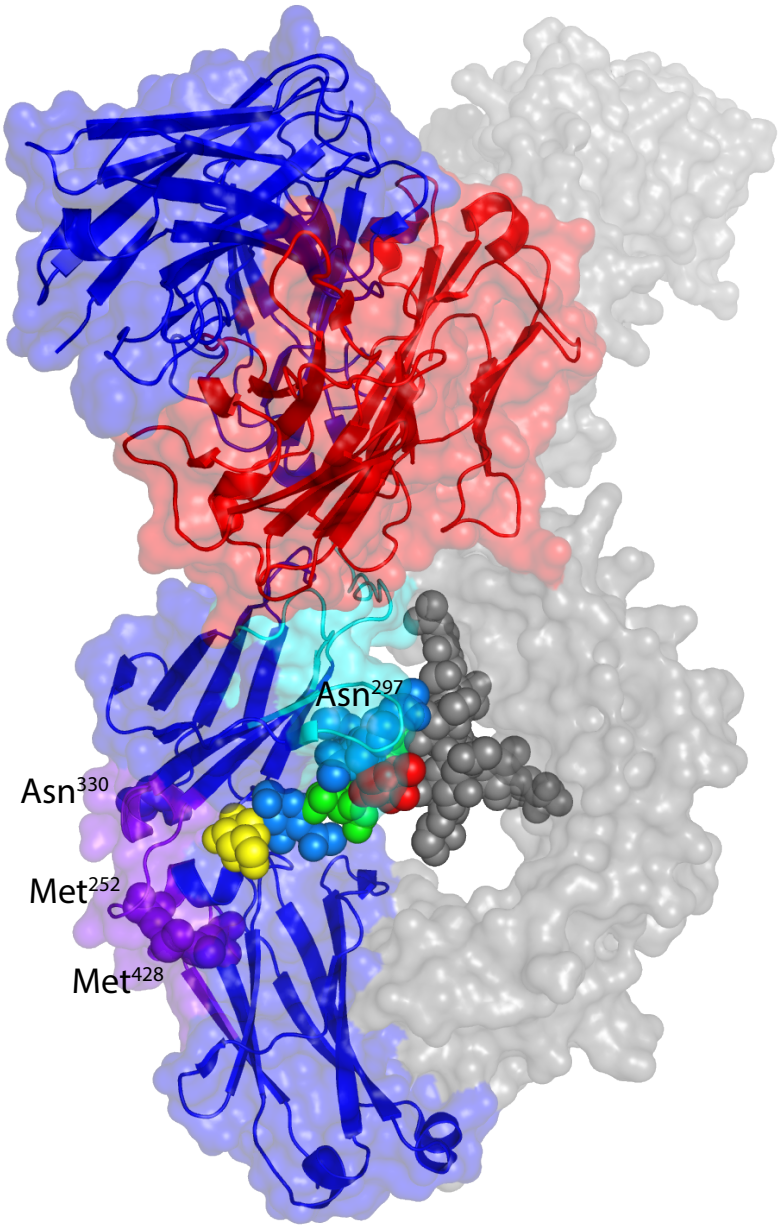

Figure 3.1. Schematic representation of IgG1 architecture based on 1HZH scaffold. The light chain is colored in red and the heavy chain is colored in blue (with FcRn binding interface highlighted in purple and FcRγ in cyan). The glycan chain is shown in spherical representation, and the secondary structure of the polypeptide chains is shown using common notations (strands, turns and helices). The side chains of two methionine residues and one asparagine residue prone to non-enzymatic PTM as shown in spherical representation.

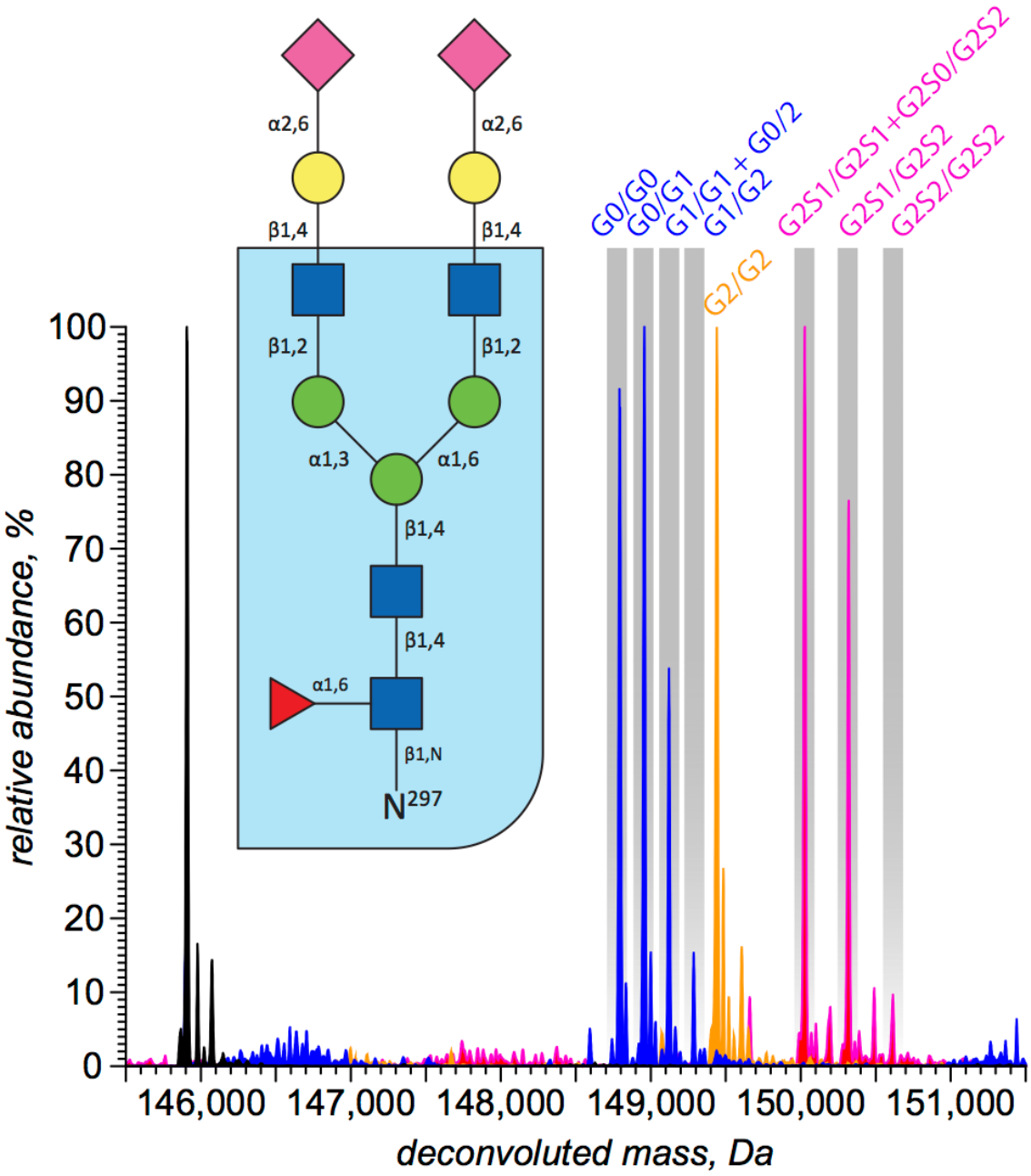

Figure 3.2. Deconvoluted mass spectra of intact (blue), fully-deglycosylated (black), hypergalactosylated (yellow), and hypersialylated (magenta) forms of IgG1. The inset shows the structure of the glycan chain.

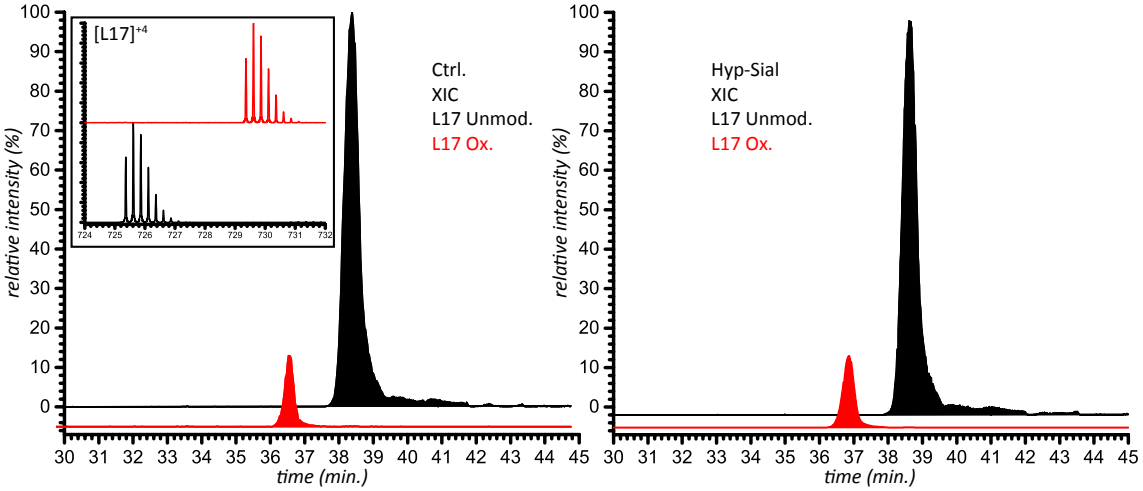

Figure 3.3. Extracted ion chromatograms for the two peptide ions representing intact (black) and oxidized (red) forms of Met^{252} (the corresponding mass spectra are shown in the inset). The peptides were produced by Lys-C digestion of the control (left panel) and hypersialylated IgG1 samples.

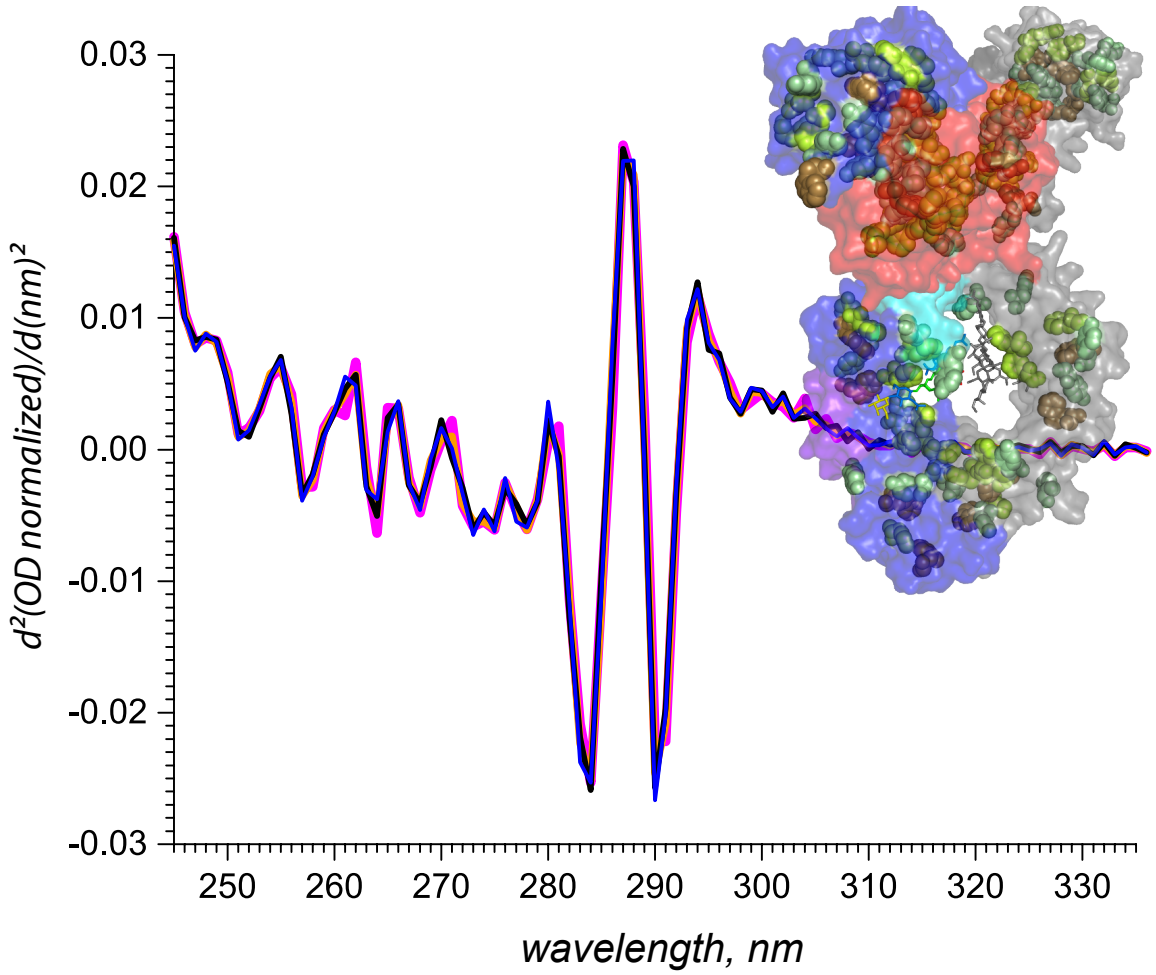

Figure 3.4. Plots of second derivatives of near-UV absorption spectra of intact (blue), fully-deglycosylated (black), hypergalactosylated (yellow), and hypersialylated (magenta) forms of IgG1. The inset shown distribution of aromatic residues within the IgG1 structure using 1HZH as a scaffold.

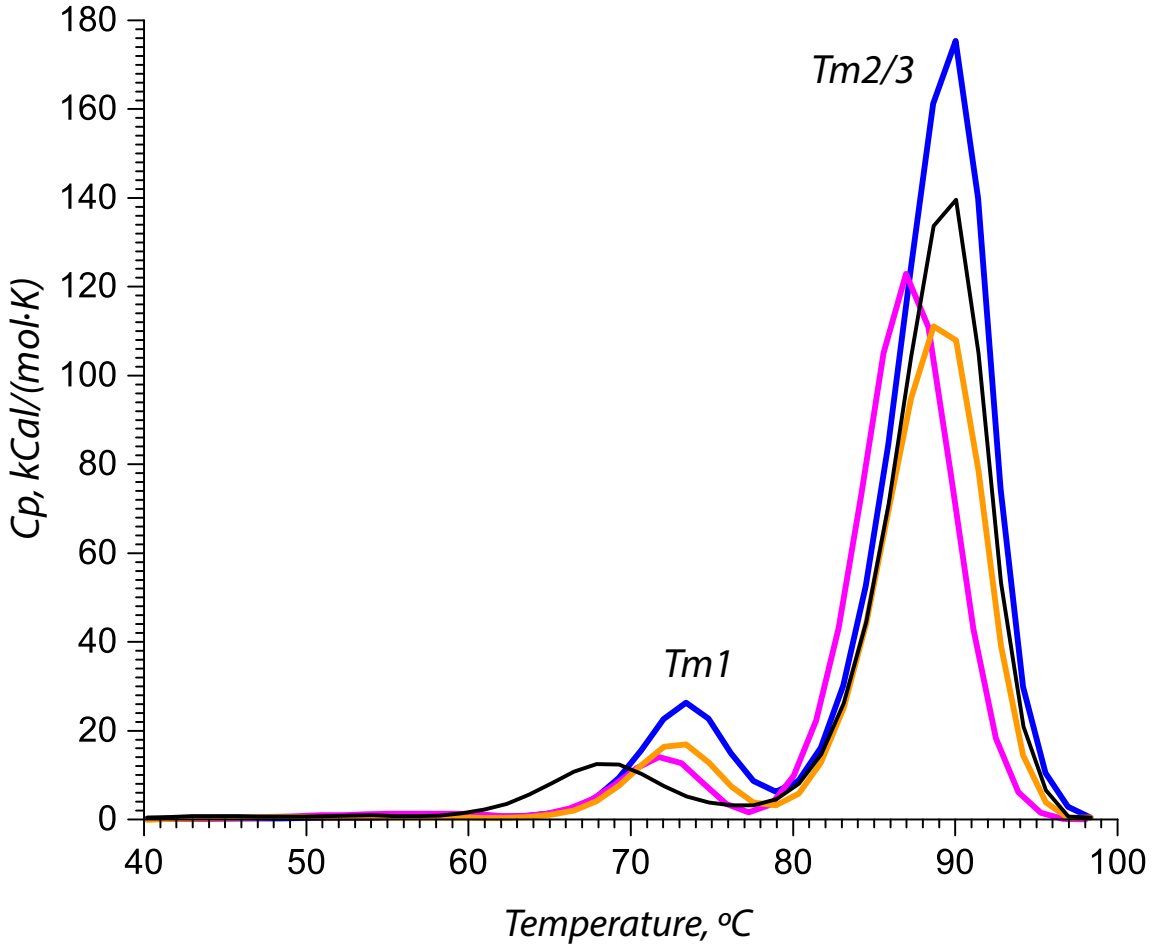

Figure 3.5. Overlay of DSC thermograms for intact (blue), fully-deglycosylated (black), hypergalactosylated (yellow), and hypersialylated (magenta) forms of IgG1 samples. T_m1 and $T_m2/3$ correspond to the CH2 and combined CH3/Fab melting points respectively. Deglycosylated IgG1 showed a decrease of its T_m1 which has been previously reported. Hypersialylated IgG1 is observed to have a global decrease of its melting points.

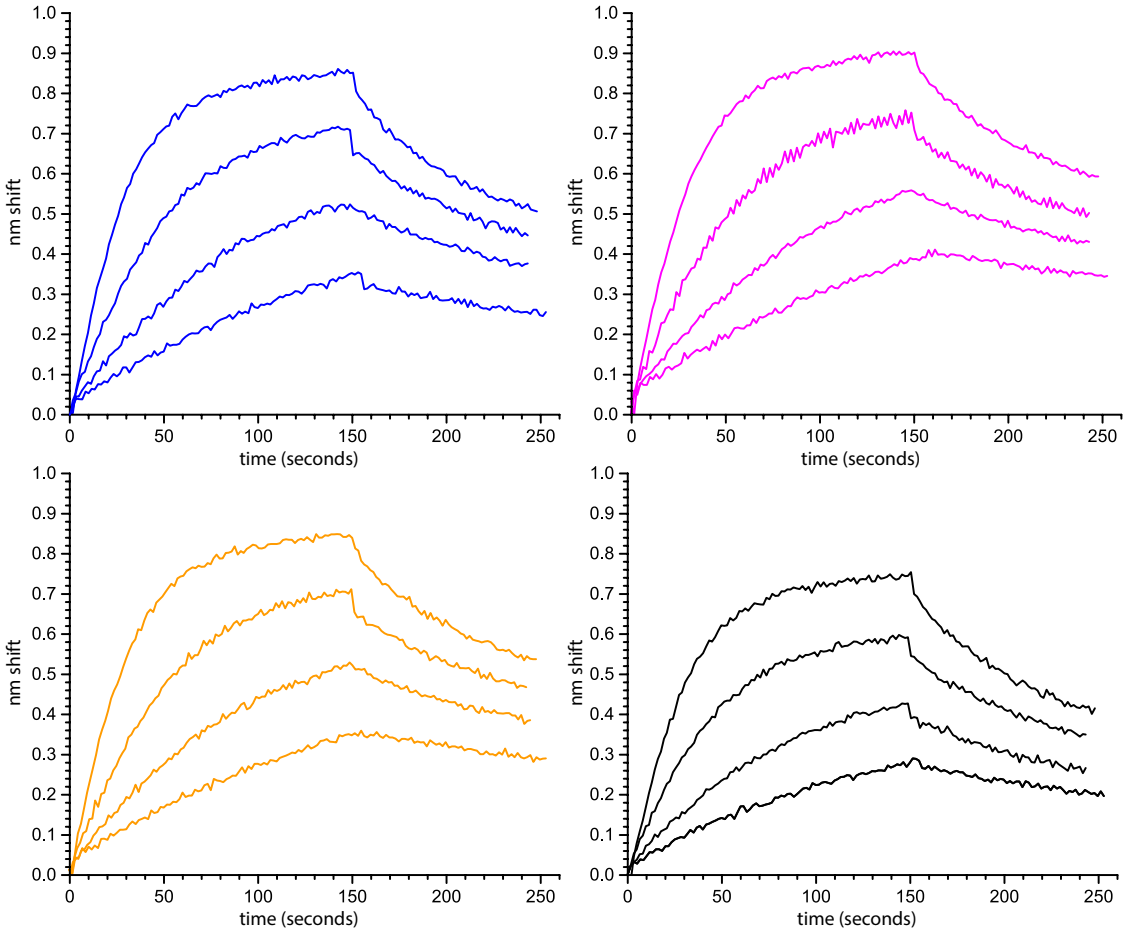

Figure 3.6. FcRn binding and dissociation curves for intact (blue), fully-deglycosylated (black), hypergalactosylated (yellow) and hypersialylated (magenta) forms of IgG1 obtained with a biolayer interferometry assay at 4.17, 8.33 nM, 16.7 nM, and 33.3 nM.

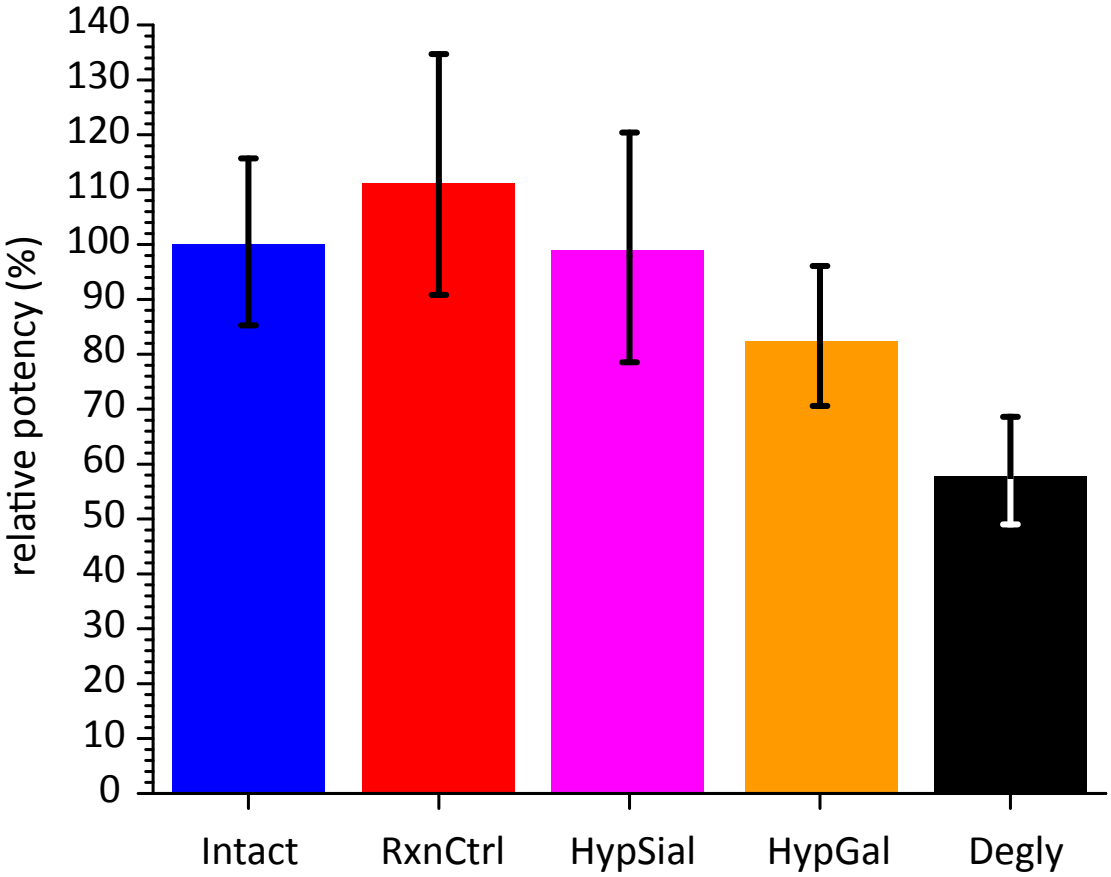

Figure 3.7. Bar graphs for intact (blue), reaction control (red), fully-deglycosylated (black), hypergalactosylated (yellow) and hypersialylated (magenta) forms of IgG1 binding to FcRn. Error bars correspond to the 95% confidence interval of each measurement. FcRn relative potency: intact (100%), reaction control (111%), fully-deglycosylated (58%), hypergalactosylated (82%) and hypersialylated (98%)

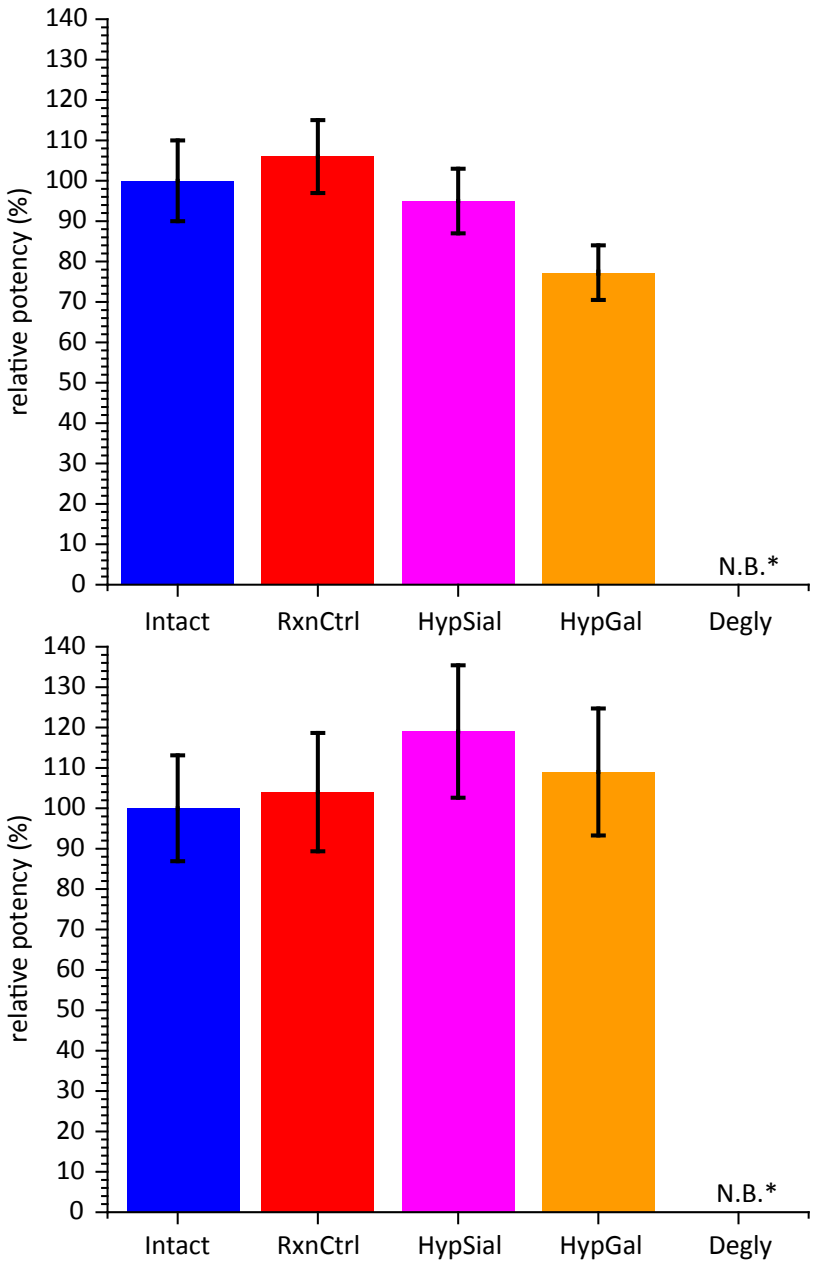

Figure 3.8. Bar graphs for intact (blue), reaction control (red), fully-deglycosylated (black), hypergalactosylated (yellow) and hypersialylated (magenta) forms of IgG1 binding to FcγRIIA (top) and FcγRIIIA (bottom). Error bars correspond to the 95% confidence interval of each measurement. FcγRIIA/ FcγRIIIA relative potency: intact (100%/100%), reaction control (106%/104%), fully-deglycosylated (N.B./N.B.), hypergalactosylated (77%/109) and hypersialylated (95%/119%)

3.10 Supplemental Figures

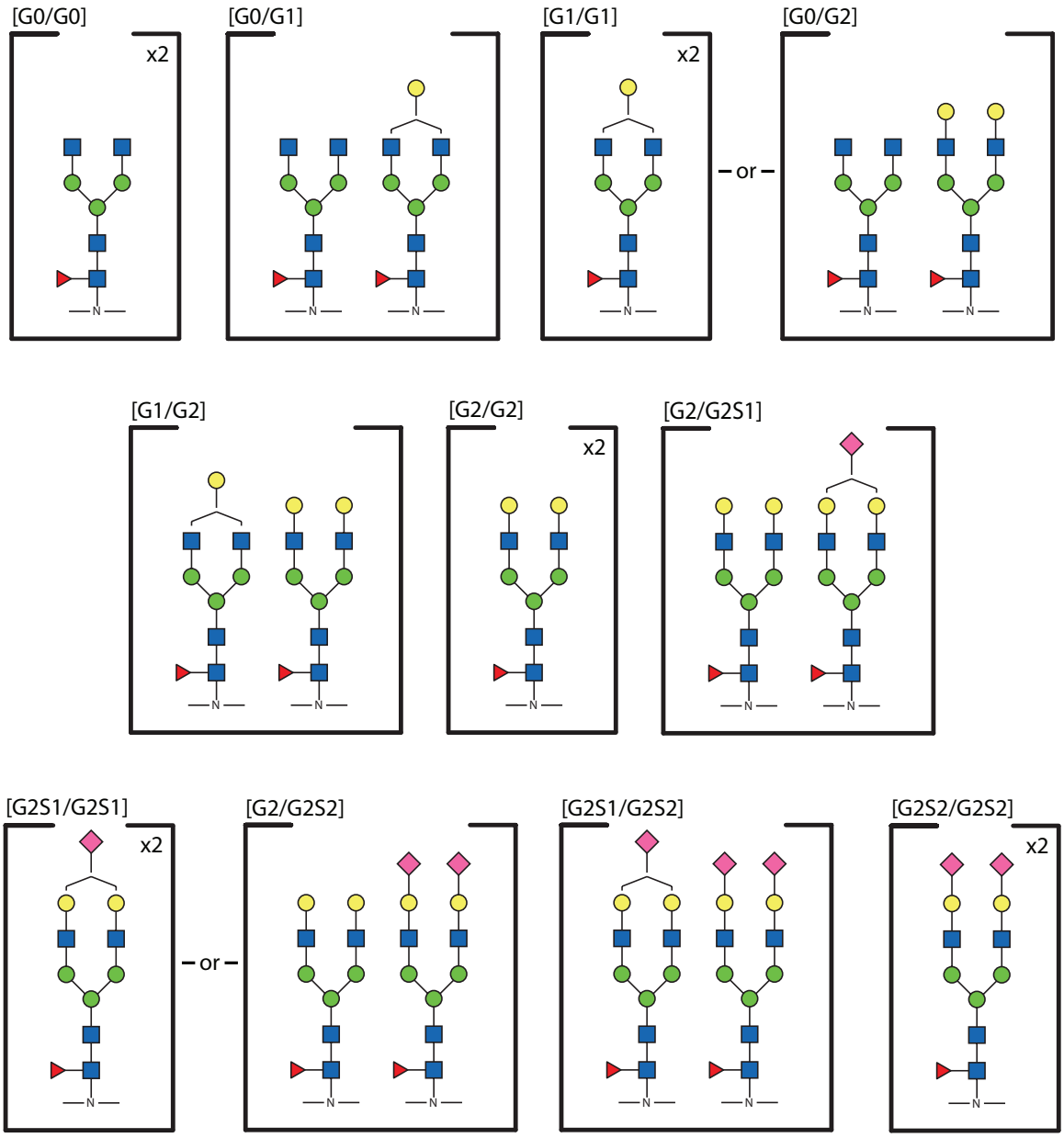

Figure S3.1. Naming convention for all observed carbohydrate chains attached to IgG1. G0/G0 is the core moiety of a complex glycan chain.

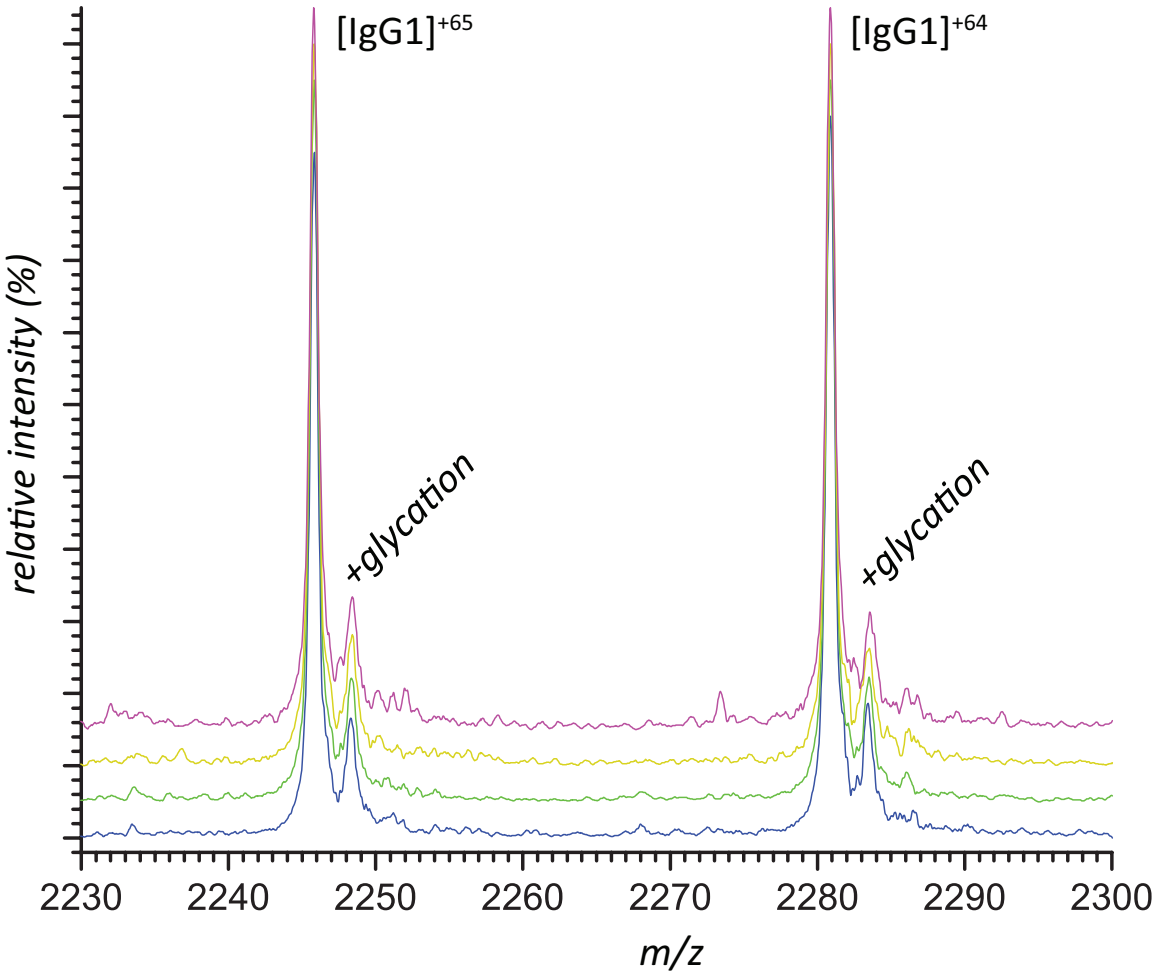

Figure S3.2. Intact (blue), reaction control (green), hyper-galactosylated (yellow), and hyper-sialylated (magenta) forms of IgG1 samples were deglycosylated and two charge states (+65/64) were looked at to assess if there increases of PTMs (glycation and oxidation).

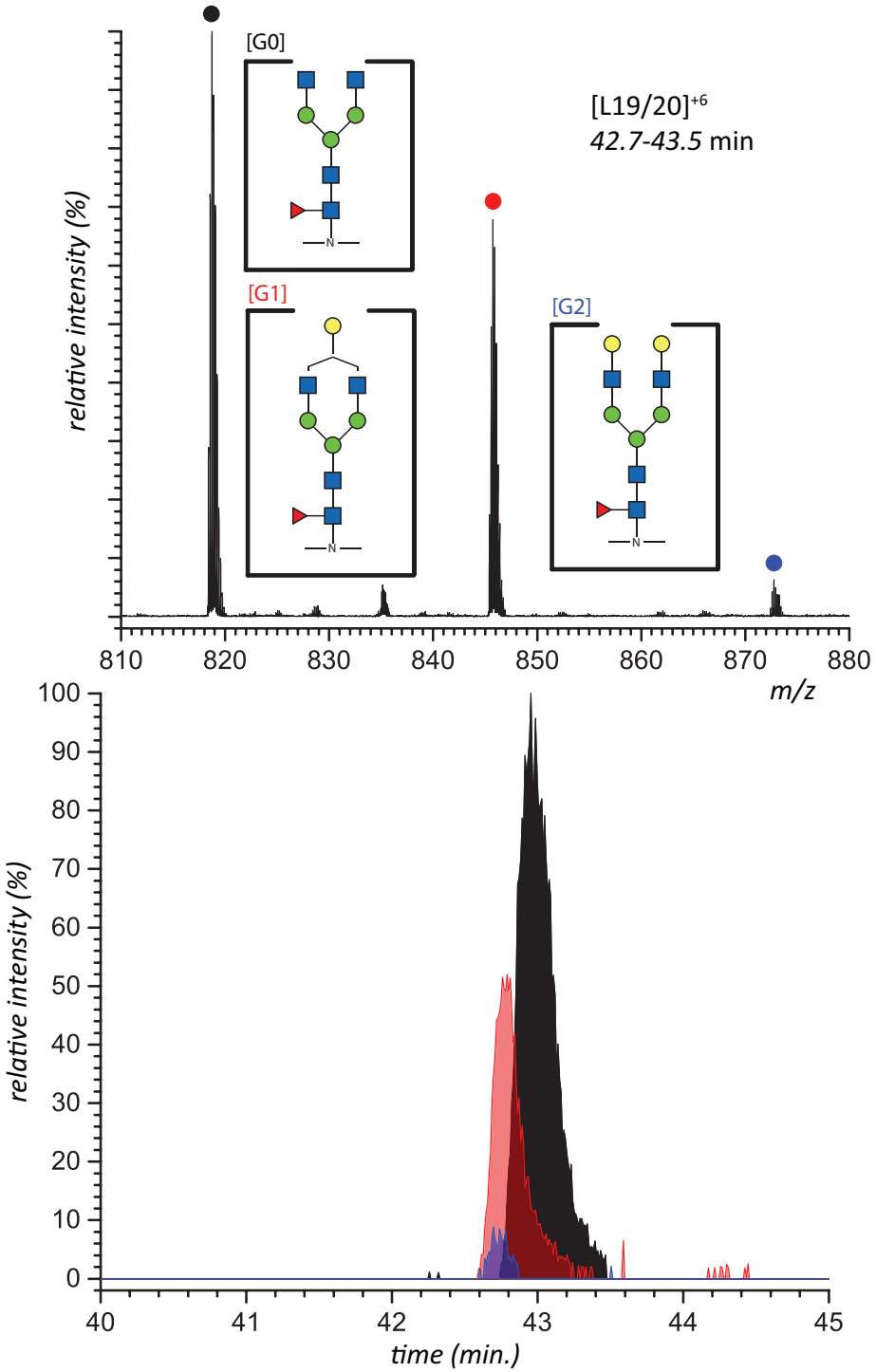

Figure S3.3. Representative extracted ion chromatograms and mass spectra for G0/G1/G2 glycopeptides.

3.11 References

1 Jefferis, R. Isotype and glycoform selection for antibody therapeutics. *Arch. Biochem. Biophys.* **526**, 159-166, doi:http://dx.doi.org/10.1016/j.abb.2012.03.021 (2012).

2 Irani, V. *et al.* Molecular properties of human IgG subclasses and their implications for designing therapeutic monoclonal antibodies against infectious diseases. *Mol. Immunol.* **67**, 171-182, doi:http://dx.doi.org/10.1016/j.molimm.2015.03.255 (2015).

3 Vidarsson, G., Dekkers, G. & Rispens, T. IgG subclasses and allotypes: from structure to effector functions. *Front. Immunol.* **5**, 520, doi:10.3389/fimmu.2014.00520 (2014).

4 Kapur, R., Einarsdottir, H. K. & Vidarsson, G. IgG-effector functions: "The Good, The Bad and The Ugly". *Immunol. Lett.* **160**, 139-144, doi:http://dx.doi.org/10.1016/j.imlet.2014.01.015 (2014).

5 Hogarth, P. M. & Pietersz, G. A. Fc receptor-targeted therapies for the treatment of inflammation, cancer and beyond. *Nat Rev Drug Discov* **11**, 311-331, doi:10.1038/nrd2909 (2012).

6 Caaveiro, J. M., Kiyoshi, M. & Tsumoto, K. Structural analysis of Fc/FcgammaR complexes: a blueprint for antibody design. *Immunol. Rev.* **268**, 201-221, doi:10.1111/imr.12365 (2015).

7 Suzuki, T. *et al.* Importance of neonatal FcR in regulating the serum half-life of therapeutic proteins containing the Fc domain of human IgG1: a comparative study of the affinity of monoclonal antibodies and Fc-fusion proteins to human neonatal FcR. *J. Immunol.* **184**, 1968-1976, doi:10.4049/jimmunol.0903296 (2010).

8 Roopenian, D. C. & Akilesh, S. FcRn: the neonatal Fc receptor comes of age. *Nat. Rev. Immunol.* **7**, 715-725 (2007).

9 Rath, T., Baker, K., Pyzik, M. & Blumberg, R. S. Regulation of Immune Responses by the Neonatal Fc Receptor and Its Therapeutic Implications. *Front. Immunol.* **5**, 664, doi:10.3389/fimmu.2014.00664 (2014).

10 Faucette, A. N., Pawlitz, M. D., Pei, B., Yao, F. & Chen, K. Immunization of pregnant women: Future of early infant protection. *Hum. Vaccin. Immunother.* **11**, 2549-2555, doi:10.1080/21645515.2015.1070984 (2015).

11 Bourdage, J. S. *et al.* Effect of double antigen bridging immunoassay format on antigen coating concentration dependence and implications for designing immunogenicity assays for monoclonal antibodies. *J. Pharm. Biomed. Anal.* **39**, 685-690, doi:https://doi.org/10.1016/j.jpba.2005.03.037 (2005).

12 Scallon, B. J., Tam, S. H., McCarthy, S. G., Cai, A. N. & Raju, T. S. Higher levels of sialylated Fc glycans in immunoglobulin G molecules can adversely impact functionality. *Molecular Immunology* **44**, 1524-1534, doi:http://dx.doi.org/10.1016/j.molimm.2006.09.005 (2007).

13 Alsenaidy, M. A. *et al.* Physical stability comparisons of IgG1-Fc variants: effects of N-glycosylation site occupancy and Asp/Gln residues at site Asn 297. *J. Pharm. Sci.* **103**, 1613-1627, doi:10.1002/jps.23975 (2014).

14 Anthony, R. M. & Ravetch, J. V. A novel role for the IgG Fc glycan: the anti-inflammatory activity of sialylated IgG Fcs. *Journal of clinical immunology* **30 Suppl 1**, S9-14, doi:10.1007/s10875-010-9405-6 (2010).

15 Crispin, M., Yu, X. & Bowden, T. A. Crystal structure of sialylated IgG Fc: Implications for the mechanism of intravenous immunoglobulin therapy. *Proc. Natl. Acad. Sci. U. S. A.* **110**, E3544-E3546, doi:10.1073/pnas.1310657110 (2013).

16 Anthony, R. M. *et al.* Recapitulation of IVIG anti-inflammatory activity with a recombinant IgG Fc. *Science* **320**, 373-376, doi:10.1126/science.1154315 (2008).

17 Raju, T. S. Terminal sugars of Fc glycans influence antibody effector functions of IgGs. *Curr Opin Immunol* **20**, 471-478, doi:10.1016/j.coi.2008.06.007 (2008).

18 Liu, L. Antibody glycosylation and its impact on the pharmacokinetics and pharmacodynamics of monoclonal antibodies and Fc-fusion proteins. *J. Pharm. Sci.* **104**, 1866-1884, doi:10.1002/jps.24444 (2015).

19 Yamaguchi, Y. *et al.* Glycoform-dependent conformational alteration of the Fc region of human immunoglobulin G1 as revealed by NMR spectroscopy.

Biochimica et Biophysica Acta (BBA) - General Subjects **1760**, 693-700, doi:http://doi.org/10.1016/j.bbagen.2005.10.002 (2006).

20 Krapp, S., Mimura, Y., Jefferis, R., Huber, R. & Sondermann, P. Structural analysis of human IgG-Fc glycoforms reveals a correlation between glycosylation and structural integrity. *J. Mol. Biol.* **325**, 979-989 (2003).

21 Shields, R. L. *et al.* Lack of fucose on human IgG1 N-linked oligosaccharide improves binding to human Fcgamma RIII and antibody-dependent cellular toxicity. *J. Biol. Chem.* **277**, 26733-26740, doi:10.1074/jbc.M202069200 (2002).

22 Morar-Mitrica, S. *et al.* Development of a stable low-dose aglycosylated antibody formulation to minimize protein loss during intravenous administration. *MAbs* **7**, 792-803, doi:10.1080/19420862.2015.1046664 (2015).

23 Saxena, A. & Wu, D. Advances in Therapeutic Fc Engineering – Modulation of IgG-Associated Effector Functions and Serum Half-life. *Front. Immunol.* **7**, doi:10.3389/fimmu.2016.00580 (2016).

24 Wang, W. *et al.* Impact of methionine oxidation in human IgG1 Fc on serum half-life of monoclonal antibodies. *Mol. Immunol.* **48**, 860-866, doi:10.1016/j.molimm.2010.12.009 (2011).

25 Stracke, J. *et al.* A novel approach to investigate the effect of methionine oxidation on pharmacokinetic properties of therapeutic antibodies. *MAbs* **6**, 1229-1242, doi:10.4161/mabs.29601 (2014).

26 Bertolotti-Ciarlet, A. *et al.* Impact of methionine oxidation on the binding of human IgG1 to FcRn and Fcγ receptors. *Mol. Immunol.* **46**, 1878-1882, doi:http://doi.org/10.1016/j.molimm.2009.02.002 (2009).

27 Sydow, J. F. *et al.* Structure-Based Prediction of Asparagine and Aspartate Degradation Sites in Antibody Variable Regions. *PLoS One* **9**, e100736, doi:10.1371/journal.pone.0100736 (2014).

28 Chelius, D., Rehder, D. S. & Bondarenko, P. V. Identification and characterization of deamidation sites in the conserved regions of human immunoglobulin gamma antibodies. *Anal. Chem.* **77**, 6004-6011, doi:10.1021/ac050672d (2005).

29 Ionescu, R. M., Vlasak, J., Price, C. & Kirchmeier, M. Contribution of variable domains to the stability of humanized IgG1 monoclonal antibodies. *Journal of pharmaceutical sciences* **97**, 1414-1426, doi:10.1002/jps.21104 (2008).

30 Zheng, K., Yarmarkovich, M., Bantog, C., Bayer, R. & Patapoff, T. W. Influence of glycosylation pattern on the molecular properties of monoclonal antibodies. *MAbs* **6**, 649-658, doi:10.4161/mabs.28588 (2014).

31 Zheng, K., Bantog, C. & Bayer, R. *mAbs* **3**, 568 (2011).

32 Bajardi-Taccioli, A. *et al.* Effect of protein aggregates on characterization of FcRn binding of Fc-fusion therapeutics. *Mol. Immunol.* **67**, 616-624, doi:10.1016/j.molimm.2015.06.031 (2015).

33 Carini, M., Regazzoni, L. & Aldini, G. Mass Spectrometric Strategies and Their Applications for Molecular Mass Determination of Recombinant Therapeutic Proteins. *Curr. Pharm. Biotechnol.* **12**, 1548-1557 (2011).

34 Kaltashov, I. A. *et al.* Advances and challenges in analytical characterization of biotechnology products: Mass spectrometry-based approaches to study properties and behavior of protein therapeutics. *Biotechnol. Adv.* **30**, 210-222 (2012).

35 Houde, D., Arndt, J., Domeier, W., Berkowitz, S. & Engen, J. R. *Anal. Chem.* **81**, 5966 (2009).

36 Kim, Y. H., Berry, A. H., Spencer, D. S. & Stites, W. E. Comparing the effect on protein stability of methionine oxidation versus mutagenesis: steps toward engineering oxidative resistance in proteins. *Protein Eng.* **14**, 343-347 (2001).

37 Mulinacci, F., Poirier, E., Capelle, M. A. H., Gurny, R. & Arvinte, T. Influence of methionine oxidation on the aggregation of recombinant human growth hormone. *Eur. J. Pharm. Biopharm.* **85**, 42-52, doi:http://doi.org/10.1016/j.ejpb.2013.03.015 (2013).

38 Kueltzo, L. A., Wang, W. e. i., Randolph, T. W. & Carpenter, J. F. Effects of Solution Conditions, Processing Parameters, and Container Materials on Aggregation of a Monoclonal Antibody during Freeze-Thawing. *J. Pharm. Sci.* **97**, 1801-1812, doi:http://doi.org/10.1002/jps.21110 (2008).

39 Mach, H. & Middaugh, C. R. Simultaneous Monitoring of the Environment of Tryptophan, Tyrosine, and Phenylalanine Residues in Proteins by Near-Ultraviolet Second-Derivative Spectroscopy. *Anal. Biochem.* **222**, 323-331, doi:http://dx.doi.org/10.1006/abio.1994.1499 (1994).

40 Kueltzo, L. A., Ersoy, B., Ralston, J. P. & Middaugh, C. R. Derivative absorbance spectroscopy and protein phase diagrams as tools for comprehensive protein characterization: a bGCSF case study. *J. Pharm. Sci.* **92**, 1805-1820, doi:10.1002/jps.10439 (2003).

41 Thakkar, S. V. *et al.* Understanding the relevance of local conformational stability and dynamics to the aggregation propensity of an IgG1 and IgG2 monoclonal antibodies. *Protein Science : A Publication of the Protein Society* **22**, 1295-1305, doi:10.1002/pro.2316 (2013).

42 Barnett, G. V. *et al.* Structural Changes and Aggregation Mechanisms for Anti-Streptavidin IgG1 at Elevated Concentration. *The Journal of Physical Chemistry B* **119**, 15150-15163, doi:10.1021/acs.jpcb.5b08748 (2015).

43 Thakkar, S. V. *et al.* Local Dynamics and Their Alteration by Excipients Modulate the Global Conformational Stability of an lgG1 Monoclonal Antibody. *J. Pharm. Sci.* **101**, 4444-4457, doi:http://doi.org/10.1002/jps.23332 (2012).

44 Rodriguez, J. *et al.* High productivity of human recombinant beta-interferon from a low-temperature perfusion culture. *J. Biotechnol.* **150**, 509-518, doi:http://doi.org/10.1016/j.jbiotec.2010.09.959 (2010).

45 Runkel, L. *et al.* Structural and functional differences between glycosylated and non-glycosylated forms of human interferon-beta (IFN-beta). *Pharm. Res.* **15**, 641-649 (1998).

46 Byrne, S. L. *et al.* Effect of glycosylation on the function of a soluble, recombinant form of the transferrin receptor. *Biochemistry* **45**, 6663-6673 (2006).

47 Latypov, R. F., Hogan, S., Lau, H., Gadgil, H. & Liu, D. Elucidation of acid-induced unfolding and aggregation of human immunoglobulin IgG1 and IgG2 Fc. *J. Biol. Chem.* **287**, 1381-1396, doi:10.1074/jbc.M111.297697 (2012).

48 Anthony, R. M., Wermeling, F., Karlsson, M. C. I. & Ravetch, J. V. Identification of a receptor required for the anti-inflammatory activity of IVIG. *Proceedings of the National Academy of Sciences* **105**, 19571-19578 (2008).

49 Kaneko, Y., Nimmerjahn, F. & Ravetch, J. V. Anti-Inflammatory Activity of Immunoglobulin G Resulting from Fc Sialylation. *Science* **313**, 670-673, doi:10.1126/science.1129594 (2006).

50 Anthony, R. M. & Ravetch, J. V. A Novel Role for the IgG Fc Glycan: The Anti-inflammatory Activity of Sialylated IgG Fcs. *J. Clin. Immunol.* **30**, 9-14, doi:10.1007/s10875-010-9405-6 (2010).

51 Raju, T. S. Terminal sugars of Fc glycans influence antibody effector functions of IgGs. *Curr. Opin. Immunol.* **20**, 471-478, doi:http://doi.org/10.1016/j.coi.2008.06.007 (2008).

52 Jung, S. T., Kang, T. H., Kelton, W. & Georgiou, G. Bypassing glycosylation: engineering aglycosylated full-length IgG antibodies for human therapy. *Curr. Opin. Biotechnol.* **22**, 858-867, doi:10.1016/j.copbio.2011.03.002 (2011).

53 Liu, L. *et al.* Pharmacokinetics of IgG1 monoclonal antibodies produced in humanized Pichia pastoris with specific glycoforms: a comparative study with CHO produced materials. *Biologicals* **39**, 205-210, doi:10.1016/j.biologicals.2011.06.002 (2011).

54 Hristodorov, D. *et al.* Generation and comparative characterization of glycosylated and aglycosylated human IgG1 antibodies. *Mol. Biotechnol.* **53**, 326-335, doi:10.1007/s12033-012-9531-x (2013).

55 Jensen, P. F. *et al.* Investigating the interaction between the neonatal Fc receptor and monoclonal antibody variants by hydrogen/deuterium exchange mass spectrometry. *Mol. Cell. Proteomics* **14**, 148-161, doi:10.1074/mcp.M114.042044 (2015).

56 Center for Drug Evaluation and Research (U.S.), C. f. B. E. a. R. U. S., & International Conference on Harmonisation. Vol. U.S. Dept. of Health and Human Services, Food and Drug Administration, Center for Drug Evaluation and Research. (ed Food and Drug Administration U.S. Dept. of Health and Human Services, Center for Drug Evaluation and Research.) (Rockville, MD, 2009).

57 Food & Drug Administration, H. H. S. International Conference on Harmonisation; Guidance on Q11 Development and Manufacture of Drug Substances; availability. Notice. *Fed. Regist.* **77**, 69634-69635 (2012).

58 Farrington G.K., L. A., Meier W., Eldredge J., Garber E., Biogen Idec. Neonatal Fc receptor (FcRn)-binding polypeptide variants, dimeric Fc binding proteins and methods related thereto. (2013).

CHAPTER 4

INTEGRATION OF ON-COLUMN CHEMIAL REACTIONS IN PROTEIN CHARACTERIZATION

This chapter has been adapted from a paper submitted as: Pawlowski, J., Carrick, I. & Kaltashov, I. A. Integration of on-column chemical reactions in protein characterization by LC/MS: cross-path reactive chromatography. *Anal. Chem.*, doi:10.1021/acs.analchem.7b04328 (2018).

4.1 Abstract

Profiling of complex proteins by means of mass spectrometry (MS) frequently requires that certain chemical modifications of their covalent structure (*e.g*., reduction of disulfide bonds) be carried out prior to the MS or MS/MS analysis. Traditionally, these chemical reactions take place in the off-line mode to allow the excess reagents (the majority of which interfere with the MS measurements and degrade the analytical signal) to be removed from the protein solution prior to MS measurements. In addition to a significant increase in the analysis time, chemical reactions may result in a partial or full loss of the protein if the modifications adversely affect its stability, *e.g*. making it prone to aggregation. In this work we present a new approach to solving this problem by carrying out the chemical reaction on-line using the reactive chromatography scheme on a size-exclusion chromatography (SEC) platform with MS detection. This is achieved by using a cross-path reaction scheme, *i.e*. by delaying the protein injection onto the SEC column (with respect to the injection of the reagent plug containing a disulfide-reducing agent), which allows the chemical reactions to be carried out inside the column for a limited (and precisely controlled) period of time, while the two plugs overlap inside the column. The reduced protein elutes separately from the unconsumed reagents, allowing the signal suppression in ESI to be avoided and enabling sensitive MS detection. The new method is used to measure fucosylation levels of a plasma protein haptoglobin at the whole protein level following on-line reduction of disulfide-linked tetrameric species to monomeric units. The feasibility of top-down fragmentation of disulfide-containing proteins is also

demonstrated using β_2-microglobulin and a monoclonal antibody (mAb). The new on-line technique is both robust and versatile, as the cross-path scheme can be readily expanded to include multiple reactions in a single experiment (as demonstrated in this work by oxidatively labeling mAb on the column, followed by reduction of its disulfide bonds and MS analysis of the extent of oxidation within each chain of the molecule).

4.2 Introduction

Analysis of protein covalent structure (which includes both amino acid sequence and post-translational modifications, PTMs) is now routinely carried out using LC/MS and LC/MS/MS. While comprehensive structural analyses have traditionally relied upon the so-called "bottom-up" approach, where proteolysis precedes the LC/MS step, analysis of the whole protein provides an attractive alternative as it allows valuable protein characteristics (including information on structural heterogeneity) to be obtained without requiring time-consuming proteolytic steps.[1] Furthermore, the progress made in recent years in the field of top-down MS[2] resulted in a dramatic expansion of the range of proteins amenable to analysis by this technique.[3-6]

By eliminating the need for proteolysis, top-down MS not only simplifies the sample handling step, but also greatly reduces the possibility of introducing artifacts.[7-10] One serious impediment that frequently complicates the top-down analysis of protein structure is the presence of multiple disulfide bonds. Indeed, even though dissociation of the thiol-thiol linkages can be achieved in the gas phase by using electron-based ion fragmentation techniques,[11] negative-ion CID[12] or ultra-violet photo-dissociation (UVPD),[13] these approaches typically work for small proteins[14] or peptides,[15] while larger proteins with multiple intact disulfide bonds remain out of reach of these techniques. Therefore, it is not surprising that in most cases successful top-down analysis of biopharmaceutical products relies on disulfide bond reduction prior to MS/MS measurements, which can be done using either conventional chemical reduction methods[4] or electrochemical cells interfaced with MS.[16,17] Above and beyond top-down MS/MS analysis of protein structure, reduction of disulfides prior to MS measurements may prove beneficial for other analytical tasks. For example, complexity and heterogeneity of

recombinant proteins, protein/drug conjugates and endogenous macromolecules used as biomarkers can frequently be assessed by measuring their masses (or, more precisely, distribution of molecular masses in analytical and/or clinical samples).[1] While this task can be readily accomplished using modern MS tools for proteins with relatively low degree of complexity, it becomes increasingly challenging as both the size and the degree of heterogeneity increase.

One of the most significant sources of heterogeneity of many proteins is their glycosylation, the most abundant type of post-translational modifications (PTMs) found in both membrane and secreted proteins.[18] Glycosylation patterns frequently have a tremendous diagnostic value, holding enormous promise in the emerging field of personalized medicine.[18] Indeed, carbohydrate composition is known to be modulated not only by congenital disorders that affect the glycosylation machinery at the genetic level,[19] but also by a variety of other pathologies, including Alzheimer's disease and other cognitive disorders,[20] diabetes,[20] immune disorders,[21] and cancer.[18,22]

The use of biomarkers in personalized medicine can be quite complicated, since frequently it is a panel of biomolecules, rather than a single reporter molecule, that needs to be considered. Therefore, sophisticated mathematical tools, such as multivariate statistical analysis,[23] are commonly used in order to provide meaningful results. Fortuitously, a number of serum glycoproteins offer unique opportunities for streamlined cancer diagnosis by exhibiting disease-specific glycosylation patterns.[24] Traditionally, protein glycan analysis is carried out in the bottom-up fashion, by isolating the protein of interest followed by enzymatic removal of the glycans and their analysis by MS and/or MS/MS.[22] Alternatively, composition of glycans can be established in favorable cases by the analysis of the intact protein mass,[25] bypassing the enzymatic step. Unfortunately, this approach is feasible only when applied to proteins with a relatively low extent of glycosylation (such as IgG molecules[25]), while extensive glycosylation inevitably results in high levels of heterogeneity preventing meaningful mass profiling.[26] In many cases, however, the extent of heterogeneity can be reduced to allow meaningful MS measurements without compromising the information encoded by glycans. For example, a number of plasma glycoproteins with high diagnostic value (haptoglobin and complex immunoglobulins) are multi-unit assemblies linked by disulfide bonds. Reduction of the

thiol-thiol linkages may produce monomeric glycoproteins that can be readily mass-profiled by MS at the whole protein level, while their glycosylation patterns remain preserved. Unfortunately, such monomeric units are frequently only marginally stable and readily aggregate/precipitate prior to MS analysis.

Above and beyond disulfide reduction, a variety of other chemical reactions are used to probe biopolymer structure, *e.g*. selective chemical labeling and cross-linking.[27,28] Top-down MS offers an elegant way to determine the chemically modified and cross-linked sites in biopolymer complexes,[29] but it cannot be applied directly to analyze modified proteins in reaction mixtures without removing all unconsumed reagents and/or quenching agents that are incompatible with the ESI process. The clean-up step not only increases the analysis time and cost, but can also lead to the protein loss should modifications render it less stable. Clearly, there is an urgent need for an experimental scheme eliminating the clean-up step and enabling protein MS characterization in an on-line fashion immediately following the completion of the chemical transformations.

The goal of this work is to explore the possibility of carrying out chemical reactions inside a chromatographic column as a means of combining protein modification and MS analysis in a one-step experiment. Reactions taking place inside chromatographic columns are commonly viewed as detrimental (*e.g*., reactions between the analyte and the mobile phase components giving rise to artifacts[30]). However, there are applications where on-column reactions are carried out intentionally in order to enhance the analyte detection while maintaining the separation fidelity (*e.g*., on-column derivatization with chromophores to enable spectrophotometric detection in LC[31,32] or with ionizable groups to enhance detection in GC/MS[33]). Integration of certain reactions with the separation process (e.g., acid/base reactions,[34] as well as a combination of metal ion complexation and redox reactions [35-37]) may also improve the LC separation selectivity. Finally, integration of chemical reactions with chromatographic separation can also be used to study organic reaction mechanisms.[38,39]

Recently, on-column chemical reactions were used to enhance the quality of biopharmaceuticals by converting trisulfide bonds to disulfides within a monoclonal antibody (mAb) captured by an affinity column.[40] Affinity capturing is a reliable way of retaining a protein while carrying out modifications that do not disrupt its native structure.

However, this approach is too restrictive with regards to the types of chemical reactions. Indeed, this scheme would not allow incorporation of chemical reactions altering the higher order structure (*i.e.*, conformation and/or quaternary assembly), nor would it be tolerant to denaturing solvents. More importantly, on-column reactions are likely to target the affinity ligand in addition to captured analytes, thereby compromising the analyte retention and damaging the column. Lastly, even though affinity separation of immunoglobulins is now a routine procedure due to the availability of a wide range of antibody-specific ligands,[41,42] high-affinity ligands for other proteins may not be available as readily.

Since our goal was to devise a versatile experimental scheme allowing a variety of chemical reactions to be carried out on the column, we focused our attention on methods of separation that utilize stationary phases remaining inert towards protein-modifying agents, such as size exclusion chromatography (SEC). Since the majority of biomolecules cannot be permanently captured in SEC, we adopted a cross-path scheme: injection of the fast-moving protein molecules is delayed with respect to the loading of slow-moving chemical regents; the chemical reactions occur inside the column during the time interval when the reagent and protein plugs overlap (**Figure 4.1**). This separates the chemically modified protein upon its elution from the unconsumed reagents, enabling on-line protein analysis by MS. The feasibility of this approach is demonstrated by carrying out on-column reduction of several disulfide-containing proteins. The new method of protein structure analysis (dubbed XP-RC/MS, or cross-path reactive chromatography with MS detection) can be expanded to accommodate multiple reactions in a single experiment (demonstrated in this work by oxidative labeling of mAb, followed by reduction of its disulfide bonds and MS analysis of each immunoglobulin chain).

4.3 Experimental

Materials. Haptoglobin 1-1 (Hp) was purchased from Athens Research (Athens, GA); β_2-microglobulin (β2m) was purchased from Lee Biosolutions (Maryland Heights, MO), and the mAb sample was generously provided by Biogen (Cambridge, MA). PNGase F (500,000 U/mL) was purchased from New England Biolabs (Ipswich, MA). Hydrogen peroxide (30%), ammonium acetate (HPLC grade), Tris and TCEP were purchased from

Thermo-Fisher Scientific (Hampton, NH). All solvents and chemicals were of analytical grade or higher.

Deglycosylation of mAb. The mAb sample was buffer exchanged into 100 mM Tris buffer (pH 7.5) followed by pipetting solution containing 25 mg of mAb (by dry weight) into a vial and diluted up to 990 μL with 100 mM Tris buffer (pH 7.5). A 10 μL aliquot of PNGase F was added to the vial, followed by incubation in a water bath at 37 ^{O}C. After incubation, deglycosylated IgG1 was buffer exchanged into a 150 mM ammonium acetate solution and stored at 2-8 ^{O}C.

On-column protein modification. On-column chemical reactions were carried out on a TSKgel SuperSW mAb HTP (Tosoh, Tokyo, Japan) SEC column used with an HP 1100 (Agilent, Santa Clara, CA) HPLC system. A 75 mM ammonium acetate solution (pH 5.5) at a flow rate of 0.15 mL/min was used as a mobile phase for the analysis of Hp glycosylation patterns; a 150 mM ammonium acetate solution (pH 3.0) at a flow rate of 0.1 mL/min was used as a mobile phase for the top-down β2m analysis; and a 9:1 (v:v) mixture of aqueous 75 mM ammonium acetate solution (pH 3.0) with acetonitrile at a flow rate of 0.15 mL/min was used as a mobile phase for the structural analyses of deglycosylated mAb. The reduction plugs were composed of 100 mM TCEP (β2m analysis), 50 mM TCEP and 4M guanidinium chloride (Hp analysis); and 0.5 M TCEP and 5M guanidinium chloride (mAb analyses) in their respective mobile phases. The plugs were introduced using a manual injector with a loop volume of 100 μL (β2m) and 150 μL (mAb and Hp), which was placed between the sample injector and the SEC column. The protein samples were injected with a delay time of 10 sec (β2m) or 1 min (mAb and Hp) following the reagent plug injection.

Sequential on-column reactions (oxidation followed by disulfide reduction) were carried out with a TSKgel 3000SW xl (Tosoh, Tokyo, Japan) SEC column used with an HP 1100 HPLC system. A 75 mM ammonium acetate solution (pH adjusted to 3.0) with 10% methanol at a flow rate of 0.5mL/min was used as a mobile phase for the analysis of deglycosylated mAb. A flow splitter was used to send ~10% of the flow to the mass spectrometer and the rest to waste. The oxidation plug was composed of 2% hydrogen peroxide, 10% methanol, and 75 mM ammonium acetate (pH 3.0). The reduction plug was composed of 100mM TCEP, 10% methanol, and 75 mM ammonium acetate (pH 3.0).

Each plug was introduced using a manual injector with a loop volume of 250 μL. The reduction and oxidation plugs were injected three and one minute prior to deglycosylated mAb injection, respectively.

MS Measurements and data analysis. All MS and MS/MS measurements were performed with a SolariX 7 (Bruker Daltonics, Billerica, MA) Fourier transform ion cyclotron resonance (FT ICR) mass spectrometer equipped with a 7.0 T superconducting magnet and a standard ESI source. Protein ions at successive charge states +11 through +14 (β2m) and +12 through +16 (mAb light chain) were isolated in the front-end quadrupole for MS/MS measurements; collision-induced dissociation (CID) in the hexapole region was used to induce ion fragmentation. The excitation voltage was set for at 22V and 30V for β2m and mAb light chain ions, respectively. MS/MS data were analyzed with DataAnalysis™ and BioTools™ software packages (Bruker Daltonics, Billerica, MA); all assignments made by BioTools™ were manually inspected to eliminate a possibility of false positives.

4.4 Results and Discussion

Feasibility of using on-column reactions in LC/MS: XP-RC MS profiling of haptoglobin. Haptoglobin 1-1 (Hp) is a plasma glycoprotein composed of four subunits (two heavy chains, H, and two light chains, L) connected by disulfide bonds as H-L-L-H.[43] There are eight glycosylation sites within this protein (residing exclusively within the H chains), making the carbohydrate content of this protein nearly 20% of the total mass (92 kDa). Such a significant extent of glycosylation gives rise to a high level of structural heterogeneity making it nearly impossible to obtain reliable MS measurements.[26] Indeed, even though an SEC/MS spectrum of intact Hp contains abundant ionic signal (**Figure 4.2A, B**), the peaks representing different charge states are broad and do not show distinct contributions from individual glycoforms. This makes it impossible to deduce any meaningful information on the composition of Hp glycans. Reduction of disulfides would be an obvious approach to glycoform profiling at the intact polypeptide level (it should produce monomeric H-chains with a mass of only 37 kDa) and lower the extent of glycosylation (four glycans per each H-chain). However, these monomeric species become unstable upon disulfide reduction, and aggregate readily during a buffer exchange step

preceding MS analysis. The new approach to disulfide reduction explored in this work (on-column chemistry followed by on-line MS detection) minimizes the time between the protein reduction and the MS measurement and provides an opportunity to vary it from tens of seconds to several minutes by selecting an appropriate delay for protein injection (**Figure 4.1**). Increasing this delay decreases the time period spent by the metastable chemically modified species inside the column, dramatically reducing the specter of on-column aggregation.

On-column reduction (with TCEP used as a reducing reagent) gives rise to an abundant ionic signal of L-chains (12 min elution) and H-chains (11 min) in SEC/MS (**Figure 4.2C**). The reduction is incomplete, as evident by the presence of covalent dimers L_2. We also note that limited aggregation of metastable polypeptides does occur, as evidenced by the SEC peak at 8 min. elution (no interpretable ionic signal could be obtained for these high molecular weight species). This highlights the intrinsic instability and aggregation propensity of monomeric H-chains. Nevertheless, the abundance of both L- and H-chains ions in the mass spectra collected at longer elution times (11-12 min) is high, allowing the assignment of all eluting species to be readily made based on their masses. In a stark contrast to intact Hp, ionic signal of monomeric H-chains displays a number of baseline-resolved peaks representing different glycoforms (**Figure 4.2D**). Measuring the mass differences between adjacent peaks allows three major clusters to be identified (as labeled in **Figure 4.2D**). The mass difference between the clusters corresponds to a segment comprising a GlcNAcGalNeuAc trisaccharide (N-acetyl-glucosamine, galactose, and N-acetylneuraminic acid). The spacing between adjacent peaks within each cluster corresponds to a fucose residue mass (142.1 Da), with the total level of fucosylation ranging from zero to four (as indicated in **Figure 4.2D**). Fucosylation patterns are highly reproducible, allowing the extent of fucosylation to be calculated with an error not exceeding 9% RSD (see ***Supporting Information***). Therefore, XP-RC MS provides a means of exploiting the high diagnostic value of Hp fucosylation patterns without the need to remove/isolate carbohydrate chains from the protein. Sufficient amounts of monomeric species are produced during Hp transient exposure to the reducing agent (TCEP) inside the column, while the cross-path scheme eliminates any interference from TCEP during the

on-line MS analysis of these monomeric polypeptides: the reagent plug does not emerge from the column until after all Hp components have eluted (**Figure 4.2A**).

Top-down sequencing of small disulfide-containing proteins: XP-RC MS/MS analysis of β2-microglobulin. Despite its modest size (11.7 kDa), β2m presents a challenge for top-down MS/MS analysis. Its single disulfide bridge (Cys^{25}-Cys^{80}) exerts a two-fold negative effect on the diagnostic value of the top-down MS/MS data. First, collision-induced dissociation (CID) of the peptide bonds within the [Cys^{25}-Cys^{80}] segment does not give rise to observable fragment ions (the two fragments are still physically connected by the thiol-thiol linkage, and the mass of this dimer is indistinguishable from that of intact protein ions). Indeed, all CID-generated *b*- and *y*-fragments of β2m with the intact disulfide are confined to the short terminal segments of the polypeptide, [Ile^{1}-Cys^{25}] and [Cys^{80}-Met^{99}] (see ***Supporting Information***). Second, the presence of the disulfide cross-link within the polypeptide chain results in a significant reduction of the conformational space it can sample in solution even under denaturing conditions. Since the physical size of the protein is the major determinant of the extent of its multiple charging in ESI,[44,45] the number of charges accommodated by β2m ions with the intact disulfide bridge will remain modest, limiting the collision energy. The highest charge state observed for β2m ions in conventional SEC/MS is +10; and the efficiency of cumulative CID of four precursor ions (from +7 to +10) is rather modest (see ***Supporting Information***).

In contrast, the extent of multiple charging of polypeptide ions produced by ESI following the on-column disulfide reduction is relatively high (extending up to a charge state +17, see ***Supporting Information***). In addition to the dramatic change in the protein ion charge state distribution, disulfide reduction also manifested itself by a mass increase of 2 Da for ions at lower *m/z*. Mass increase for ions at lower charge states (<+9) was also evident, although the overall shift was less than 2 Da, indicating the presence of both disulfide-reduced and surviving disulfide-intact proteins. CID of ions corresponding to the disulfide-reduced β2m (charge states +11 through +15 were selected as precursors) gives rise to a large number of fragments (see ***Supporting Information***). In addition to a significant gain in the overall intensity of fragment ions, the fragmentation pattern also changes dramatically, with half of the observed fragment ions resulting from amide bond cleavages within the [Cys^{25}-Cys^{80}] segment, which failed to generate distinguishable

fragment ions without on-column protein reduction. Clearly, on-line reduction of β2m results in a dramatic increase of the quality of information that can be extracted from the top-down MS/MS measurements while minimizing both sample preparation and analysis time.

Top-down analysis of a disulfide-connected protein assembly's subunit: on-line mAb's light chain analysis. While the XP-RC MS/MS analysis of β2m yields sequence information not accessible via CID of the disulfide-intact protein, it should be remembered that β2m is a rather modest protein whose single disulfide bond can be cleaved in the gas phase using electron capture dissociation.[14] The vast majority of biopharmaceuticals are significantly larger and contain multiple disulfide bonds (which could both reinforce the conformation of a single polypeptide chain by providing intra-chain cross-links, and connect several monomeric units in a multi-unit assembly). These features are epitomized by mAbs, recombinant proteins based on the IgG1 structural template.

There are sixteen disulfide bonds in the mAb used in our work. This includes twelve internal thiol-thiol connections, two in each of the light chains (L) and four in each of the heavy chains (H), and four inter-chain linkages (with each L/H pair being connected by a single disulfide bond, and the remaining two thiol-thiol linkages connecting the two H-chains). The inter-chain bonds are more labile, as they can be reduced under native conditions, when the intra-chain bonds remain intact.[46] Since our goal was to explore the utility of top-down MS for structural characterization of mAbs, we used low-pH conditions to maximize the reduction of all disulfide bonds. The chromatogram of mAb that underwent on-column reduction has a convoluted shape; on-line MS analysis reveals the presence of both monomers (L and H) and incompletely reduced assemblies (HL, H_2 and H_2L), see ***Supplementary Material*** for more detail.

While the effective reduction of external disulfide bonds in XP-RC is evident due to the presence of L- and H-chain ions, mass spectra acquired on-line do not produce direct evidence that the on-column reduction also succeeded in eliminating the internal disulfide bonds. Some indirect evidence is provided by the charge state distributions of the L- and H-chain ions. Indeed, the bimodal character of the charge state distributions, as well as the presence of ionic species with high charge density (in the low *m/z* regions of the spectra) suggest that at least some internal disulfides have been reduced. In order to determine if

any internal disulfide bonds were indeed eliminated as a result of the on-column reduction, on-line MS/MS analysis of the L-chain was carried out. Five charge states (+16 through +12) were mass-selected as precursors for CID. The presence of 5 M guanidinium chloride in the reagent plug results in the most facile fragmentation (as judged by both overall intensity of the fragment ions and the number of amide bonds undergoing dissociation, see **Figure 4.3** and ***Supplementary Material***). The detected high-abundance fragment ions (both *b*- and *y*-type) correspond to cleavages of nearly half of the amide bonds within the constant region of the L-chain (fifty-two out of one hundred and thirteen).

Guanidinium chloride is a very effective chaotrope frequently used as a protein unfolding agent. Its presence in the reagent plug likely results in more efficient unfolding of mAb chains, exposing the disulfide bonds to the reducing agent. Guanidinium chloride cannot be used in ESI MS measurements; however, in our scheme this interference is eliminated by separating polypeptide chains from the chaotrope prior to MS analysis. Importantly, twenty fragment ions detected in the XP-RC/MS/MS analysis of the L-chain correspond to the region of the polypeptide chain flanked by two cysteines (Cys^{134} and Cys^{194}) forming an internal disulfide bond (**Figure 4.3**). This provides unequivocal evidence that this internal disulfide had been successfully eliminated during protein exposure to the reagent plug inside the column. A comparable sequence coverage was obtained in XP-RC MS/MS measurements in the absence of guanidinium chloride in the reagent plug, but the overall abundance of the fragment ions was noticeably lower (see ***Supplementary Material***). As an alternative approach to MS/MS, in-source fragmentation of ions without mass selection was carried out within the time window corresponding to the elution of L-chains (14-20 min, see ***Supplementary Material*** for more detail). Although the total fragment ion abundance was lower compared to the on-line MS/MS experiments, the extent of the sequence coverage was comparable, suggesting that XP-RC MS can be implemented on inexpensive MS platforms lacking tandem capabilities.

Since the presence of guanidinium chloride appears to favor dissociation of disulfide bonds, it seems reasonable to assume that other chaotropic agents may also prove beneficial as far as breaking thiol/thiol linkages. One particularly attractive possibility lies with the use of co-solvents that do not have to be confined to the reagent plug, but instead can be used as a part of the mobile phase. For example, addition of alcohols to the mobile

phase is likely to destabilize the tertiary structure of the proteins, while keeping the secondary structure largely intact. This should increase the solvent exposure of disulfide bridges (and, therefore, reduction efficiency) without raising the specter of protein aggregation. Indeed, addition of even relatively modest amount of methanol to the mobile phase (10% by volume) results in a notable decrease of the relative abundance of all partially reduced species (H_2L, H_2, and HL), and near-complete elimination of the ionic signal of the surviving intact assembly H_2L_2 (see ***Supplementary Material*** for more detail). An important question that should be addressed in connection with the on-column disulfide reduction is the possibility of recombination of free thiol groups outside of the reagent plug. Should this process occur, it would lead to (re)formation of disulfides prior to MS/MS detection. Above and beyond its obvious negative effect on the overall efficiency of the XP-RC process, thiol/thiol recombination can give rise to artifacts (*e.g.*, formation of disulfide bonds that were not present in the original protein). We note, however, that all multimeric species observed in the XP-RC MS of the mAb sample appear to be "legitimate" products of partial disulfide reduction (*e.g.*, H_2L, H_2, and HL), while any signs of *de novo* disulfide formation are absent (*e.g.*, HL_2, L_2, *etc*.). This provides a reasonable assurance that no disulfide recombination occurs under the conditions employed in XP-RC measurements following the on-column disulfide reduction.

It is interesting to compare the results of XP-RC/MS/MS analysis of mAb in this work with the top-down characterization of IgG molecules carried out using common approaches. Due to their large size, structural analyses of antibodies by MS until recently were almost exclusively carried out using the bottom-up approaches, where gas-phase fragmentation is preceded by proteolysis in solution. This is now beginning to change mainly due to the rapidly increasing demands for the high-throughput analysis of mAbs and mAb-related products in the biopharmaceutical sector, with several groups actively exploring the feasibility of the top-down approach.[6,16,47] Not surprisingly, intact disulfide bonds present a formidable problem for the top-down analysis of mAb: while electron-based ion dissociation techniques allow some thiol-thiol linkages to be cleaved in the gas phase, the large number of disulfides typically present in mAbs limits the number of fragment ions derived from polypeptide segments flanked by disulfide-connected cysteine residues.[47] Chemical reduction of disulfides prior to antibody analysis by top-down MS

results in a dramatic increase of the number of structurally diagnostic fragments and the extent of sequence coverage. Interestingly, sequence coverage of the variable regions is highly antibody-specific. For example, Marshall and co-workers observed that despite the 88% sequence identity between the variable domains of the light chains of Adalimumab and Efalizumab, the sequence coverage in this region differed by nearly six-fold, while the coverage of the constant regions was nearly identical between the two antobodies.[6] Therefore, a meaningful comparison of two different techniques *vis-à-vis* the extent of mAb sequence coverage should focus on the constant (κ) region, rather than compare the overall sequence coverage across the entire polypeptide chain. The number of the amide bonds within the constant region of mAb light chains that dissociate under ETD/CID combination giving rise to structurally diagnostic fragment ions reported by Marshall and co-workers for disulfide-reduced proteins is 61-62.[6] This number far exceeds the extent of sequence coverage that can be obtained without the reduction step prior to dissociation (up to 23 for the same segment[47]), but is comparable with that obtained in XP-RC MS/MS experiments (50 in the constant region of the light chain, as shown in **Figure 4.3**).
Interestingly, the fragmentation efficiency of the light chain of a mAb molecule subjected to the top-down MS/MS analysis following the on-line reduction in an electrochemical cell was relatively modest in comparison: even though the intra-chain disulfides were successfully reduced, the number of structurally diagnostic fragments derived from the light chain was relatively low, and their localization within the sequence was consistent with the notion of the internal thiol-thiol linkages remaining intact.[16] Clearly, XP-RC MS appears to be a more robust method for on-line reduction coupled to top-down MS analysis of monoclonal antibodies. Another important advantage offered by this technique is its versatility, as it allows various types of chemical modifications to be carried out prior to MS analysis (*vide infra*). Furthermore, multi-step modification procedures can be implemented in a single experiment, as outlined in the following section.

Feasibility of using multiple reactions in XP-RC MS: sequential on-column oxidative labeling of mAb and reduction of disulfide bonds. All examples of protein analysis with XP-RC MS considered so far utilize a single reagent plug. However, one can envision using multiple plugs containing different reagents in a single experiment. As long as all reagents fall under the permeation limit, the plugs will travel inside the SEC column

along parallel trajectories, and the protein injected with a delay will be exposed to these reagents in a sequential manner (**Figure 4.4**). This would provide an opportunity to expand the use of XP-RC MS to probing higher order structure of proteins and protein assemblies, *e.g*. by employing chemical labeling as a probe of solvent accessibility.[48] The feasibility of this approach was evaluated using a scheme depicted in **Figure 4.4**, where oxidative labeling of mAb was carried out by using a plug of a 2% H_2O_2 solution, followed by exposure of the labeled protein to the TCEP plug. The ensuing disulfide dissociation generates L- and H-chains along with partially reduced species (H_2L, H_2, and HL), as previously observed in a "single-reaction" XP-RC MS/MS analysis of mAb. On-line MS detection provides clear evidence for the three oxidation events occurring within the H-chain (manifested by a mass shift of 50±2 Da), but not in the L-chain (see the top panels in **Figure 4.4**). The mass shifts observed within the partially reduced species and the intact assembly are also consistent with the notion of the H-chain undergoing oxidation at three sites, while the L-chain does not suffer any oxidative damage (48±3 Da shift for HL, 97±2 for H_2, and 98±3 for H_2L).

While H_2O_2 is hardly the best choice as a labeling reagent in terms of its efficiency with respect to protein labeling and the effect on the column longevity, the multiple reaction XP-RC scheme can be used for probing higher order protein structure with a variety of labeling reagents in the first plug, including amino-acid specific labeling reagents.[27] Another application where the multiple-reaction feature of XP-RC MS will be advantageous is the ranking of disulfide susceptibility to reduction using isotopically labeled thiol-capping reagents.[49]

4.5 Conclusions

Top-down MS analysis of proteins is a powerful tool for elucidation of various aspects of both covalent[50-52] and higher order structure.[53-56] Many applications of top-down MS require chemical treatment of proteins prior to MS analysis, which inevitably introduces ESI-incompatible low-molecular weight components (unconsumed reagents, quenchers, *etc*.) that must be removed prior to the MS analysis. This creates problems for proteins where the chemically modified forms are metastable and undergo aggregation/precipitation during the sample clean-up step. Furthermore, even for proteins that remain stable throughout the clean-up step, the latter results in a significant increase

of the sample handling/analysis time. The cross-path reactive chromatography (XP-RC) presented in this work as a means of facilitating top-down MS protein analysis solves this problem by initiating the chemical transformations inside the chromatographic column, and separating the high-molecular weight products (modified proteins) from the low-molecular weight reagents prior to the on-line MS analysis.

In this initial report we focus primarily on disulfide reduction as a means of increasing the value of information provided by on-line MS and MS/MS measurements for proteins that have traditionally been challenging for the top-down MS analysis. This new approach offers a straightforward way to control the extent of chemical modifications by varying either the width of the reagent plug or the reagent concentration (or both). It also provides a means of controlling the undesirable post-reaction processes (*e.g.*, aggregation of metastable chemically modified species) by allowing the time interval between the analyte's exposure to the regent plug and its elution from the column to be minimized by selecting an appropriate injection delay. An additional benefit offered by this technique is the (partial) separation of the reaction products, which allows the spectral crowding to be reduced and the quality of the MS data to be enhanced.

Above and beyond disulfide reduction, XP-RC allows other reactions to be implemented, including those that can be used to probe protein higher order structure. In some ways, the cross-path scheme presented in this work resembles the "catch-me-if-you-can" approach introduced by Krylov and co-workers as a means to measure kinetics of non-covalent interactions of proteins with small ligands.[57] A unique advantage of the cross-path scheme demonstrated in our work is the possibility of carrying out multiple reactions in sequence during a single experiment (*e.g.*, oxidative labeling followed by disulfide reduction to assist on-line MS characterization). Lastly, even though all experiments presented in this work had been carried out using SEC, the XP-RC methodology can be implemented on a variety of other LC platforms, provided the chemically treated protein(s) can be separated from the unconsumed reagents prior to the on-line MS analysis (we are currently exploring the utility of ion exchange chromatography for this purpose)

4.6 Acknowledgments

The authors are grateful to Dr. Tyler Carlage (Biogen, Cambridge, MA) for providing a sample of a monoclonal antibody. This work was supported by a grant CHE-1709552 from the National Science Foundation. The FT ICR mass spectrometer was acquired through a grant CHE-0923329 from the National Science Foundation and is a part of the Mass Spectrometry Core facility at UMass-Amherst.

4.7 Tables

Table 4.1. Distribution of fucosylation within the $[NeuAc_2Gal_2Man_3GlcNac_4]_4/Fuc_x$ glycoforms based on the ionic peak heights in the on-line mass spectra of Hp H-chains produced upon on-column disulfide reduction

Total number of fucose residues	Relative abundance (based on the peak heights)	95% confidence interval (based on a set of three replicate measurements)
0	13%	2%
1	12%	2%
2	38%	5%
3	29%	3%
4	8%	1%

4.8 Figures

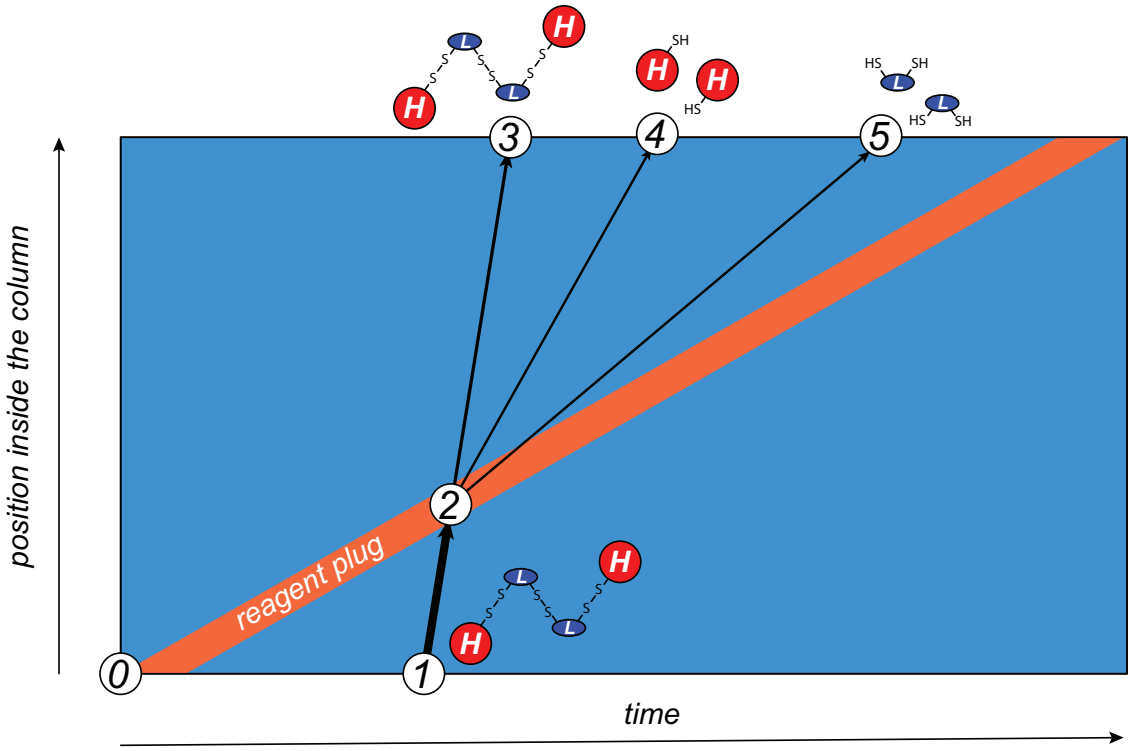

Figure 4.1. Schematic representation of the XP-RC using a 2-D depiction of the chromatographic process. The numerals on the diagram indicate injection of the low-molecular weight reagent plug (0), injection of the protein (1), chemical reaction between the protein and the reagent (2), and elution of the unreacted protein species (3) and the products of the chemical reaction (4 and 5).

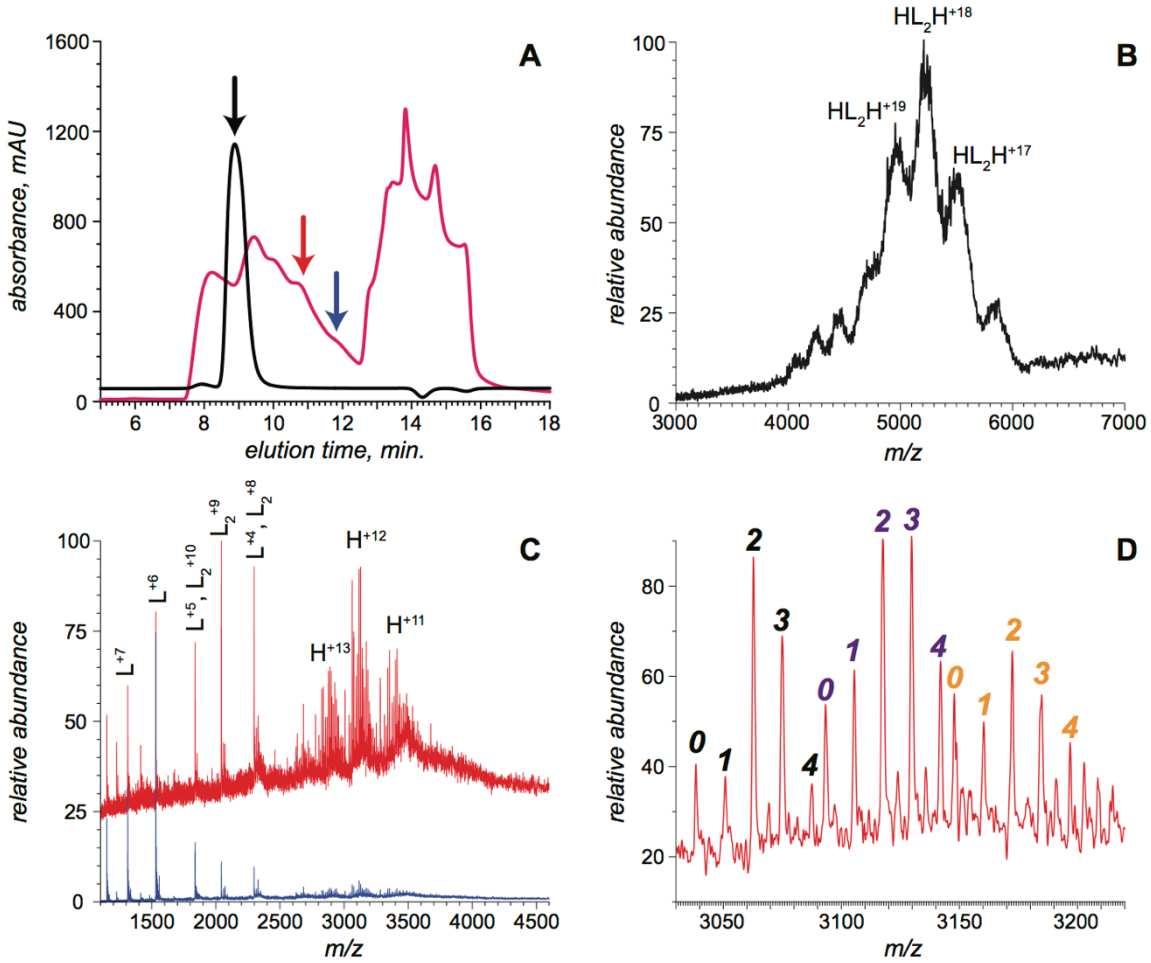

Figure 4.2. XP-RC MS analysis of haptoglobin 1-1. **A**: A UV chromatogram of a control Hp injection without the on-column disulfide reduction (black trace) and the XP-RC chromatogram (magenta). **B**: On-line mass spectrum of the control Hp injection (averaged across the 9-10 min elution window). **C**: On-line mass spectra acquired in XP-RC of Hp (the colored arrows in panel **A** show where the two mass spectra were acquired). **D**: a zoomed view of the on-line mass spectrum of the H-chain of Hp produced by on-column reduction. Three clusters of peaks represent the following glycoforms (based on the measured masses): $[NeuAc_2Gal_2Man_3GlcNac_4]_4/Fuc_x$ (black labels), $[NeuAc_2Gal_2Man_3GlcNac_4]_3/NeuAc3Gal3Man3GlcNac5/Fuc_x$ (purple) and $[NeuAc_2Gal_2Man_3GlcNac_4]_2/[NeuAc_3Gal_3Man_3GlcNac_5]_2/Fuc_x$ (gold); the numerals indicate the number of fucose units (x) within each species.

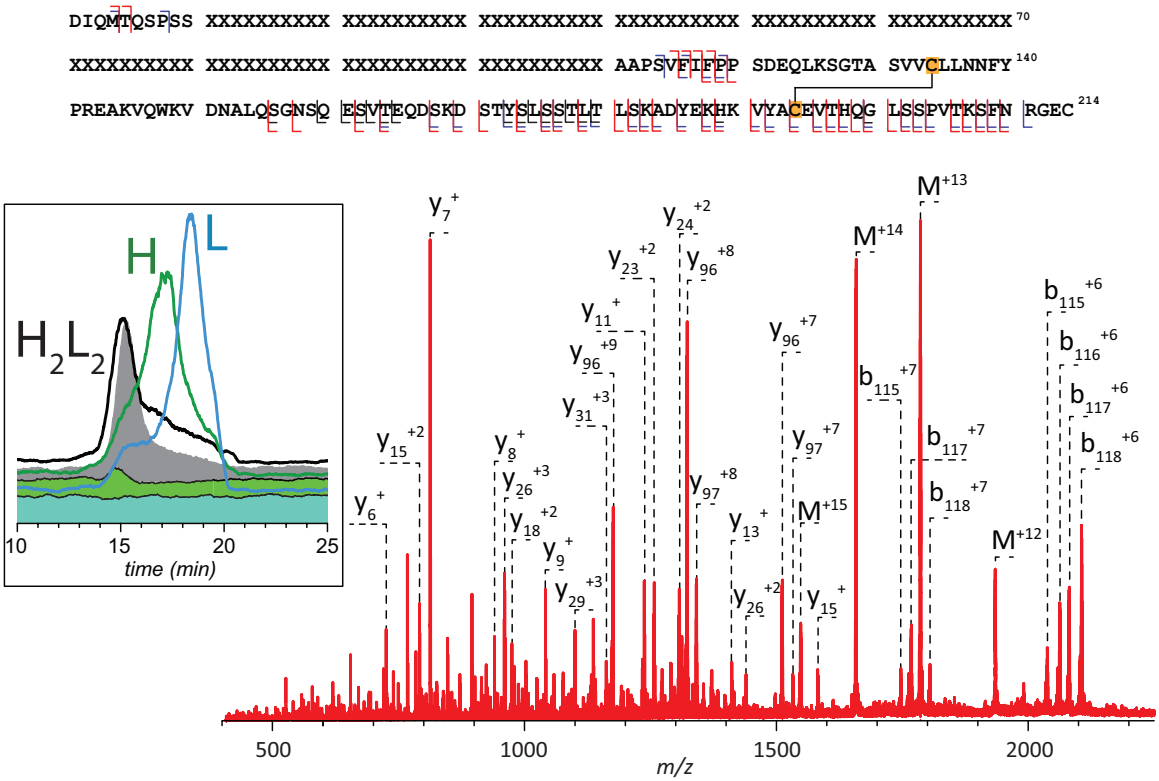

Figure 4.3. XP-RC MS/MS of mAb showing CID mass spectrum and fragmentation pattern of the L-chain produced upon the on-column reduction of the intact protein. Amino acid sequence is shown only for the constant region of the L-chain; the vertical lines indicate amide bonds whose cleavage gives rise to the detected *b*- and *y*-ions (red lines correspond to this data set; blue line correspond to XP-RC MS/MS measurements carried out without using guanidinium chloride in the reagent plug; and black lines correspond to fragments generated in XP-RC MS using in-source collisional activation). The inset shows selected extracted ion chromatograms for several ionic species in XP-RC chromatogram (reference XICs obtained in the absence of the reducing agent in the reagent plug are shown as color-filled curves). The complete set of XICs with representative mass spectra (MS1) is shown in the **Supplementary Material** section.

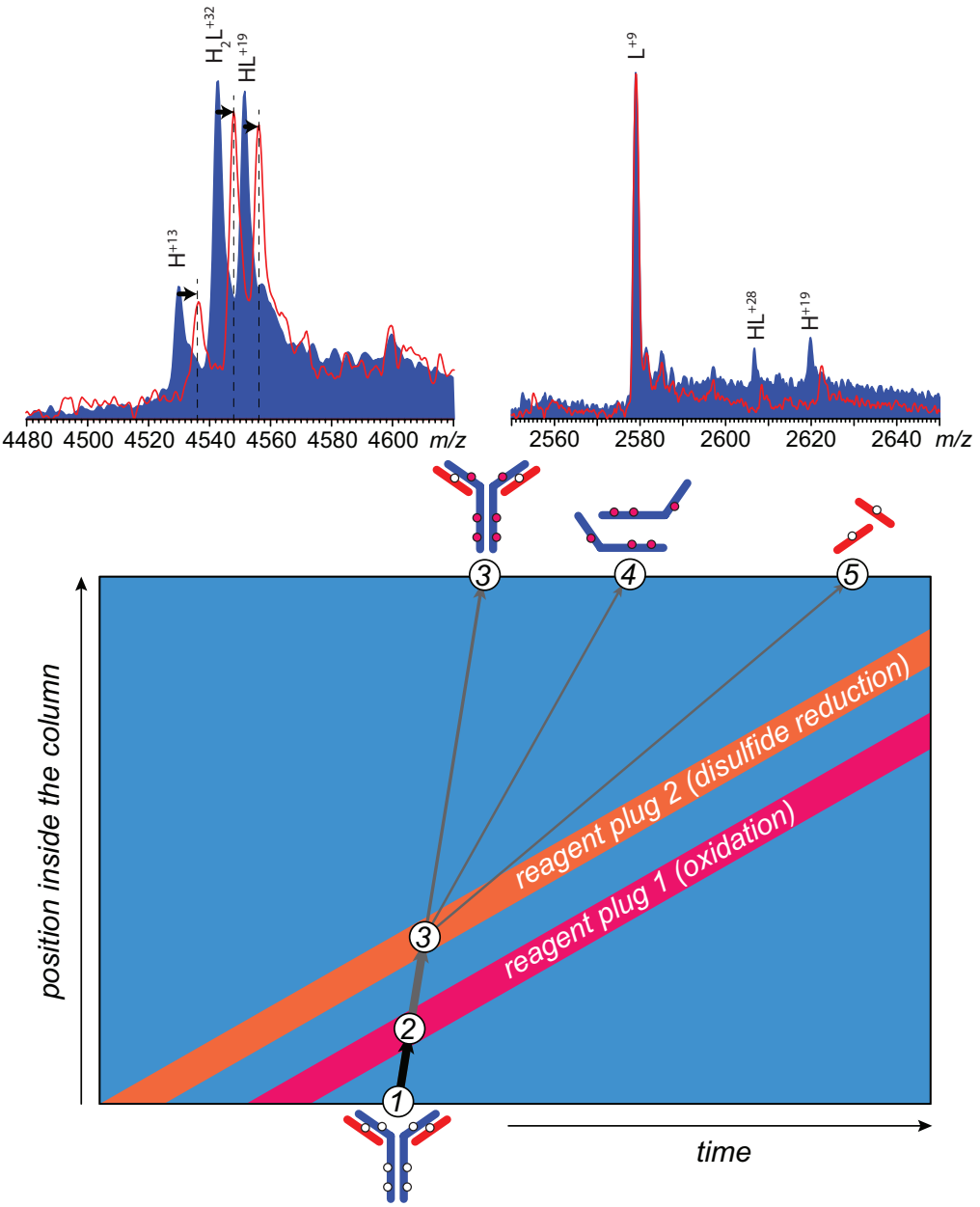

Figure 4.4. A schematic diagram of an XP-RC experiment employing two reagent plugs and the mass spectra of the constituents of mAb produced by the on-column reduction with TCEP (reagent plug 2) following the on-column oxidative labeling with hydrogen peroxide (reagent plug 1). The numerals on the diagram indicate injection of the protein (1), chemical reaction between the protein and the reagent 1, *e.g.* oxidation with H_2O_2 (2), chemical reaction between the protein and the reagent 2, *e.g.* reduction of disulfide bonds (3), and elution of the unreduced (disulfide-intact) protein species (4) and the products of the external disulfide reduction (5 and 6).

4.8 Supplemental Figures

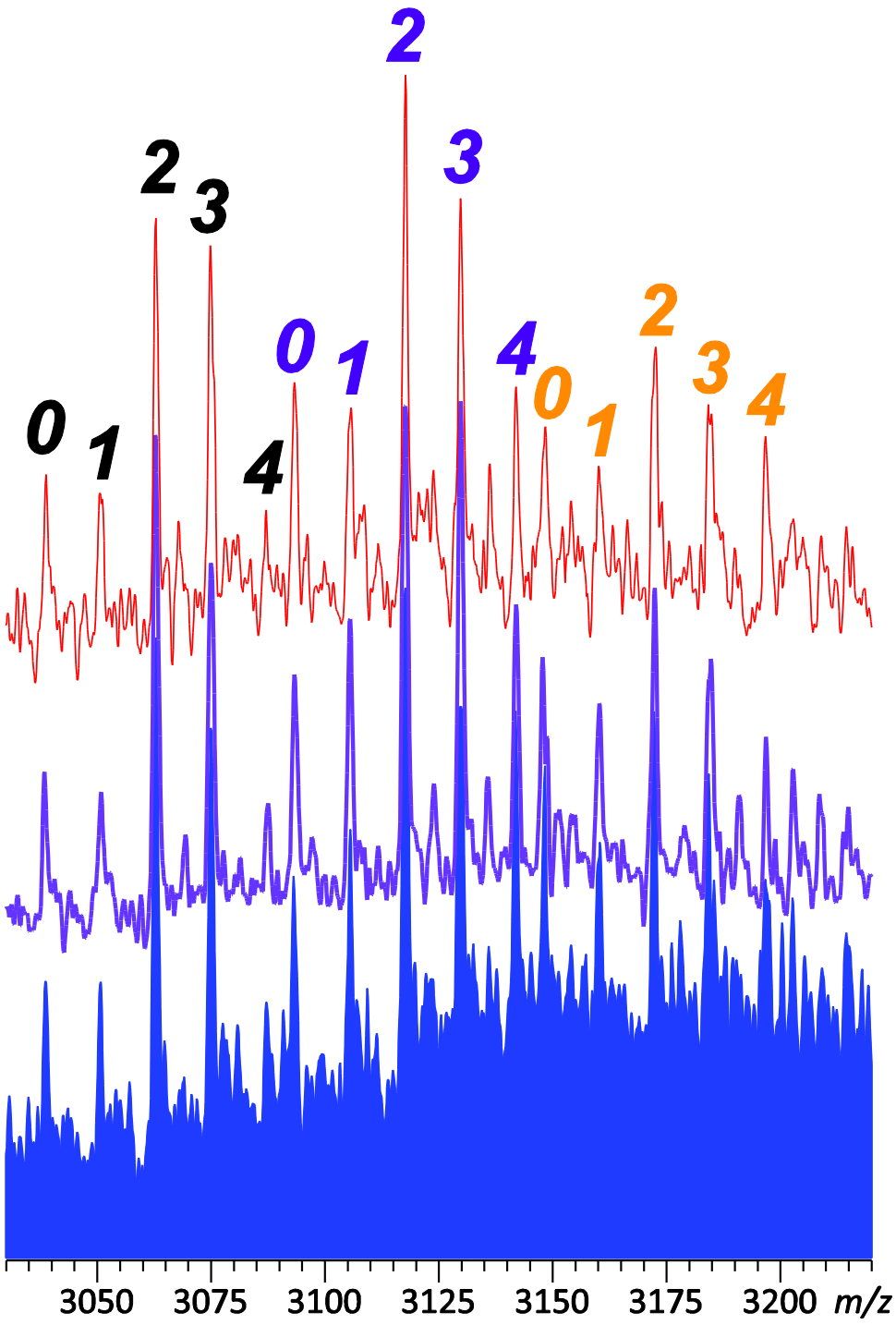

Figure S4.1. Reproducibility of Hp fucosylation patterns obtained with XP-RC MS (TCEP in the reagent plug). Three different data sets are shown for the monomeric H-chain at charge state +12; labeling of individual glycoforms is the same as in **Figure 4.2D**.

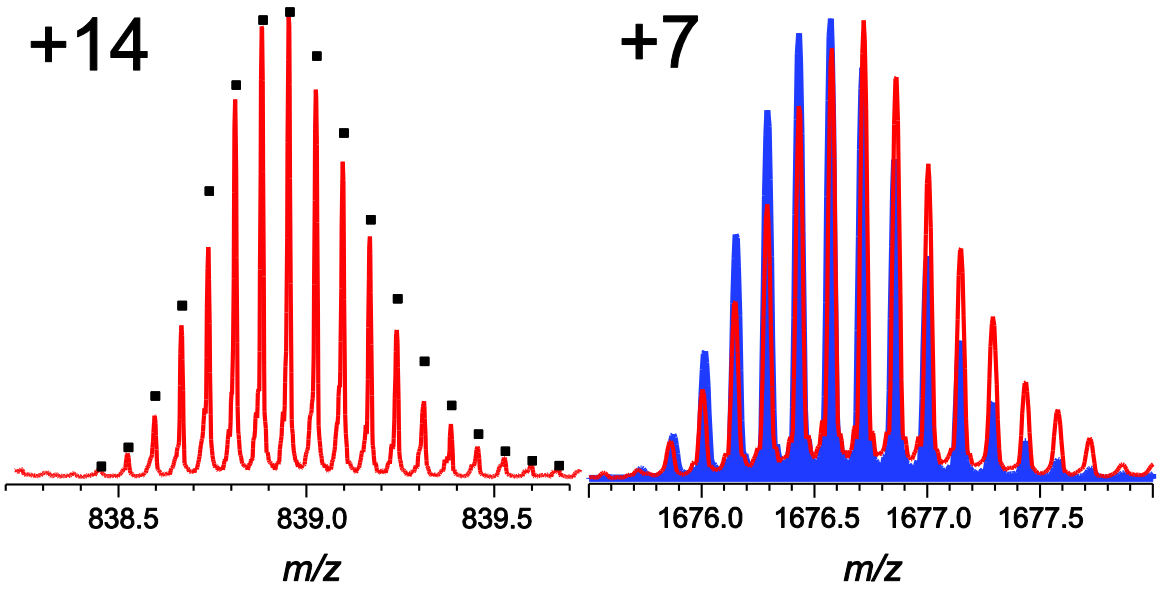

Figure S4.2. Isotopic distributions of β2m ions (charge states +7 and +14) produced by XP-RC MS with TCEP in the reagent plug. Black squares in the left-hand panel show the calculated isotopic distribution of a β2m ion at charge state +14 with a reduced disulfide bond. The blue trace in the right-hand side diagram shows the isotopic distribution of a β2m ion (charge state +7) produced by SEC MS (no on-column reduction).

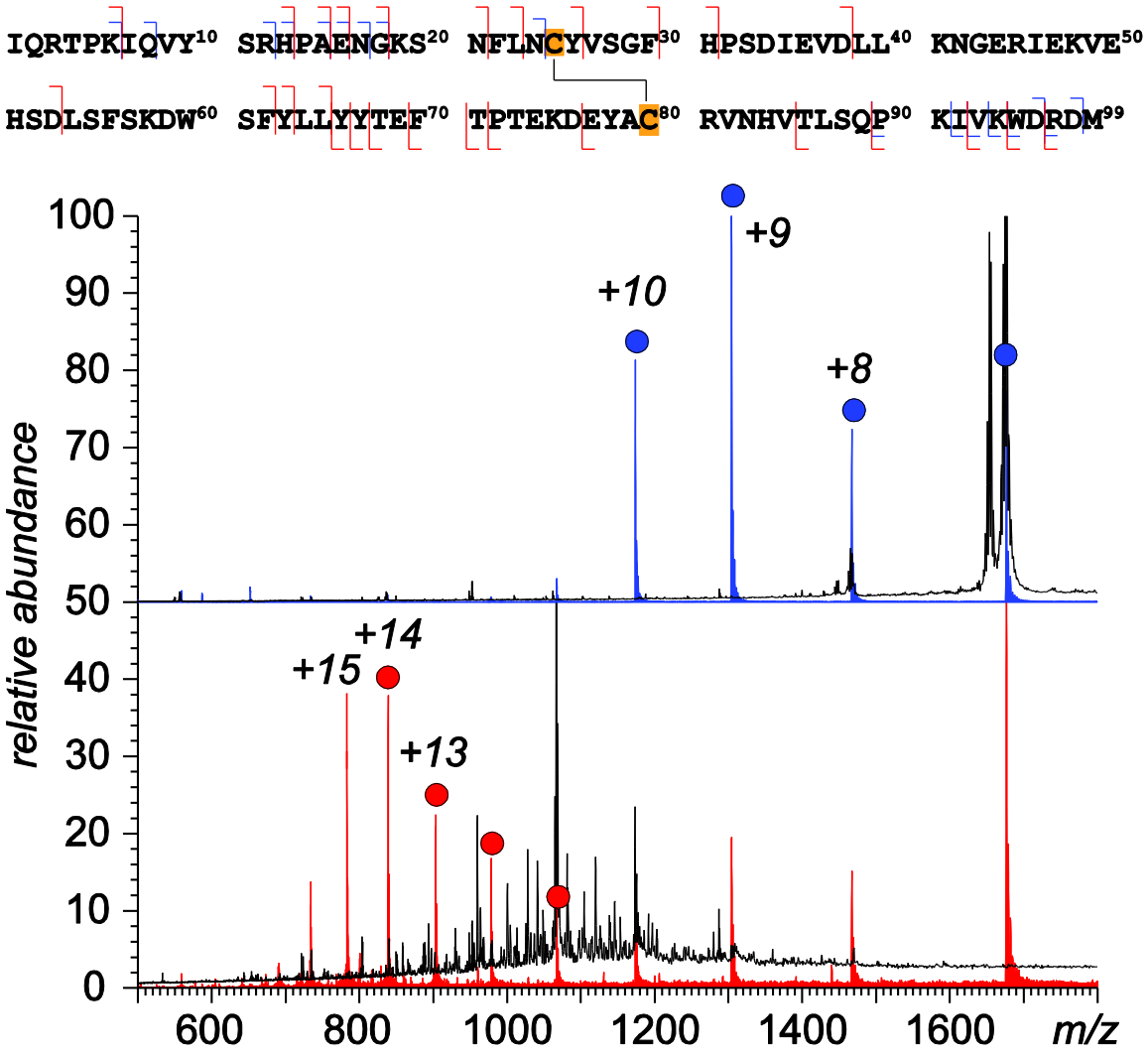

Figure S4.3. SEC MS/MS (top panel) and XP-RC MS/MS (bottom) analysis of β2m. The colored traces in each panel show mass spectra of intact protein (no collisional activation), and circles indicate protein ion used as precursors in CID measurements. The fragmentation patterns are shown at the top of the figure for both SEC MS/MS (blue lines) and XP-RC MS/MS (red).

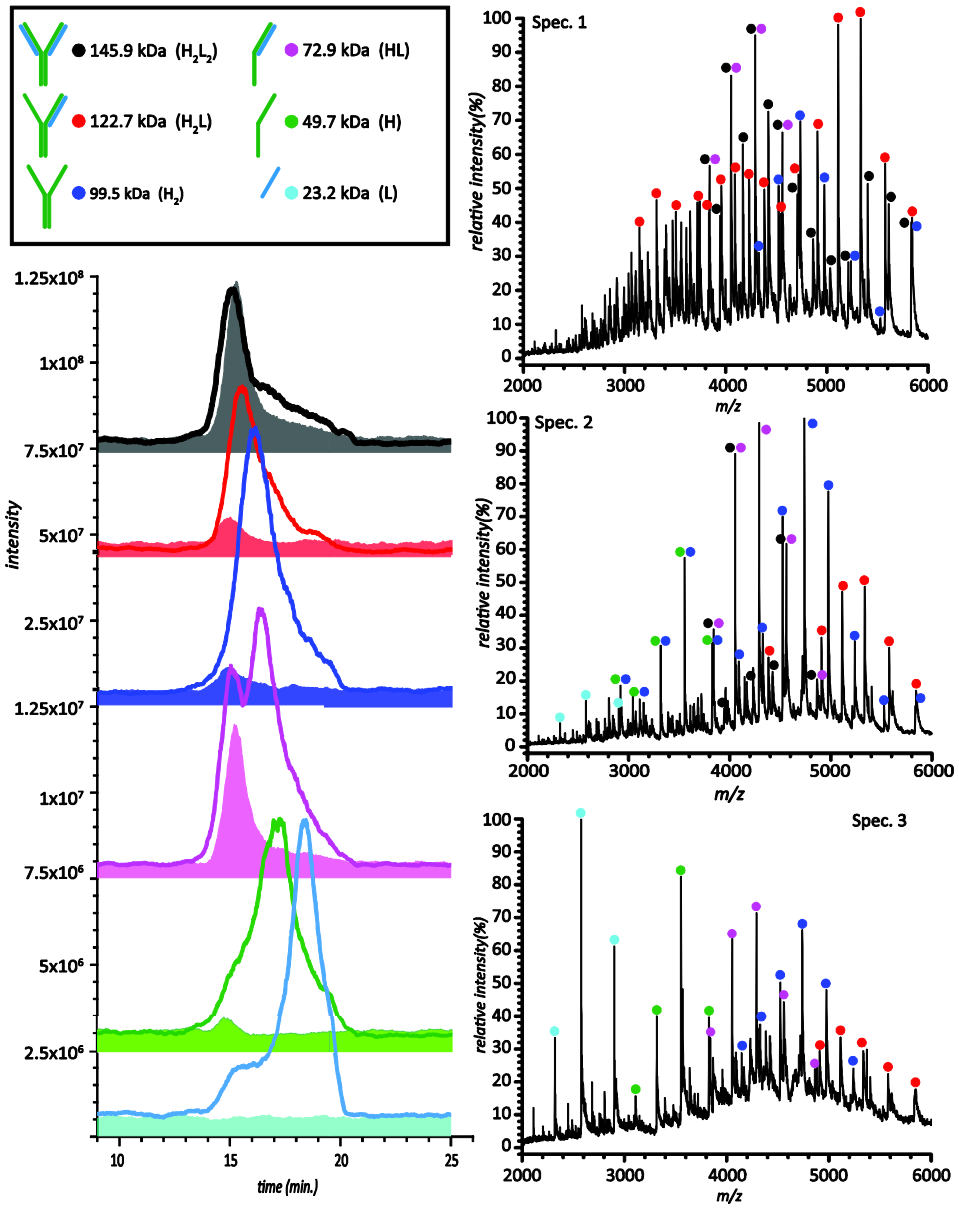

Figure S4.4. Extracted ion chromatograms for fully-, partially- and non-reduced species of mAb detected in SEC MS without on-column reduction (filled curves) and XP-RC MS experiments (150 mM ammonium acetate solution, pH adjusted to 3.0; TCEP in the reagent plug). The three representative on-line mass spectra shown on the right-hand side were averaged across the following elution windows: 14-16 min (top), 16-17 min (middle), and 17-19 min (bottom). The XICs were generated by plotting ionic signals for the following species: H_2L_2, charge state +33 (m/z window 4419-4423); H_2L, charge state +23 (m/z window 5332-5336); H_2, charge state +21 (m/z window 4736-4740); HL, charge state +17 (m/z window 4289-4293); H, charge state +14 (m/z window 3552-3556); and L, charge state +9 (m/z window 2576-2580). Note that the early-eluting peaks of partially- and fully-reduced species are artifacts due to the interfering signal of the intact mAb (e.g., it is impossible to distinguish the ionic signal of HL^{+17} from that of $H_2L_2^{+34}$).

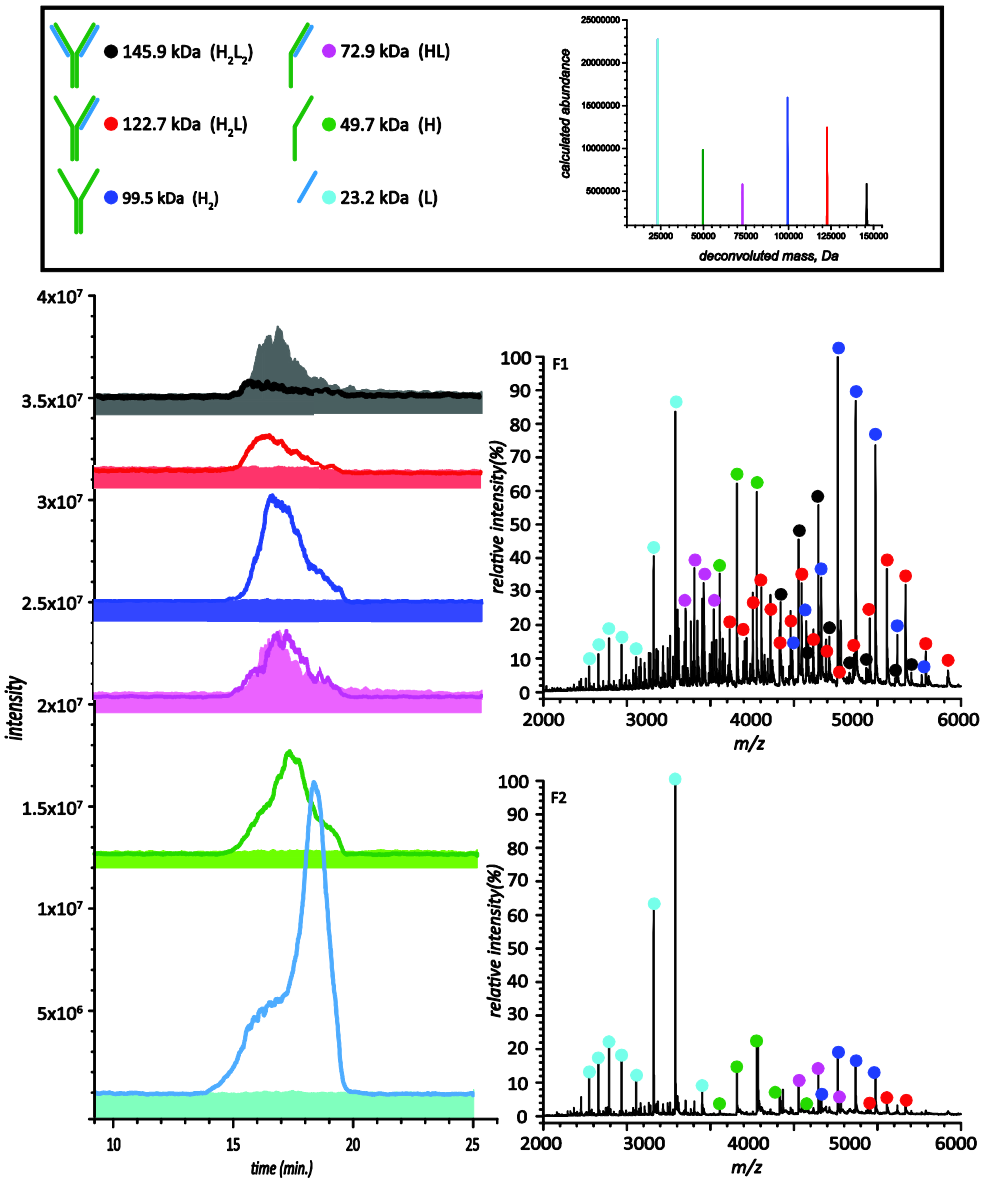

Figure S4.5. Extracted ion chromatograms for fully-, partially- and non-reduced species of mAb detected in SEC MS without on-column reduction (filled curves) and XP-RC MS experiments (150 mM aqueous ammonium acetate solution, pH adjusted to 3.0, with 10% methanol by volume; TCEP/10% methanol in the reagent plug). The three representative on-line mass spectra shown on the right-hand side were averaged across the following elution windows: 15-17 min (top) and 17-19 min (bottom). The XICs were generated by plotting ionic signals for the following species: H_2L_2, charge state +33 (m/z window 4419-4423); H_2L, charge state +23 (m/z window 5332-5336); H_2, charge state +21 (m/z window 4736-4740); HL, charge state +17 (m/z window 4289-4293); H, charge state +14 (m/z window 3552-3556); and L, charge state +9 (m/z window 2576-2580). Note that the early-eluting peaks of partially- and fully-reduced species are artifacts due to the interfering signal of the intact mAb (e.g., it is impossible to distinguish the ionic signal of HL^{+17} from that of $H_2L_2^{+34}$).

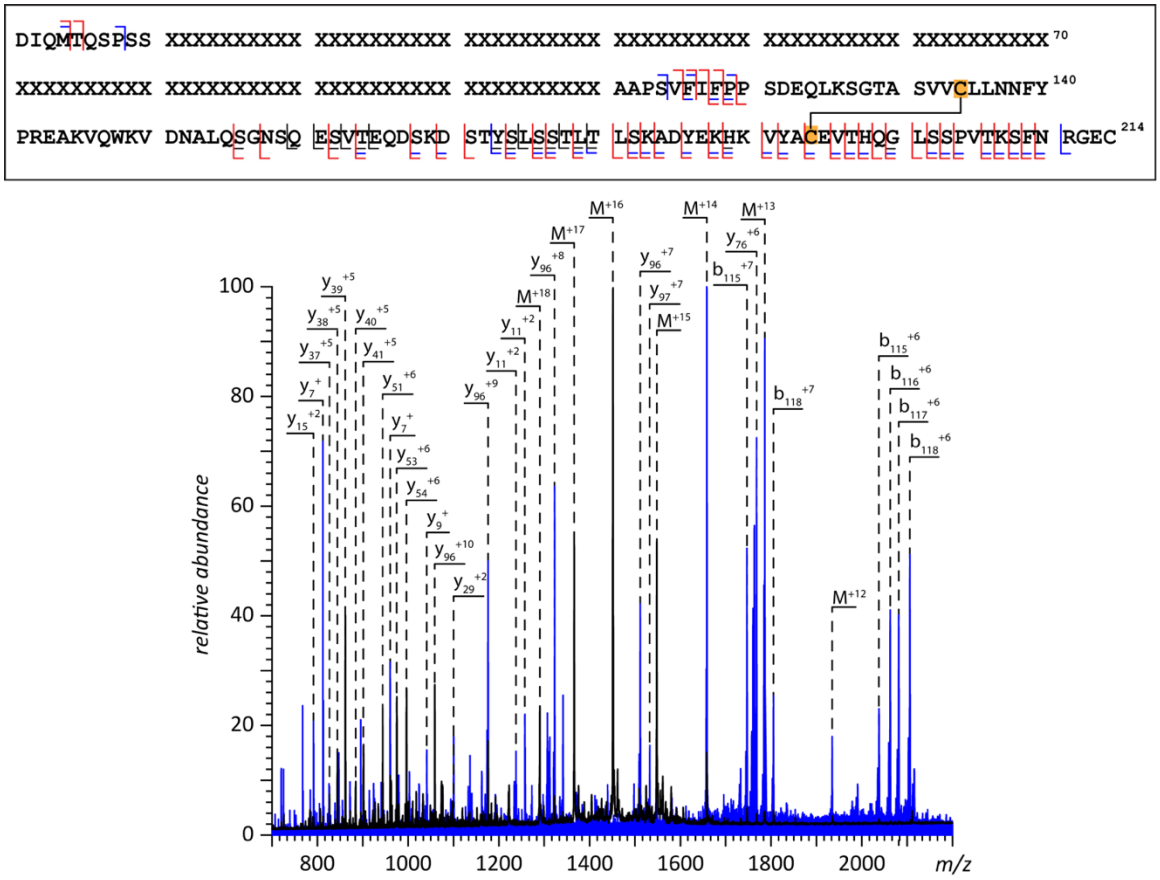

Figure S4.6. XP-RC MS/MS analysis of mAb: fragment ion spectra of the L-chain generated by on-column disulfide reduction of mAb (TCEP in the reagent plug). Fragmentation was induced by collisional activation of ions of monomeric L-chains at charge states +12 through +16 (blue-filled curve) and by collisional activation of all ions in the ESI interface without precursor ion selection (in-source fragmentation, black trace). The two fragmentation patterns are overlaid in the top diagram (the amino acid sequence is shown only for the constant region of the L-chain).

4.10 References

1 Carini, M., Regazzoni, L. & Aldini, G. Mass Spectrometric Strategies and Their Applications for Molecular Mass Determination of Recombinant Therapeutic Proteins. *Curr. Pharm. Biotechnol.* **12**, 1548-1557 (2011).

2 Kelleher, N. L. *et al.* Top down versus bottom up protein characterization by tandem high-resolution mass spectrometry. *J. Am. Chem. Soc.* **121**, 806-812 (1999).

3 Leurs, U., Mistarz, U. H. & Rand, K. D. Getting to the core of protein pharmaceuticals – Comprehensive structure analysis by mass spectrometry. *European Journal of Pharmaceutics and Biopharmaceutics* **93**, 95-109, doi:http://dx.doi.org/10.1016/j.ejpb.2015.03.012 (2015).

4 Bondarenko, P. V., Second, T. P., Zabrouskov, V., Makarov, A. A. & Zhang, Z. Q. Mass measurement and top-down HPLC/MS analysis of intact monoclonal antibodies on a hybrid linear quadrupole ion trap-orbitrap mass spectrometer. *J. Am. Soc. Mass Spectrom.* **20**, 1415-1424, doi:10.1016/j.jasms.2009.03.020 (2009).

5 Zhang, H., Cui, W. & Gross, M. L. Mass spectrometry for the biophysical characterization of therapeutic monoclonal antibodies. *FEBS Letters* **588**, 308-317, doi:http://dx.doi.org/10.1016/j.febslet.2013.11.027 (2014).

6 He, L. *et al.* Analysis of Monoclonal Antibodies in Human Serum as a Model for Clinical Monoclonal Gammopathy by Use of 21 Tesla FT-ICR Top-Down and Middle-Down MS/MS. *J. Am. Soc. Mass Spectrom.* **28**, 827-838, doi:10.1007/s13361-017-1602-6 (2017).

7 Wang, S., Bobst, C. E. & Kaltashov, I. A. Pitfalls in protein quantitation using acid-catalyzed O^{18} labeling: Hydrolysis-driven deamidation. *Anal. Chem.* **83**, 7227-7232, doi:10.1021/ac201657u (2011).

8 Ren, D. *et al.* An improved trypsin digestion method minimizes digestion-induced modifications on proteins. *Anal. Biochem.* **392**, 12-21, doi:10.1016/j.ab.2009.05.018 (2009).

9 Dick, L. W., Jr., Mahon, D., Qiu, D. & Cheng, K. C. Peptide mapping of therapeutic monoclonal antibodies: improvements for increased speed and fewer

artifacts. *J. Chromatogr. B Analyt. Technol. Biomed. Life Sci.* **877**, 230-236, doi:10.1016/j.jchromb.2008.12.009 (2009).

10 Hao, P., Ren, Y., Datta, A., Tam, J. P. & Sze, S. K. Evaluation of the effect of trypsin digestion buffers on artificial deamidation. *Journal of proteome research* **14**, 1308-1314, doi:10.1021/pr500903b (2015).

11 Zubarev, R. A. *et al.* Electron capture dissociation of gaseous multiply-charged proteins is favored at disulfide bonds and other sites of high hydrogen atom affinity. *J. Am. Chem. Soc.* **121**, 2857-2862 (1999).

12 Bilusich, D. *et al.* Direct identification of intramolecular disulfide links in peptides using negative ion electrospray mass spectra of underivatised peptides. A joint experimental and theoretical study. *Rapid Commun. Mass Spectrom.* **19**, 3063-3074 (2005).

13 Fung, Y. M. E., Kjeldsen, F., Silivra, O. A., Chan, T. W. D. & Zubarev, R. A. Facile disulfide bond cleavage in gaseous peptide and protein cations by ultraviolet photodissociation at 157 nm. *Angew. Chem. Int. Ed.* **44**, 6399-6403, doi:10.1002/anie.200501533 (2005).

14 Wang, G. & Kaltashov, I. A. A new approach to characterization of the higher order structure of disulfide-containing proteins using hydrogen/deuterium exchange and top-down mass spectrometry. *Anal. Chem.* **86**, 7293-7298 (2014).

15 Zhang, M. & Kaltashov, I. A. Mapping of protein disulfide bonds using negative ion fragmentation with a broadband precursor selection. *Anal. Chem.* **78**, 4820-4829 (2006).

16 Nicolardi, S., Deelder, A. M., Palmblad, M. & van der Burgt, Y. E. M. Structural Analysis of an Intact Monoclonal Antibody by Online Electrochemical Reduction of Disulfide Bonds and Fourier Transform Ion Cyclotron Resonance Mass Spectrometry. *Anal. Chem.* **86**, 5376-5382, doi:10.1021/ac500383c (2014).

17 Cramer, C. N., Haselmann, K. F., Olsen, J. V. & Nielsen, P. K. Disulfide Linkage Characterization of Disulfide Bond-Containing Proteins and Peptides by Reducing Electrochemistry and Mass Spectrometry. *Anal. Chem.* **88**, 1585-1592, doi:10.1021/acs.analchem.5b03148 (2016).

18 Almeida, A. & Kolarich, D. The promise of protein glycosylation for personalised medicine. *Biochim Biophys Acta* **1860**, 1583-1595, doi:10.1016/j.bbagen.2016.03.012 (2016).

19 Sparks, S. E. in *In: Glycobiology and Human Diseases* (ed G. edited by Wiederschain) Ch. 16, 284-312 (CRC Press, 2016).

20 Miura, Y. & Endo, T. Glycomics and glycoproteomics focused on aging and age-related diseases — Glycans as a potential biomarker for physiological alterations. *Biochim. Biophys. Acta* **1860**, 1608-1614, doi:http://dx.doi.org/10.1016/j.bbagen.2016.01.013 (2016).

21 Lauc, G., Pezer, M., Rudan, I. & Campbell, H. Mechanisms of disease: The human N-glycome. *Biochimica et Biophysica Acta (BBA) - General Subjects* **1860**, 1574-1582, doi:http://dx.doi.org/10.1016/j.bbagen.2015.10.016 (2016).

22 Kailemia, M. J., Park, D. & Lebrilla, C. B. Glycans and glycoproteins as specific biomarkers for cancer. *Anal Bioanal Chem* **409**, 395-410, doi:10.1007/s00216-016-9880-6 (2017).

23 Marengo, E. & Robotti, E. Biomarkers for pancreatic cancer: recent achievements in proteomics and genomics through classical and multivariate statistical methods. *World J. Gastroenterol.* **20**, 13325-13342, doi:10.3748/wjg.v20.i37.13325 (2014).

24 Meany, D. L. & Chan, D. W. Aberrant glycosylation associated with enzymes as cancer biomarkers. *Clin. Proteomics* **8**, 7, doi:10.1186/1559-0275-8-7 (2011).

25 Pawlowski, J. W. *et al.* Influence of glycan modification on IgG1 biochemical and biophysical properties. *submitted*.

26 Abzalimov, R. R. & Kaltashov, I. A. Electrospray ionization mass spectrometry of highly heterogeneous protein systems: Protein ion charge state assignment via incomplete charge reduction. *Anal. Chem.* **82**, 7523-7526, doi:10.1021/ac101848z (2010).

27 Mendoza, V. L. & Vachet, R. W. Probing protein structure by amino acid-specific covalent labeling and mass spectrometry. *Mass Spectrom. Rev.* **28**, 785-815 (2009).

28 Yu, E. T., Hawkins, A., Eaton, J. & Fabris, D. MS3D structural elucidation of the HIV-1 packaging signal. *Proc. Natl. Acad. Sci. U. S. A.* **105**, 12248-12253, doi:10.1073/pnas.0800509105 (2008).

29 Kellersberger, K. A., Yu, E., Kruppa, G. H., Young, M. M. & Fabris, D. Top-down characterization of nucleic acids modified by structural probes using high-resolution tandem mass spectrometry and automated data interpretation. *Anal. Chem.* **76**, 2438-2445, doi:10.1021/ac0355045 (2004).

30 Myers, D. P. *et al.* On-column nitrosation of amines observed in liquid chromatography impurity separations employing ammonium hydroxide and acetonitrile as mobile phase. *J. Chromatogr. A* **1319**, 57-64, doi:10.1016/j.chroma.2013.10.021 (2013).

31 Glowacki, R., Bald, E. & Jakubowski, H. An on-column derivatization method for the determination of homocysteine-thiolactone and protein N-linked homocysteine. *Amino acids* **41**, 187-194, doi:10.1007/s00726-010-0521-7 (2011).

32 Ma, L. & Kang, J. Determination of mercury ion by MEKC with on-column derivatisation and LIF detection. *J. Sep. Sci.* **31**, 888-892, doi:10.1002/jssc.200700606 (2008).

33 Halket, J. M. & Zaikin, V. G. Derivatization in mass spectrometry --7. On-line derivatisation/degradation. *Eur. J. Mass Spectrom.* **12**, 1-13, doi:10.1255/ejms.785 (2006).

34 Foley, J. P. & May, W. E. Optimization of secondary chemical equilibria in liquid chromatography: variables influencing the self-selectivity, retention, and efficiency in acid-base systems. *Anal. Chem.* **59**, 110-115, doi:10.1021/ac00128a023 (1987).

35 Shibukawa, M., Unno, A., Miura, T., Nagoya, A. & Oguma, K. On-Column Derivatization Using Redox Activity of Porous Graphitic Carbon Stationary Phase: An Approach to Enhancement of Separation Selectivity of Liquid Chromatography. *Anal. Chem.* **75**, 2775-2783, doi:10.1021/ac020705e (2003).

36 Saitoh, K. *et al.* On-column electrochemical redox derivatization for enhancement of separation selectivity of liquid chromatography use of redox reaction as secondary chemical equilibrium. *J. Chromatogr. A* **1180**, 66-72, doi:10.1016/j.chroma.2007.12.003 (2008).

37 Saitoh, K., Soeta, N., Minamisawa, H. & Shibukawa, M. On-line redox derivatization liquid chromatography for selective separation of Fe(II) and Fe(III) cyanide complexes using porous graphitic carbon. *Anal. Sci.* **29**, 715-721 (2013).

38 Troendlin, J., Rehbein, J., Hiersemann, M. & Trapp, O. Integration of catalysis and analysis is the key: rapid and precise investigation of the catalytic asymmetric Gosteli-Claisen rearrangement. *J. Am. Chem. Soc.* **133**, 16444-16450, doi:10.1021/ja207091x (2011).

39 Stockinger, S. & Trapp, O. Integrating reaction and analysis: investigation of higher-order reactions by cryogenic trapping. *Beilstein J. Org. Chem.* **9**, 1837-1842, doi:10.3762/bjoc.9.214 (2013).

40 Aono, H. *et al.* Efficient on-column conversion of IgG1 trisulfide linkages to native disulfides in tandem with Protein A affinity chromatography. *J. Chromatogr. A* **1217**, 5225-5232, doi:10.1016/j.chroma.2010.06.029 (2010).

41 Bolton, G. R. & Mehta, K. K. The role of more than 40 years of improvement in protein A chromatography in the growth of the therapeutic antibody industry. *Biotechnol. Prog.* **32**, 1193-1202, doi:10.1002/btpr.2324 (2016).

42 Choe, W., Durgannavar, T. A. & Chung, S. J. Fc-Binding Ligands of Immunoglobulin G: An Overview of High Affinity Proteins and Peptides. *Materials (Basel, Switzerland)* **9**, 994-1010, doi:10.3390/ma9120994 (2016).

43 Fatunmbi, O., Abzalimov, R. R., Savinov, S. N., Gershenson, A. & Kaltashov, I. A. Interactions of Haptoglobin with Monomeric Globin Species: Insights from Molecular Modeling and Native Electrospray Ionization Mass Spectrometry. *Biochemistry* **55**, 1918-1928, doi:10.1021/acs.biochem.5b00807 (2016).

44 Kaltashov, I. A. & Abzalimov, R. R. Do ionic charges in ESI MS provide useful information on macromolecular structure? *J. Am. Soc. Mass Spectrom.* **19**, 1239-1246 (2008).

45 Testa, L., Brocca, S. & Grandori, R. Charge-surface correlation in electrospray ionization of folded and unfolded proteins. *Anal. Chem.* **83**, 6459-6463 (2011).

46 Liu, H., Chumsae, C., Gaza-Bulseco, G., Hurkmans, K. & Radziejewski, C. H. Ranking the susceptibility of disulfide bonds in human IgG1 antibodies by

reduction, differential alkylation, and LC-MS analysis. *Anal. Chem.* **82**, 5219-5226, doi:10.1021/ac100575n (2010).

47 Fornelli, L. *et al.* Top-down analysis of immunoglobulin G isotypes 1 and 2 with electron transfer dissociation on a high-field Orbitrap mass spectrometer. *J. Proteomics* **159**, 67-76, doi:https://doi.org/10.1016/j.jprot.2017.02.013 (2017).

48 Sharp, J. S., Becker, J. M. & Hettich, R. L. Protein surface mapping by chemical oxidation: Structural analysis by mass spectrometry. *Anal. Biochem.* **313**, 216-225 (2003).

49 Wang, S. & Kaltashov, I. A. Identification of reduction-susceptible disulfide bonds in transferrin by differential alkylation using O(16)/O(18) labeled iodoacetic acid. *J. Am. Soc. Mass Spectrom.* **26**, 800-807, doi:10.1007/s13361-015-1082-5 (2015).

50 Siuti, N. & Kelleher, N. L. Decoding protein modifications using top-down mass spectrometry. *Nat. Meth.* **4**, 817-821 (2007).

51 Gregorich, Z. R. & Ge, Y. Top-down proteomics in health and disease: challenges and opportunities. *Proteomics* **14**, 1195-1210, doi:10.1002/pmic.201300432 (2014).

52 Li, H., Wolff, J. J., Van Orden, S. L. & Loo, J. A. Native top-down electrospray ionization-mass spectrometry of 158 kDa protein complex by high-resolution Fourier transform ion cyclotron resonance mass spectrometry. *Anal. Chem.* **86**, 317-320, doi:10.1021/ac4033214 (2014).

53 Xie, Y., Zhang, J., Yin, S. & Loo, J. A. Top-down ESI-ECD-FT-ICR mass spectrometry localizes noncovalent protein-ligand binding sites. *J. Am. Chem. Soc.* **128**, 14432-14433 (2006).

54 Wang, G., Abzalimov, R. R., Bobst, C. E. & Kaltashov, I. A. Conformer-specific characterization of non-native protein states using hydrogen exchange and top-down mass spectrometry. *Proc. Natl. Acd. Sci. U.S.A.* **110**, 20087-20092 (2013).

55 Pan, J., Han, J., Borchers, C. H. & Konermann, L. Hydrogen/deuterium exchange mass spectrometry with top-down electron capture dissociation for characterizing structural transitions of a 17 kDa protein. *J. Am. Chem. Soc.* **131**, 12801-12808 (2009).

56 Zhang, H., Cui, W., Wen, J., Blankenship, R. E. & Gross, M. L. Native electrospray and electron-capture dissociation FTICR mass spectrometry for top-down studies of protein assemblies. *Anal. Chem.* **83**, 5598-5606, doi:10.1021/ac200695d (2011).

57 Bao, J. *et al.* Pre-equilibration kinetic size-exclusion chromatography with mass spectrometry detection (peKSEC-MS) for label-free solution-based kinetic analysis of protein-small molecule interactions. *Analyst* **88**, 4063-4070, doi:10.1039/c4an02232g (2015).

CHAPTER 5

CONCLUSIONS AND FUTURE DIRECTIONS

5.1 Conclusion

MS and LC are excellent characterization tools as demonstrated by this thesis. MS allows for precise and accurate mass measurements that are extremely valuable for protein identification and quality. Additionally, these measurements can be used for discovery and quantitation of PTMs. LC provides the ability to separate components in a complex sample by a variety of physical and chemical properties. The ability to separate proteins by a specific property creates opportunities to tailor a method to separate out an analyte of interest. This thesis describes a diverse set of novel LC and MS methods to analyze proteins with biotherapeutic potential.

In chapter II, a method was developed to analyze the metal and synergistic anion composition of Tf. LC and native MS usefulness were both highlighted with their ability to purify and measure the composition of a non-covalent complex, respectively. To purify Tf from serum a 2D separation strategy was required due to the complexity of the sample. SEC was used to collect a Tf-containing fraction while a BDR column was used to deplete the abundant serum albumin. Native MS was mandatory to preserve the metal and synergistic anion composition of Tf which would be lost under denaturing conditions. One of the six serum samples was observed to have oxalate as the synergistic anion instead of the typical carbonate. Tf with bound oxalate is known to negatively affect iron homeostasis as iron is unable to be released in cells. Current clinical tests can measure the amount of oxalate in the blood but are unable to detect Tf-bound oxalate. The developed method has

great potential to discover any potential link between oxalate-bound Tf and disruption to iron homeostasis and its role in iron-related diseases.

Chapter III presented work on the glycan modification of a mAb and the effect on its effector functions and biophysical properties. An IgG1 was enzymatically modified to produce three different glycan-modified forms (deglycosylated, hypergalactosylated, and hypersialylated). All three forms were characterized by various analytical methods for comparison to each other and the unmodified IgG1. The goal of these experiments was to understand how the glycan composition of a mAb affects its biophysical properties and effector functions. Biophysical measurements did not reveal any significant changes (excluding the loss of stability for the CH2 domain of deglycosylated IgG1 which has been previously reported) in the higher order structure or stability of any of the three modified IgGs. Removal of the glycan chain appears to abrogate any effector functions of IgG1 while maintaining its long half-life. If a mAb's mechanism of action is drug delivery or imagine, using a deglycosylated or aglycosylated mAb may be an attractive choice due to its lack of effector function while maintaining a long half-life. Hypersialylation and hypergalactosylation of an IgG1 were not shown to have a significant effect on half-lives and effector functions. The lack of a significant effect allows for more variability of an IgG1's glycosylation composition during production without potentially affecting a mAb's *in vivo* function. An increase of terminal galactose(s) on a IgG1's glycan chain is known to correlate with a greater complement dependent cytotoxicity which might be attractive for cancer targeting mAbs. Additionally, sialylated IgGs are known to possess anti-inflammatory properties making its incorporation during production attractive for treating inflammatory-related diseases. It is very important to establish how PTMs (glycosylation

in this case) may affect the biophysical properties of a protein. If it can be determined that PTMs will not affect a protein's function or provide an alternative use for a biotherapeutic, it provides more flexibility in producing a biotherapeutic.

A novel XP-RC/MS method was presented in chapter IV. A reagent plug is first injected onto a column after which a protein sample is injected following a specified time delay. At some point inside the column the two traveling peaks will cross and a chemical reaction can take place. Due to SEC separating molecules by their hydrodynamic radius, proteins will have a faster velocity than the reagent plug allowing them to be separated during elution. Three proteins (β2m, IgG1, and Hp 1-1) were used to demonstrate the versatility and usefulness of this approach. All three proteins were successfully reduced on column using a TCEP-containing reagent plug. Each reduced protein was analyzed on-line by MS to confirm that reduction was successful. Reduction of Hp 1-1 allowed for determining of the glycosylation of the heavy chain: such a determination is impossible at the whole protein level due the heterogeneity of Hp 1-1. Specifically, the amount of fucosylation of Hp 1-1 could be measured and is known to be relevant for certain disease diagnoses. β2m and IgG1's LC were both top-down sequenced by MS/MS after on column reduction. XP-RC/MS is a powerful method as it allows for on column reduction of disulfide containing proteins for MS and MS/MS analysis.

To further demonstrate the versatility of XP-RC/MS, a two reagent plug method was implemented to first oxidize and then reduce IgG1. Eluting oxidized and reduced species were detected on-line by MS to identify where oxidation is occurring on IgG1. Based on measured mass shifts, only the HC was oxidized while the LC was unaffected. A two reagent plug method suggests numerous possibilities in which a protein can be

modified and then reduced. XP-RC/MS is a powerful tool for protein characterization that greatly reduces sample analysis time and is suitable for proteins that are unstable after reduction. The methods presented in this thesis demonstrate the wide range of usefulness of LC- and MS-based methods for characterization of proteins with biotherapeutic potential.

5.2 Future Directions

5.2.1 Quantitation of Iron Occupancy in Tf

The maximum concentration of iron that can be bound by serum Tf, from an individual, is known as the total iron bound concentration (TIBC).[1] TIBC is a colorimetric assay that utilizes an iron binding molecule (chromazurol B) to measure free iron released from Tf in solution. A TIBC measurement is used for a diagnosis of anemia, hereditary hemochromatosis, and other iron deficiency disorders.[1-3] However, TIBC does not provide information with regard to the concentration of apo-, monoferric-, or holo-Tf in serum which may be important to iron homeostasis in an individual. Holo-Tf binds to Tf receptor (at pH 7.4) with the highest affinity followed by monoferric-Tf while apo-Tf has a very weak affinity.[4] Further information may be gathered by measuring the concentration or percentage of apo-, monoferric-, or holo-Tf in a patient's serum. It has been reported the distribution of holo-Tf in is ~11 to 27%[4] in serum. A plausible scenario of the importance of being able to measure the concentrations of apo-, monoferric-, or holo-Tf is as follows. Two patients are determined to have the same TIBC value but differ in their distribution of monoferric- and holo-Tf which would not be detected by TIBC. Measuring the

concentration of monoferric- and holo-Tf could be useful when diagnosing iron related diseases. Currently, urea gel analysis is used to estimate the different iron occupancy states of Tf in serum.[4] However this is not a high throughput assay that could be implemented as a clinical test. Presented below is a method to measure the amount of apo-, monoferric-, or holo-Tf in serum.

Figure 5.1 describes the general procedure for the purification of Tf from serum and its analysis. First, serum is injected onto an SEC column and the eluting Tf fraction is collected. To separate holo-Tf from apo- and monoferric-Tf a BDR column is used. As show in figure 5.2, holo-Tf is not retained by the resin while monoferric- and apo-Tf are. Separation of holo-Tf from apo- and monoferric-Tf allows for their concentrations to be indirectly measured by a using chromazurol B. Free iron is bound by chromazurol B and the concentration iron is calculated by measuring the 660nm absorbance and comparing it to a calibration curve. The general strategy to measure the concentration of apo-, monoferric-, and holo-Tf involves the adjustment of the solution's pH to promote Tf to bind or release iron. Both Tf-containing fractions (holo-Tf and monoferric-/apo-Tf) are first added to a low pH (4.5) solution with iron and chromazurol B. Released iron results in the increased absorbance at 660 nm and is used to calculate the concentration of iron bound by Tf. For the holo-Tf sample, the measured iron concentration is halved to calculate holo-Tf's concentration. The iron concentration for the monoferric-/apo-Tf sample is equal to the concentration of monoferric-Tf. To determine the concentration of apo-Tf, a neutral carbonate buffer (pH 7.0) is added to the low pH monoferric-/apo-Tf solution. Raising the pH to near neutral permits Tf to bind iron and results in the decrease of 660 nm absorbance. The concentration of iron bound is calculated by the decrease of

660 nm absorbance and the concentration of Tf is equal to half of the measured iron concentration. However, it is important to keep in mind that monoferric-Tf was converted to apo-Tf in the previous step so the measured concentration of Tf is the combined concentration of (previously) monoferric- and apo-Tf. Subtracting monoferric-Tf's concentration from the total Tf concentration results in the concentration of apo-Tf. Importantly, an automated plate reader with liquid transfer capabilities is able to handle the chromazurol B absorbance detection making this assay to be high throughput.

It is the goal of this proposed method to accurately quantitate the amount of apo-, monoferric-, or holo-Tf in serum. The generated data may help relate iron-related disease symptoms with the iron occupancy of Tf. With this additional information, it may be possible to establish additional biomarkers (such as % of holo-Tf or total concentration) to assist with iron-related disease diagnosis.

5.2.2 Cross Path Reactive Chromatography

XP-RC/MS is a very versatile method due to the variety and number of plug that can be employed. As shown in chapter IV, multiple plugs can be injected to facilitate different protein reactions. This leads to the enticing possibility of performing online HDX inside an SEC column. An HDX XP-RC/MS schematic is shown in figure 5.3. By adjusting the time between plugs, a protein can be detected very quickly after exchange and reduction. Furthermore unlike traditional HDX experiments there will be no dilution (excluding diffusion of the protein plug inside the column) of the protein sample as it passes through the deuterium plug. Additionally, the reduction plug can be removed if global

HDX measurements are of interest. Reducing the time between exchange and detection will help with back exchange that is major issue affecting current HDX measurements.

Other types of chromatography can be used for XP-RC/MS as long as the analyte and reactive plugs can be separated. Ion exchange chromatography is a possible alternative to SEC due to its ability to retain a molecule for significant amount of time under the correct mobile phase conditions. By reversing the order of plugs in an SEC experiment, a protein can first be injected followed by any number of reactive plugs, as shown in figure 5.4. Once the reactive plugs elute from the column, a step gradient can be used to elute the modified protein. This has the added benefit over SEC XP-RC/MS which has a limited range of the number of plugs that can be effectively injected. XP-RC/MS is a compartmental method where different plugs or types chromatographies can be implemented to tackle the unique requirements of an experiment.

5.3 Figures

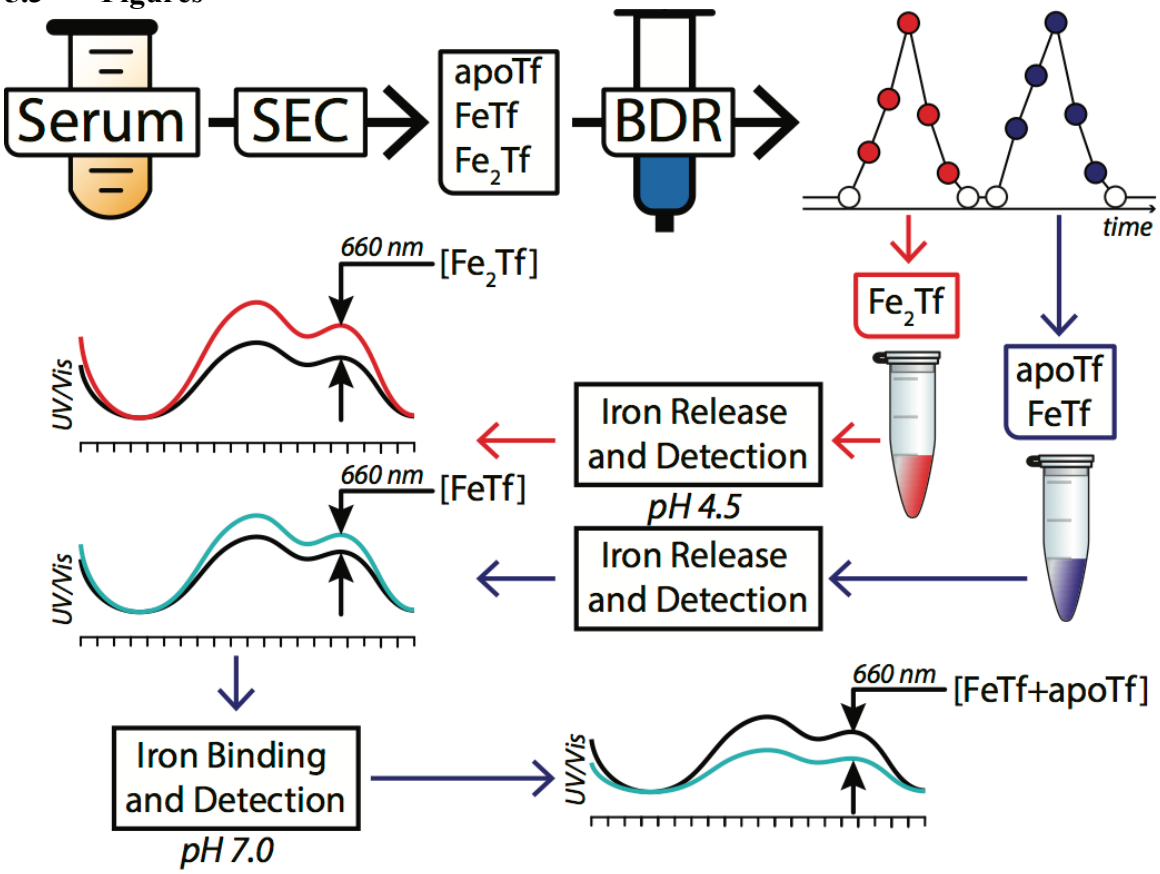

Figure 5.1 General schematic for quantitation of apo-, monoferric-, and holo-Tf. Serum is injected onto an SEC column and a fraction containing Tf is collected. A BDR column (cibacron F3GA) is used to separate holo-Tf from apo- and monoferric-Tf. Holo-Tf is added to a low pH solution (4.5) containing iron and chromazurol B. The change in 660 nm absorbance is measured to calculate the concentration of holo-Tf. Apo- and monoferric-Tf are added to a low pH solution (4.5) containing iron and chromazurol B. The change in 660 nm absorbance is measured to calculate the concentration of monoferric-Tf. Next, a carbonate buffer, pH 7.0, is added to the solution to allow Tf to bind iron. The change in 660 nm absorbance is measured to calculate the concentration of total Tf in solution. This concentration is subtracted by the previously measured monoferric-Tf concentration to calculate the concentration of apo-Tf.

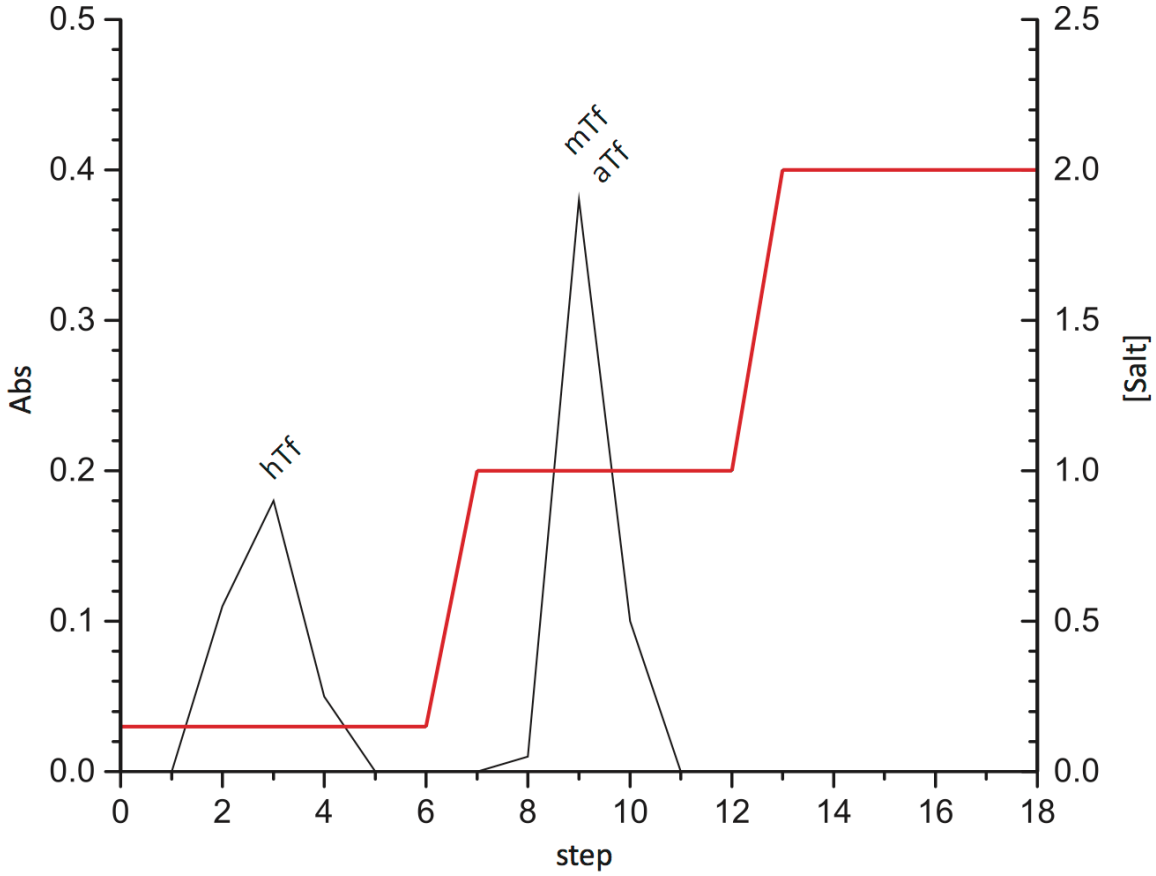

Figure 5.2 Separation of holo-Tf from monoferric- and apo-Tf on a cibacron F3GA column using a salt gradient (red). The identity of Tf in each eluting peak was confirmed by MS.

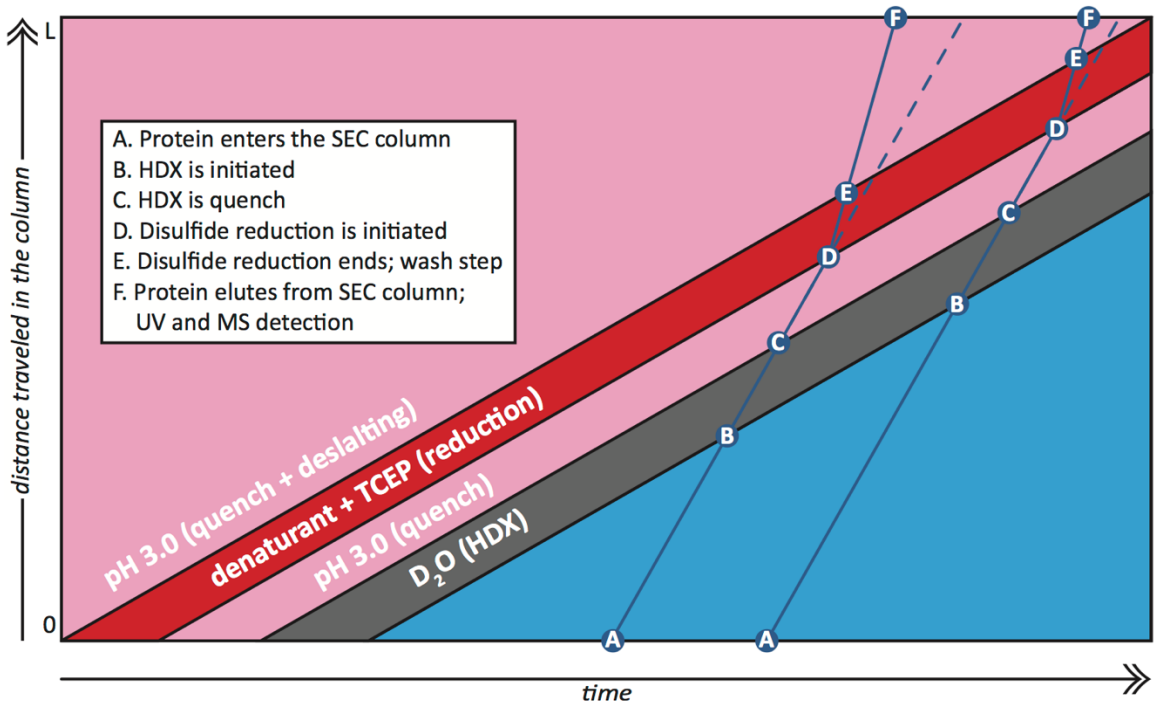

Figure 5.3 Schematic for an online HDX assay inside an SEC column.

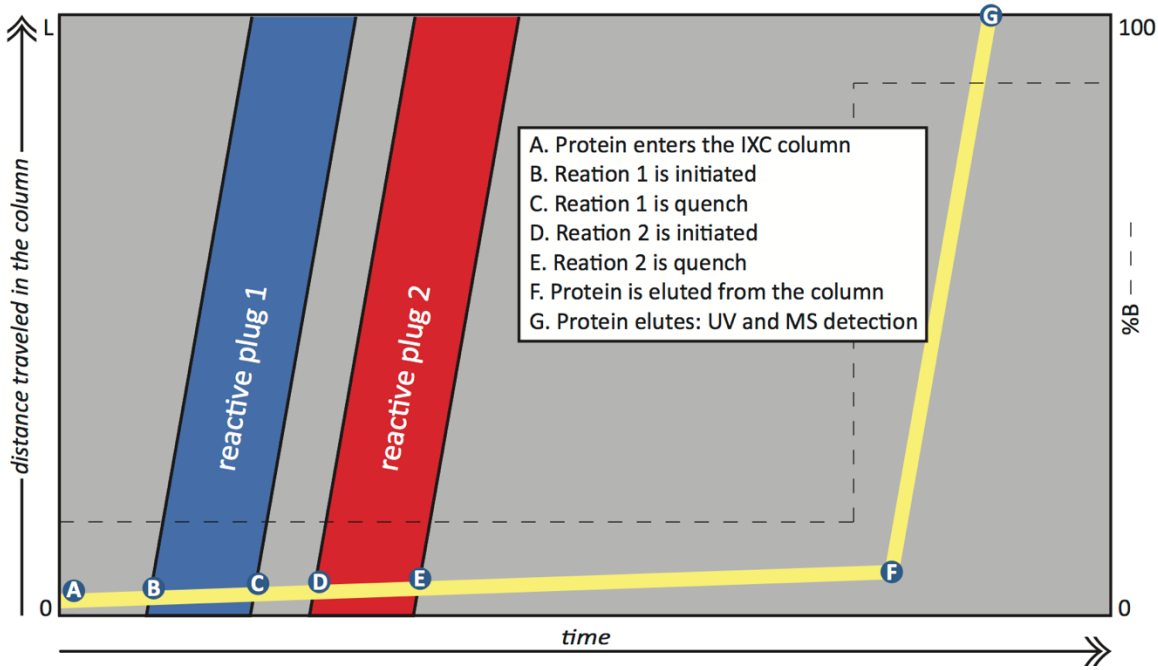

Figure 5.4 Representative workflow for an XP-RC-MS experiment in an IXC column.

5.4 References

1 Siek, G., Lawlor, J., Pelczar, D., Sane, M. & Musto, J. Direct Serum Total Iron-binding Capacity Assay Suitable for Automated Analyzers. *Clin. Chem.* **48**, 161-166 (2002).

2 Imperatore, G. *et al.* Hereditary hemochromatosis: Perspectives of public health, medical genetics, and primary care. *Genet. Med.* **5**, 1-8 (2003).

3 Hawkins, R. C. Total iron binding capacity or transferrin concentration alone outperforms iron and saturation indices in predicting iron deficiency. *Clin. Chim. Acta* **380**, 203-207, doi:10.1016/j.cca.2007.02.032 (2007).

4 Luck, A. N. & Mason, A. B. in *Current Topics in Membranes* Vol. 69 (eds José M. Argüello & Svetlana Lutsenko) 3-35 (Academic Press, 2012).

APPENDIX A

PURIFICATION AND ANALYSIS OF TF AND HUMAN SERUM ALBUMIN FROM SERUM SAMPLES.

A.1 Introduction

Using the method developed in chapter II Tf was purified and measured from several different serum samples. Additionally, human serum albumin (HSA) was also measured by buffer exchanging HSA from the high salt fractions of the BDR runs into a MS-friendly buffer. The objective was to determine the metal and synergistic anion composition for Tf to determine if other Tf samples contained oxalate as the synergistic anion. In addition, any PTMs of Tf and HSA were identified. Of particular interest was the presence of glycation on Tf and HSA as it is a potential biomarker for diabetes mellitus.[1-3] Glycation has also been shown to negatively affect Tf's ability bind iron thus affect iron homeostasis in the body.[4,5] Briefly, it was found at a physiologically relevant time scale and glucose concentration Tf was able to be glycated at lysine^{534}.[4] Lysine^{534} is a component of the secondary pH sensitive shell that is responsible for Tf's ability to bind and release iron. Glycation of lysine^{534} appears to disrupt Tf's C-lobe to bind iron. Therefore, it is important to determine if Tf is glycated as it may play a role in disrupting iron homeostasis in the body.

A.2 Results and Discussion

All five HSA samples (Figures A.6-A.10) were observed to be modified by glycation and cysteinylation. The relative abundance of glycation and cysteinylation for each sample is different with respect to each other and unmodified HSA. Unfortunately,

the health status of the serum sample patients is unknown. Consequently, no meaningful correlation between glycation and or cysteinylation can be made to any ailments.

Of the five serum Tf samples two were observed with oxalate bound to iron. Also observed was three of the Tf samples were glycated as shown in figures A.2-4. Additionally, all five Tf samples appear to have different levels of apo-, monoferric-, and holo-Tf. While it is tempting to make conclusions from the observed iron saturation and synergistic anion composition, without the full medical history of the serum sample donors this would be a imprudent decision. What can be discussed is out of the 7 (5 in this appendix and 2 from the published paper) different Tf samples analyzed, three had oxalate present as the synergistic anion. Moreover, three of the Tf samples were also observed to be glycated. While this is a small sample set, oxalate bound to iron in Tf appears to be common as well as glycation. To confirm this hypothesis and to attempt a link between oxalate and glycation to iron related diseases, a large set of Tf samples would need to be analyzed.

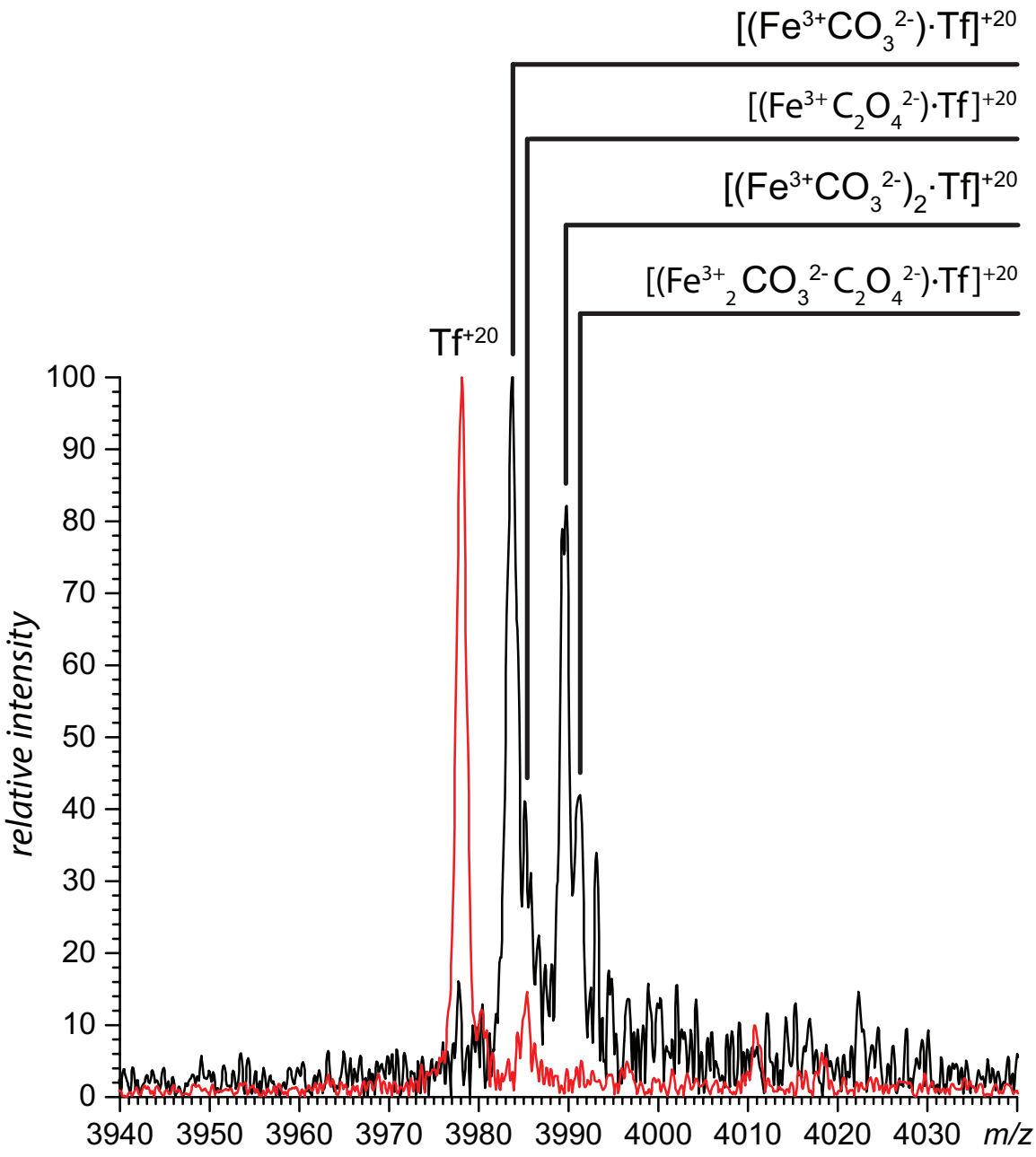

A.1 Tf from serum was found to be bound to iron with carbonate and/or oxalate as its synergistic anion. The black trace corresponds to native Tf and the red trace corresponds to Tf at pH 3.7.

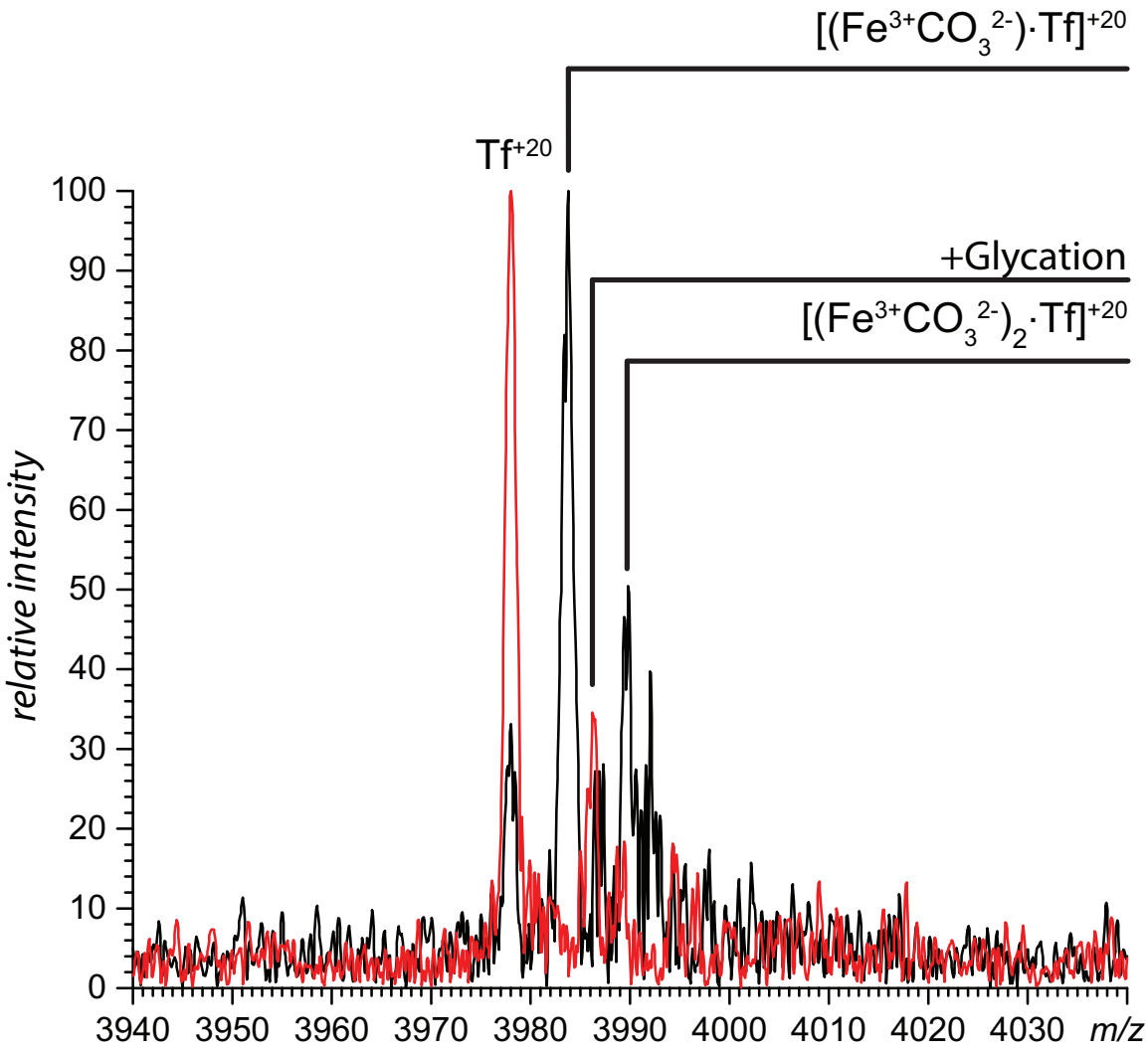

A.2 Tf from serum was found to be bound to iron with carbonate as its synergistic anion. Glycation of Tf was also observed. The black trace corresponds to native Tf and the red trace corresponds to Tf at pH 3.7.

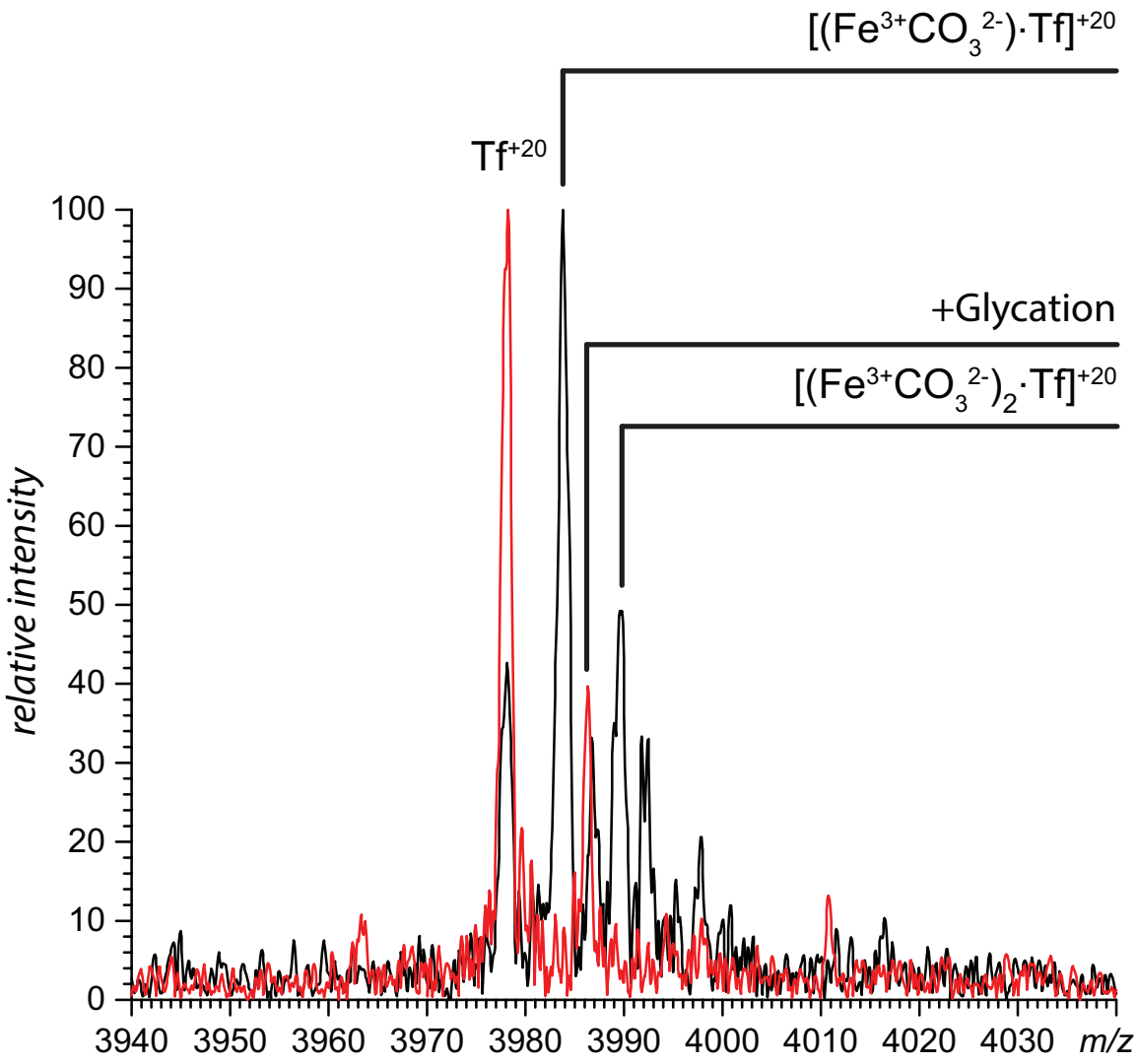

A.3 Tf from serum was found to be bound to iron with carbonate as its synergistic anion. Glycation of Tf was also observed. The black trace corresponds to native Tf and the red trace corresponds to Tf at pH 3.7.

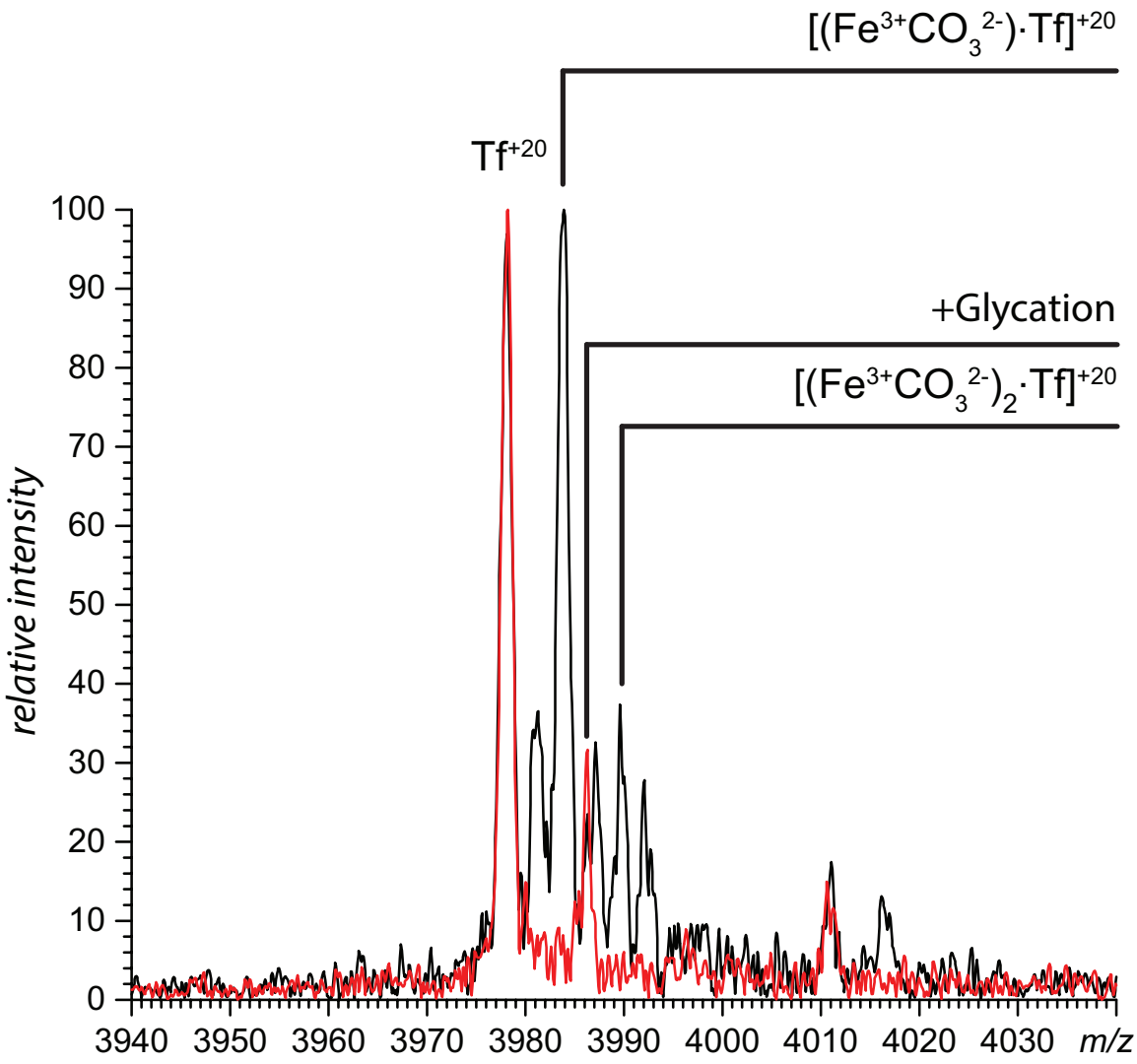

A.4 Tf from serum was found to be bound to iron with carbonate as its synergistic anion. Glycation of Tf was also observed. The black trace corresponds to native Tf and the red trace corresponds to Tf at pH 3.7.

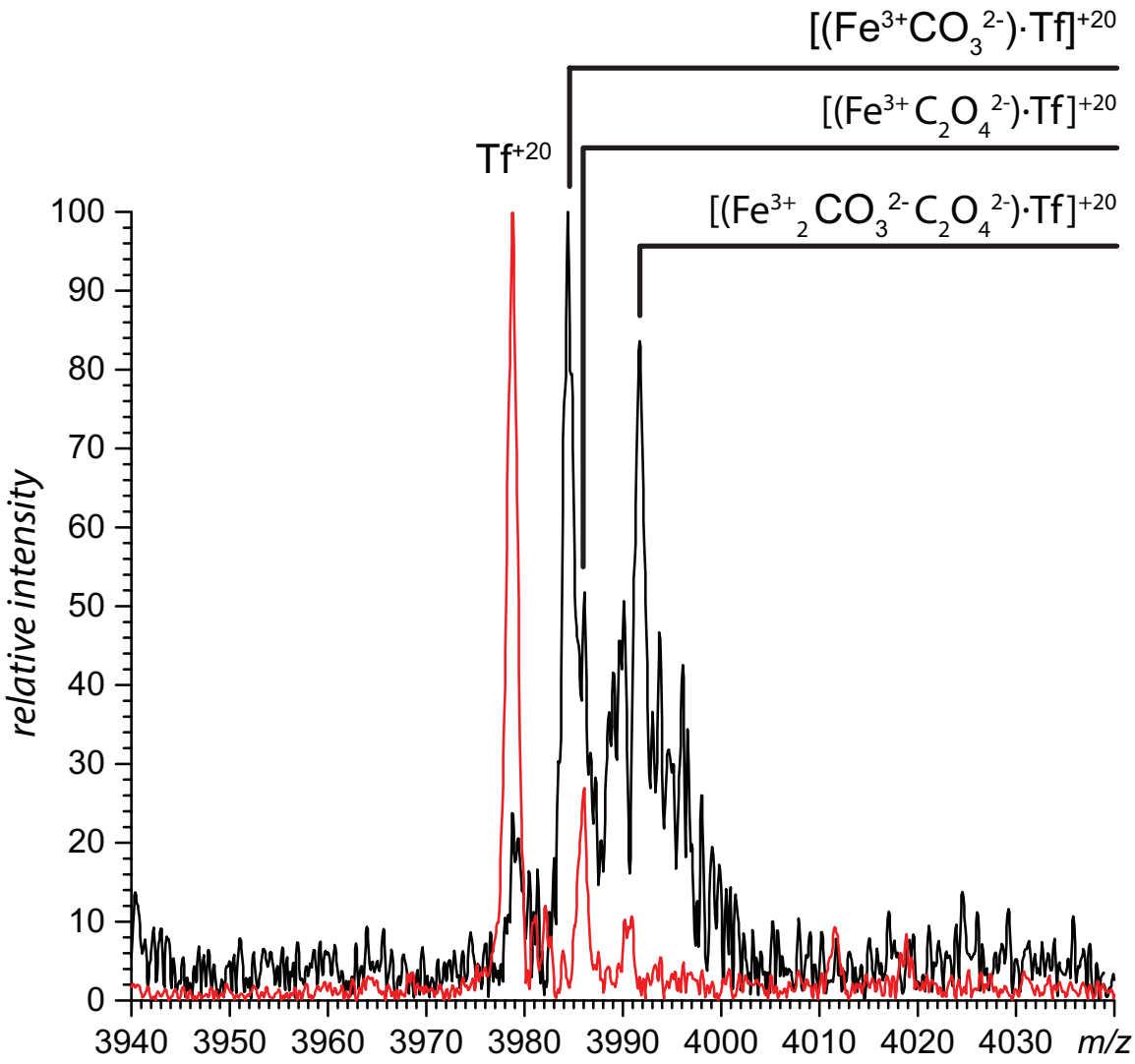

A.5 Tf from serum was found to be bound to iron with carbonate and/or oxalate as its synergistic anion. The black trace corresponds to native Tf and the red trace corresponds to Tf at pH 3.7.

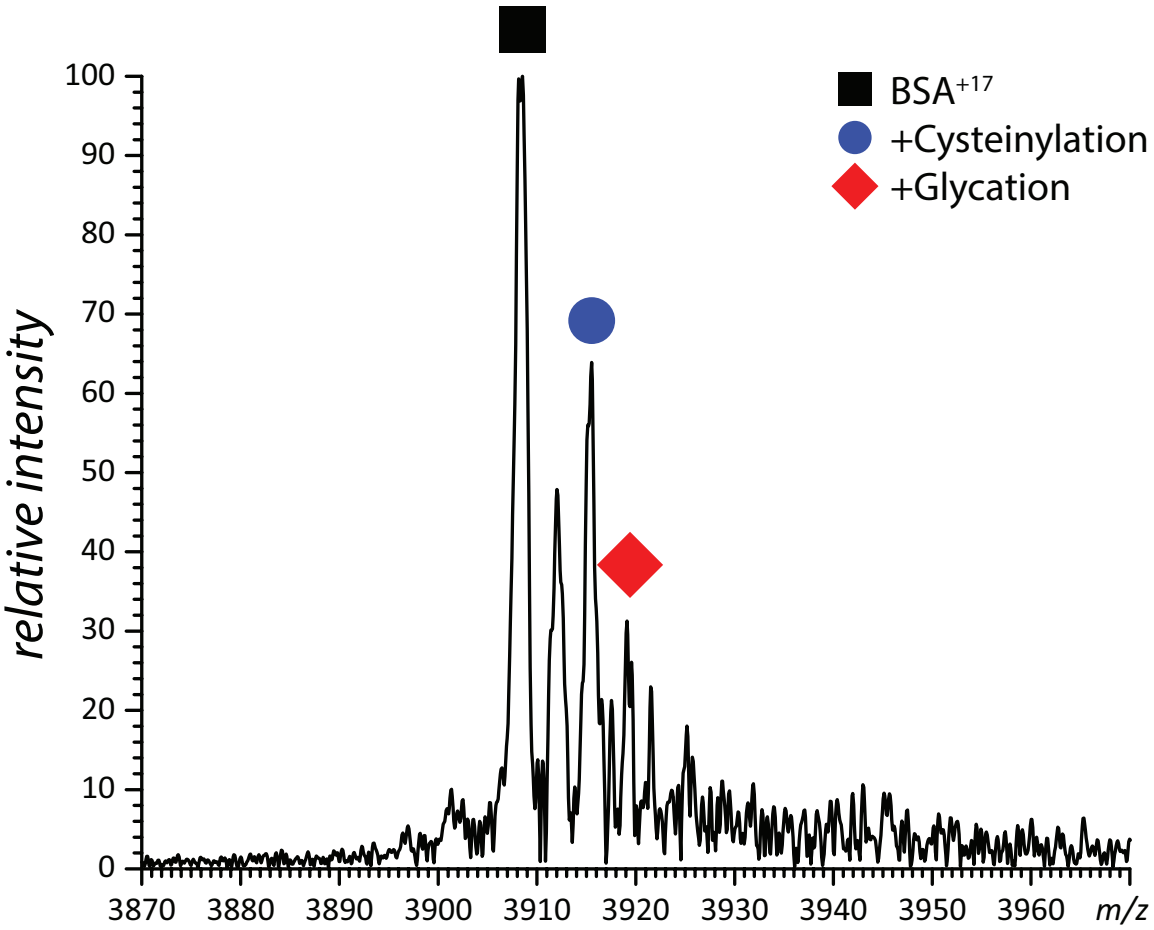

A.6 Zoomed in mass spectrum of the +17-charge state of HSA. Peaks corresponding to cysteinylation and glycation are labeled with a blue circle and red diamond respectively.

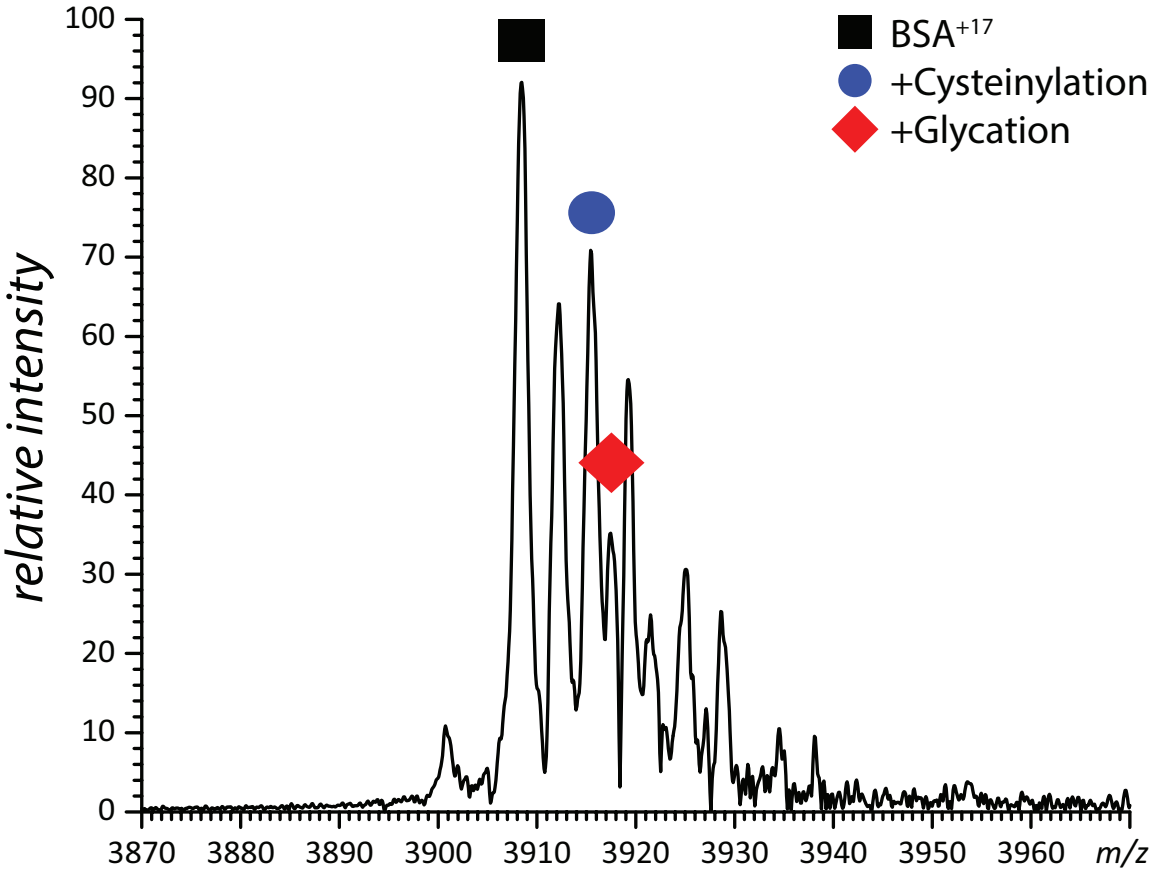

A.7 Zoomed in mass spectrum of the +17-charge state of HSA. Peaks corresponding to cysteinylation and glycation are labeled with a blue circle and red diamond respectively.

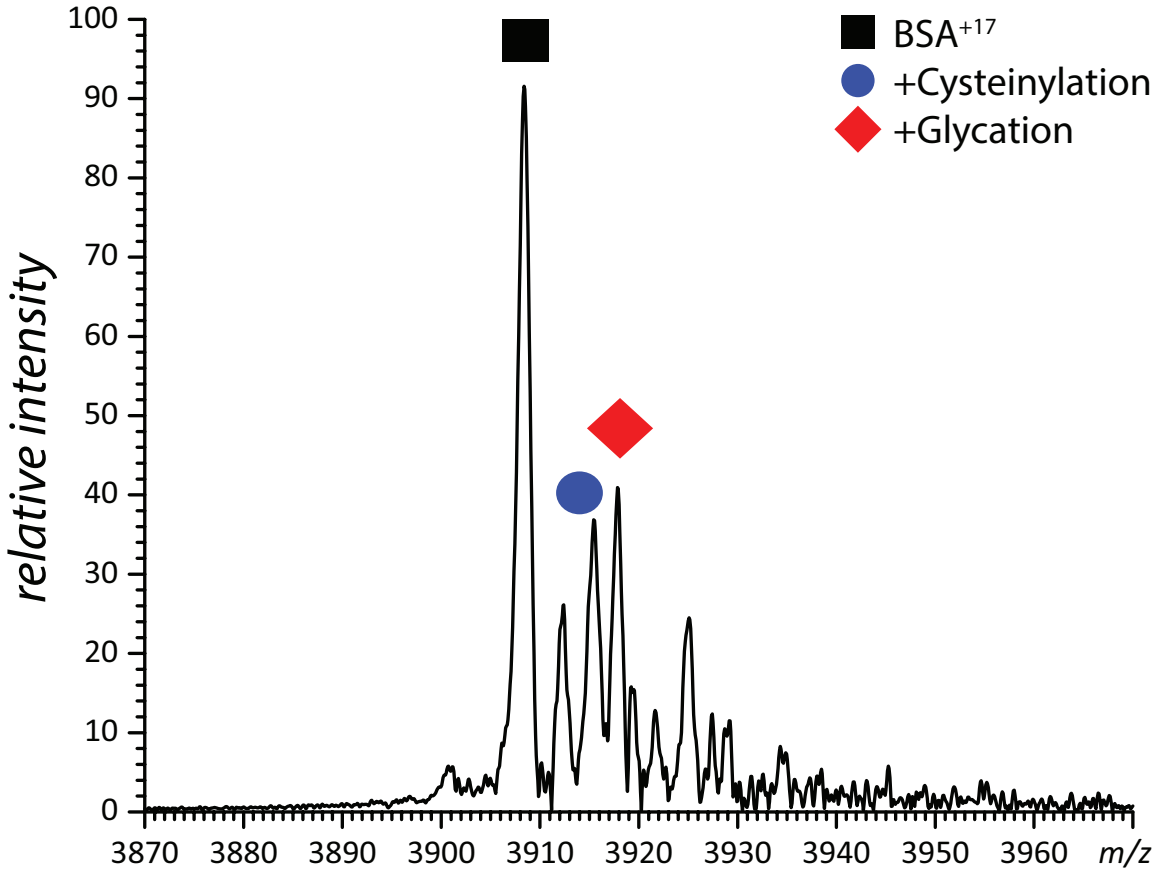

A.8 Zoomed in mass spectrum of the +17-charge state of HSA. Peaks corresponding to cysteinylation and glycation are labeled with a blue circle and red diamond respectively

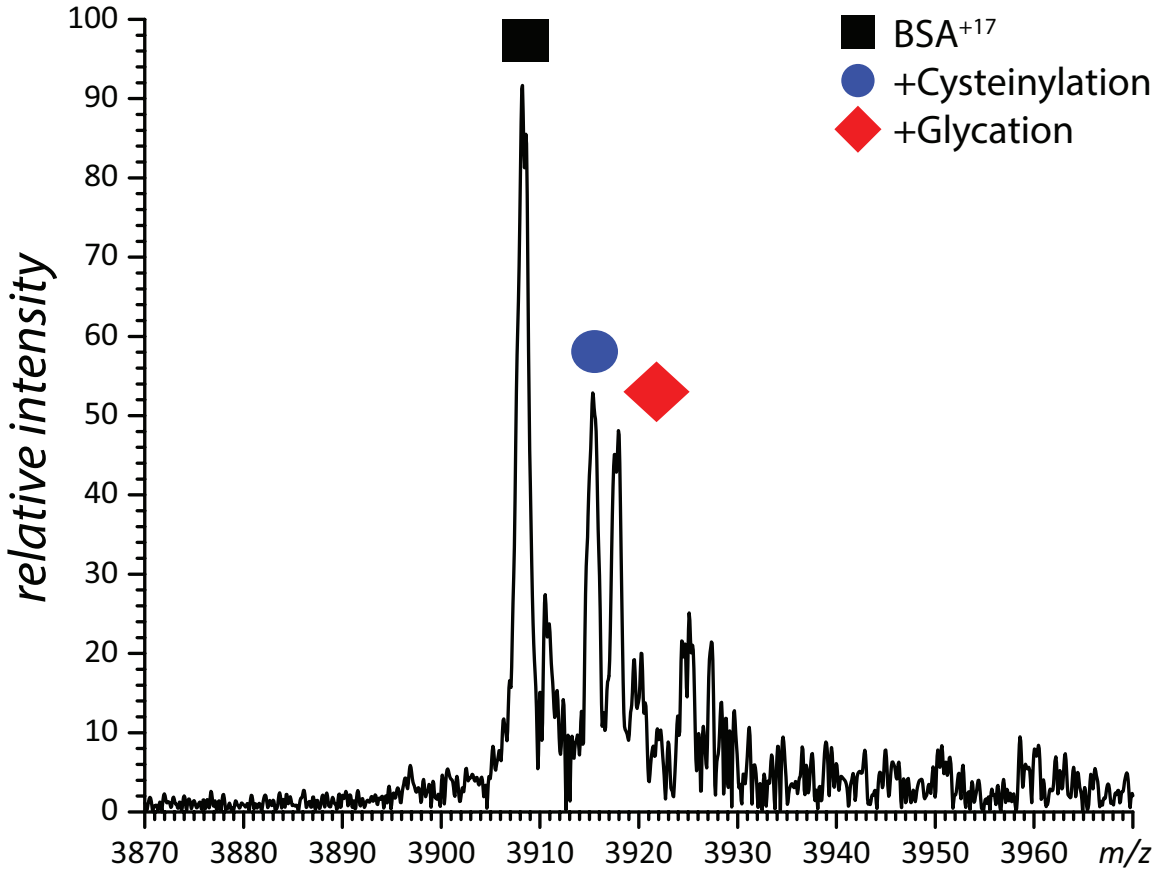

A.9 Zoomed in mass spectrum of the +17-charge state of HSA. Peaks corresponding to cysteinylation and glycation are labeled with a blue circle and red diamond respectively

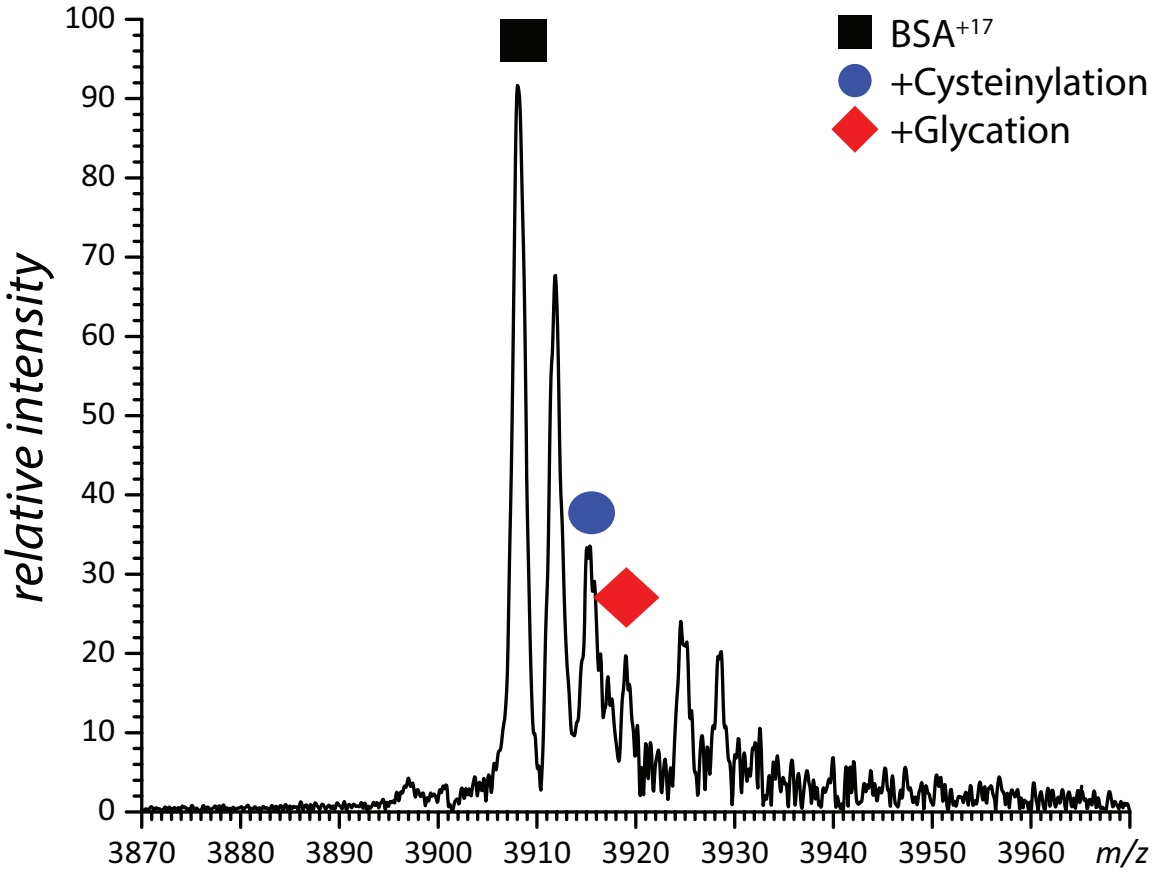

A.10 Zoomed in mass spectrum of the +17-charge state of HSA. Peaks corresponding to cysteinylation and glycation are labeled with a blue circle and red diamond respectively.

A.3 References

1 Dorcely, B. *et al.* Novel biomarkers for prediabetes, diabetes, and associated complications. *Diabetes Metab. Syndr. Obes.* **10**, 345-361, doi:10.2147/dmso.s100074 (2017).

2 Freitas, P. A. C., Ehlert, L. R. & Camargo, J. L. Glycated albumin: a potential biomarker in diabetes. *Archives of endocrinology and metabolism* **61**, 296-304, doi:10.1590/2359-3997000000272 (2017).

3 Van Campenhout, A. *et al.* A novel method to quantify in vivo transferrin glycation: Applications in diabetes mellitus. *Clin. Chim. Acta* **370**, 115-123, doi:https://doi.org/10.1016/j.cca.2006.01.028 (2006).

4 Silva, André M. N. *et al.* The glycation site specificity of human serum transferrin is a determinant for transferrin's functional impairment under elevated glycaemic conditions. *Biochem. J.* **461**, 33-42, doi:10.1042/bj20140133 (2014).

5 Van Campenhout, A., Van Campenhout, C., Lagrou, A. & Manuel-y-Keenoy, B. Iron-induced oxidative stress in haemodialysis patients: a pilot study on the impact of diabetes. *Biometals* **21**, 159-170, doi:10.1007/s10534-007-9104-9 (2008).

APPENDIX B

CALCULATIONS AND SIMULATIONS FOR XP-RC-LC

B.1 Calculating the residency time of an analyte in the reactive plug

In order for XP-RC-LC to considered as a robust analytical technique additional details about the interaction of the analyte and reactive plug as they cross paths is required. One important detail is the time an analyte spends in the reagent plug which is necessary for determining the reaction kinetics. **Figure B.1** describes the relationship of an analyte's residency in the reactive plug to the difference in elution between analyte and reactive plug. From the graph, it is clear the smaller difference between an analyte's and reactive plug's elution time the more time they spend interacting which intuitively makes sense. To calculate the time an analyte spends interacting (describe in detail *vide infra*) with the reactive plug the reactive plug is treated as stationary to the analyte. This can be modeled by subtracting the velocity of the analyte by the reactive plug to calculate an adjusted analyte velocity. By dividing the volume of the reactive plug by the adjusted analyte velocity, the time an analyte spends interacting with the reactive plug is calculated. From this simple calculation, it is clearly seen that the time an analyte spends interacting with the reactive plug can be easily controlled. One option is to change the volume of the reactive plug while the other is to change the flow rate of mobile phase. Both options allow for a great degree of control of the time an analyte interacts with the reactive plug.

Analyte residency time in the reactive plug calculation:

To calculate the analyte's residency time in the reactive plug several values must be experimentally determined.

(**1**) *Column volume*: Inject a small volume (20µL) of a 5% acetone solution onto the SEC column. Calculate the elution time from the maximum of the eluting peak's absorbance (280nm). Multiply the elution time by the flow rate of the mobile phase to calculate the column volume.

(**2**) *Reactive plug's velocity (v_p)*: Assuming the reactive plug is composed of small molecules far below the SEC column's permeation limit and will not interact with the stationary phase, the v_p will be equal to the flow rate of the mobile phase.

(**3**) *Analyte's velocity (v_a)*: Inject a small volume of the analyte onto the SEC column. Calculate the elution time from the maximum of the eluting peak's absorbance (280nm). Divide the column volume by the analyte's retention time to calculate v_a.

(**4**) *Analyte's adjusted velocity (v'_a)*: To calculate the analyte's residency time in the reactive plug, it will be treated as if the plug is stationary (as a point of reference) to the analyte. The velocity of the analyte *(v_a)* will be subtracted by the velocity of the reactive plug *(v_p)* to calculate the adjusted velocity *(v'_a)*.

(**5**) *Residency time in reactive plug*: The volume of the reactive plug is divided by the analyte's adjusted velocity *(v'_a)* to calculate the analyte's time spent in the reactive plug.

****Note**** Diffusion of the plug and analyte in the SEC column was not considered for these calculations.

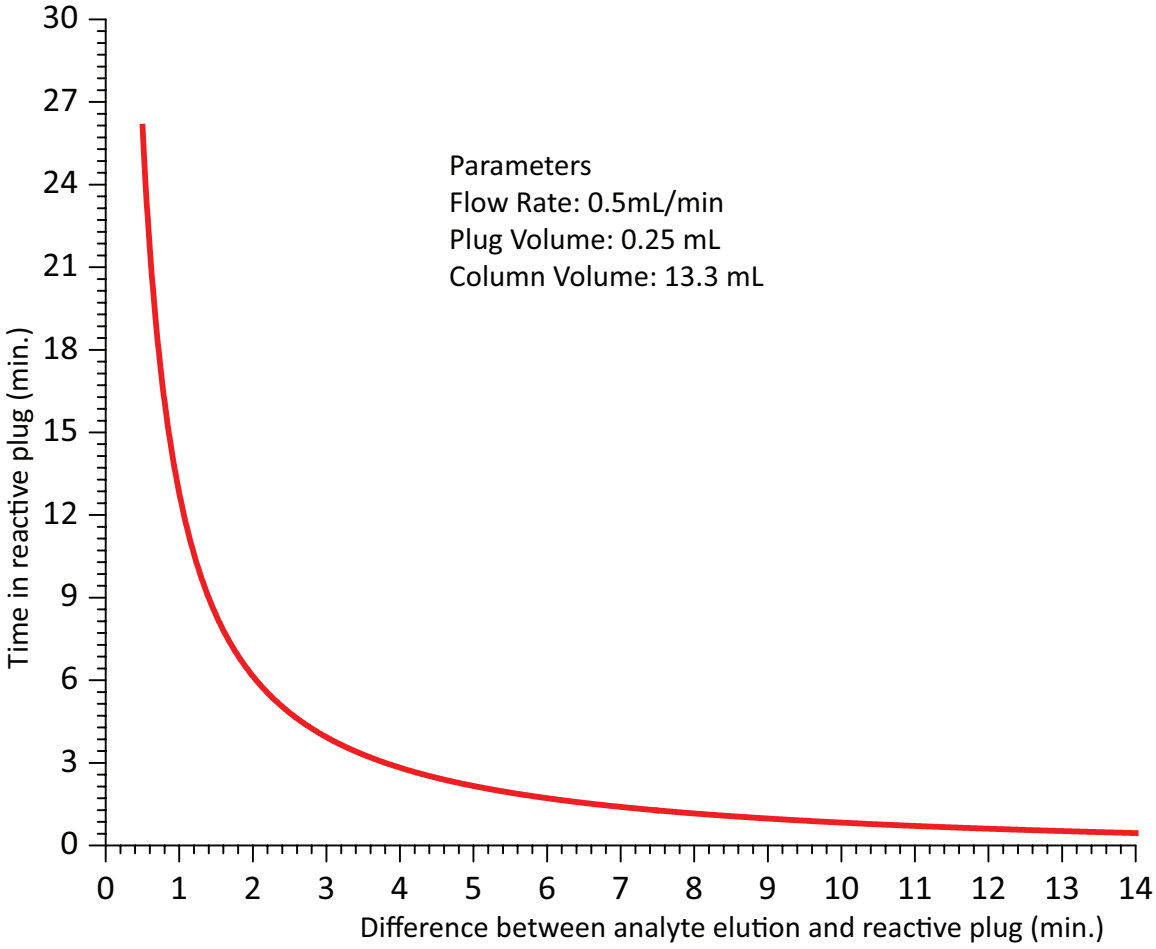

B.1 The graph depicts the relationship of the difference of elution time for the analyte and reactive plug to the amount of time an analyte spends in the reactive plug.

B.2 Diffusion of reactive plug inside an SEC column

To further understand the reaction kinetics for XP-RC-LC the shape of the reactive plug must be more fully defined. As the reactive plug travels through the SEC it will diffuse longitudinally as described in the Van Deemter equation for chromatography. This diffusion will lead to a concentration gradient that the analyte will interact with as it passes through the reactive plug. To assess how shape of a plug changes as it travels through an SEC column, a 300μL plug of 0.5% acetone was run at three different (100, 250, 500 μL/min) flow rates. For each flow rate a measurement was taken where the UV/VIS detector was place pre- and post-SEC column as shown by figure **B.2**. When the peaks from the respective flowrates are scaled and overlaid (figure **B.3**) it is clear there is minimal longitudinal diffusion. Not surprisingly was the lowest flow rate (100μL/min) had the most diffusion due to its increased time spent traveling through the column.

Also thought to be contributing to the band broadening is the introduction of the plug to the SEC column. For all these experiments (and those performed in chapter IV) a manual injector was used with a sample loop. The sample loop has a larger diameter than the tubing coming from the pump and leading to the column. It is suspected as the manual injector is turned and thus introducing the plug to the SEC column the mobile phase is spiked through a portion of the reactive plug due to laminar flow. This would create a mixture of mobile phase and reactive plug that will alter the concentration of the active component(s) in the plug as well as lead to an increase of the plug's volume. New plumbing schemes will be needed to help minimize these issues to give a more uniform reactive plug.

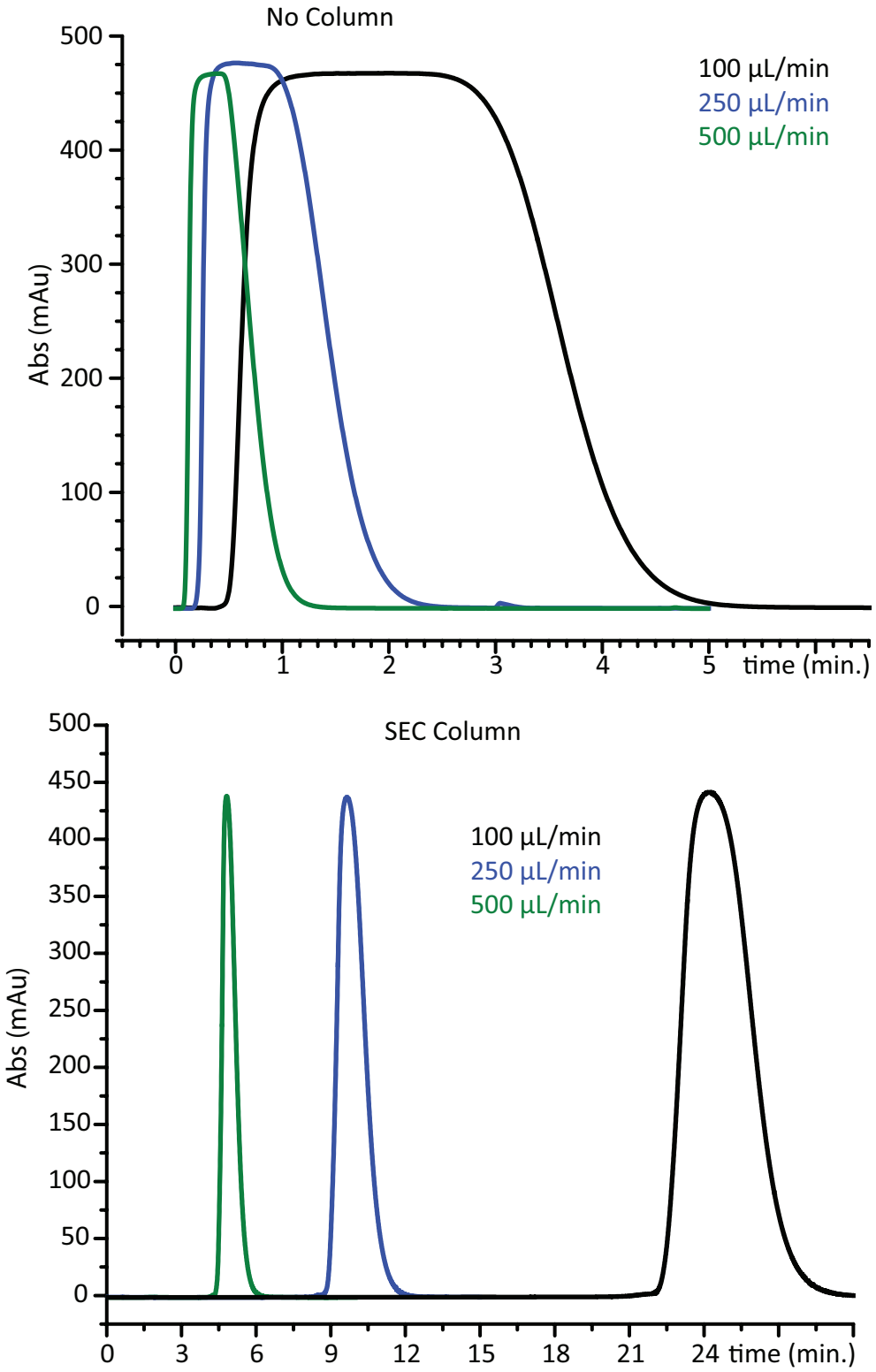

B.2 UV/VIS detector placed before (top) and after (bottom) the SEC column.

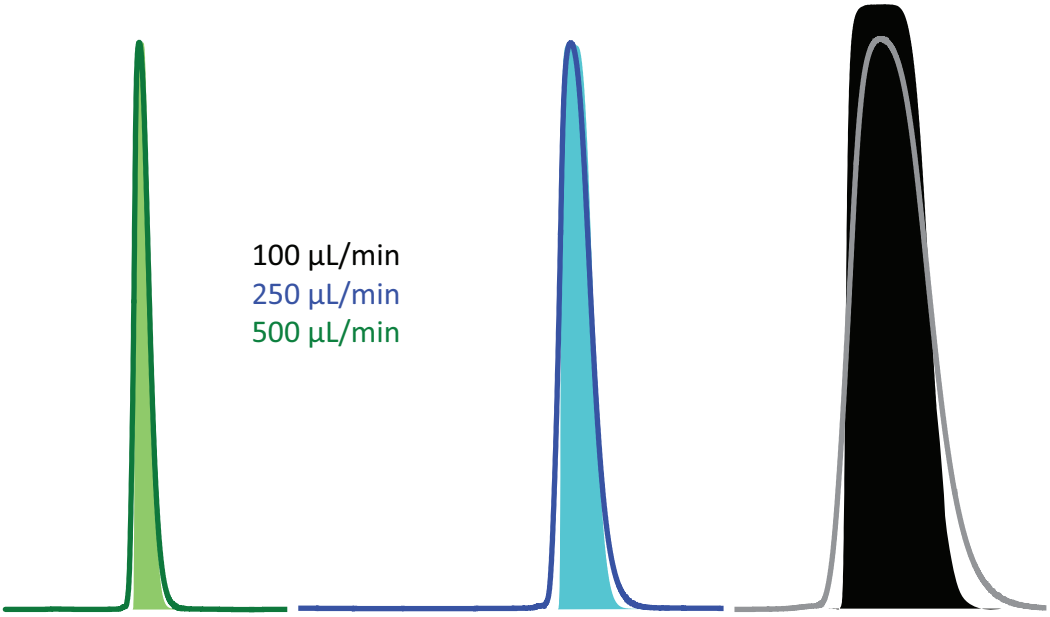

B.3 Overlay of the elution of the 0.5% acetone peak pre- (filled) and post- (outlined) SEC column at the three different flow rates.

BIBLIOGRAPHY

Abzalimov, R. R. *et al.* Electrospray ionization mass spectrometry of highly heterogeneous protein systems: Protein ion charge state assignment via incomplete charge reduction. *Anal. Chem.* **82**, 7523-7526, doi:10.1021/ac101848z (2010).

Aisen, P. Transferrin, the transferrin receptor, and the uptake of iron by cells. *Met. Ions Biol. Syst.* **35**, 585-631 (1998).

Aitken, K. J. Dietary interventions in autism spectrum disorders why they work when they do, why they don't when they don't. (2009).

Almeida, A. *et al.* The promise of protein glycosylation for personalised medicine. *Biochim Biophys Acta* **1860**, 1583-1595, doi:10.1016/j.bbagen.2016.03.012 (2016).

Alsenaidy, M. A. *et al.* Physical stability comparisons of IgG1-Fc variants: effects of N-glycosylation site occupancy and Asp/Gln residues at site Asn 297. *J. Pharm. Sci.* **103**, 1613-1627, doi:10.1002/jps.23975 (2014).

Anthony, R. M. *et al.* Recapitulation of IVIG anti-inflammatory activity with a recombinant IgG Fc. *Science* **320**, 373-376, doi:10.1126/science.1154315 (2008).

Anthony, R. M. *et al.* A Novel Role for the IgG Fc Glycan: The Anti-inflammatory Activity of Sialylated IgG Fcs. *J. Clin. Immunol.* **30**, 9-14, doi:10.1007/s10875-010-9405-6 (2010).

Anthony, R. M. *et al.* A novel role for the IgG Fc glycan: the anti-inflammatory activity of sialylated IgG Fcs. *Journal of clinical immunology* **30 Suppl 1**, S9-14, doi:10.1007/s10875-010-9405-6 (2010).

Anthony, R. M. *et al.* Identification of a receptor required for the anti-inflammatory activity of IVIG. *Proceedings of the National Academy of Sciences* **105**, 19571-19578 (2008).

Aono, H. *et al.* Efficient on-column conversion of IgG1 trisulfide linkages to native disulfides in tandem with Protein A affinity chromatography. *J. Chromatogr. A* **1217**, 5225-5232, doi:10.1016/j.chroma.2010.06.029 (2010).

Arndt, T. Carbohydrate-deficient transferrin as a marker of chronic alcohol abuse: a critical review of preanalysis, analysis, and interpretation. *Clinical chemistry* **47**, 13-27 (2001).

Bajardi-Taccioli, A. *et al.* Effect of protein aggregates on characterization of FcRn binding of Fc-fusion therapeutics. *Mol. Immunol.* **67**, 616-624, doi:10.1016/j.molimm.2015.06.031 (2015).

Bao, J. *et al.* Pre-equilibration kinetic size-exclusion chromatography with mass spectrometry detection (peKSEC-MS) for label-free solution-based kinetic analysis of protein-small molecule interactions. *Analyst* **88**, 4063-4070, doi:10.1039/c4an02232g (2015).

Barnett, G. V. *et al.* Structural Changes and Aggregation Mechanisms for Anti-Streptavidin IgG1 at Elevated Concentration. *The Journal of Physical Chemistry B* **119**, 15150-15163, doi:10.1021/acs.jpcb.5b08748 (2015).

Beard, J. One person's view of iron deficiency, development, and cognitive function. *Am. J. Clin. Nutr.* **62**, 709-710 (1995).

Berkowitz, S. A. *et al.* Analytical tools for characterizing biopharmaceuticals and the implications for biosimilars. *Nat Rev Drug Discov* **11**, 527-540 (2012).

Berkowitz, S. A. *et al.* in *Biophysical Characterization of Proteins in Developing Biopharmaceuticals* 1-21 (Elsevier, 2015).

Bertolotti-Ciarlet, A. *et al.* Impact of methionine oxidation on the binding of human IgG1 to FcRn and Fcγ receptors. *Mol. Immunol.* **46**, 1878-1882, doi:http://doi.org/10.1016/j.molimm.2009.02.002 (2009).

Bhasin, B. *et al.* Primary and secondary hyperoxaluria: Understanding the enigma. *World J. Nephrol.* **4**, 235-244, doi:10.5527/wjn.v4.i2.235 (2015).

Bilgic, A. *et al.* Iron deficiency in preschool children with autistic spectrum disorders. *Res. Autism Spectr. Disord.* **4**, 639-644, doi:10.1016/j.rasd.2009.12.008 (2010).

Bilusich, D. *et al.* Direct identification of intramolecular disulfide links in peptides using negative ion electrospray mass spectra of underivatised peptides. A joint experimental and theoretical study. *Rapid Commun. Mass Spectrom.* **19**, 3063-3074 (2005).

Bolton, G. R. *et al.* The role of more than 40 years of improvement in protein A chromatography in the growth of the therapeutic antibody industry. *Biotechnol. Prog.* **32**, 1193-1202, doi:10.1002/btpr.2324 (2016).

Bondarenko, P. V. *et al.* Mass measurement and top-down HPLC/MS analysis of intact monoclonal antibodies on a hybrid linear quadrupole ion trap-orbitrap mass spectrometer. *J. Am. Soc. Mass Spectrom.* **20**, 1415-1424, doi:10.1016/j.jasms.2009.03.020 (2009).

Bourdage, J. S. *et al.* Effect of double antigen bridging immunoassay format on antigen coating concentration dependence and implications for designing immunogenicity assays for monoclonal antibodies. *J. Pharm. Biomed. Anal.* **39**, 685-690, doi:https://doi.org/10.1016/j.jpba.2005.03.037 (2005).

Broek, J. A. C. *et al.* The need for a comprehensive molecular characterization of autism spectrum disorders. *International Journal of Neuropsychopharmacology* **17**, 651-673, doi:10.1017/s146114571300117x (2014).

Burtis, C. A. *et al. Tietz Textbook of Clinical Chemistry*. 3 edn, (W.B. Saunders, 1999).

Byrne, S. L. *et al.* Effect of glycosylation on the function of a soluble, recombinant form of the transferrin receptor. *Biochemistry* **45**, 6663-6673 (2006).

Caaveiro, J. M. *et al.* Structural analysis of Fc/FcgammaR complexes: a blueprint for antibody design. *Immunol. Rev.* **268**, 201-221, doi:10.1111/imr.12365 (2015).

Carini, M. *et al.* Mass Spectrometric Strategies and Their Applications for Molecular Mass Determination of Recombinant Therapeutic Proteins. *Curr. Pharm. Biotechnol.* **12**, 1548-1557 (2011).

Center for Drug Evaluation and Research (U.S.), C. f. B. E. a. R. U. S., & International Conference on Harmonisation. Vol. U.S. Dept. of Health and Human Services, Food and Drug Administration, Center for Drug Evaluation and Research. (ed Food and Drug Administration U.S. Dept. of Health and Human Services, Center for Drug Evaluation and Research.) (Rockville, MD, 2009).

Chelius, D. *et al.* Identification and characterization of deamidation sites in the conserved regions of human immunoglobulin gamma antibodies. *Anal. Chem.* **77**, 6004-6011, doi:10.1021/ac050672d (2005).

Choe, W. *et al.* Fc-Binding Ligands of Immunoglobulin G: An Overview of High Affinity Proteins and Peptides. *Materials (Basel, Switzerland)* **9**, 994-1010, doi:10.3390/ma9120994 (2016).

Cornely, K. Biopharmaceuticals: Biochemistry and biotechnology, 2nd edition: Walsh, Gary, John Wiley & Sons. *Biochem. Mol. Biol. Educ.* **32**, 137-138, doi:10.1002/bmb.2004.494032029997 (2004).

Coulter-Mackie, M. B. *et al.* Primary Hyperoxaluria Type 1. *GeneReviews* (2014).

Cramer, C. N. *et al.* Disulfide Linkage Characterization of Disulfide Bond-Containing Proteins and Peptides by Reducing Electrochemistry and Mass Spectrometry. *Anal. Chem.* **88**, 1585-1592, doi:10.1021/acs.analchem.5b03148 (2016).

Crispin, M. *et al.* Crystal structure of sialylated IgG Fc: Implications for the mechanism of intravenous immunoglobulin therapy. *Proc. Natl. Acad. Sci. U. S. A.* **110**, E3544-E3546, doi:10.1073/pnas.1310657110 (2013).

Daugherty, A. L. *et al.* Formulation and delivery issues for monoclonal antibody therapeutics. *Advanced Drug Delivery Reviews* **58**, 686-706, doi:http://dx.doi.org/10.1016/j.addr.2006.03.011 (2006).

Dick, L. W., Jr. *et al.* Peptide mapping of therapeutic monoclonal antibodies: improvements for increased speed and fewer artifacts. *J. Chromatogr. B Analyt. Technol. Biomed. Life Sci.* **877**, 230-236, doi:10.1016/j.jchromb.2008.12.009 (2009).

Dorcely, B. *et al.* Novel biomarkers for prediabetes, diabetes, and associated complications. *Diabetes Metab. Syndr. Obes.* **10**, 345-361, doi:10.2147/dmso.s100074 (2017).

Dosman, C. F. *et al.* Children with autism: Effect of iron supplementation on sleep and ferritin. *Pediatr. Neurol.* **36**, 152-158, doi:10.1016/j.pediatrneurol.2006.11.004 (2007).

Dosman, C. F. *et al.* Ferritin as an indicator of suspected iron deficiency in children with autism spectrum disorder: prevalence of low serum ferritin concentration. *Dev. Med. Child Neurol.* **48**, 1008-1009, doi:10.1017/s0012162206232225 (2006).

Dozier, J. K. *et al.* Site-Specific PEGylation of Therapeutic Proteins. *Int. J. Mol. Sci.* **16**, 25831-25864, doi:10.3390/ijms161025831 (2015).

Dumont, J. *et al.* Human cell lines for biopharmaceutical manufacturing: history, status, and future perspectives. *Crit. Rev. Biotechnol.* **36**, 1110-1122, doi:10.3109/07388551.2015.1084266 (2016).

Dunlop, R. A. *et al.* Oxidized proteins: mechanisms of removal and consequences of accumulation. *IUBMB Life* **61**, 522-527, doi:10.1002/iub.189 (2009).

Dyachenko, A. *et al.* Tandem Native Mass-Spectrometry on Antibody–Drug Conjugates and Submillion Da Antibody–Antigen Protein Assemblies on an Orbitrap EMR Equipped with a High-Mass Quadrupole Mass Selector. *Anal. Chem.* **87**, 6095-6102, doi:10.1021/acs.analchem.5b00788 (2015).

Estes, S. *et al.* Mammalian cell line developments in speed and efficiency. *Adv. Biochem. Eng. Biotechnol.* **139**, 11-33, doi:10.1007/10_2013_260 (2014).

Farrington G.K., L. A., Meier W., Eldredge J., Garber E., Biogen Idec. Neonatal Fc receptor (FcRn)-binding polypeptide variants, dimeric Fc binding proteins and methods related thereto. (2013).

Fatunmbi, O. *et al.* Interactions of Haptoglobin with Monomeric Globin Species: Insights from Molecular Modeling and Native Electrospray Ionization Mass Spectrometry. *Biochemistry* **55**, 1918-1928, doi:10.1021/acs.biochem.5b00807 (2016).

Faucette, A. N. *et al.* Immunization of pregnant women: Future of early infant protection. *Hum. Vaccin. Immunother.* **11**, 2549-2555, doi:10.1080/21645515.2015.1070984 (2015).

Foley, J. P. *et al.* Optimization of secondary chemical equilibria in liquid chromatography: variables influencing the self-selectivity, retention, and efficiency in acid-base systems. *Anal. Chem.* **59**, 110-115, doi:10.1021/ac00128a023 (1987).

Food *et al.* International Conference on Harmonisation; Guidance on Q11 Development and Manufacture of Drug Substances; availability. Notice. *Fed. Regist.* **77**, 69634-69635 (2012).

Fornelli, L. *et al.* Top-down analysis of immunoglobulin G isotypes 1 and 2 with electron transfer dissociation on a high-field Orbitrap mass spectrometer. *J. Proteomics* **159**, 67-76, doi:https://doi.org/10.1016/j.jprot.2017.02.013 (2017).

Freitas, P. A. C. *et al.* Glycated albumin: a potential biomarker in diabetes. *Archives of endocrinology and metabolism* **61**, 296-304, doi:10.1590/2359-3997000000272 (2017).

Fung, Y. M. E. *et al.* Facile disulfide bond cleavage in gaseous peptide and protein cations by ultraviolet photodissociation at 157 nm. *Angew. Chem. Int. Ed.* **44**, 6399-6403, doi:10.1002/anie.200501533 (2005).

Gao, X. *et al.* Effect of individual Fc methionine oxidation on FcRn binding: Met252 oxidation impairs FcRn binding more profoundly than Met428 oxidation. *J. Pharm. Sci.* **104**, 368-377, doi:10.1002/jps.24136 (2015).

Gau, B. C. *et al.* Fast Photochemical Oxidation of Proteins Footprints Faster than Protein Unfolding. *Anal. Chem.* **81**, 6563-6571, doi:10.1021/ac901054w (2009).

Gaza-Bulseco, G. *et al.* Effect of methionine oxidation of a recombinant monoclonal antibody on the binding affinity to protein A and protein G. *Journal of Chromatography B* **870**, 55-62, doi:http://dx.doi.org/10.1016/j.jchromb.2008.05.045 (2008).

Ghaderi, D. *et al.* Implications of the presence of N-glycolylneuraminic acid in recombinant therapeutic glycoproteins. *Nat. Biotechnol.* **28**, 863-867, doi:10.1038/nbt.1651 (2010).

Glowacki, R. *et al.* An on-column derivatization method for the determination of homocysteine-thiolactone and protein N-linked homocysteine. *Amino acids* **41**, 187-194, doi:10.1007/s00726-010-0521-7 (2011).

Gordon, N. Iron deficiency and the intellect. *Brain Dev.* **25**, 3-8, doi:http://dx.doi.org/10.1016/s0387-7604(02)00148-1 (2003).

Graumann, K. *et al.* Manufacturing of recombinant therapeutic proteins in microbial systems. *Biotechnol J* **1**, 164-186, doi:10.1002/biot.200500051 (2006).

Gregorich, Z. R. *et al.* Top-down proteomics in health and disease: challenges and opportunities. *Proteomics* **14**, 1195-1210, doi:10.1002/pmic.201300432 (2014).

Griffith, W. P. *et al.* Highly asymmetric interactions between globin chains during hemoglobin assembly revealed by electrospray ionization mass spectrometry. *Biochemistry* **42**, 10024-10033 (2003).

Gu, S. *et al.* Characterization of trisulfide modification in antibodies. *Anal. Biochem.* **400**, 89-98, doi:10.1016/j.ab.2010.01.019 (2010).

Gumerov, D. R. *et al.* Dynamics of iron release from transferrin N-lobe studied by electrospray ionization mass spectrometry. *Anal. Chem.* **73**, 2565-2570 (2001).

Gumerov, D. R. *et al.* Interlobe communication in human serum transferrin: metal binding and conformational dynamics investigated by electrospray ionization mass spectrometry. *Biochemistry* **42**, 5421-5428 (2003).

Halbrooks, P. J. *et al.* The oxalate effect on release of iron from human serum transferrin explained. *J. Mol. Biol.* **339**, 217-226 (2004).

Halket, J. M. *et al.* Derivatization in mass spectrometry --7. On-line derivatisation/degradation. *Eur. J. Mass Spectrom.* **12**, 1-13, doi:10.1255/ejms.785 (2006).

Hao, P. *et al.* Evaluation of the effect of trypsin digestion buffers on artificial deamidation. *Journal of proteome research* **14**, 1308-1314, doi:10.1021/pr500903b (2015).

Hawkins, R. C. Total iron binding capacity or transferrin concentration alone outperforms iron and saturation indices in predicting iron deficiency. *Clin. Chim. Acta* **380**, 203-207, doi:10.1016/j.cca.2007.02.032 (2007).

He, L. *et al.* Analysis of Monoclonal Antibodies in Human Serum as a Model for Clinical Monoclonal Gammopathy by Use of 21 Tesla FT-ICR Top-Down and Middle-Down MS/MS. *J. Am. Soc. Mass Spectrom.* **28**, 827-838, doi:10.1007/s13361-017-1602-6 (2017).

Heck, A. J. Native mass spectrometry: a bridge between interactomics and structural biology. *Nat Methods* **5**, 927-933, doi:10.1038/nmeth.1265 (2008).

Higdon, R. *et al.* The Promise of Multi-Omics and Clinical Data Integration to Identify and Target Personalized Healthcare Approaches in Autism Spectrum Disorders. *Omics* **19**, 197-208, doi:10.1089/omi.2015.0020 (2015).

Hogarth, P. M. *et al.* Fc receptor-targeted therapies for the treatment of inflammation, cancer and beyond. *Nat Rev Drug Discov* **11**, 311-331, doi:10.1038/nrd2909 (2012).

Houde, D. *et al. Anal. Chem.* **81**, 5966 (2009).

Houde, D. J. *et al.* in *Biophysical Characterization of Proteins in Developing Biopharmaceuticals* 23-47 (Elsevier, 2015).

Hristodorov, D. *et al.* Generation and comparative characterization of glycosylated and aglycosylated human IgG1 antibodies. *Mol. Biotechnol.* **53**, 326-335, doi:10.1007/s12033-012-9531-x (2013).

Huang, C.-J. *et al.* Industrial production of recombinant therapeutics in Escherichia coli and its recent advancements. *J. Ind. Microbiol. Biotechnol.* **39**, 383-399, doi:10.1007/s10295-011-1082-9 (2012).

Hyung, S. W. *et al.* Microscale depletion of high abundance proteins in human biofluids using IgY14 immunoaffinity resin: analysis of human plasma and cerebrospinal fluid. *Anal Bioanal Chem* **406**, 7117-7125, doi:10.1007/s00216-014-8058-3 (2014).

Imperatore, G. *et al.* Hereditary hemochromatosis: Perspectives of public health, medical genetics, and primary care. *Genet. Med.* **5**, 1-8 (2003).

Ionescu, R. M. *et al.* Contribution of variable domains to the stability of humanized IgG1 monoclonal antibodies. *Journal of pharmaceutical sciences* **97**, 1414-1426, doi:10.1002/jps.21104 (2008).

Irani, V. *et al.* Molecular properties of human IgG subclasses and their implications for designing therapeutic monoclonal antibodies against infectious diseases. *Mol. Immunol.* **67**, 171-182, doi:http://dx.doi.org/10.1016/j.molimm.2015.03.255 (2015).

Jackson, D. A. *et al.* Biochemical Method for Inserting New Genetic Information into DNA of Simian Virus 40: Circular SV40 DNA Molecules Containing Lambda Phage Genes and the Galactose Operon of Escherichia coli. *Proc. Natl. Acad. Sci. U. S. A.* **69**, 2904-2909 (1972).

Jandera, P. Stationary and mobile phases in hydrophilic interaction chromatography: a review. *Anal. Chim. Acta* **692**, 1-25, doi:10.1016/j.aca.2011.02.047 (2011).

Jandl, J. H. *et al.* The plasma-to-cell cycle of transferrin. *J. Clin. Invest.* **42**, 314-326, doi:10.1172/JCI104718 (1963).

Jáuregui-Lobera, I. Iron deficiency and cognitive functions. *Neuropsychiatr. Dis. Treat.* **10**, 2087-2095, doi:10.2147/NDT.S72491 (2014).

Jefferis, R. Isotype and glycoform selection for antibody therapeutics. *Arch. Biochem. Biophys.* **526**, 159-166, doi:http://dx.doi.org/10.1016/j.abb.2012.03.021 (2012).

Jensen, P. F. *et al.* Investigating the interaction between the neonatal Fc receptor and monoclonal antibody variants by hydrogen/deuterium exchange mass spectrometry. *Mol. Cell. Proteomics* **14**, 148-161, doi:10.1074/mcp.M114.042044 (2015).

Jung, S. T. *et al.* Bypassing glycosylation: engineering aglycosylated full-length IgG antibodies for human therapy. *Curr. Opin. Biotechnol.* **22**, 858-867, doi:10.1016/j.copbio.2011.03.002 (2011).

Kailemia, M. J. *et al.* Glycans and glycoproteins as specific biomarkers for cancer. *Anal Bioanal Chem* **409**, 395-410, doi:10.1007/s00216-016-9880-6 (2017).

Kaltashov, I. A. *et al.* Do ionic charges in ESI MS provide useful information on macromolecular structure? *J. Am. Soc. Mass Spectrom.* **19**, 1239-1246 (2008).

Kaltashov, I. A. *et al.* Advances and challenges in analytical characterization of biotechnology products: Mass spectrometry-based approaches to study properties and behavior of protein therapeutics. *Biotechnol. Adv.* **30**, 210-222 (2012).

Kaltashov, I. A. *et al.* Emerging mass spectrometry-based approaches to probe protein-receptor interactions: focus on overcoming physiological barriers. *Adv Drug Deliv Rev* **65**, 1020-1030, doi:10.1016/j.addr.2013.04.014 (2013).

Kaltashov, I. A. *et al.* Transferrin as a model system for method development to study structure, dynamics and interactions of metalloproteins using mass spectrometry. *Biochim. Biophys. Acta* **1820**, 417-426 (2012).

Kaltashov, I. A. *et al. Mass spectrometry in biophysics : conformation and dynamics of biomolecules*. (Hoboken, N.J. : John Wiley, 2005., 2005).

Kaneko, Y. *et al.* Anti-Inflammatory Activity of Immunoglobulin G Resulting from Fc Sialylation. *Science* **313**, 670-673, doi:10.1126/science.1129594 (2006).

Kapur, R. *et al.* IgG-effector functions: "The Good, The Bad and The Ugly". *Immunol. Lett.* **160**, 139-144, doi:http://dx.doi.org/10.1016/j.imlet.2014.01.015 (2014).

Kelleher, N. L. *et al.* Top down versus bottom up protein characterization by tandem high-resolution mass spectrometry. *J. Am. Chem. Soc.* **121**, 806-812 (1999).

Kellersberger, K. A. *et al.* Top-down characterization of nucleic acids modified by structural probes using high-resolution tandem mass spectrometry and automated data interpretation. *Anal. Chem.* **76**, 2438-2445, doi:10.1021/ac0355045 (2004).

Kiese, S. *et al.* Shaken, not stirred: mechanical stress testing of an IgG1 antibody. *J. Pharm. Sci.* **97**, 4347-4366, doi:10.1002/jps.21328 (2008).

Kim, Y. H. *et al.* Comparing the effect on protein stability of methionine oxidation versus mutagenesis: steps toward engineering oxidative resistance in proteins. *Protein Eng.* **14**, 343-347 (2001).

Konermann, L. *et al.* Acid-Induced Unfolding of Cytochrome c at Different Methanol Concentrations: Electrospray Ionization Mass Spectrometry Specifically Monitors Changes in the Tertiary Structure. *Biochemistry* **36**, 12296-12302, doi:10.1021/bi971266u (1997).

Konofal, E. *et al.* Impact of restless legs syndrome and iron deficiency on attention-deficit/hyperactivity disorder in children. *Sleep Med.* **8**, 711-715, doi:http://dx.doi.org/10.1016/j.sleep.2007.04.022 (2007).

Konstantynowicz, J. *et al.* A potential pathogenic role of oxalate in autism. *Eur. J. Paediatr. Neurol.* **16**, 485-491, doi:http://dx.doi.org/10.1016/j.ejpn.2011.08.004 (2012).

Krapp, S. *et al.* Structural analysis of human IgG-Fc glycoforms reveals a correlation between glycosylation and structural integrity. *J. Mol. Biol.* **325**, 979-989 (2003).

Krokhin, O. Peptide retention prediction in reversed-phase chromatography: proteomic applications. *Expert Review of Proteomics* **9**, 1-4, doi:10.1586/epr.11.79 (2012).

Kueltzo, L. A. *et al.* Derivative absorbance spectroscopy and protein phase diagrams as tools for comprehensive protein characterization: a bGCSF case study. *J. Pharm. Sci.* **92**, 1805-1820, doi:10.1002/jps.10439 (2003).

Kueltzo, L. A. *et al.* Effects of Solution Conditions, Processing Parameters, and Container Materials on Aggregation of a Monoclonal Antibody during Freeze-Thawing. *J. Pharm. Sci.* **97**, 1801-1812, doi:http://doi.org/10.1002/jps.21110 (2008).

Latypov, R. F. *et al.* Elucidation of acid-induced unfolding and aggregation of human immunoglobulin IgG1 and IgG2 Fc. *J. Biol. Chem.* **287**, 1381-1396, doi:10.1074/jbc.M111.297697 (2012).

Lauc, G. *et al.* Mechanisms of disease: The human N-glycome. *Biochimica et Biophysica Acta (BBA) - General Subjects* **1860**, 1574-1582, doi:http://dx.doi.org/10.1016/j.bbagen.2015.10.016 (2016).

Lei, Q. P. *et al.* Electrospray mass spectrometry studies of non-heme iron-containing proteins. *Anal. Chem.* **70**, 1838-1846 (1998).

Leurs, U. *et al.* Getting to the core of protein pharmaceuticals – Comprehensive structure analysis by mass spectrometry. *European Journal of Pharmaceutics and Biopharmaceutics* **93**, 95-109, doi:http://dx.doi.org/10.1016/j.ejpb.2015.03.012 (2015).

Li, H. *et al.* Native top-down electrospray ionization-mass spectrometry of 158 kDa protein complex by high-resolution Fourier transform ion cyclotron resonance mass spectrometry. *Anal. Chem.* **86**, 317-320, doi:10.1021/ac4033214 (2014).

Liu, H. *et al.* Ranking the susceptibility of disulfide bonds in human IgG1 antibodies by reduction, differential alkylation, and LC-MS analysis. *Anal. Chem.* **82**, 5219-5226, doi:10.1021/ac100575n (2010).

Liu, L. Antibody glycosylation and its impact on the pharmacokinetics and pharmacodynamics of monoclonal antibodies and Fc-fusion proteins. *J. Pharm. Sci.* **104**, 1866-1884, doi:10.1002/jps.24444 (2015).

Liu, L. *et al.* Pharmacokinetics of IgG1 monoclonal antibodies produced in humanized Pichia pastoris with specific glycoforms: a comparative study with CHO produced materials. *Biologicals* **39**, 205-210, doi:10.1016/j.biologicals.2011.06.002 (2011).

Lopez, A. *et al.* Iron deficiency anaemia. *Lancet*, in press, doi:10.1016/s0140-6736(15)60865-0 (2015).

Lossl, P. *et al.* Boundaries of mass resolution in native mass spectrometry. *J. Am. Soc. Mass Spectrom.* **25**, 906-917, doi:10.1007/s13361-014-0874-3 (2014).

Lozoff, B. *et al.* Iron Deficiency and Brain Development. *Sem. Pediatr. Neurol.* **13**, 158-165, doi:http://dx.doi.org/10.1016/j.spen.2006.08.004 (2006).

Luck, A. N. *et al.* Human serum transferrin: is there a link among autism, high oxalate levels, and iron deficiency anemia? *Biochemistry* **52**, 8333-8341, doi:10.1021/bi401190m (2013).

Luck, A. N. *et al.* Human serum transferrin: Is there a link between autism, high oxalate and iron deficiency anemia? *Biochemistry* **52**, 8333-8341, doi:10.1021/bi401190m (2013).

Luck, A. N. *et al.* in *Current Topics in Membranes* Vol. 69 (eds José M. Argüello & Svetlana Lutsenko) 3-35 (Academic Press, 2012).

Luck, A. N. *et al.* in *Metal Transporters* Vol. 69 *Current Topics in Membranes* (eds S. Lutsenko & J. M. Arguello) 3-35 (Elsevier Academic Press Inc, 2012).

Luck, A. N. *et al.* Transferrin-mediated cellular iron delivery. *Curr. Top. Membr.* **69**, 3-35, doi:10.1016/b978-0-12-394390-3.00001-x (2012).

Lutgens, F. K. *et al. Essentials of geology*. (Boston : Pearson, [2015] Twelfth edition., 2015).

Lutsenko, S. *et al. Metal transporters. [electronic resource]*. (San Diego : Elsevier Science, 2012., 2012).

Ma, L. *et al.* Determination of mercury ion by MEKC with on-column derivatisation and LIF detection. *J. Sep. Sci.* **31**, 888-892, doi:10.1002/jssc.200700606 (2008).

Maa, Y. F. *et al.* Protein denaturation by combined effect of shear and air-liquid interface. *Biotechnol. Bioeng.* **54**, 503-512, doi:10.1002/(sici)1097-0290(19970620)54:6<503::aid-bit1>3.0.co;2-n (1997).

Mach, H. *et al.* Simultaneous Monitoring of the Environment of Tryptophan, Tyrosine, and Phenylalanine Residues in Proteins by Near-Ultraviolet Second-Derivative Spectroscopy. *Anal. Biochem.* **222**, 323-331, doi:http://dx.doi.org/10.1006/abio.1994.1499 (1994).

Mahajan, R. *et al.* The Effect of Inert Atmospheric Packaging on Oxidative Degradation in Formulated Granules. *Pharm. Res.* **22**, 128-140, doi:10.1007/s11095-004-9018-y (2005).

Mann, M. *et al.* Proteomic analysis of post-translational modifications. *Nat. Biotechnol.* **21**, 255-261, doi:10.1038/nbt0303-255 (2003).

Marengo, E. *et al.* Biomarkers for pancreatic cancer: recent achievements in proteomics and genomics through classical and multivariate statistical methods. *World J. Gastroenterol.* **20**, 13325-13342, doi:10.3748/wjg.v20.i37.13325 (2014).

Mastrangeli, R. *et al.* Biological Functions of Interferon beta-1a Are Enhanced By Deamidation. *J. Interferon Cytokine Res.* **36**, 534-541, doi:10.1089/jir.2016.0025 (2016).

McCann, J. C. *et al.* An overview of evidence for a causal relation between iron deficiency during development and deficits in cognitive or behavioral function. *Am. J. Clin. Nutr.* **85**, 931-945 (2007).

Meany, D. L. *et al.* Aberrant glycosylation associated with enzymes as cancer biomarkers. *Clin. Proteomics* **8**, 7, doi:10.1186/1559-0275-8-7 (2011).

Mendoza, V. L. *et al.* Probing protein structure by amino acid-specific covalent labeling and mass spectrometry. *Mass Spectrom. Rev.* **28**, 785-815, doi:10.1002/mas.20203 (2009).

Mertz, J. E. *et al.* Cleavage of DNA by R(1) Restriction Endonuclease Generates Cohesive Ends. *Proc. Natl. Acad. Sci. U. S. A.* **69**, 3370-3374 (1972).

Milstein, C. The hybridoma revolution: an offshoot of basic research. *Bioessays* **21**, 966-973 (1999).

Miura, Y. *et al.* Glycomics and glycoproteomics focused on aging and age-related diseases — Glycans as a potential biomarker for physiological alterations. *Biochim. Biophys. Acta* **1860**, 1608-1614, doi:http://dx.doi.org/10.1016/j.bbagen.2016.01.013 (2016).

Mizejewski, G. J. *et al.* Newborn screening for autism: in search of candidate biomarkers. *Biomark. Med.* **7**, 247-260, doi:10.2217/bmm.12.108 (2013).

Morar-Mitrica, S. *et al.* Development of a stable low-dose aglycosylated antibody formulation to minimize protein loss during intravenous administration. *MAbs* **7**, 792-803, doi:10.1080/19420862.2015.1046664 (2015).

Mulinacci, F. *et al.* Influence of methionine oxidation on the aggregation of recombinant human growth hormone. *Eur. J. Pharm. Biopharm.* **85**, 42-52, doi:http://doi.org/10.1016/j.ejpb.2013.03.015 (2013).

Murphy, K. *et al. Janeway's immunobiology*. (Garland Science, 2012).

Myers, D. P. *et al.* On-column nitrosation of amines observed in liquid chromatography impurity separations employing ammonium hydroxide and acetonitrile as mobile phase. *J. Chromatogr. A* **1319**, 57-64, doi:10.1016/j.chroma.2013.10.021 (2013).

Nemirovskiy, O. V. *et al.* Determination of calcium binding sites in gas-phase small peptides by tandem mass spectrometry. *J. Am. Soc. Mass Spectrom.* **9**, 1020-1028 (1998).

Nguyen, S. N. *et al.* Mass Spectrometry-Guided Optimization and Characterization of a Biologically Active Transferrin–Lysozyme Model Drug Conjugate. *Mol. Pharm.*, doi:10.1021/mp400026y (2013).

Nicolardi, S. *et al.* Structural Analysis of an Intact Monoclonal Antibody by Online Electrochemical Reduction of Disulfide Bonds and Fourier Transform Ion Cyclotron Resonance Mass Spectrometry. *Anal. Chem.* **86**, 5376-5382, doi:10.1021/ac500383c (2014).

Nielsen, J. Production of biopharmaceutical proteins by yeast: Advances through metabolic engineering. *Bioengineered* **4**, 207-211, doi:10.4161/bioe.22856 (2013).

Otero, G. A. *et al.* Working memory impairment and recovery in iron deficient children. *Clin. Neurophysiol.* **119**, 1739-1746, doi:http://dx.doi.org/10.1016/j.clinph.2008.04.015 (2008).

Pan, J. *et al.* Hydrogen/deuterium exchange mass spectrometry with top-down electron capture dissociation for characterizing structural transitions of a 17 kDa protein. *J. Am. Chem. Soc.* **131**, 12801-12808 (2009).

Pan, J. *et al.* Higher-order structural interrogation of antibodies using middle-down hydrogen/deuterium exchange mass spectrometry. *Chemical Science* **7**, 1480-1486, doi:10.1039/C5SC03420E (2016).

Pantopoulos, K. *et al.* Mechanisms of mammalian iron homeostasis. *Biochemistry* **51**, 5705-5724, doi:10.1021/bi300752r (2012).

Pawlowski, J. W. *et al.* Influence of glycan modification on IgG1 biochemical and biophysical properties. *submitted*.

Phillips, J. J. *et al.* Rate of Asparagine Deamidation in a Monoclonal Antibody Correlating with Hydrogen Exchange Rate at Adjacent Downstream Residues. *Anal. Chem.* **89**, 2361-2368, doi:10.1021/acs.analchem.6b04158 (2017).

Pollitt, E. IRON-DEFICIENCY AND COGNITIVE FUNCTION. *Annu. Rev. Nutr.* **13**, 521-537, doi:10.1146/annurev.nutr.13.1.521 (1993).

Raju, T. S. Terminal sugars of Fc glycans influence antibody effector functions of IgGs. *Curr. Opin. Immunol.* **20**, 471-478, doi:http://doi.org/10.1016/j.coi.2008.06.007 (2008).

Raju, T. S. Terminal sugars of Fc glycans influence antibody effector functions of IgGs. *Curr Opin Immunol* **20**, 471-478, doi:10.1016/j.coi.2008.06.007 (2008).

Ratanji, K. D. *et al.* Immunogenicity of therapeutic proteins: influence of aggregation. *J. Immunotoxicol.* **11**, 99-109, doi:10.3109/1547691x.2013.821564 (2014).

Ratanji, K. D. *et al.* Immunogenicity of therapeutic proteins: Influence of aggregation. *J. Immunotoxicol.* **11**, 99-109, doi:10.3109/1547691X.2013.821564 (2014).

Rath, T. *et al.* Regulation of Immune Responses by the Neonatal Fc Receptor and Its Therapeutic Implications. *Front. Immunol.* **5**, 664, doi:10.3389/fimmu.2014.00664 (2014).

Rathore, A. S. *et al.* Establishing analytical comparability for "biosimilars": filgrastim as a case study. *Anal. Bioanal. Chem.* **406**, 6569-6576, doi:10.1007/s00216-014-7887-4 (2014).

Ren, D. *et al.* An improved trypsin digestion method minimizes digestion-induced modifications on proteins. *Anal. Biochem.* **392**, 12-21, doi:10.1016/j.ab.2009.05.018 (2009).

Reslan, L. *et al.* Understanding and circumventing resistance to anticancer monoclonal antibodies. *mAbs* **1**, 222-229 (2009).

Reynolds, A. *et al.* Iron Status in Children With Autism Spectrum Disorder. *Pediatrics* **130**, S154-S159, doi:10.1542/peds.2012-0900M (2012).

Robinson, N. E. *et al.* Molecular clocks. *Proc. Natl. Acad. Sci. U. S. A.* **98**, 944-949, doi:10.1073/pnas.98.3.944 (2001).

Rodriguez, J. *et al.* High productivity of human recombinant beta-interferon from a low-temperature perfusion culture. *J. Biotechnol.* **150**, 509-518, doi:http://doi.org/10.1016/j.jbiotec.2010.09.959 (2010).

Roopenian, D. C. *et al.* FcRn: the neonatal Fc receptor comes of age. *Nat. Rev. Immunol.* **7**, 715-725 (2007).

Runkel, L. *et al.* Structural and functional differences between glycosylated and non-glycosylated forms of human interferon-beta (IFN-beta). *Pharm. Res.* **15**, 641-649 (1998).

Saitoh, K. *et al.* On-column electrochemical redox derivatization for enhancement of separation selectivity of liquid chromatography use of redox reaction as secondary chemical equilibrium. *J. Chromatogr. A* **1180**, 66-72, doi:10.1016/j.chroma.2007.12.003 (2008).

Saitoh, K. *et al.* On-line redox derivatization liquid chromatography for selective separation of Fe(II) and Fe(III) cyanide complexes using porous graphitic carbon. *Anal. Sci.* **29**, 715-721 (2013).

Saxena, A. *et al.* Advances in Therapeutic Fc Engineering – Modulation of IgG-Associated Effector Functions and Serum Half-life. *Front. Immunol.* **7**, doi:10.3389/fimmu.2016.00580 (2016).

Scallon, B. J. *et al.* Higher levels of sialylated Fc glycans in immunoglobulin G molecules can adversely impact functionality. *Molecular Immunology* **44**, 1524-1534, doi:http://dx.doi.org/10.1016/j.molimm.2006.09.005 (2007).

Scallon, B. J. *et al.* Higher levels of sialylated Fc glycans in immunoglobulin G molecules can adversely impact functionality. *Mol. Immunol.* **44**, 1524-1534, doi:10.1016/j.molimm.2006.09.005 (2007).

Schiestl, M. *et al.* Acceptable changes in quality attributes of glycosylated biopharmaceuticals. *Nat Biotech* **29**, 310-312, doi:http://www.nature.com/nbt/journal/v29/n4/abs/nbt.1839.html - supplementary-information (2011).

Schlabach, M. R. *et al.* The synergistic binding of anions and Fe3+ by transferrin. Implications for the interlocking sites hypothesis. *J. Biol. Chem.* **250**, 2182-2188 (1975).

Schlothauer, T. *et al.* Analytical FcRn affinity chromatography for functional characterization of monoclonal antibodies. *MAbs* **5**, 576-586, doi:10.4161/mabs.24981 (2013).

Sharp, J. S. *et al.* Protein surface mapping by chemical oxidation: Structural analysis by mass spectrometry. *Anal. Biochem.* **313**, 216-225 (2003).

Shibukawa, M. *et al.* On-Column Derivatization Using Redox Activity of Porous Graphitic Carbon Stationary Phase: An Approach to Enhancement of Separation Selectivity of Liquid Chromatography. *Anal. Chem.* **75**, 2775-2783, doi:10.1021/ac020705e (2003).

Shields, R. L. *et al.* Lack of fucose on human IgG1 N-linked oligosaccharide improves binding to human Fcgamma RIII and antibody-dependent cellular toxicity. *J. Biol. Chem.* **277**, 26733-26740, doi:10.1074/jbc.M202069200 (2002).

Siegel, G. J. *et al. Basic Neurochemistry: Molecular, Cellular, and Medical Aspects*. (Lippincott Williams & Wilkins, 1999).

Siek, G. *et al.* Direct Serum Total Iron-binding Capacity Assay Suitable for Automated Analyzers. *Clin. Chem.* **48**, 161-166 (2002).

Silva, André M. N. *et al.* The glycation site specificity of human serum transferrin is a determinant for transferrin's functional impairment under elevated glycaemic conditions. *Biochem. J.* **461**, 33-42, doi:10.1042/bj20140133 (2014).

Simakajornboon, N. *et al.* Diagnosis and management of restless legs syndrome in children. *Sleep Med. Rev.* **13**, 149-156, doi:http://dx.doi.org/10.1016/j.smrv.2008.12.002 (2009).

Siuti, N. *et al.* Decoding protein modifications using top-down mass spectrometry. *Nat. Meth.* **4**, 817-821 (2007).

SolÁ, R. J. *et al.* Effects of Glycosylation on the Stability of Protein Pharmaceuticals. *J. Pharm. Sci.* **98**, 1223-1245, doi:10.1002/jps.21504 (2009).

Sparks, S. E. in *In: Glycobiology and Human Diseases* (ed G. edited by Wiederschain) Ch. 16, 284-312 (CRC Press, 2016).

Steel, L. F. *et al.* Efficient and specific removal of albumin from human serum samples. *Mol. Cell. Proteomics* **2**, 262-270, doi:10.1074/mcp.M300026-MCP200 (2003).

Stockinger, S. *et al.* Integrating reaction and analysis: investigation of higher-order reactions by cryogenic trapping. *Beilstein J. Org. Chem.* **9**, 1837-1842, doi:10.3762/bjoc.9.214 (2013).

Stracke, J. *et al.* A novel approach to investigate the effect of methionine oxidation on pharmacokinetic properties of therapeutic antibodies. *MAbs* **6**, 1229-1242, doi:10.4161/mabs.29601 (2014).

Strege, M. A. Hydrophilic Interaction Chromatography−Electrospray Mass Spectrometry Analysis of Polar Compounds for Natural Product Drug Discovery. *Anal. Chem.* **70**, 2439-2445, doi:10.1021/ac9802271 (1998).

Suganya, V. *et al.* Urine proteome analysis to evaluate protein biomarkers in children with autism. *Clinica Chimica Acta* **450**, 210-219, doi:http://dx.doi.org/10.1016/j.cca.2015.08.015 (2015).

Suzuki, T. *et al.* Importance of neonatal FcR in regulating the serum half-life of therapeutic proteins containing the Fc domain of human IgG1: a comparative study of the affinity of monoclonal antibodies and Fc-fusion proteins to human neonatal FcR. *J. Immunol.* **184**, 1968-1976, doi:10.4049/jimmunol.0903296 (2010).

Sydow, J. F. *et al.* Structure-Based Prediction of Asparagine and Aspartate Degradation Sites in Antibody Variable Regions. *PLoS One* **9**, e100736, doi:10.1371/journal.pone.0100736 (2014).

Sykes, N. H. *et al.* Autism: the quest for the genes. *Expert Reviews in Molecular Medicine* **9**, 1-15, doi:doi:10.1017/S1462399407000452 (2007).

Testa, L. *et al.* Charge-surface correlation in electrospray ionization of folded and unfolded proteins. *Anal. Chem.* **83**, 6459-6463 (2011).

Thakkar, S. V. *et al.* Local Dynamics and Their Alteration by Excipients Modulate the Global Conformational Stability of an lgG1 Monoclonal Antibody. *J. Pharm. Sci.* **101**, 4444-4457, doi:http://doi.org/10.1002/jps.23332 (2012).

Thakkar, S. V. *et al.* Understanding the relevance of local conformational stability and dynamics to the aggregation propensity of an IgG1 and IgG2 monoclonal antibodies. *Protein Science : A Publication of the Protein Society* **22**, 1295-1305, doi:10.1002/pro.2316 (2013).

Troendlin, J. *et al.* Integration of catalysis and analysis is the key: rapid and precise investigation of the catalytic asymmetric Gosteli-Claisen rearrangement. *J. Am. Chem. Soc.* **133**, 16444-16450, doi:10.1021/ja207091x (2011).

Van Campenhout, A. *et al.* Iron-induced oxidative stress in haemodialysis patients: a pilot study on the impact of diabetes. *Biometals* **21**, 159-170, doi:10.1007/s10534-007-9104-9 (2008).

Van Campenhout, A. *et al.* A novel method to quantify in vivo transferrin glycation: Applications in diabetes mellitus. *Clin. Chim. Acta* **370**, 115-123, doi:https://doi.org/10.1016/j.cca.2006.01.028 (2006).

Varki, A. *Essentials of glycobiology*. (Cold Spring Harbor Laboratory Press, 2009).

Vidarsson, G. *et al.* IgG subclasses and allotypes: from structure to effector functions. *Front. Immunol.* **5**, 520, doi:10.3389/fimmu.2014.00520 (2014).

Walsh, G. Post-translational modifications of protein biopharmaceuticals. *Drug Discovery Today* **15**, 773-780, doi:http://dx.doi.org/10.1016/j.drudis.2010.06.009 (2010).

Wang, G. *et al.* Conformer-specific characterization of non-native protein states using hydrogen exchange and top-down mass spectrometry. *Proc. Natl. Acd. Sci. U.S.A.* **110**, 20087-20092 (2013).

Wang, G. *et al.* A new approach to characterization of the higher order structure of disulfide-containing proteins using hydrogen/deuterium exchange and top-down mass spectrometry. *Anal. Chem.* **86**, 7293-7298 (2014).

Wang, H. *et al.* Potential serum biomarkers from a metabolomics study of autism. *J. Psychiatry Neurosci.* **40**, in press, doi:10.1503/jpn.140009 (2015).

Wang, S. *et al.* Pitfalls in protein quantitation using acid-catalyzed O^{18} labeling: Hydrolysis-driven deamidation. *Anal. Chem.* **83**, 7227-7232, doi:10.1021/ac201657u (2011).

Wang, S. *et al.* Identification of reduction-susceptible disulfide bonds in transferrin by differential alkylation using O(16)/O(18) labeled iodoacetic acid. *J. Am. Soc. Mass Spectrom.* **26**, 800-807, doi:10.1007/s13361-015-1082-5 (2015).

Wang, W. *et al.* Antibody Structure, Instability, and Formulation. *J. Pharm. Sci.* **96**, 1-26, doi:http://dx.doi.org/10.1002/jps.20727 (2007).

Wang, W. *et al.* Impact of methionine oxidation in human IgG1 Fc on serum half-life of monoclonal antibodies. *Mol. Immunol.* **48**, 860-866, doi:10.1016/j.molimm.2010.12.009 (2011).

Wei, B. *et al.* Glycation of antibodies: Modification, methods and potential effects on biological functions. *MAbs* **9**, 586-594, doi:10.1080/19420862.2017.1300214 (2017).

Weiss, G. *et al.* Anemia of chronic disease. *N. Engl. J. Med.* **352**, 1011-1023, doi:10.1056/NEJMra041809 (2005).

Weykamp, C. *et al.* Toward standardization of carbohydrate-deficient transferrin (CDT) measurements: III. Performance of native serum and serum spiked with disialotransferrin proves that harmonization of CDT assays is possible. *Clin. Chem. Lab. Med.* **51**, 991-996, doi:10.1515/cclm-2012-0767 (2013).

Xie, Y. *et al.* Top-down ESI-ECD-FT-ICR mass spectrometry localizes noncovalent protein-ligand binding sites. *J. Am. Chem. Soc.* **128**, 14432-14433 (2006).

Xu, C. *et al.* Glycosylation-directed quality control of protein folding. *Nat. Rev. Mol. Cell Biol.* **16**, 742-752, doi:10.1038/nrm4073 (2015).

Yager, J. Y. *et al.* Neurologic manifestations of iron deficiency in childhood. *Pediatr. Neurol.* **27**, 85-92, doi:http://dx.doi.org/10.1016/S0887-8994(02)00417-4 (2002).

Yamaguchi, Y. *et al.* Glycoform-dependent conformational alteration of the Fc region of human immunoglobulin G1 as revealed by NMR spectroscopy. *Biochimica et Biophysica Acta (BBA) - General Subjects* **1760**, 693-700, doi:http://doi.org/10.1016/j.bbagen.2005.10.002 (2006).

Yan, B. *et al.* Human IgG1 hinge fragmentation as the result of H2O2-mediated radical cleavage. *J. Biol. Chem.* **284**, 35390-35402, doi:10.1074/jbc.M109.064147 (2009).

Yang, M. *et al.* Disulfide-Bond Scrambling Promotes Amorphous Aggregates in Lysozyme and Bovine Serum Albumin. *The Journal of Physical Chemistry B* **119**, 3969-3981, doi:10.1021/acs.jpcb.5b00144 (2015).

Yu, E. T. *et al.* MS3D structural elucidation of the HIV-1 packaging signal. *Proc. Natl. Acad. Sci. U. S. A.* **105**, 12248-12253, doi:10.1073/pnas.0800509105 (2008).

Yu, X. *et al.* Assessment of metals in reconstituted metallothioneins by electrospray mass spectrometry. *Anal. Chem.* **65**, 1355-1359 (1993).

Zavodszky, M. *et al.* Disulfide bond effects on protein stability: Designed variants of Cucurbita maxima trypsin inhibitor-V. *Protein Science : A Publication of the Protein Society* **10**, 149-160 (2001).

Zhang, H. *et al.* Mass spectrometry for the biophysical characterization of therapeutic monoclonal antibodies. *FEBS Letters* **588**, 308-317, doi:http://dx.doi.org/10.1016/j.febslet.2013.11.027 (2014).

Zhang, H. *et al.* Native electrospray and electron-capture dissociation FTICR mass spectrometry for top-down studies of protein assemblies. *Anal. Chem.* **83**, 5598-5606, doi:10.1021/ac200695d (2011).

Zhang, M. *et al.* Indirect detection of protein-metal binding: Interaction of serum transferrin with In^{3+} and Bi^{3+}. *J. Am. Soc. Mass Spectrom.* **15**, 1658-1664 (2004).

Zhang, M. *et al.* Mapping of protein disulfide bonds using negative ion fragmentation with a broadband precursor selection. *Anal. Chem.* **78**, 4820-4829 (2006).

Zhao, H. *et al.* Evaluation of Nonferrous Metals as Potential In Vivo Tracers of Transferrin-Based Therapeutics. *J. Am. Soc. Mass Spectrom.* **27**, 211-219, doi:10.1007/s13361-015-1267-y (2016).

Zheng, K. *et al.* The impact of glycosylation on monoclonal antibody conformation and stability. *MAbs* **3**, 568-576, doi:10.4161/mabs.3.6.17922 (2011).

Zheng, K. *et al.* Influence of glycosylation pattern on the molecular properties of monoclonal antibodies. *MAbs* **6**, 649-658, doi:10.4161/mabs.28588 (2014).

Zubarev, R. A. *et al.* Electron capture dissociation of gaseous multiply-charged proteins is favored at disulfide bonds and other sites of high hydrogen atom affinity. *J. Am. Chem. Soc.* **121**, 2857-2862 (1999).

Zühlsdorf, A. *et al.* It Is Not Always Alcohol Abuse—A Transferrin Variant Impairing the CDT Test. *Alcohol Alcohol.*, doi:10.1093/alcalc/agv099 (2015).